Modelling Vaccine Hesitancy and Strategies to Address It



Muhammad Firdaus Kasim

Exeter College
Nuffield Department of Medicine
University of Oxford

A thesis submitted for the degree of
Doctor of Philosophy
Hilary 2026

Acknowledgement

The last four years have been the most intellectually rewarding and challenging for me. The writing of this thesis has summarised the academic work I have conducted over the four-year period, and this thesis is a celebration of the journey. On this occasion, I would like to acknowledge people whose contributions have been invaluable in finalizing this study.

I want to express my gratitude to my supervisors Professor Ricardo Aguas, Professor Nathaniel Hupert and Professor Lisa White, for being the best role models of academics who elevate their students and explore their hidden potentials. Their intellectually intense yet enjoyable discussions through the years enabled me to discover lots of fascinating ideas covering multiple scientific disciplines which I humbly explore in this thesis.

I would like to acknowledge the Indonesian government through the Indonesian Endowment Fund for Education (Lembaga Pengelola Dana Pendidikan) which has provided financial support during my study and enabled me to pursue my dream. We have laid out our constitutional responsibility for education, and I stand as a testament to that commitment. Hopefully we can maintain this development course which emphasises the importance of education through the changing of regimes in Indonesia.

Many foundational ideas of this thesis were flourished through discussions with my wife, *Elvita Bellani*, who has been kind to introduce me to behavioural science and nurture my interest ever since. Our shared mission of developing people around us gives me reason to pursue this thesis topic. I am looking forward to our more flourishing discussions in addressing our ever-changing societal problems.

To all my family and friends whom I encountered during the study, I would like to express my sincere gratitude for the support, companionship and engaging discussions.

I submit this thesis in loving memory of my mother, *Farida Kasim*, who always looked at the world with compassion.

Table of Contents

List of Figures ..... **vii**

List of Tables ..... **x**

Declaration of the Use of Generative Artificial Intelligence ..... **xii**

Chapter 1 Introduction **1**

1.1 Background **1**

1.2 Evidence gap and research questions **5**

1.3 Project aim and objectives **8**

1.4 Thesis outline **8**

Chapter 2 Modelling Vaccine Hesitancy **9**

2.1. Introduction **9**

2.2 The Decision Update Model **11**

2.2.1 Perception of vaccination 12

2.2.2 Social influence 17

2.2.3 Individual's willingness to vaccinate 19

2.3 The Opinion Formation Model **21**

2.3.1 Failure of information deficit hypothesis 22

2.3.2 Modelling opinion formation along with the biased assimilation 23

2.3.3 External events effect to opinion formation 27

2.3.4 Integration of the opinion formation to the vaccine decision rule 28

2.4. The Measles Transmission Model **29**

2.4.1 Evidence on measles transmission 30

2.4.2 The measles model description 32

2.5. The Social Network Model **37**

2.5.1 Network clustering and the vulnerability against outbreak 38

2.5.2 Network structure 38

2.6. Conclusions **42**

Chapter 3 Vaccination decision dynamics **43**

3.1 Introduction **43**

3.2 Methods **45**

3.2.1 Vaccination willingness, behaviour and epidemiological outcomes 46

3.2.2 Opinion formation, inter-community interaction and external events 50

3.3 Results and Discussion **53**

3.3.1 Vaccination willingness 54

3.3.2 Vaccination behaviour 57

3.3.3 Epidemiological outcomes 60

3.3.4 Behavioural vaccine effectiveness 63

3.3.5 Opinion formation 65

3.3.6 Inter-community interaction 70

3.3.7 External events 72

3.4 Conclusions **81**

3.5 Limitations **83**

Chapter 4 Estimating Perceived Relative Cost of Vaccination **84**

4.1 Introduction **84**

4.2 Methods **85**

4.2.1 Dataset 86

4.2.2 Parameter calibration 87

4.2.3 Generalized Expectation-Maximization implementation 91

4.2.4 Perceived vaccination relative cost (vRC) estimation and reconciliation 97

4.2.5 In-sample model fit and uncertainty quantification 99

4.2.6 Out-of-sample validation 101

4.3 Results **104**

4.3.1 Measles vaccination and incidence trends in Indonesia 104

4.3.2 In-sample model fit 106

4.3.3 Estimated perceived vaccination relative cost (vRC) 110

4.3.4 Out-of-sample validation 116

4.4 Discussions **119**

4.5 Conclusions **123**

Chapter 5 Strategies to Address Vaccine Hesitancy **125**

5.1 Introduction **125**

5.2 Methods **127**

5.2.1 Network, vaccination and disease models 127

5.2.2 Parameters 128

5.2.3 Interventions model 129

5.3 Results **134**

5.3.1 Communication Strategies 135

5.3.2 Influencer-Based Strategies 138

5.3.3 Mandatory Vaccination Strategy 139

5.4 Discussion **141**

5.4.1 Communication interventions: perception change under social influences and assimilation bias 141

5.4.2 Influencers strategies: evaluating most popular promoter myth 143

5.4.3 Mandatory vaccination: decoupling willingness from behaviour 144

5.4.4 Implications for scaling interventions 145

5.5 Conclusions **146**

Chapter 6 General Discussions and Conclusions **149**

6.1 Summary of findings **149**

6.2 Context **151**

6.3 Strengths, limitations and further works **155**

6.4 Conclusions **158**

Appendix **160**

Appendix A Reported data adjustment **160**

Appendix B Seasonality analysis of measles **163**

Appendix C Parameter estimation **167**

Appendix D Basic and effective reproductive number **168**

Appendix E Estimated vRC list **170**

Bibliography **175**

List of Figures

Figure 2.1. Probability of switching from non-vaccinated to vaccinated status as a function of perceived vaccination relative cost (v_{RC}).....16
Figure 2.2. The vaccine decision update rule 20
Figure 2.3. The biased opinion formation (BOF) update function 27
Figure 2.4. Proposed measles transmission model 33
Figure 2.5. Probability distribution of the state transition periods 34
Figure 2.6. Hypothetical measles outbreak simulation. 36
Figure 2.7. The ecological model of the social network implemented in this study. 37
Figure 2.8. Degree (*d*) distribution of empirical social networks. 40
Figure 3.1. Simulation setup of vaccination and measles dynamics in an under-vaccinated community. 47
Figure 3.2. Modelled inter-community interaction of the under-vaccinated community with other communities. 51
Figure 3.3. Individual's willingness to vaccinate 55
Figure 3.4. Probability of vaccination comparison of two decision models 57
Figure 3.5. Collective vaccination behaviour in under-vaccinated communities with and without outbreak. 58
Figure 3.6. Epidemiological dynamics of measles outbreaks in under-vaccinated communities. 61
Figure 3.7. Behavioural vaccine effectiveness (BVE) in under-vaccinated communities against measles infection. 64
Figure 3.8. Perception of vaccination relative cost (v_{RC}) and vaccination dynamics in under-vaccinated and neighbouring pro-vaccination communities. 66
Figure 3.9. Update of perceived vaccination relative cost in an under-vaccinated community following interaction with other communities. 68
Figure 3.10. Final vaccinated household (Vf) in the under-vaccinated community following opinion updates about vaccination. 69
Figure 3.11. Final vaccinated household (Vf) in an under-vaccinated community influenced by inter-community opinion exchange. 71

Figure 3.12. Perception of vaccination relative cost (v_{RC}) trend comparison under different vaccine risk scenarios. 74
Figure 3.13. Perception of vaccination relative cost (v_{RC}) and vaccination coverage dynamics among households in under-vaccinated community and other communities when there is no measles outbreak. 76
Figure 3.14. Perception of vaccination relative cost (v_{RC}) and vaccination coverage dynamics among households in under-vaccinated community and other communities when there is measles outbreak. 77
Figure 3.15. Final vaccinated household percentage following vaccine scare in under-vaccinated community without an outbreak. 78
Figure 3.16. Final vaccinated and infected household percentages following vaccine and disease scares in an under-vaccinated community with an outbreak. 79
Figure 3.17. Final vaccinated and infected household percentages following vaccine and disease scares in an under-vaccinated community with an outbreak. 80
Figure 4.1. Indonesian reported measles vaccination uptake and incidence 105
Figure 4.2. Evaluation of model accuracy for MCV-1 uptake and measles incidence across Indonesian provinces. 107
Figure 4.3. Posterior predictive distribution of provincial measles-containing vaccine dose 1 (MCV-1) uptake in Indonesia, 2017–2023. 108
Figure 4.4. Posterior predictive distribution of provincial measles incidence in Indonesia, 2017–2023 109
Figure 4.5. Trend of perceived vaccination relative cost (v_{RC}) in Indonesian provinces along with the reported MCV-1 uptake and mean monthly measles incidence, 2017 – 2023. 111
Figure 4.6. Spatial distribution and temporal evolution of provincial perceived vaccination relative cost (v_{RC}) in Indonesia, 2017 to 2023. 113
Figure 4.7. Correlation of annual measles-containing-vaccine dose 1 (MCV-1) and mean monthly measles incidence with perceived vaccination relative cost (v_{RC}) in Indonesian provinces, 2017 – 2023. 114
Figure 4.8. Association of annual measles-containing-vaccine dose 1 (MCV-1) uptake and perceived vaccination relative cost (v_{RC}) with poverty rate and distance to primary care facilities in Indonesian provinces, 2017-2023. 115
Figure 4.9. Mean absolute error (MAE) of the models prediction along with the share of error across provinces. 117

Figure 4.10. Predicted-reported data association and skill score of various information settings against baseline models.....118
Figure 5.1. Communication strategies gate receptivity (g) based on prior perceived vaccination cost of households.....130
Figure 5.2. Vaccination uptake stability as a function of perceived vaccination relative cost (v_{RC}).....135
Figure 5.3. Effect of risk communication to increase vaccination uptake in one community, based on prior vaccination popularity (Vp) and assimilation bias (b).....136
Figure 5.4. Effect of misinformation against vaccination to decrease uptake in one community, based on prior vaccination popularity (Vp) and assimilation (b).....137
Figure 5.5. Efficacy of communication strategies to increase uptake under influence of misinformation against vaccination.....138
Figure 5.6. Comparisons of influencers strategies effectiveness to vaccination uptake.....139
Figure 5.7. Efficacy of mandatory vaccination in a community.....140

List of Tables

Table 1. Descriptions parameters in the measles transmission model. 35
Table 2. Global parameter values used in simulations. 49
Table 3. Global parameter values for opinion dynamics simulations 53
Table 4. Carry-forward rule of the behavioural parameters and the force of infection. 102
Table 5. Information settings of the prediction model. 103
Table 6. Global parameter values in interventions to address vaccine hesitancy simulation. 128

Abstract

Vaccine hesitancy limits the potential of vaccination as a public health intervention, yet the complex mechanisms underlying the phenomenon remain insufficiently understood. This thesis aims to model vaccine hesitancy and strategies to address it, through an integrated framework that combines health behaviour theories, evolutionary game theory, opinion formation, social network model and measles epidemiology. The vaccination decision model implements two key behavioural drivers derived from the Theory of Planned Behaviour and the Increasing Vaccination Model: self-perception and social influence, operationalised through perceived vaccination relative cost and social learning within synthetic network structures. The integrated model is evaluated through agent-based simulations of vaccination and measles dynamics in under-vaccinated communities.

The results demonstrate that social influence transforms individual perception of vaccination into collective dynamics that constraint behaviour, and that a critical threshold of perceived vaccination relative cost determines whether herd immunity is achievable. Assimilation bias, moderated by community isolation, entrenches opposition to vaccination and fosters polarisation between under-vaccinated communities and the surrounding population. These mechanisms explain the persistence of hesitancy during outbreaks and the limited utility of reactive vaccination when perceived vaccination relative cost exceeds the critical threshold.

To infer temporal dynamics of vaccination perception at the population level, the agent-based model is transformed into a deterministic form and implemented within a Generalized Expectation Maximization framework. This estimation model is applied to provincial measles vaccination uptake and incidence data in Indonesia, with uncertainty quantified through Bayesian Markov Chain Monte Carlo sampling. The results demonstrate that the model can estimate perceived vaccination relative cost, a hidden psychological construct distinct from observed vaccination behaviour, providing a foundation to monitor vaccine perception trajectories complementing routinely reported vaccine uptake and incidence data.

Finally, the integrated model is used to simulate communication, influencer and mandatory vaccination interventions, demonstrating that risk communication yields the greatest benefit in the most under-vaccinated communities, while mandatory vaccination achieves high uptake without corresponding improvement in willingness to vaccinate.

Declaration of the Use of Generative Artificial Intelligence

Generative artificial intelligence (GenAI) was used, in compliance with the University, divisional and departmental guidance, in research underlying this thesis, to generate Python code for the implementation of simulations, analytical tasks and visualisations. In all instances of the GenAI implementation, the model structure, mathematical formulations, parameter definitions, simulation logic and expected analytical outputs were specified by the author independently prior to any interaction with GenAI tools. GenAI was used solely to translate these pre-determined specifications into executable code. The resulting code was subsequently reviewed by the author for logical coherence and verified against expected simulation behaviour and outputs. The code was also manually edited by the author to correct errors or inconsistencies.

The author transitioned between several platforms of GenAI tools as the technology evolved during the 2023 to 2025 period. The tools used were ChatGPT (OpenAI, various versions) and Claude (Anthropic, various versions), accessed via their respective web interfaces, desktop applications and, specifically for Claude, also through Claude Code, a command-line interface for agentic coding tasks.

GenAI tools were also used to proofread the written text of this thesis for grammatical checking and correction. No substantive intellectual content, analytical arguments, model interpretations, or conclusions were generated or altered through this process. All suggested corrections were reviewed by the author prior to incorporation into this thesis.

No GenAI tool was used for other substantive use in the research cycle underlying this thesis, such as the review of literature, the identification of research gaps, the formulation of research aims, the design of research methodology, the formulation of model structure or parameters, the interpretation of simulation outputs or estimated results, the determination of analytical objectives, or the drawing of conclusions. The author accepts full responsibility for the integrity of the work presented in this thesis.

Chapter 1 Introduction

1.1 Background

Vaccination is one of the most successful public health interventions to date. Currently available vaccines can prevent mortality and morbidity from more than 30 diseases (World Health Organization, 2026). Since the launch of the Expanded Programme on Immunization (EPI) by the World Health Organization (WHO) in 1974, there have been more than 150 million deaths averted, contributing to 40% decline of infant mortality globally (Shattock et al., 2024). Moreover, vaccination is estimated to have yielded eight hundred and twenty billion US Dollar of economic and social value in lower middle-income countries from 2001 to 2020 (Ozawa et al., 2017).

To achieve the optimal benefit from vaccination, a significant percentage of the population should be vaccinated to reach the herd immunity threshold. Herd immunity occurs when a sufficiently high percentage of the population is immune, either through vaccination or infection, thereby preventing the transmission of vaccine-preventable diseases and protecting the remaining susceptible individuals in the population. Reaching herd immunity through vaccination requires a sustained level of vaccination coverage, as new susceptible individuals are continuously introduced through birth and waning immunity over time. Yet attaining herd immunity through natural infection is not acceptable due to the morbidity and mortality it would incur, which are preventable by vaccination. Furthermore, achieving and maintaining sufficient vaccination coverage to confer herd immunity and protect the population from vaccine-preventable diseases remains a challenge (Eagan et al., 2023).

Vaccination strategies are prone to controversy, where misinformation and misattribution can depress vaccine uptake even when there is extensive scientific evidence to refute those claims. Over the last decades, EPI efforts to ensure life-saving vaccines can be accessed by all children globally, have been undermined by several mischaracterisations of vaccines as being harmful and proposed links between vaccines and several diseases (Cowan et al., 1993; Gilmour et al., 2013; Wakefield, 1999). Although further empirical evidence has proven that the overwhelming misperceptions of vaccine safety are unfounded (Ben-Menachem, 2011;

DeStefano and Thompson, 2004; Ikeda et al., 2019), the latter have contributed to a substantial decrease in vaccine uptake over the last decade and widespread vaccination concerns in today's society (de Figueiredo et al., 2021).

Population vaccination adherence is extremely sensitive to social contexts, with social, economic and political factors combining to play a significant role in shaping people's stance toward vaccination. Fridman et al. (2021) found that people are not responsive to increasing threat of disease, and that unresponsiveness is related with political partisanship, in which self-identified Republican participants showed negative attitude and low willingness to vaccinate. In those participants, there is a correlation between a less favourable attitude toward vaccination and disease complacency. Along with the partisanship, confidence toward vaccination is also confounded with having more unvaccinated individuals within one person's immediate social network (Facciani et al., 2023). Partisanship is also associated with low vaccination behaviour outcome (Backhaus et al., 2023; Kennedy, 2019; Kreps and Kriner, 2023), along with income (Dong et al., 2024).

Nevertheless, right-leaning individuals do not always vaccinate less. Unlike in the USA, supporters of Conservative parties in the UK are associated with higher COVID-19 vaccination rates compared with Labour supporters (Klymak and Vlandas, 2022). This vaccination support is related to the fact that the political party they support is in power and endorses vaccination. Vaccination behaviour is therefore not solely related to the identity individuals uphold, but rather to how individuals align their decisions with others who share a similar identity.

It has been reported that determinants of non-vaccination are not limited to personal judgement of the risks and benefits of vaccination only but also extend to a complex social context that emerges from interactions among individuals. In this thesis, judgment of vaccination risk and benefit is defined as *self-learning*, following the terminology in the Increase Vaccination Model (Brewer, 2021; Brewer et al., 2017), and is operationalised as perceived vaccination relative cost (v_{RC}). The social context determinants are operationalised through perceived vaccination popularity based on the individuals' location in the social network and defined as *social learning*.

To describe decision making mechanisms of failure to vaccinate, the term vaccine hesitancy was implemented, and defined as delaying or refusing vaccination when the vaccine is available (MacDonald, 2015). Vaccine hesitancy is a constraint for vaccination to reap its

potential population level benefits. It is a global phenomenon which has been reported in more than 90% countries around the world based on joint reporting from WHO and UNICEF data (Lane et al., 2018). The phenomenon has been credited for the re-emergence of vaccine preventable diseases in several countries where those diseases had been previously eliminated (Gostin et al., 2020; Hotez, 2019; Phadke et al., 2016). Given the magnitude of the problem, vaccine hesitancy has been declared by WHO as one of the major public health threats in 2019 (World Health Organization, 2019).

Although vaccine hesitancy can be objectively operationalised and easily measured through vaccination behaviour, this behaviour can mask the complexities of true perception towards the vaccine. People can decide to vaccinate even when their hesitancy persists. For example, when vaccine mandates are in place, people will comply with vaccination to maintain access to public services, which can sometimes result in reduced willingness to adopt other voluntary vaccinations and protective behaviours (Sprengholz et al., 2022).

Therefore, due to the incongruence between human behaviour and its psychological determinants, vaccine hesitancy should be defined in the psychological state rather than at the behavioural outcome of vaccination (Bussink-Voorend et al., 2022; Goldenberg, 2021; Larson, 2022). The antecedent psychological states, which produce vaccination behaviour outcome, include perception of vaccination relative cost, confidence or willingness to vaccinate, and can be measured through surveys (Eagan et al., 2023; Figueiredo et al., 2020) to complement vaccination uptake data which is routinely collected by EPI programs. Although important, the psychological state measurement is not readily available like routinely reported vaccination uptake.

Vaccination behaviour is not homogenous in a population. Clusters of under-vaccinated communities are evident despite a high vaccination coverage in general population (Brownwright et al., 2017; Klinkenberg et al., 2022; Masters et al., 2020). These under-vaccinated pockets are more responsible for re-emergence of vaccine preventable diseases than case importation in populations where vaccination is widely available (Dimala et al., 2021; Leong and Wilder-Smith, 2019; Phadke et al., 2016).

To understand how the vaccination behaviour outcome arises from the complexities of its determinants, mechanistic mathematical model offers an avenue to understand the underlying mechanisms and causal processes of vaccine hesitancy. Several approaches have been

implemented to study vaccination through mathematical modelling, and network-based approaches are increasingly used to capture heterogeneity of vaccination behaviour (Wang et al., 2016).

Modelling vaccination through social networks offers a more realistic representation of social interaction in a heterogenous setting. Vaccination in a population is a collective outcome from interacting behaviours of individuals who make individualised vaccination decisions. These decisions are well suited to agent-based (ABM) or individual-based (IBM) modelling, while the resulting collective decision dynamics are represented using an evolutionary game framework (Traulsen and Hauert, 2009).

Measles is an excellent use case to study vaccine hesitancy through mathematical modelling, due to its high transmissibility and the fact that both natural and vaccine induced immunity elicit lifelong immunity against disease (Griffin et al., 2018; Schenk et al., 2021). The basic reproduction number (R_0) for measles, defined as the average number of secondary infections following a primary infection in wholly susceptible population, is commonly cited as a range of 14-18 (Anderson and May, 1982). However, R_0 is not a fixed biological constant, and the reproduction rate may vary in different contexts: in least developed, high density or high birth rate areas, the case reproductive number can be substantially higher (Guerra et al., 2017). Based on the range of measles R_0, the implied herd immunity threshold of 1 - $1/R_0$ is approximately 93-94%. However, considering vaccine effectiveness against infection is not 100%, at least 95% of under five years old children should be vaccinated to prevent measles transmission within a population and reach herd immunity (Funk et al., 2019). Due to the high transmissibility and the high vaccination coverage required to confer herd immunity, measles outbreaks are often regarded as an early signal of childhood immunisation system failure (Kiang et al., 2025).

Beyond its high transmissibility, measles also poses an equity concern. An infection can trigger immune amnesia, a condition in which the immune system's memory of previously encountered pathogens is diminished, due to depletion of memory B and T cells (Laksono et al., 2020). This immune suppression phenomenon is only found on previously unvaccinated children who are infected with measles (Mina et al., 2019), and can last from a few weeks to several years (Mina et al., 2015). Measles infections can also alter vaccine-acquired immunity for other pathogens (Petrova et al., 2019), rendering children who have been vaccinated with

vaccines other than measles also vulnerable to secondary infection following measles infection. Due to the immune amnesia effect, children who live in environments with inadequate sanitation and limited healthcare access are disproportionately affected following a measles infection.

Despite its rapid spread and potential to compromise a child's immune defences, measles is preventable through vaccination. Current measles vaccines provide robust protection against all known circulating strains (Di Pietrantonj et al., 2021), while the degree of waning immunity is considered to be negligible (Schenk et al., 2021). The safety profile of the measles vaccine is also well-established, with side effects generally minimal and predominantly mild (Di Pietrantonj et al., 2021), Severe adverse events are extremely rare, making the measles vaccine one of the safest and most cost-effective public health interventions currently available.

Overall, this background summarises that vaccine hesitancy limits the potential of vaccination strategies, and that underlying psychological states should be distinguished from observed vaccination outcomes when defining vaccine hesitancy. The hesitancy phenomenon is due to complex interactions of self-learning and social determinants, in which the hesitant individuals are clustered within populations. Mathematical modelling provides useful tools to study the complex mechanism of vaccine hesitancy through evolutionary game theory in network-based ABM. As the use case, measles is implemented in this study as the disease prevented by the vaccination, due to the high transmissibility and the high vaccination coverage it requires to reach herd immunity, yet currently available vaccine is optimal to provide protection against measles.

1.2 Evidence gap and research questions

Despite the standard use of vaccination modelling for policy design (Shankar et al., 2024; Wang et al., 2016), several gaps persist. Many vaccination models are not explicitly grounded in behavioural theory or social science (Bedson et al., 2021; Weston et al., 2018), even though a large body of behavioural and social science literature has described the phenomenon of vaccine hesitancy (Brewer et al., 2017; Yaqub et al., 2014). This gap provides an opportunity to model the inherent mechanisms of vaccination decision-making through mathematical models, that are grounded in behavioural and social science, to better understand the underlying dynamics.

Social networks implemented in vaccination decision models are frequently not empirically inspired. This is understandable given the limitations of empirical network construction, although several studies have provided evidence on the shape of real-world networks (Banerjee et al., 2013; Harris et al., 2019). Nevertheless, discussions of social network topology have largely converged on whether connectivity follows a scale-free or a log-normal distribution (Broido and Clauset, 2019; Serafino et al., 2021). Those current empirical observations and emerging understanding of social network patterns provide a foundation for constructing synthetic social networks that more closely reflect reality.

Although helpful for representing heterogeneity, networks constructed in vaccination models are often specified at the general population level (Pastor-Satorras et al., 2015; Wang et al., 2016), rather than at the community level. Such population-level models can obscure local vulnerabilities and dynamics, as pockets of under-vaccinated communities can persist despite high vaccination coverage in the general population (Brownwright et al., 2017; Klinkenberg et al., 2022; Masters et al., 2020). Therefore, given that vaccine-hesitant individuals tend to cluster within smaller under-vaccinated communities, models that focus on these communities can provide a better understanding of vaccine hesitancy.

Several empirical observations regarding the social phenomenon of vaccine hesitancy are not always captured by current approaches. One is the persistence of hesitancy during outbreaks. If vaccination was driven solely by judgements about the benefits of vaccination relative to the risk of contracting diseases, then increased vaccination during an outbreak would be expected. However, some communities remain reluctant to vaccinate even under outbreak conditions (Christianson et al., 2020; Zucker et al., 2020; Parker et al., 2006). Information deficit also offers a limited explanation for this persistence of hesitancy. Evidence suggests that providing corrective information about vaccination does not necessarily increase confidence and, in some settings, may even backfire (Nyhan et al., 2014). Together, these findings are consistent with cognitive biases shaping vaccination decisions (Goldenberg, 2021), specifically assimilation bias (Lord et al., 1979). The persistence of hesitancy during outbreak and assimilation bias are both observed phenomena lacking an adequate explanatory mechanism. Existing modelling frameworks exploring vaccination do not integrate these determinants to explore the dynamics of vaccination in social network settings.

Several interventions to address vaccine hesitancy have been implemented, including routine monitoring of vaccination uptake, reactive vaccination following outbreaks, and proactive

strategies to increase uptake such as communication, community activation, or mandatory vaccination. However, these approaches also face important limitations. Although vaccination uptake is routinely monitored through EPI programmes, underlying psychological determinants cannot be directly inferred from uptake alone, and approaches to monitor psychological determinants alongside behavioural uptake data remain limited. Due to the importance of the psychological state in measuring vaccine hesitancy (Bussink-Voorend et al., 2022; Goldenberg, 2021; Larson, 2022), monitoring the hidden psychological variable that shapes vaccination behaviour is warranted, in addition to routinely reported uptake. Reactive vaccination, while widely used, is resource-intensive (Martin et al., 2021; Zucker et al., 2020), needs to be administered rapidly to be effective (Marinović et al., 2012), and can face substantial implementation challenges in hesitant communities (Robinson et al., 2021). Finally, proactive strategies show mixed effects on increasing vaccination coverage/uptake (Banas and Rains, 2010; de Figueiredo et al., 2021; Gualano et al., 2019; Parsons et al., 2018; Smith et al., 2021). Yet their efficacy is measured in controlled observational or experimental settings or assessed primarily through observed outcomes, rather than through the underlying mechanisms. Consequently, evidence remains limited on how these proactive strategies perform when implemented in under-vaccinated communities under realistic behavioural and social complexity.

Therefore, based on the research gaps elaborated above, this thesis proceeds with the following research questions:

1. Why do under-vaccinated communities remain hesitant to vaccinate even during disease outbreaks?
2. How effective is reactive vaccination in controlling outbreaks in under-vaccinated communities?
3. What role do cognitive biases play in shaping vaccine hesitancy and its consequences?
4. How to monitor perceived vaccination relative cost complementing reported vaccination uptake and incidence?
5. Under what conditions interventions to address vaccine hesitancy can be effective in increasing vaccine uptake?

1.3 Project aim and objectives

This study aims to model vaccine hesitancy and strategies to address it, in order to understand the complex mechanisms underlying the phenomenon. To achieve this aim, this study sets the following objectives:

1. To formulate a vaccination decision model integrating multidisciplinary understandings of the vaccine hesitancy phenomenon.
2. To elucidate complex mechanisms of vaccine hesitancy.
3. To infer temporal dynamics of vaccination perception from routine administrative data of vaccination uptake and incidence.
4. To simulate implementations of interventions to address vaccine hesitancy.

1.4 Thesis outline

Each subsequent chapter delivers an objective of the study. In Chapter 2, methods to develop a unified vaccination model from multidisciplinary perspectives are presented. Literature reviews related to the specific construction of each part of the model are also elaborated in Chapter 2. Testing of the developed modelling framework is presented in Chapter 3, which answers research questions 1 to 3. After this testing, the model is implemented to estimate the hidden variable of perceived vaccination relative cost from routine administrative data available from the EPI programme, as presented in Chapter 4. In Chapter 5, the model is also implemented to simulate interventions to address vaccine hesitancy, by integrating findings from observational and experimental studies within the complexity of social interaction and assimilation bias. Finally, Chapter 6 presents the general discussion and conclusions of the thesis.

Chapter 2 Modelling Vaccine Hesitancy

2.1. Introduction

This chapter presents a literature review on modelling vaccination decisions, grounded in current understandings of the vaccine hesitancy problem. The evidence from this review informs the development of integrated models of vaccination decision-making, which are also elaborated in this chapter. The integrated decision models are implemented to guide us in understanding vaccine hesitancy phenomena. These models are developed and implemented based on insights from behavioural, cognitive, social, physics, epidemiological, and networks sciences, offering a multidisciplinary perspective on vaccine hesitancy. To the best of the author's knowledge, the work contained in this thesis introduces a novel methodological approach by integrating theoretical and empirical insights from multiple scientific disciplines to model the complex dynamics of vaccine hesitancy.

Here, I will explore decision-making models exploring how individuals make choices about vaccination, as a function of their cognitive biases, underlying disease transmission dynamics, and their social interactions. The integrated vaccine uptake decision-making model is composed of four key components which are elaborated in each section in this chapter: (i) the vaccination decision rule, (ii) the opinion formation, (iii) the disease transmission model, and (iv) the social network structure.

Section 2.2 below elaborates the decision update model to describe individuals' decision to vaccinate. This model which represents individuals' willingness to receive vaccination is grounded by two health behaviour theories: The Theory of Planned Behaviour (TPB) (Ajzen, 1991) and the Increasing Vaccination Model (IVM) (Brewer, 2021; Brewer et al., 2017) . Two key elements are incorporated into the decision rule model: individual's beliefs towards vaccination and social influence. The beliefs mentioned here are akin to the "attitude toward the behaviour" from TPB and "what people think and feel" from IVM, while the social influence is equivalent with "subjective norm" from TPB and "social process" from IVM. These elements of self and social learning ultimately influence an individual's willingness to vaccinate, which is quantified as the probability of adopting the behaviour. The decision rule

is established with an assumption that there is no accessibility problem, to focus on the study of vaccination demand side.

Individuals' vaccination decisions are influenced by the choices of those around them and their perceived threat in facing infectious disease. Evolutionary game theory (EGT) is implemented to simulate each individual's decision-making processes and to model collective behaviour. The EGT approach captures these decision dynamics through an iterative process, as individuals will make the decision for each time step of vaccination schedule. The Fermi-Dirac like function (Perc et al., 2017) is implemented to model how individual's willingness to be vaccinated is affected by interactions within their sphere of influence. For this study, we defined sphere of influence as the set of people with whom a person has direct interactions with and anyone else within that set is designated as neighbour.

Section 2.3 introduces 2.3 The Opinion Formation Model. Opinion formation plays a crucial role in shaping vaccination behaviour, particularly under the influence of cognitive biases. Here, opinions shape individual's perception of vaccination. I chose to implement a biased assimilation model (Dandekar et al., 2013), which assumes that individuals are more likely to accept an opinion that is closer to their pre-existing belief (Lord et al., 1979). The biased assimilation model extends the De Groot social learning framework (DeGroot, 1974).

To explore the interplay between vaccination decisions and disease dynamics, this study incorporates individual-based measles transmission model, which is described in Section 2.4:2.4. The Measles Transmission Model. The biological parameters of the transmission model are estimated from evidence of measles infection and vaccination. The model accounts for two-dose vaccination regimens against measles. Individuals can be vaccinated based on their immunisation record and if they do not exhibit any symptoms for infection. Those vaccination requirements reflect real-world guidelines for measles immunisation.

Finally, social networks provide a structural environment for vaccination decision-making and disease transmission dynamics, which is elaborated in Section 2.5: 2.5. The Social Network Model. The network can influence individuals' willingness to vaccinate directly through enforcement of social norm or indirectly through opinion formation. This study employs empirical and synthetic network models to investigate transmission of vaccination behaviour and disease. Here, the node in the network can represent household or individual. The empirical network is derived from household connection data in 75 villages in India (Banerjee et al.,

2013). While the synthetic network is constructed based on log-normal degree distribution when the network size is small and scale free when a larger network is implemented. The choice between log-normal and scale free network topologies is informed by a survey conducted by Serafino et al. (2021), which found that finite-size effects cause deviations from scale-free distributions in smaller networks, making them more likely to resemble log-normal structures.

The following sections detail the modelling approaches for vaccine hesitancy, structured around the four integrated components developed in this study. The chapter begins with a discussion of how individuals update their vaccination decisions, followed by models of opinion formation, disease transmission and social networks. Together, these components form an integrated framework to capture the cognitive, social and epidemiological dynamics underlying vaccine hesitancy.

2.2 The Decision Update Model

Vaccination is not without risk; no vaccine is free from side effects, but most have very low probability of adverse events. Within the context of routine immunisation, it is reasonable to assume that individuals can construct perceptions about vaccination risks, which they subsequently evaluate against the perceived benefit of protection from the disease the vaccine tries to prevent. This conceptualization aligns with global survey evidence, highlighting that evaluations of benefit and risks, like fears regarding side effects and vaccine safety, has been cited as the most frequent reason behind vaccine hesitancy (Lane et al., 2018).

Given their perception of both benefit and risk, individuals can establish an expected utility about vaccination before performing the behaviour. This expectation is constructed through self-learning. However, vaccination decision cannot be exclusively made by personal judgement alone. For every decision with an inherent cost (for vaccination, the expected risk is the cost), a social reinforcement is needed to assess whether a behaviour can legitimately be adopted (Guilbeault et al., 2018).

Given the importance of social influence in vaccination behaviour, this study employs decision theories that explicitly incorporate social cues. The Theory of Planned Behaviour (TPB) is applied, where intention to adopt a behaviour depends on three main components: attitude toward the behaviour, subjective norm and perceived behavioural control (Ajzen, 1991). The three elements from TPB align with those of the Increasing Vaccination Model (IVM): self-

learning (what people think and feel), social process and direct behaviour change (Brewer, 2021; Brewer et al., 2017). Although TPB was developed as a general framework for behaviour change and IVM focuses specifically on vaccination, both models incorporate social coordination in vaccination decision-making, reflected as "subjective norm" in TPB and "social process" in IVM.

As a focus on the demand side of the vaccination, the decision update model only focuses on the self-learning process to construct a perception toward vaccination, and the social learning process to assess the legitimacy of the behaviour within the sphere of influence. The two processes are elaborated in the two following subsections. The 2.2.1 Perception of vaccination section elaborates the expected utility assessment, and the subsequent 2.2.2 Social influence section complements the vaccination decision rule. Both deliberation processes influence probability of vaccination which is elaborated in 2.2.3 Individual's willingness to vaccinate section.

2.2.1 Perception of vaccination

Since vaccination is not entirely without risk, individuals bear a non-zero perceived cost from potential side effects or other barriers, even when they perceive to gain significant protection against disease. Therefore, the expected utility toward vaccination is shaped by how individuals perceive both the protection a vaccine offers, and the risk involved if they decide to vaccinate. In this study, the expected relative utility is represented as perceived vaccination relative cost (v_{RC}).

Definition. **Perceived vaccination relative cost (v_{RC})** is a psychological measure of how people perceive the cost of being vaccinated relative to the perceived cost of being infected. v_{RC} is within [0, 1] range, where 0 denotes vaccination perceived as costless relative to infection and 1 denotes vaccination perceived as costly as infection. In opinion formation model (Sub Chapter 2.3), 0 denotes support and 1 denotes opposition to vaccination. In this thesis, the $v_{RC}$is a model construct and it is not measured directly but inferred either by assumption (Chapters 3 and 5) or by fitting to routine administrative data (Chapter 4).

In relation to behavioural theories' concepts, v_{RC}plays the role of *attitude toward behaviour* within the Theory of Planned Behaviour (Ajzen, 1991), and it represents what *people think and feel* within the Increasing Vaccination Model (Brewer, 2021; Brewer et al., 2017). Furthermore,

the v_{RC} is a composite ratio of Health Belief Model (Becker et al., 1974; Rosenstock, 1974a, 1974b) elements as expressed in Eq. 2.3.

The v_{RC} is deliberately focused on model construct of psychological dimension, in which individuals weigh the perceived cost of vaccinating against the perceived cost of being infected with the disease. Although the term is framed as cost, it is not intended to capture a monetary quantity. The v_{RC} is also not intended to capture structural barriers to access, since the decision model in this thesis assumes vaccination is available on demand (as elaborated in Section 2.2.3 Individual's willingness to vaccinate). This deliberate exclusion of accessibility barrier to v_{RC} construct is consistent with a result reported in Chapter 4 (**Figure 4.8**), where the estimated v_{RC} shows no statistically significant association with provincial poverty rate or travel time to primary care, while measles vaccination uptake is significantly associated with both structural barriers.

The next question arises on how to model vaccine adoption based on the vaccination perceived cost. To answer the question, a series of assumptions must be made about the domain problem: whether the social network is homogenous or heterogenous, finite or infinite, and whether the dynamics are based on fitness function or pairwise-comparison (Jusup et al., 2022). For the vaccine hesitancy problem, it has been shown that vaccine-hesitant individuals tend to cluster with the other hesitant individuals (Brownwright et al., 2017; Klinkenberg et al., 2022; Omer et al., 2008; Pingali et al., 2019; Stefkovics et al., 2024). This clustering phenomenon can result in pockets of under vaccinated communities, despite a high coverage in general population (Anis et al., 2021; Masters et al., 2020). Therefore, a finite network setting is more appropriate to capture the phenomenon of vaccine-hesitancy clustering and the heterogeneity of vaccine uptake in general population.

To better capture the vaccination decision dynamics in the finite and heterogenous network, an evolutionary game-theoretic (EGT) approach is incorporated. In the EGT, individuals compare their payoff with those of their neighbours. The comparison is conducted iteratively based on vaccination schedule, and the "evolutionary" term in the EGT reflects this iterative decision making.

In the vaccination dilemma, individuals can decide to vaccinate and bear the cost of vaccination. If individuals decide not to vaccinate, they have a chance to become infected and subsequently bear the cost of disease. Because of the expected cost after each event, the payoff

in this thesis is defined as **posterior cost (p)**. Before making each decision, individual i compares the posterior cost at time t ($p_{(i,t)}$) with a random neighbour j's posterior cost ($p_{(j,t)}$) through pair-wise comparison. The posterior cost function is defined as:

$$p_{(i,t)} = \begin{cases} v_{RC}, & if\ vaccinated \\ 0, & if\ not\ vaccinated \end{cases} \qquad p_{(j,t)} = \begin{cases} 1, & if\ infected \\ 0, & if\ not\ infected \end{cases} \tag{2.1}$$

One can evaluate the posterior cost function related to the neighbour's outcome for infection based on either absolute case numbers or the prevalence of infection in the sphere of influence. Additionally, one can choose between local or global case comparisons, where the local level reflects outbreaks occurring within the direct social contacts, and the global level refers to outbreaks in the broader population but not within the direct social contacts. The neighbour's posterior cost function in this study adopts result from a modelling study which found that local infection count is most sensitive toward protective action during an outbreak (Herrera-Diestra and Meyers, 2019). Therefore, the infection-related posterior cost assessment of neighbour j is modelled via a local level comparison by checking whether a random neighbour is infected or not. The randomization of neighbour selection is conducted to account for stochasticity in each decision step.

For finite population, the pair-wise comparison in the EGT is more suitable to be modelled by a Fermi-Dirac function (Traulsen and Hauert, 2009). The Fermi-Dirac is a sigmoid function which models probabilistic decision-making and originates from quantum statistical mechanics, a subfield of statistical physics. It describes the probability that a state is occupied by a particle, and in behavioural modelling, this function has been adapted to represent the probabilistic adoption of strategy in human cooperation (Jusup et al., 2022).

At each iteration, individual i updates their decision to be vaccinated based on their personal posterior cost at time t ($p_{(i,t)}$) and a random neighbour j's outcome against the disease ($p_{(j,t)}$), whether infected or not, based on the Fermi-Dirac function (Perc et al., 2017):

$$\Pi_{V \leftarrow NV} = \frac{1}{1 + \exp\left(\frac{p_{(i,t)} - p_{(j,t)}}{k}\right)} \tag{2.2}$$

$\Pi_{V \leftarrow NV}$ expresses the probability of individual i updating their decision from not vaccinated (NV) to vaccinated (V). In the decision update rule, a noise k ($0 < k < +\infty$) is introduced. The assumption is that each individual has a limitation to represent the problem they encounter akin

to the concept of bounded rationality (Simon, 1997, 1990). The smaller k means that individuals have a better understanding of the risk involved from both vaccination and the disease. Therefore, the k parameter can be considered disease- and vaccine-specific, as different pathogens and vaccines may vary in how easily individuals can comprehend their associated risks.

In principle, individuals could update their k values as they gain more information. With better understanding, they may become more confident in assessing risks, which would reduce the effects of bounded rationality. However, in this model, k is assumed to remain relatively stable over time. Moreover, due to empirical challenges in measuring k, it is treated as a fixed parameter within each simulation scenario. The value is chosen based on the assumed clarity with which individuals can assess a particular disease, such as routine immunisation for vaccine-preventable diseases compared to vaccination during a pandemic caused by an emerging pathogen. For the latter scenario, a higher k can be applied into the model.

Figure 2.1. illustrates the probability of an individual choosing to vaccinate ($\Pi_{V \leftarrow NV}$) based on the comparison of posterior costs between the individual and a randomly selected neighbour ($p_{(i,t)} - p_{(j,t)}$), moderated by decision noise (k). For simplicity, the individual's posterior cost is assumed to equal the perceived vaccination relative cost (v_{RC}) as when the individual decides to vaccinate ($p_{(i,t)} = v_{RC}$).

As shown in **Figure 2.1**, smaller values of k result in a steeper vaccination probability curve: in the absence of an infected neighbour, individuals choose to vaccinate only when the vaccination relative cost (v_{RC}) is very low, whereas in the presence of an infected neighbour, individuals maintain a high probability to vaccinate even when v_{RC} approaches the perceived cost of infection.

Similar to decision noise (k), the perceived vaccination relative (v_{RC}) is also disease- and vaccine-specific. However, v_{RC} is more dynamic over time, as it reflects evolving perceptions of the risks and benefits associated with vaccination. Therefore, v_{RC} is treated as variable in the model.

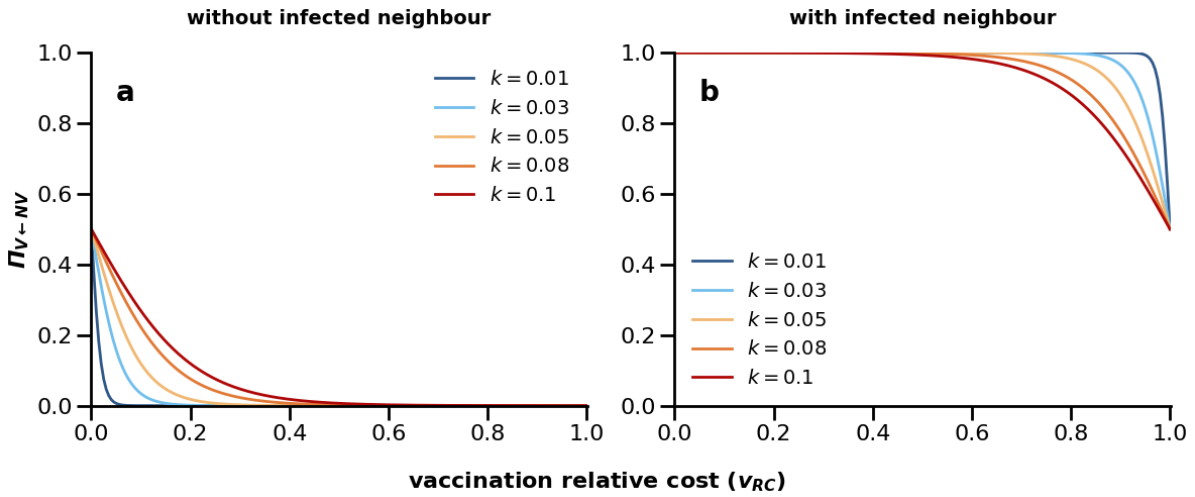


Figure 2.1. Probability of switching from non-vaccinated to vaccinated status as a function of perceived vaccination relative cost (v_{RC}). The $\Pi_{V \leftarrow NV}$ is given by the Fermi-Dirac update rule (Eq.2.2) and plotted against v_{RC} for five values of decision noise (k). **(a)** Households without infected neighbour ($p_{(j,t)}$= 0). **(b)** Households with infected neighbour ($p_{(j,t)}$= 1). Lower k values reflect more deterministic decision-making, where individuals are more likely to vaccinate when exposed to infection and refrain from vaccinating in the absence of infection.

The vaccination relative cost (v_{RC}) serves as a proxy for attitude toward vaccination. Because the v_{RC} stems from an individual's judgement of vaccination risk and benefit, the Health Belief Model (HBM) framework is utilized (Becker et al., 1974; Rosenstock, 1974a, 1974b) to calculate the v_{RC}. According to HBM, the likelihood of taking a preventative behaviour is increased as the perceived benefits approach and surpass the perceived cost. The judgement of v_{RC} is a function of perceived cost of vaccination (c_v) relative to perceived benefit of protection from vaccination (b_v), which can be extended to account for all elements of the HBM. Here, vaccination works to prevent infection, therefore b_v is equal to cost of infection (i_C). The v_{RC} is then given by:

$$v_{RC} = \frac{c_v}{b_v} = \frac{c_v}{v_c . r_i} = \frac{c_v}{v_c . Su . Se} \tag{2.3}$$

The v_c captures individual's confidence in the vaccine effectiveness and trust in the vaccination program, whereas the risk of infection (r_i) reflects the perceived susceptibility (Su) and severity (Se) of the disease.

Dividing the perceptions about vaccination into different elements enables a focus on specific elements that ultimately contribute to vaccination decision making and can be modulated through tailored interventions. For example, communicating disease risk can increase risk perception of the disease (Parsons et al., 2018), although the effect to vaccination behaviour is

inconclusive. While Parsons et al. (2018) found that no effect of disease risk perception to vaccination intention and behaviour, Brewer et al. (2007) found that the risk perception is significantly predictive of vaccination behaviour.

Other intervention prone elements to vaccination decision are presented in the 2.2.3 Individual's willingness to vaccinate section, where the IVM model also accounts for direct behavioural change (DBC) by reducing psychological barriers toward vaccination. The IVM proposed that DBC is proven to increase vaccination (Brewer et al., 2017). A reduction in psychological barriers can be achieved by interventions such as schedule reminder or appointment default. Although the IVM posits that the DBC "leverages on favourable intentions" without altering individuals' perception of vaccination, in the model applied in this study, the DBC is assumed to influence the perceived cost to vaccination (c_v) element within the HBM framework. The integration of the DBC to c_v assumption enables an objective simulation of the DBC's effect on vaccination uptake dynamics.

2.2.2 Social influence

Individuals need to coordinate with others before they make any inherently risky decision, to assess whether the behaviour is legitimate. This social coordination also applies in vaccination adoption. Perception of vaccine coverage among immediate contacts is correlated with vaccination (Bruine De Bruin et al., 2019). Empirical evidences suggest that social coordination also guides people in any health decision along with vaccination, like adoption of health behaviour in online communities (Centola, 2010), smoking cessation (Cole-Lewis et al., 2016), running activity (Aral and Nicolaides, 2017), and even there is a higher neural receptivity to health messages promoting physical activity when individuals are within proximity of active close contacts (Pandey et al., 2021). Those health decisions have inherent psychological cost when individuals adopt the new behaviour, like discomfort of performing the new behaviour or risk of failure to be consistent in adopting the behaviour. The social coordination influence also extends beyond the health domain, as demonstrated by phenomena such as patterns of social media subscription (Toole et al., 2012), novel telecommunication application usage (Karsai et al., 2014), microfinance adoption (Banerjee et al., 2013), or cultural events like the Amyotrophic Lateral Sclerosis Ice Bucket Challenge (Sprague and House, 2017).

Because of the multiple reinforcements needed to motivate individuals to adopt one behaviour, the decision under risk cannot be modelled with a simple contagion. In a simple contagion, even a single exposure can lead to transmission, as in the case with pathogen spread. In contrast, vaccination behaviour is more appropriate to be modelled as a gradual shift in behaviour under social influence, where multiple and reinforcing signals from peers are needed before individuals adopt the behaviour. This social influence formulation is motivated by the concept of complex contagion (Centola, 2021; Centola and Macy, 2007), which established that costly behaviours require multiple reinforcement to be transmitted in a way that pathogens do not.

Social influence in this model is captured by the fraction of neighbours who have adopted vaccination, reflecting the evidence that an individual's probability of adoption is linearly equivalent to the prevalence of adopters in their immediate social circle (Karsai et al., 2014). Following Szolnoki et al. (2012), individual i's social influence is defined as:

$$\left(\frac{N_0}{Z}\right)^{\alpha} \tag{2.4}$$

where N_0 is number of neighbours who have been successfully vaccinated from a total of Z number of neighbours. The fraction of vaccine adopters is modulated by social norm index α ($0 < \alpha \leq 1$) which defines the degree to which individuals conform with the majority decision in their sphere of influence. Accordingly, α is treated as a behavioural parameter which that varies across social groups, reflecting differences in the degree of conformity within each group.

The social norm index α represents the degree of general conformity to local vaccination behaviour, rather than a requirement for near-unanimous local uptake. Because $0 < \alpha \leq 1$, the social term $\left(\frac{N_0}{Z}\right)^{\alpha}$ never falls below the fraction of vaccinated neighbours. Willingness scales proportionally with local uptake when $\alpha = 1$ and depends less on neighbours as α decreases. A near-unanimity requirement would instead require $\alpha > 1$ or an explicit adoption threshold, neither of which is implemented in this thesis. The only legitimacy condition is that at least one neighbour must be vaccinated, since the social term is zero otherwise. The empirical value $\alpha = 0.7$ (Chu et al., 2021) implemented in Chapter 3, derived from the association between subjective norms and willingness, likewise reflects the strength of normative influence rather than an unanimity threshold.

The social influence model in this thesis does not implement complex contagion concept in strict sense, which incorporate threshold dynamics. There is no fixed number of reinforcing exposure that should be accumulated before adoption becomes possible, due to empirical limitation on the evidence of threshold level for vaccination. Therefore, the mechanism modelled here is a gradual shift of behaviour under social influence rather than complex contagion as formalised through threshold rules. The term "complex contagion" is used only to situate the work in this thesis with the literature.

2.2.3 Individual's willingness to vaccinate

Finally, by integrating the perception of vaccination cost and the social coordination, the individual's willingness to vaccinate (Ψ) is defined as:

$$\Psi_{(i,t)} = \left(\frac{N_0}{Z}\right)^{\alpha} \frac{1}{1 + \exp\left(\frac{p_{(i,t)} - p_{(j,t)}}{k}\right)} \tag{2.5}$$

where $\Psi_{(i,t)}$ calculate individual i's probability to vaccinate at time t. Recall that the $\frac{N_0}{Z}$ represents the fraction of vaccinated neighbours moderated by how individual i conforms to the social norm (α), and the second part $\frac{1}{1+\exp\left(\frac{p_{(i,t)} - p_{(j,t)}}{k}\right)}$ is an update rule by assigning individual i's judgment in the evolutionary game. **Figure 2.2** illustrates how those components interact in the vaccine decision update rule:

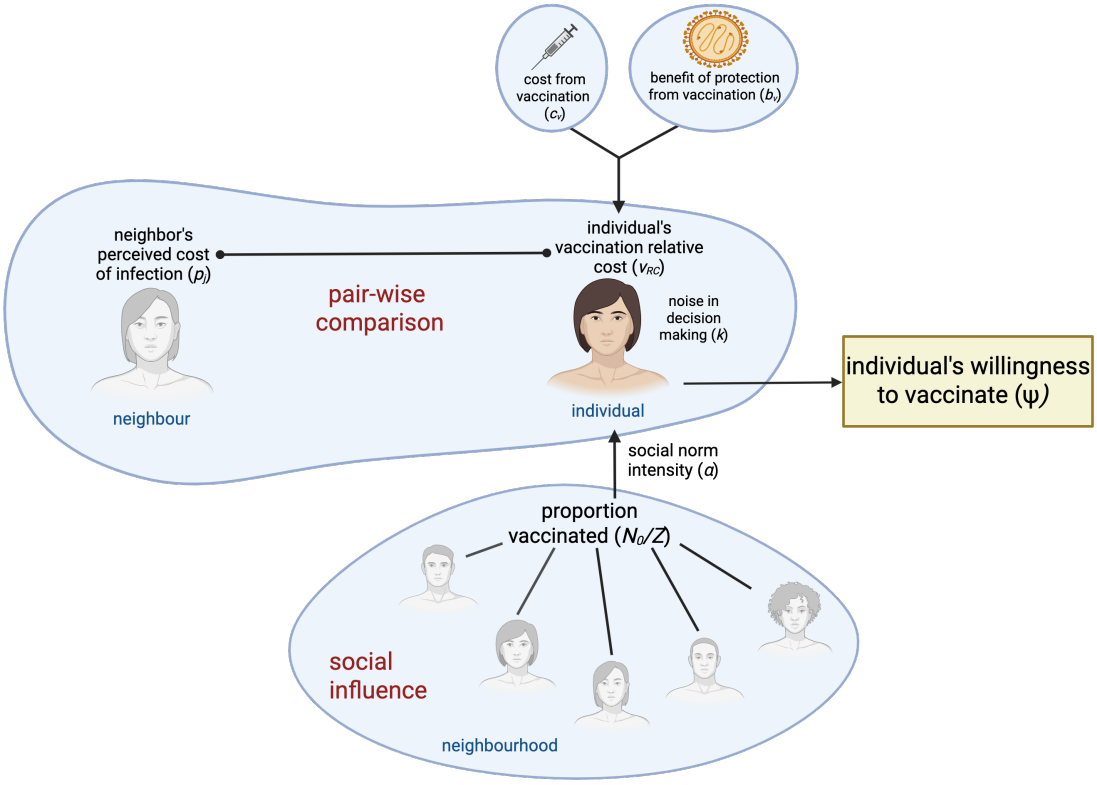


Figure 2.2. The vaccine decision update rule. Individuals construct their perceived vaccination relative cost (v_{RC}) by looking at the benefit of vaccination compared its risk. The v_{RC} is then compared with a random neighbour's posterior cost toward infection through pair-wise comparison. To complement the self-learning, individuals also look at the neighbourhood to assess how many of the neighbours have adopted vaccination.

The decision rule model is assumed to be not constrained by accessibility problems. Individuals are able to vaccinate whenever they choose, provided it aligns with the recommended vaccination schedule (e.g. measles immunisation administered to children aged 9–12 months in high-incidence areas). This assumption allows the model to focus specifically on the demand side of vaccination. The emphasis is on how vaccination perception and the proportion of vaccinated individuals in one's social environment influence collective vaccination behaviour.

The "perceived behavioural control" from TPB or in similar term of self-efficacy (Bandura, 2001) measures how confident one individual to undertake the behaviour. Individuals with limited access to vaccination can have a reduction of perceived behavioural control. Therefore, when there is no problem in vaccine access, we can assign that the TPB or self-efficacy obstacle is negligible.

The "direct behaviour change" from IVM posits that individuals can be nudged to be vaccinated based on their favourable intentions to vaccinate by reducing logistic and psychological barriers, such as making default appointments, or schedule reminders. This

approach is modelled by reducing perceived vaccination cost (c_v) based on the HBM framework implemented in this study and integrating the perceived cost into the self-perception element. Other forms of the direct behavioural change can be more stringent, shaping behaviour through incentive, disincentive or mandating vaccine uptake. I illustrate the interventions that transform the c_v through mandatory vaccination policy in Chapter 5 Strategies to Address Vaccine Hesitancy.

The vaccine decision rule model used to compute willingness in Eq.2.5 was implemented by Wu and Zhang (2013) to analyse the effect of social influence (termed as "peer-pressure" in their paper) on vaccination behaviour. In this thesis, the effect of social influence, together with perceived vaccination relative cost (v_{RC}), is further extended by considering opinion formation and the underlying bias.

2.3 The Opinion Formation Model

In the vaccine decision model, behavioural adoption depends on how individuals in a community perceive vaccination relative cost (v_{RC}). When vaccination is viewed as more costly, people are less inclined to vaccinate. In this study, "cost" encompasses perceived barriers to vaccination which are comprehensively defined in psychological dimension, rather than monetary expense alone. In the previous Decision Update Model (sub chapter 2.2), the Health Belief Model (HBM) (Rosenstock, 1974a, 1974b) is implemented to disentangle elements of individual's perception of vaccination cost into perceived barriers, severity, susceptibility and confidence. The perception can be shaped either independently for each element in the HBM framework or combined as the v_{RC} through social network interaction. Accordingly, this section will outline methods for modelling the perception dynamics among individuals.

From this point forward, the term opinion will be used instead of perception to align with terminology commonly employed in the mathematical modelling of opinion formation. Although the concept of social learning also applies when modelling the dynamics of opinion, the two approaches differ in the outcome they measure. Several social learning models focus primarily on final behavioural decisions at each time step, while opinion formation models emphasize individuals' underlying opinions about vaccination. In this sense, opinion functions similarly to attitude as defined in the Theory of Planned Behaviour (TPB) (Ajzen, 1991). Conversely, the act of vaccination itself is modelled explicitly as a behavioural outcome, with

its probability calculated as the individual's willingness to vaccinate (W). Therefore, this section will focus on opinion dynamic as represented by opinion formation models, instead of vaccination adoption behaviours.

This section begins by reviewing evidence on how individuals acquire and shape their opinions about vaccination. It then provides a general overview of opinion formation concepts related to vaccination decisions. Subsequently, distinct modelling categories are discussed, followed by elaboration of the specific method employed in this study. Prior to detailing these methods, this section first examines how individuals acquire and shape their opinions about vaccination.

2.3.1 Failure of information deficit hypothesis

It has long been a general assumption that people are hesitant toward vaccination primarily due to an information deficit (Goldenberg, 2016; Ramsay, 2001; Ratzan, 2011). Accordingly, strategies to address vaccine hesitancy have traditionally focused on providing more "correct" information about vaccination to redress misconceptions. Thus, mass communication campaigns have been tailored to close the assumed informational gaps, working under the belief that accurate knowledge would reduce hesitancy.

However, empirical evidence indicates that merely supplying vaccine-hesitant individuals with corrective information offers little benefit and may even backfire. Instead of reducing hesitancy, such interventions often leave individuals equally or even more hesitant toward vaccination (Nyhan et al., 2014). For those who already hold hesitant views, exposure to information contradicting their existing beliefs frequently fails to alter their perceptions and may even reinforce their initial hesitancy. Therefore, the information deficit hypothesis is insufficient for explaining the phenomenon of vaccine hesitancy.

An alternative to the information deficit hypothesis is cognitive bias (Goldenberg, 2021). In the context of vaccination decisions, biased assimilation (Lord et al., 1979) describes the tendency of individuals to respond primarily to opinions that align with their prior beliefs. This concept is closely related to the more widely recognized term motivated reasoning (Kunda, 1990). Specifically for vaccine hesitancy, motivated reasoning involves a directional purpose in which people tend to accept information to support their current stance. Hence, individuals who oppose vaccination are more inclined to embrace anti-vaccination arguments, while those who support vaccination are more receptive to a pro-vaccine perspective.

People who are vaccine hesitants tend to connect with others who share similar opinions and thus more susceptible to social influence from like-minded peers (Alvarez-Zuzek et al., 2022). These social selection and social influence processes result in the clustering of individuals with similar attitudes, creating distinct groups with divergent views. In this situation, the social network serves as a filter of information to be distributed within the group, and creating echo chambers which also contribute to the phenomenon of vaccine hesitancy (Müller et al., 2022).

Biased assimilation is also responsible for attitude polarization (Lord et al., 1979). When presented with identical evidence, different groups may respond differently depending on their initial attitudes. Within each group, individuals perceive evidence supporting their initial beliefs as more credible, while discounting contradictory information (Fryer et al., 2019). Consequently, repeated exposure of same evidence to opposing groups tends to widen the gap between them and reinforcing polarization over time. Furthermore, when people are exposed to opposing views, their stance often does not moderate but instead becomes even stronger, substantially increasing polarization (Bail et al., 2018).

The opinion formation model presented herein implements the biased assimilation hypothesis. Before focusing on biased assimilation in the opinion formation process, a discussion is provided on methods for modelling opinion formation. The following section outlines the types of opinion formation models and the rationale for the model type selected in this study.

2.3.2 Modelling opinion formation along with the biased assimilation

There are two distinct categories of opinion formation models: (1) The Bayesian update rule and (2) The heuristic (rule-of-thumb) rule (Acemoglu and Ozdaglar, 2011). Bayesian learning assumes that individuals have an accurate representation of the world and that the likelihood of events can be predicted reliably. However, this condition cannot always be fulfilled by every individual when facing complex problems. Therefore, the heuristic learning approach can be an alternative in decision making when the problem cannot be perfectly represented. Heuristic learning models focus on how individuals form their opinions while having access to naturally occurring information and limited cognitive capacity.

In the Bayesian framework, each individual has a formed initial opinion about some state $\varphi \in \phi$, like the perception of barriers, severity, likelihood or confidence toward vaccination, along

with the prior belief of that opinion probability to be true $P(\varphi)$. Subsequently, individuals receive signals $s \in S$ from observations about φ (e.g. how likely I will be infected with the disease? How are the risk of adverse event from vaccination? How trusted are the government which supervises the immunisation program?). Bayesian learning posits that individuals will update their probability of state φ given signals s, $P(\varphi \mid s)$, according to:

$$P(\varphi \mid s) = \frac{P(s \mid \varphi) \, . P(\varphi)}{P(s)} \tag{2.6}$$

The $P(s \mid \varphi)$ implies that individuals know what signal to expect when their opinion is φ, along with the probability that their opinion is true $P(\varphi)$ and the probability that they will receive signals $P(s)$.

While Bayesian learning assumes individuals have complete information before forming an opinion, the heuristic learning model resolves the decision making with incomplete information assumption. When the decision maker is at risk, the heuristic learning fits observations from empirical results better (Chandrasekhar et al., 2020). This aligns with Simon's theory of bounded rationality (Simon, 1997, 1990), which proposes that individuals do not always make optimal decisions but instead seek satisfactory options within the limits of their cognitive capacity, available time, and information. To reduce decision making complexity, individuals often draw on prior experiences and develop habitual responses. Therefore, the heuristic learning model is likely to be more suitable for decision making processes related to vaccination uptake.

In the heuristic model, opinion can be modelled as a binary or continuous variable. In the binary opinion model, individuals' opinion is labelled as 0 and 1, fully endorsing or rejecting a potential behaviour. An example of the binary model is voter model (Clifford and Sudbury, 1973; Holley and Liggett, 1975). For the continuous opinion model, individuals can grade their level of support or opposition towards an opinion. The most popular implementation of the continuous opinion model is DeGroot model (DeGroot, 1974). As can be seen in Eq.2.3 which represents Health Belief Model (Rosenstock, 1974a, 1974b), the continuous model is better at capturing how individuals construct their opinion. Therefore, the DeGroot model is implemented in the opinion formation model.

In the DeGroot opinion formation model, individual i re-evaluates their opinion (x_i) at each time step based on observations of all the neighbour's opinions x_j, by weighing their trust in each neighbour's opinion alongside their own opinion, w_{ij}. The signal received by each individual over time ($s_i(t)$) is defined as:

$$s_i(t) = \sum_{j \in N\,(i)} w_{ij} x_j(t) \tag{2.7}$$

In this heuristic model of opinion formation, individual i consider all the neighbours' j opinion over time and weighted by how they trust each neighbour (w_{ij}). The connection weights w_{ij} may differ based on group membership, with individuals assigning greater weight to others within the same group.

Individuals also consider the sum of connection weight to all of its neighbours (d_i) in their information assimilation process:

$$d_i = \sum_{j \in N\,(i)} w_{ij} \tag{2.8}$$

In the DeGroot model, individuals update their opinion based on two extreme-degrees of support ($x = 1$) and opposition ($1 - x = 0$). At each time step, each individual i takes on weighted average support of an opinion in the neighbourhood along with their own support.

In this section, the x opinion is applied to perceived vaccination relative cost (v_{RC}) and the individual i's opinion about relative cost of vaccination follows this equation:

$$v_{RC\,i}(t+1) = \frac{w_{ii} v_{RC\,i}(t) + s_i(t)}{w_{ii} + d_i} \tag{2.9}$$

where w_{ii} describes how individual i weighs their own opinion about v_{RC}. Recall that v_{RC} reflects how individuals perceive the cost of vaccination relative to the benefit of protection against disease. When $v_{RC} = 1$, vaccination is perceived to be equally as costly as contracting the disease.

However, the DeGroot model does not account for biased assimilation where individuals are more likely to accept an opinion which conforms with their existing belief (Lord et al., 1979).

Therefore, to account for biased assimilation, the DeGroot model is extended in accordance with the biased opinion formation (BOF) model by Dandekar et al. (2013):

$$v_{RC_i}(t+1) = \frac{w_{ii} v_{RC_i}(t) + \left(v_{RC_i}(t)\right)^{b_i} s_i(t)}{w_{ii} + \left(v_{RC_i}(t)\right)^{b_i} s_i(t) + \left(1 - v_{RC_i}(t)\right)^{b_i} \left(d_i - s_i(t)\right)} \tag{2.10}$$

The biased assimilation process is represented by $\left(v_{RC_i}(t)\right)^{b_i}$. In the BOF model, i considers neighbours' support toward an opinion by $\left(v_{RC_i}(t)\right)^{b_i} s_i(t)$ and neighbours' opposition by $\left(1 - v_{RC_i}(t)\right)^{b_i} s_i(t)$. The $b_i \geq 0$ is a parameter to represent the bias that i will assimilate the neighbour's opinion. It can be observed that when the $b_i = 0$, the opinion formation process follows the unbiased averaging process of the DeGroot model in Eq. 2.9.

Figure 2.3 illustrates the biased opinion formation (BOF) function implemented in this study. Each simulation models an interaction between individual i and a neighbour j, where each agent holds their own opinion on vaccination, expressed as a relative cost (v_{RC}) ranging from 0 to 1. A value of 0 indicates full support for vaccination (no perceived cost), while a value of 1 indicates complete opposition (perceived cost equal to having the disease). Thus, opinions span the spectrum from total support ($v_{RC} = 0$) to total opposition ($v_{RC} = 1$).

According to the DeGroot model (DeGroot, 1974), individuals update their opinions based on those around them. In **Figure 2.3**, the horizontal lines in each subplot represent the neighbour's opinion under a no-assimilation-bias scenario, corresponding to the classic DeGroot assumption. When individuals place no weight on their own prior opinion (i.e. $w_{ii} = 0$) and rely entirely on the opinions of others, their updated stance directly reflects the surrounding viewpoint.

As shown in **Figure 2.3**, the BOF model illustrates how increased assimilation bias (b_i) amplifies individuals' prior opinion toward vaccination. In panel a, where the neighbour is neutral ($v_{RC_j} = 0.5$), a bias more than one magnifies individual's existing view. If previously individuals oppose vaccination ($v_{RC_i}(t) > 0.5$), interacting with a neutral neighbour results in heightened opposition, reflected by an increased updated perceived vaccination relative cost. Conversely, if the individual initially supports vaccination, the same interaction leads to stronger support.

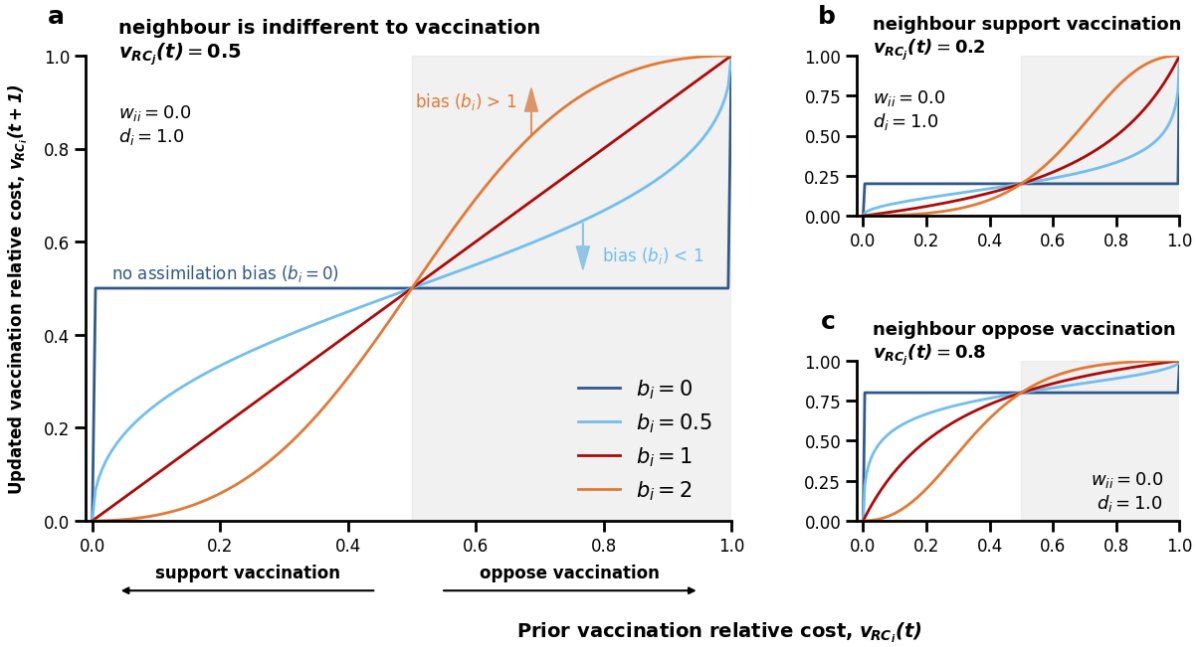


Figure 2.3. The biased opinion formation (BOF) update function. Opinion updates for individual i with assimilation bias b_i when exposed to one neighbour j's opinion. The x-axis shows the prior vaccination relative cost $v_{RC_i}(t)$ for i; the y-axis shows the updated cost $v_{RC_i}(t+1)$ after interaction. Opinions range from 0 (full support for vaccination) to 1 (complete opposition). There are three scenarios are simulated: **(a)** When neighbour is indifferent ($v_{RC_j}(t)$=0.5), **(b)** When neighbour is supportive ($v_{RC_j}(t)$=0.2), and **c**. When neighbour is opposing ($v_{RC_j}(t)$= 0.8) toward vaccination. In all panels shown, neighbour weight d_i=w_{ij}= 1 and self-weight w_{ii}= 0, isolating the effect of bias b_i to opinion formation.

Assimilation bias (b_i) can produce opinion polarization when individuals are exposed to opposing views. As can be seen in **Figure 2.3b**, when individuals who oppose vaccination ($v_{RC_i}(t) > 0.5$), interact with vaccine supporter neighbour, their opposition will be increased when their bias is more than 1. Similarly, in **Figure 2.3c**, when individuals who support vaccination ($v_{RC_i}(t) < 0.5$) interact with vaccine opponent neighbour, their support will be increased after the interaction. This opinion polarization phenomenon has also been found in a social media context (Bail et al., 2018), where individuals can interact without geographical constraints.

2.3.3 External events effect to opinion formation

As described in the previous section, the opinion formation model accounts only for how individuals navigate through their existing biases and the opinions of those within their sphere of influence. The current model focuses solely on the existing opinions circulated through interpersonal communication. However, opinion exchange can also be influenced by external events occurring within a community, such as disease outbreaks or vaccine scares, which can

alter the dynamics of opinion formation. To account for these external events, the opinion formation model is extended by introducing a term $\eta.h_i(t)$ into the model. Here, the $\eta \geq 0$ is a scaling factor that controls the magnitude of an external event's impact on individual i. The term $h_i(t)$ represents the effect of the external event on individual i at time t, and is formally defined as follows:

$$h_i(t) \begin{cases} h > 0 & if\ there\ is\ vaccine\ scare; \\ h < 0 & if\ there\ is\ a\ disease\ outbreak \end{cases} \quad (2.11)$$

The $h_i(t)$ value is assigned temporarily based on occurrence of external events in the network. It can be noted in the h direction from the $h_i(t)$ function that the opinion is denoted as 1 when the vaccine is perceived as dangerous and 0 if the opposite is believed. By adding the external event term, the opinion formation model is then extended and represented by equation:

$$v_{RC_i}(t+1) = \frac{w_{ii} v_{RC_i}(t) + \left(v_{RC_i}(t)\right)^{b_i} s_i(t)}{w_{ii} + \left(v_{RC_i}(t)\right)^{b_i} s_i(t) + \left(1 - v_{RC_i}(t)\right)^{b_i} \left(d_i - s_i(t)\right)} + \eta.h_i(t) \quad (2.12)$$

At each time step, individual i updates their opinion about perceived vaccination relative cost (v_{RC}) by incorporating the impact of external events to complement the biased assimilation process. Consider a hypothetical scenario involving a community with low vaccine coverage facing an imminent outbreak. In this scenario, the external event ($h < 0$) is activated during the outbreak, prompting individuals to shift their opinion toward vaccination. As vaccination rates rise, however, the probability of adverse events also increases. Should an adverse event occur, information about the unintended outcome could spread and trigger a vaccine scare. During dissemination of the vaccine scare, the external event element $h > 0$ becomes activated, increasing the perceived vaccination relative cost and thereby reducing individuals' intention to vaccinate.

2.3.4 Integration of the opinion formation to the vaccine decision rule

In the previous section, it can be seen that the opinion formation model can be integrated directly to perceived vaccination relative cost (v_{RC}), by assigning $x_i = v_{RC} = 1$ when individuals support the opinion that vaccination is costly (the same cost as the disease), or $x_i = v_{RC} = 0$ (when the relative cost of vaccination is zero). In this setting, the perceived benefit of

vaccination (b_v) and the cost of infection (i_c) is 1. Within the vaccine decision rule, this translation directly influences individuals' intention to vaccinate (Ψ) by shaping their v_{RC} opinion.

The opinion formation can also be implemented into specific elements constructing the v_{RC} based on Health Belief Model (HBM) (Rosenstock, 1974a, 1974b) as described in equation (2.3), in which the two extremes [0, 1] denote support or opposition toward vaccination, respectively. The perceived severity of the disease, likelihood to be infected, barrier to vaccinate and trust to vaccination programs can be treated as opinion dynamics among individuals. For example, individual can completely support an opinion that the disease is harmful (perceived with infection risk r_i) with x_i = 1 or oppose opinion that vaccination provision (reflected on confidence on vaccination v_c) can be trusted with the assigned value of v_c opinion as 0.

2.4. The Measles Transmission Model

In this study, measles is selected as the use case because it is regarded as one of the most transmissible among all vaccine-preventable diseases, along with its potential to compromise children's immunity. Each infected individual on average can spread the virus to 14-18 susceptible contacts (Anderson and May, 1982), which means that at least 95% of the population must be immunized to achieve sufficient herd immunity, although the reproduction rate may vary in different contexts (Guerra et al., 2017). Moreover, there is immune suppression phenomenon found on unvaccinated children and infected with measles (Laksono et al., 2020), that can last up to several years (Mina et al., 2015) to reduce immunity against other pathogens, including the vaccine-acquired immunity (Petrova et al., 2019). Children without vaccination protection against measles are also vulnerable for secondary infection for other pathogens following measles infection.

Nevertheless, measles is preventable through vaccination. Currently available vaccines provide robust protection against known circulation strains (Di Pietrantonj et al., 2021), with a life-long protection (Schenk et al., 2021). Furthermore, the side effects are minimal and predominantly mild (Di Pietrantonj et al., 2021)

Considering the above, this study integrates current evidence on measles virus biology and vaccine effectiveness to inform the development of the implemented measles model. This

section elaborates on these evidence in greater detail, focusing on how they inform the modelling approach. This provides a robust framework for assessing measles outbreak in relation to the dynamics of vaccination behaviour.

2.4.1 Evidence on measles transmission

Measles virus is transmitted through airborne particles or direct contact with infectious droplets through contaminated surfaces (fomite). The infection commonly manifests with fever, followed by erythematous maculopapular or morbilliform (measles-like) rash. The two symptoms: fever and rash are considered as cornerstone of measles detection in the community (World Health Organization, 2018). The typical measles rash generally begins from the head or neck and gradually spreads to the trunk and extremities. The two typical manifestations of measles are also accompanied by at least one of the "3 C" symptoms: cough, coryza or conjunctivitis.

In unvaccinated individuals, measles has an incubation period of 10 – 14 days, following a log-normal probability distribution (Hübschen et al., 2022). The incubation ends upon rash onset, just after the infected individuals entered the prodromal phase, characterized by fever and the 3 C symptoms. The infectious period begins during the prodromal phase, starting four days before rash onset and continuing for four days afterward (Strebel et al., 2018). Clinical diagnosis is often supported by the presence of Koplik spots – white spots with irregular red lesions on the oral buccal mucosa, which appear 1 – 2 days before the rash emerges. In uncomplicated cases, symptoms typically resolve within seven days after rash onset, although they may persist until up to 21 days (Hübschen et al., 2022).

Although most unvaccinated individuals or those without prior measles exposure develop symptoms when infected (Rota et al., 2016), asymptomatic case can still occur, where infected individuals do not exhibit any symptoms (Lievano et al., 2004; Sonoda and Nakayama, 2001). The inapparent measles cases can happen in younger infants who are still protected by maternal immunity. Although there is a possibility of asymptomatic measles, transmission from this case has not been proven (Lievano et al., 2004). Furthermore, since the measles symptoms are the manifestation of immune reaction to the virus infection, the immunocompromised individuals often present with milder symptoms or remain asymptomatic, making the diagnosis for this group particularly challenging.

Even though individuals who recover from measles typically develop lifelong immunity against reinfection (Griffin et al., 2018), the case fatality ratio (CFR) remains high, particularly among children in resource-constrained areas. In low- and middle-income countries (LMICs), measles accounts for approximately 13 deaths per 1,000 cases (Sbarra et al., 2023). The CFR is even higher among younger children, with an estimated 30 deaths per 1,000 cases in infants (under one year old). In comparison, the CFR is significantly lower in more developed countries, such as the United States, where measles leads to approximately 1 – 3 deaths per 1,000 cases (Centers for Disease Control and Prevention, 2025). However, it should be noted that the CFR estimates in both LMICs, and high-income countries (HIC) settings exclude long-term measles-related mortality. This includes death from subacute sclerosing panencephalitis, which can occur more than one year after the measles infection (Hübschen et al., 2022), as well as deaths from non-measles infectious diseases related with immune amnesia induced by measles (Mina et al., 2015).

The widely available measles vaccine has high effectiveness in preventing transmission and symptomatic disease. There is a reduction of 0.81 transmission probability for individuals who have been vaccinated with one dose vaccine, and 0.85 if followed by the second dose. The vaccine also has 95% effectiveness in preventing symptomatic cases after one dose, and the effectiveness is increased to 96% after two doses (Di Pietrantonj et al., 2021). Vaccine induced antibody titres have a similar profile to those raised following natural infection with protective levels being reached approximately 6 – 10 days after vaccination, with log-normal probability distribution of the immune response (Strebel et al., 2018). Vaccine is usually and legitimately assumed to provide life-long protection, since the immunity waning rate following vaccination is a mere 0.009 per year (Schenk et al., 2021).

Modified measles, an infection in previously vaccinated individual is uncommon. In these infections, both symptom severity and transmission probability are negligible due to vaccine-induced immunity. While the incubation period for modified measles is slightly longer than that of primary infection, the difference is not statistically significant (Kobayashi and Nishiura, 2022). Clinical symptoms may still appear in modified measles cases, but they tend to resolve quickly (Rota et al., 2016), with the duration typically being half that of a primary measles infection (de Oliveira et al., 2000).

The evidence presented in this section further informs the measles transmission model developed for this study. The following section outlines the methods used in constructing the

disease model, followed by descriptions of parameter values derived from biological evidence and assigned to the measles model. This approach ensures that the model is grounded in the current biological understanding of the disease.

2.4.2 The measles model description

An SVEIR individual-based model incorporating two-dose vaccination regimen was developed to simulate measles disease transmission dynamics. Each individual's health state is classified into one of the following categories: susceptible (S), vaccinated (V), exposed (E), infected (I) and recovered (R). Here the I state is not defined by the onset of a rash, but rather by the period when an individual becomes infectious, which begins four days before the rash onset.

To better capture real-world vaccination dynamics, the model extends these SVEIR states to account for various immunisation scenarios. For instance, individuals in states V_{10} or V_{21} have been vaccinated but have not yet developed immunity from the vaccine, whereas those in V_{11} or V_{22} have fully acquired vaccine-induced protection. During the incubation period, when no visible symptoms are present, individuals may still choose to vaccinate. The state transitions of vaccination during the incubation periods are expressed as $E \rightarrow EV_1$ or $Em_1 \rightarrow EV_2$. The former transition is to exhibit vaccination decision during incubation period for individuals without prior vaccination, while the latter is to exhibit second-dose vaccination decision while in incubation period of modified measles. Noted here that the modified measles is defined as an infection after being vaccinated.

Individual's states are transitioned to recovery based on their history of vaccination, either R, V_1R or V_2R. Furthermore, since prior infection history is not one of the exclusion criteria for measles vaccination, recovered individuals can still receive the vaccine and transition into states. The V_1R compartment then represents recovered individuals who receive one vaccination dose and V_2R is when they receive two vaccine doses.

In the measles model, it is also assumed that some infections might result in an asymptomatic measles (represented by A, AV_1, AIm_1, AV_2, or AIm_2) with probability given by As for naïve infection. When individuals have been protected with vaccine but still become infected with measles, the probability of having asymptomatic case is determined by VED_1or VED_2, depending on their immunisation history.

Figure 2.4 illustrates the state transition flows within the proposed measles transmission model:

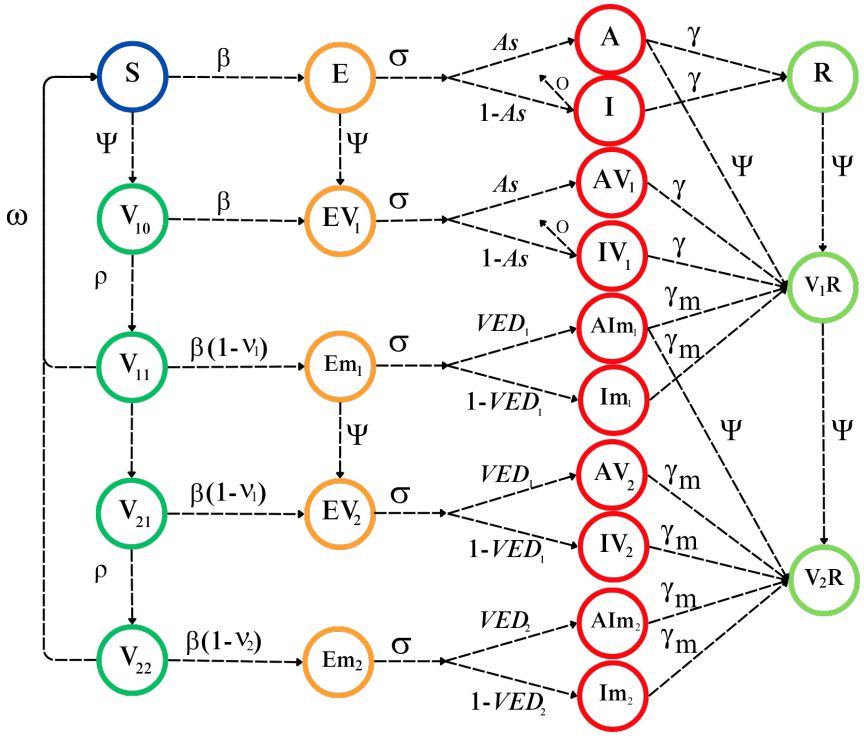


Figure 2.4. Proposed measles transmission model. At each time step, individual can only be in one state as depicted in the figure. The diseases transmission is based on individual-based model, which is iterated through stochastic states transitions in discrete time-step. The susceptible state is denoted with blue circle, while the vaccinated states are denoted with green circle. The disease transmission is started with exposed states which is pictured with orange circle, followed with infected states with red circle. Probabilities are assigned for each states transition, like infection probability (β), probable durations before transitioning to next states (σ, γ, γ_m or ρ), conditional probabilities (As or VED), or event probabilities (W or o).

Along with the various vaccination and asymptomatic scenarios, the model also incorporates modified measles, which occurs when previously vaccinated individuals experience breakthrough infections. These cases are denoted by states containing the m symbol.

Measles transmission occurs with probability $p\,.\,c$, determined by the infection probability from infectious contacts (p) and all their potentially infectious contacts per unit time (c). In the model, only symptomatic individuals contribute to disease transmission and individuals who are asymptomatic throughout all their clinical course are assumed to not be able to transmit the disease. The transmission rate (β) is defined by the following equation:

$$\beta = p\,(I + IV_1 + Im_1 + IV_2 + Im_2) \tag{2.13}$$

Transition between states occurs in discrete time steps, with time measured in days. Individuals vaccinate with probability Ψ, determined by the vaccination decision rule in Eq.2.5. The incubation (σ), seroconversion from vaccination (ρ), recovery from primary infection (γ), and recovery from modified measles (γ_m) periods are simulated based on their probability distributions from which random draws are taken to assign durations of each process to all individuals. The probability distributions for σ, ρ, γ, and γ_m is illustrated in **Figure 2.5**:

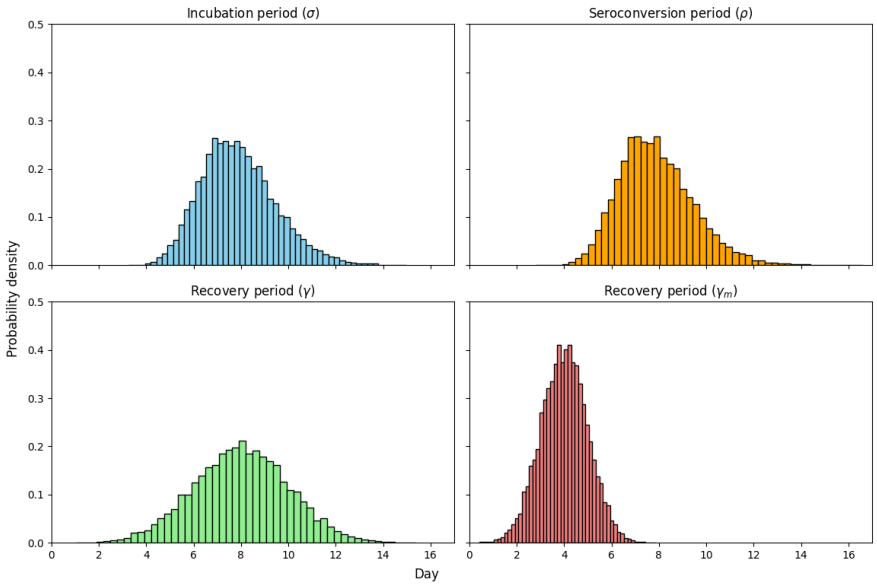


Figure 2.5. Probability distribution of the state transition periods. The incubation and seroconversion periods have similar distribution of length duration with log-normal probability distribution. The recovery period for modified measles is half of recovery period following naïve infection in unvaccinated individuals, with both events have normal distribution probability.

Other state transition parameters are assigned as probabilities, including the likelihood of asymptomatic case (As), vaccine effectiveness (VED_1, VED_2, ν_1, ν_2), the case fatality ratio (o) and waning immunity from vaccination (ω). For each exposed individual who has not been protected by vaccination (E or EV_1), a randomization process determines whether they will develop symptomatic or asymptomatic measles based on the probability As. For vaccinated individuals, their likelihood of developing symptoms is determined by VED_1 or VED_2, while ν_1 and ν_2 reduce their probability of infection upon exposure to an infectious contact. Only individuals without vaccine protection who develop symptomatic measles have an associated probability of death (o). Furthermore, waning immunity from vaccination (ω) is modelled as a probability function over time (t), meaning that the longer the time since vaccination, the greater the probability of losing immunity. **Table 1** presents the parameter values implemented in the measles transmission model:

Table 1. Descriptions parameters in the measles transmission model.

Parameters	Description	Value	References
σ	Incubation period rate	6 – 10 days	Hübschen et al. (2022); Strebel et al. (2018)
Ψ	Vaccination probability	measured	-
p	Infection probability from infectious contacts	fitted	-
ρ	Seroconversion rate after vaccination	6 – 10 days	Strebel et al. (2018)
As	Asymptomatic probability	0.05	Lievano et al. (2004)
VED_1	Vaccine dose 1 efficacy to prevent disease	0.95	Di Pietrantonj et al. (2021)
VED_2	Vaccine dose 2 efficacy to prevent disease	0.96	Di Pietrantonj et al. (2021)
ν_1	Vaccine dose 1 efficacy to prevent infection	0.81	Di Pietrantonj et al. (2021)
ν_2	Vaccine dose 2 efficacy to prevent infection	0.85	Di Pietrantonj et al. (2021)
ω	Waning immunity rate from vaccination	0.009 * (1/365)	Schenk et al. (2021)
o	Death probability of primary infection in lower-middle income countries	0.013	Sbarra et al. (2023)
	Death probability of primary infection in upper income countries	0.001	Centers for Disease Control and Prevention (2025)
γ	Recovery rate of naïve infection	Mean = 8 days (SD = 2)	Hübschen et al. (2022)
γ_m	Recovery rate of modified measles	Mean = 4 days (SD = 1)	de Oliveira et al. (2000)

Using the parameters described in **Table 1**, a measles outbreak is simulated in a synthetic network representing a susceptible population of 10,000 individuals with no prior vaccination record. The network connection is modelled with log-normal degree distribution. The mean degree follows the degree distribution statistics of the empirical network of 75 villages in India (Banerjee et al., 2013).

To reflect the measles reproduction number (R_0) range of 14 to 18, the probability of contact with an infectious number is fitted to $p = 0.1$. The case fatality ratio (o) is set to 0.013, consistent with estimates for LMIC. The outbreak is initiated with a single infectious individual as the index case at $t = 0$. Figure **2.6** illustrates the simulated measles outbreak dynamics.

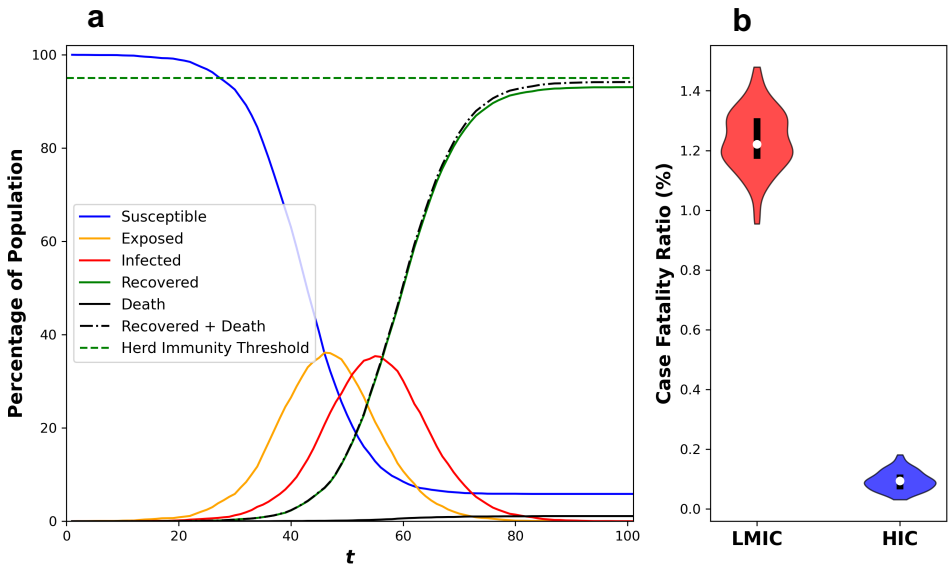


Figure 2.6. Hypothetical measles outbreak simulation. At the start of simulation, one node is infected into the susceptible population. The contact probability (p) is assigned as 0.1 and consistent through all-time steps. Panel **(a)** shows the measles model transmission dynamic through 100 time-steps in days. The simulation is conducted following Lower Middle-Income Countries (LMIC) setting where the case fatality ratio (o) is 13 out of 1000 cases. Panel **(b)** shows the violin plot of case fatality ratio (CFR) comparison between LMIC (red) and High-Income Countries (HIC) (blue) through 100 simulation runs. The white dots represent the median and the black dots represent range of the first and third quartiles data points of the CFR.

Due to its high transmissibility, a measles outbreak can spread rapidly, reaching the entire population and approaching the herd immunity threshold in less than 100 days. However, the burden of infection is not evenly distributed between children in LMICs and HICs. In the simulation, measles-related mortality disproportionately affects children in LMICs.

In LMICs, the median fraction of individuals who die after the outbreak subsides is nearly 10%, with a high degree of variability in the mortality outcomes. This implies that a measles outbreak can result in the death of approximately one in every ten children in LMICs. In contrast, the mortality in HICs is minimal by comparison, reflecting the substantial disparity in the measles-related mortality. In addition, it is important to note that the simulated mortality estimates do not account for long-term measles-related deaths, such as those caused by subacute sclerosing panencephalitis or secondary infections due to immune amnesia.

2.5. The Social Network Model

In section 2.2, I demonstrate that decisions around vaccination does not occur in isolation. Individuals instead update their decision based on local comparison, either by assessing posterior cost difference with their neighbours or through social coordination reinforced by their surrounding network. Consequently, the individual vaccination decision model is especially sensitive to the heterogeneity of the social network, as the structure of an individual's connections influence decision-making dynamics. Therefore, this section elaborates on approaches to modelling social networks, where the transmission of both disease and behaviour occurs simultaneously.

In this study, multiple levels of social networks are defined based on the ecological model proposed by Krug et al. (2002). The social network is represented as a graph, where each node (or vertex) represents a decision-maker agent which can be either represented by a single individual or household, and the agent can also be infected with a vaccine preventable disease.

Figure 2.7 illustrates the hierarchy of the ecological levels definition of the social network implemented in this study.

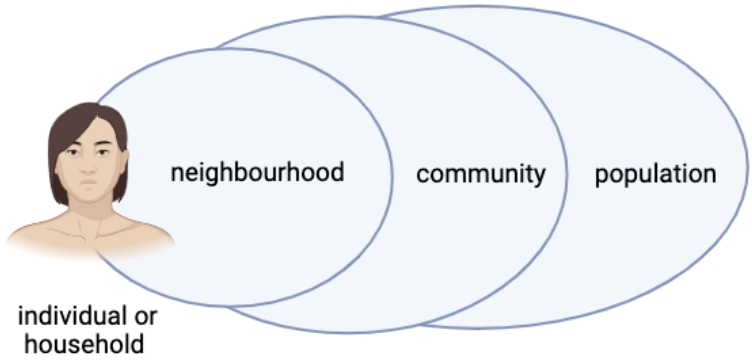


Figure 2.7. The ecological model of the social network implemented in this study. The microlevel of vaccination decision is conducted by each individual or household by assessing proportion of vaccinators in the neighbourhood. Neighbourhood is the direct contact an agent has. Sets of neighbourhoods construct a community, which is distinct with other community, and at the higher level, groups of communities are constructed into a population.

The **neighbourhood** is defined as the set of direct connections surrounding a node. Beyond the neighbourhood lies the **community,** characterized by tightly connected nodes within the group, and relatively more sparse connection between groups (Newman, 2006). At the largest scale, the entire set of nodes forms the **population**. Both the terms "community" and "population"

can correspond to real-world contexts, such as when discussing under-vaccinated or vaccine-hesitant communities within a general population in a specific administrative region.

2.5.1 Network clustering and the vulnerability against outbreak

Empirical evidence demonstrates that vaccine-hesitant individuals tend to cluster within specific network subgroups (Brownwright et al., 2017; Klinkenberg et al., 2022; Omer et al., 2008; Pingali et al., 2019). This clustering is driven by two interrelated social processes: social selection and social influence (Alvarez-Zuzek et al., 2022). Therefore, hesitant individuals are more likely to form connections with others who share similar views and reinforcing their hesitancy through mutual influence. Together, these social processes lead to the formation of under-vaccinated pockets, despite a high vaccination coverage in the general population (Jenness et al., 2021; Khan et al., 2018; Klinkenberg et al., 2022)

When a disease in introduced into a high-knit community with low vaccination coverage, it can spread rapidly and result in large outbreak. In the United States over the past two decades, highly interconnected under-vaccinated communities have been the primary sites of large measles outbreaks. The majority (88%) of outbreaks involving more than fifty cases have occurred within that setting (Centers for Disease Control and Prevention, 2024). When a region has entered post-elimination phase due to herd immunity coverage of vaccination in the general population, the reoccurrence of vaccine-preventable diseases is more likely to be driven by pockets of under-vaccinated communities compared to case importation (Dimala et al., 2021; Leong and Wilder-Smith, 2019; Phadke et al., 2016). Thus, a high vaccine coverage in general population cannot be directly translated as a comprehensive protection across all communities (Anis et al., 2021; Masters et al., 2020). This phenomenon highlights the limitation of assuming a homogenous population structure to model disease and behaviour transmissions for vaccine-preventable diseases. Community clustering significantly alters outbreak dynamics, underscoring the need for a network-based approach to accurately assess the risk associated with vaccine hesitancy.

2.5.2 Network structure

A key structural property of a network is its degree distribution, which describes the number of mean connections (or edges) each node has. Early research on social network structures, particularly in large-scale systems like the World-Wide Web, suggested that the degree

distribution often follows a scale-free power-law (Albert et al., 1999; Barabási and Albert, 1999), where a small number of highly connected nodes (hubs) are linked with a majority of sparsely connected nodes. This structure emerges due to preferential attachment, a process in which new nodes are more likely to connect to already well-connected nodes, leading to a network with a heavy-tailed degree distribution. The scale-free degree probability $P(d)$ is expressed by:

$$P(d) \sim d^{-\delta} \tag{2.14}$$

where $P(d)$ represents the probability that a node has d connections, and δ is the exponent that determines the shape of the power-law distribution. This preferential attachment mechanism results in a small number of highly connected "hubs" and a large number of sparsely connected nodes.

Although the long-tailed distribution of scale free often appears to match degree distribution of real-world social network, Broido and Clauset (2019) found that a log-normal distribution provides a better fit for many observed social networks. If node connectivity follows a log-normal distribution, the probability distribution is given by equation:

$$P(d) = \frac{1}{d\tau\sqrt{2\pi}} \exp\left(-\frac{(log\, d - \mu)^2}{2\tau^2}\right) \tag{2.15}$$

where μ and τ represent the mean and standard deviation of the logarithm of the degree, and $\sqrt{2\pi}$ is the normalization factor to ensure that the total probability integrates to 1. **Figure 2.8** shows the differences of scale-free and log-normal degree distribution among several empirical social networks.

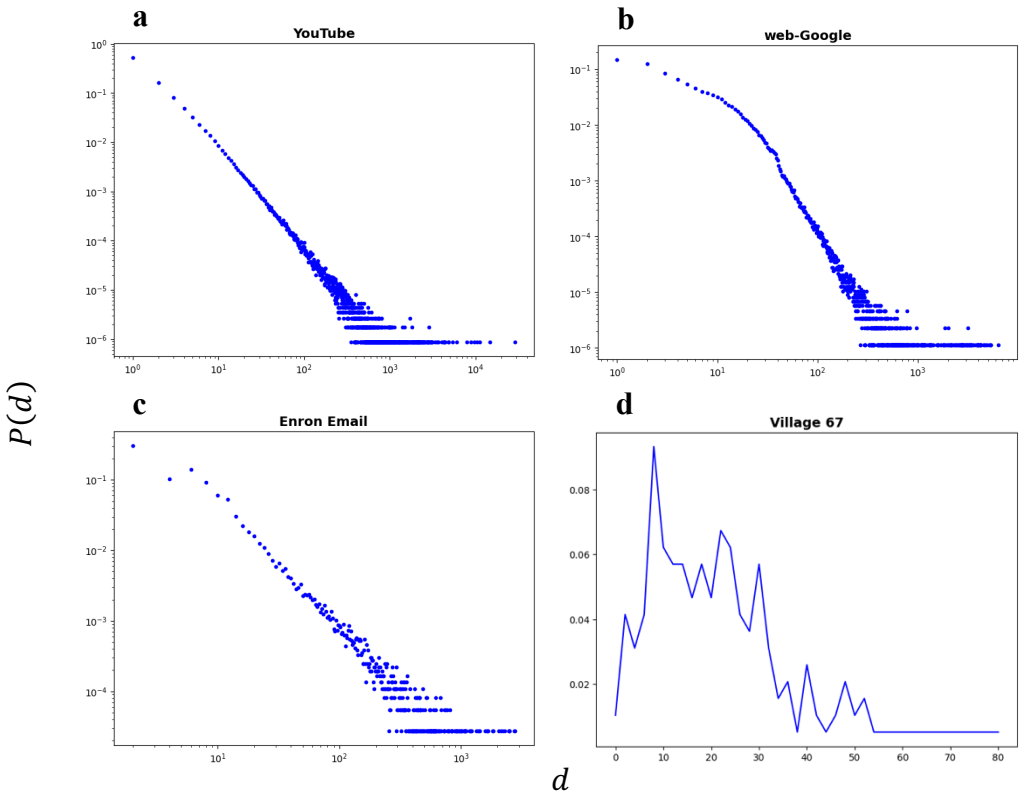


Figure 2.8. Degree (*d*) distribution of empirical social networks. Plot (a-c) illustrate scale-free degree distributions, while plot (d) shows a log-normal degree distribution, as the comparison shows finite size effect, in which smaller network appears to deviate from scale-free. **(a)** YouTube account network, where connections are determined by following relationships between accounts. **(b)** Webpage connections indexed by Google, representing hyperlink structures. **(c)** Email communication network among Enron employees. **(d)** Household connections within a village in India (Banerjee et al., 2013). Plots (a-c) are generated from the Standford Large Network Dataset Collection (Leskovec and Krevl, 2014). All the nodes connection in the networks are undirected.

To contribute to the discussion whether social network degree distribution follows scale-free or log-normal pattern, Serafino et al. (2021) further demonstrated that finite-size effect can obscure the power-law (scale-free) degree distribution. The finite-size effect refers to deviations in structural properties of a network that arise when the network has a limited (finite) number of nodes. In smaller networks, this effect cause deviations from a scale-free structure, making the degree distribution appears log-normal. Their findings suggest that while social networks may fundamentally follow a scale-free pattern, empirical observations in smaller samples or limited network realizations often make the social network indistinguishable from alternative distributions, such as log-normal.

In the context of synthetic network construction, a practical question is raised: How should one choose between scale-free and log-normal degree distribution? Consistent with Serafino et al.

(2021), larger networks may exhibit a scale-free structure, while smaller networks may appear log-normal due to finite-size effects. The next logical step is determining how small a network must be, to be treated as a log-normal rather than scale-free. One can appeal to Dunbar's theory, which posits a cognitive limit on the number of stable social relationships an individual can maintain. Based on the size of the neocortex of *Homo sapiens*, the predicted size of groups for humans are around 150 individuals (Dunbar, 1993; Hill and Dunbar, 2003), and the online interaction also resembles the offline social network (Dunbar et al., 2015). If the group size exceeds the number, information overload occurs, making the group unstable and prone to fragmentation. In such cases, information circulates mainly within smaller, tightly knit clusters, rather than across the entire network. Consequently, larger populations are often formed by joining together multiple smaller communities, each with its own intense internal interaction (Dunbar, 1992). Based on these points of evidence of network size threshold and following the ecological model as depicted on **Figure 2.7.**, it can be assumed that most behavioural process happens in communities.

Based on the former evidence on finite-size effect and the latter on network size threshold, the rule-of-thumb for constructing a synthetic network can be attained. When the network size is around or below the network size threshold, the finite-size effect becomes more pronounced, making the log-normal degree distribution a reasonable choice for modelling the social network with equal or less size of 150 nodes. For larger size networks, a scale-free assumption is more appropriate.

In this study, both empirical and synthetic networks are implemented to simulate the co-transmission of disease and behaviour. For the empirical network, the household network from 75 villages in India (Banerjee et al., 2013) is utilized, capturing real-world social structures that shape decision-making regarding vaccination and disease spread. The villages in the dataset are mutually exclusive to each other, and connections between villages are simulated as fractions of households in a village who interacting with other villages. This connection proportion is conceptually similar to what is sometimes referred to in social network analysis as "bridge width", a term used to describe the extent or intensity of intergroup connections. For the synthetic network, a log-normal degree distribution is constructed when the collective decision making, and disease transmission is simulated in a community of 150 or less decision makers. The decision makers can be individuals or households. Conversely, a scale-free network is generated to simulate the dual transmission dynamics in larger populations.

2.6. Conclusions

This chapter has presented an exploration of the theoretical and methodological foundations used to model vaccine hesitancy in this study. Grounded in health behaviour theories, opinion formation, epidemiological dynamics and network science, this chapter combines these perspectives to construct an integrated modelling framework that captures both individual and collective vaccination behaviour.

The vaccination decision model developed in this study implements two key drivers: self-perception of vaccination and social influence, derived from the Theory of Planned Behaviour and the Increasing Vaccination Model. These elements inform an individual's willingness to vaccinate, which is quantified probabilistically. Decision-making of individuals within a social network unfolds through an evolutionary-game theoretic framework using a Fermi-Dirac function to model individuals' judgement of vaccine utility, along with a social influence model that assess the fraction of neighbours who have adopted vaccination. To capture the cognitive mechanisms underlying opinion formation toward vaccination, the model incorporates biased assimilation model, reflecting how individuals are prone to adopting opinions that align with their existing beliefs. These behavioural dynamics are coupled with an individual-based transmission model that is fitted with parameters of measles biological evidence. Finally, synthetic social networks are deployed to simulate co-evolving behaviour and disease spread through a community and a population.

In summary, this chapter lays the groundwork for understanding vaccine hesitancy in an integrative manner, embedding significant elements for vaccination decision-making based on current understanding of the hesitancy phenomenon. In the following chapter (Chapter 3), the complex dynamics of individual and collective vaccination decision are presented based on simulations of the integrated models elaborated in this chapter, along with the epidemiological consequences following the behaviour. Subsequently, Chapter 4 describes the model implementation to estimate unobserved variable of perceived vaccination relative cost from reported data of vaccination uptake and measles incidence, and Chapter 5 explores targeted interventions to address vaccine hesitancy.

Chapter 3 Vaccination decision dynamics

3.1 Introduction

This chapter presents simulation results of vaccination decision dynamics using methods described in Chapter 2 (Modelling Vaccine Hesitancy). The simulations are not intended as an empirical validation of the models, but rather as an examination of the internal behaviour of the models and assess whether its outputs are qualitatively consistent with established theory and observations of vaccination behaviour. As a reminder, this study applies an integrative modelling approach, combining four distinct models: vaccination decision update, opinion formation, measles transmission and social network models. The simulation results presented in this chapter are based on theoretical frameworks and parameterized using empirical values outlined in Chapter 2, aimed to show that the integrated model produces plausible behaviour across a range of scenario.

Beyond establishing simulation plausibility, the primary aim of this chapter is to explore the complex dynamics of vaccination behaviour. Through simulations, this chapter addresses one of the key objectives of this study: understanding the mechanisms driving vaccine hesitancy. In exploring the complex dynamics of vaccination behaviour and the resulting vaccine hesitancy phenomenon, this chapter will guide us through answering several social and behavioural questions:

1. **Why do under-vaccinated communities remain hesitant to vaccinate even during disease outbreaks?**

   There is a phenomenon whereby under-vaccinated communities remain hesitant to vaccinate even during disease outbreaks (Christianson et al., 2020; Zucker et al., 2020; Parker et al., 2006). This study investigates, through model simulations, the reasons underlying the suppressed willingness to vaccinate and low vaccination uptake observed in these communities during outbreak.
2. **How effective is reactive vaccination in controlling outbreaks in under-vaccinated communities?**

Often described as the "canary in the coal mine," measles is frequently the first vaccine-preventable disease to re-emerge due to low vaccination coverage (Kiang et al., 2025). One common public health response is reactive vaccination following an outbreak in under-vaccinated communities. This chapter explores the effectiveness of reactive vaccination strategies in controlling outbreaks and the extent to which vaccine hesitancy undermines their impact.

3. **What role do cognitive biases play in shaping vaccine hesitancy and its consequences?**
   Considering evidence that information deficit alone does not fully explain vaccine hesitancy (Nyhan et al., 2014) and acknowledging the role of cognitive biases in assimilating conflicting vaccination information (Goldenberg, 2021), this chapter also examines the role of assimilation bias (Lord et al., 1979) in shaping opinion dynamics, and their impact on vaccination uptake and measles transmission.

This chapter focuses on an under-vaccinated community composed of interconnected households. As vaccination against vaccine-preventable diseases (VPDs) becomes more accessible, many regions have entered a post-elimination phase due to high coverage in the general population. However, under-vaccinated communities continue to emerge even in areas with overall high vaccination rates (Jenness et al., 2021; Khan et al., 2018; Klinkenberg et al., 2022). In such settings, the re-emergence of VPDs is more likely to be driven by clusters of under-vaccinated individuals than by case importation (Dimala et al., 2021; Leong and Wilder-Smith, 2019; Phadke et al., 2016).

Given the epidemiological significance of under-vaccinated communities, this chapter focuses on analysing vaccination dynamics within these settings, with the use case of measles outbreak. To reflect the community-level context, the analysis centres on household vaccination decisions. Here, the individual refers to parents within a household deciding whether to vaccinate their children. Throughout this chapter, the term “individual” is also used to represent a household.

This chapter’s analysis begins with a focus of vaccination dynamic in an under-vaccinated community without interaction with households outside of the community. For the analysis, it is assumed that the perception about vaccination is fixed and homogenous across households. To do the analysis, the decision update, measles transmission and social network models as outlined in Chapter 2 are implemented. With the dynamic is isolated within the community, it

is simulated that given the perception of vaccination, what would be the vaccination uptake and the measles transmission dynamic under one vaccination season which is simulated as one year.

Subsequently, the vaccination dynamic analysis is extended by simulating interaction with other community. To conduct this analysis, the perception of vaccination is assumed to be dynamic based on opinion exchange around households which is introduced through interaction with different communities. To simulate the opinion dynamics due to the exchange, opinion formation model is implemented along with the three previously implemented models.

Based on the Health Belief Model (HBM) (Rosenstock, 1974a, 1974b), there are several constructs of vaccination perception, like the perceived adverse event probability, the severity and likelihood of disease prevented by vaccine, and how confident a community toward vaccination program. To avoid unnecessary complexity, here the perception about vaccination is assigned as relative vaccination cost (v_{RC}), the composite of all judgment related with vaccination which assigns how costly a vaccine is perceived compared to the cost of disease burden.

This chapter is structured into four main sections: methods, results-discussion, conclusions and limitations. First, the modelling methods for both fixed and dynamic vaccination perceptions are presented (3.2 Methods). The results and discussions (Section 3.3) elaborate analysis of individual willingness, collective vaccination behaviour, and measles transmission dynamics to examine whether the model behaves plausibly across various scenarios and to answer social and behavioural questions related with vaccine hesitancy. The chapter concludes with a summary of conclusions (Section 3.4) which synthesizes findings in this chapter and also limitations of this study (Section 3.5).

3.2 Methods

This section outlines the modelling approach used to analyse the dynamics of individual perception of vaccination relative cost (v_{RC}), willingness to vaccinate (Ψ), collective vaccination behaviour (measured as final vaccination coverage, V_f), and the epidemiological dynamics. The methods build on the foundations established in Chapter 2 and are applied here to examine those models while addressing key social and behavioural questions about vaccine

hesitancy. The structure sequence of this sub chapter parallels that of Sub Chapter 3.3 Results and Discussion.

3.2.1 Vaccination willingness, behaviour and epidemiological outcomes

Willingness to vaccinate (Ψ) is modelled as probability that a household intends to vaccinate its children, based on Eq.2.5 in Chapter 2. In simulating the Ψ, there are four psychological parameters analysed: perceived vaccination relative cost (v_{RC}), neighbourhood vaccine coverage (θ), social norm degree (α), and decision noise (k).

$$\Psi_{(i,t)} = \left(\frac{N_0}{Z}\right)^{\alpha} \frac{1}{1 + \exp\left(\frac{p_{(i,t)} - p_{(j,t)}}{k}\right)} \tag{2.5}$$

In this study, vaccination adoption is modelled as a gradual shift in behaviour under social influence (Section 2.2.2 Social influence), in which households need to evaluate whether their neighbours have been vaccinated as well before decide to vaccinate their children. We will compare scenarios of with and without social influence on vaccination willingness under simulations of with and without outbreak.

A social network of 150 households is simulated to represent an under-vaccinated community, reflecting Dunbar's number as an optimal group size for maintaining stable social relationships (Dunbar, 1993; Hill and Dunbar, 2003). Each node in the network represents a household consisting of parents and children. The parents will decide to vaccinate their children against measles, and the children will be infected with measles based on the vaccination decision of the parents. To make the decision, parents are influenced by vaccination decision of their neighbours, and measles transmission occurs through inter-household contact to simulate community-level outbreak. **Figure 3.1a** illustrates the social network structure, where both vaccination decisions and infections events take place within and between households.

Children in the community are assumed to interact primarily through household-based connections, reflecting preschool-age contact patterns. Adults are considered immune due to prior measles infection or vaccination, while children are fully susceptible, as no outbreaks have previously occurred within their vaccination-eligible cohorts. Outbreaks are initiated with a single index case, and transmission proceeds according to the established household

interaction structure. Post-exposure prophylaxis is not incorporated, as vaccination is assumed to occur only when households actively decide to vaccinate their children. This design keeps the analysis focused on household vaccination decision-making as the primary driver of epidemiological outcomes.

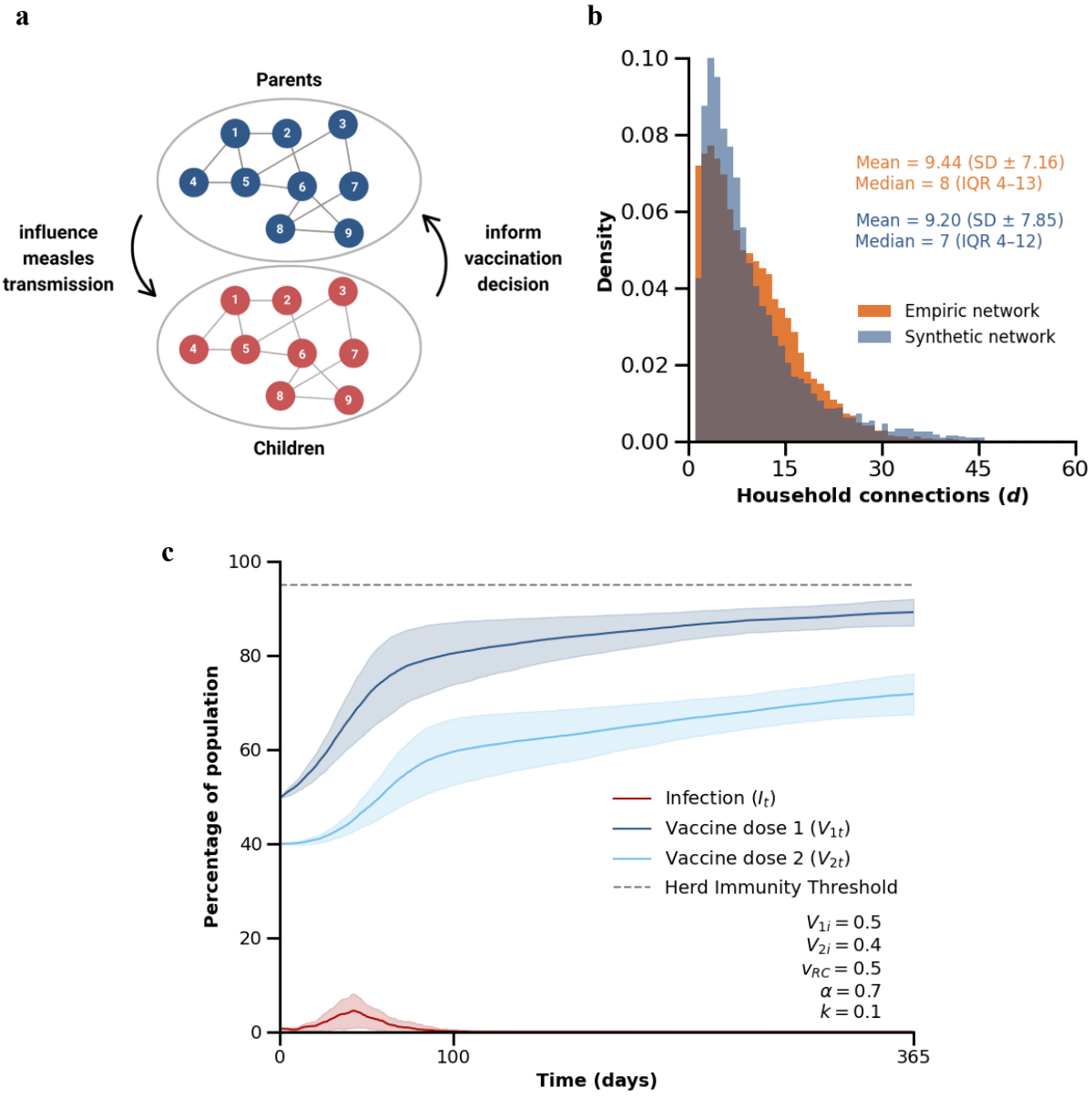


Figure 3.1. Simulation setup of vaccination and measles dynamics in an under-vaccinated community. **(a)** Social network representation, where each node denotes a household. Parents make vaccination decisions within each household, and children can become infected with measles depending on those decisions. Measles transmission among children subsequently influences parental vaccination decisions. **(b)** Degree distributions of the synthetic network used in the simulations compared with the empirical network from 75 villages in India (Banerjee et al., 2013). The synthetic network closely reproduces the mean and median of the empiric network. **(c)** Vaccination and infection dynamics over time, based on 100 simulation runs using global parameter values shown in the graph.

Inter-household interactions are constructed based on an empirically derived connection (d) distribution from 75 villages in India (Banerjee et al., 2013), with a mean of 9.44 (SD ± 7.16) and a median of 8 (IQR 4-13). As discussed in Chapter 2, social network structures are often well approximated by a log-normal distribution (Broido and Clauset, 2019), particularly in smaller networks (Serafino et al., 2021). The household connections in the Indian villages were fitted to a log-normal distribution using Scipy framework (Virtanen et al., 2020), yielding a shape parameter $\sigma = 0.8823$ and scale parameter $\mu_{1/2} = 6.8084$. Synthetic household networks were then generated based on these fitted statistics. The number of neighbours (d) is capped at 45, approximating the upper end of the mid-level social layer in the discrete hierarchy of human social group sizes reported by Zhou et al. (2005). A comparison between the empirical and synthetic network degree distribution is shown in **Figure 3.1b**.

Disease transmission and vaccination behaviour are simulated on a daily basis over the course of one year. Due to the high transmissibility of measles, the outbreak window in a single community is relatively short. As shown in **Figure 3.1c**, a measles outbreak in one community typically lasts around 100 days. While this short duration might be attributed to self-isolation, it is important to note that measles is often transmitted during the pre-symptomatic phase, which can begin up to four days before the onset of rash (Strebel et al., 2018). This one-year timeframe aligns with the routine immunisation schedule, which provides a one-year window for each vaccine dose. According to WHO recommendations, the first dose is administered at 12-15 months of age, or as early as 9 months in high-incidence settings, and the second dose is typically given at 15-18 months of age. Therefore, the one-year simulation period is chosen under that assumption that disease-vaccination dynamics reach a steady state within this time frame.

Measles transmission follows the states transition dynamics and parameter values described in Chapter 2, incorporating a two-dose vaccination regimen. However, because the measles outbreak unfolds over a relatively short time frame within a single community, children infected during the outbreak are not assumed to receive vaccination post-infection. This simplification reflects the short-term nature of outbreak dynamics, even though under routine immunisation programmes, a history of prior infection is not a contraindication for measles vaccination. Consequently, in this outbreak scenario, transitions from the recovered (R) states to vaccinated recovered (V_1R or V_2R) are not included in the simulation.

The vaccination coverage in both the neighbourhood (θ) and the broader community (V_i) is set to 0.5, indicating that half of the population is vaccinated while the other half has not been vaccinated. The social norm degree (α) is set to 0.7, based on empirical evidence of Pearson's correlation coefficient of subjective norm with vaccination willingness (Chu et al., 2021). The decision noise parameter k can range from 0 to ∞, with smaller values reflect greater clarity to represent the problem. Individuals with lower k values are more likely to choose a decision with a better payoff. Since k lacks direct empirical measurement, a moderate value of 0.1 is selected for the simulation. Notably, if k were set too low (e.g., below 0.01), the resulting vaccination relative cost (v_{RC}) would become exceedingly small, making the influence on decisions difficult to visualize clearly in the plots.

The simulation primarily focuses on the psychological and behavioural factors influencing vaccination dynamics. Therefore, the analysis emphasizes parameters related to both psychological attitudes and behavioural decision-making. When a particular parameter is not under investigation, global parameter values are applied, as listed in **Table 2**.

Table 2. Global parameter values used in simulations.

Parameters	Description	Value
θ	Vaccination coverage in the neighbourhood	0.5
V_i	Initial vaccination coverage in the community	0.5
α	Degree of social norm influence	0.7
k	Decision noise	0.1

Vaccination services during an outbreak are assumed to be available daily. Once a household decides to vaccinate its children, the vaccination can be administered the following day without delays. This accessibility assumption allows the model to focus exclusively on the demand-side dynamics of vaccination behaviour.

3.2.2 Opinion formation, inter-community interaction and external events

In this context, the term *opinion* is used as a proxy for *attitude* toward vaccination. This opinion is represented by the perceived vaccination relative cost (v_{RC}). It is important to distinguish *attitude* from *willingness to vaccinate*, as willingness is constructed by attitude based on Theory of Planned Behaviour (Ajzen, 1991). A household may show a high willingness to vaccinate while still holding an unsupportive attitude toward vaccination. For example, when a household encounters an infection in its surroundings, the willingness to vaccinate may increase; however, the underlying perception of vaccination relative cost (v_{RC}) remains unchanged. As during outbreak, parents can have a high willingness to vaccinate their children, but at the same time project a lower willingness when the outbreak has been subsided (Christianson et al., 2020).

In the previous section, the perceived vaccination relative cost (v_{RC}) was assumed to be fixed and homogeneous across all households within the under-vaccinated community, and there is no interaction with other community. In this section, interaction is introduced with neighbouring communities that have lower v_{RC} values and, consequently, achieve higher vaccination coverage sufficient to reach herd immunity. By contrast, the under-vaccinated community maintains a higher perceived vaccination relative cost and is simulated with $v_{RC} \geq 0.5$. This setting resembles condition of persistent low coverage community which is surrounded by high vaccination coverage in general population (Jenness et al., 2021; Khan et al., 2018; Klinkenberg et al., 2022).

The simulations in this section explore whether opinion exchange with other community influences the vaccination dynamics within the under-vaccinated community. To model the interaction, the perceived vaccination relative cost (v_{RC}) is assumed to be dynamic, changing in response to inter-community interaction and governed by opinion formation process.

To simulate opinion formation, the biased assimilation model proposed by Dandekar et al. (2013) is implemented, and described in Eq.2.10 in Chapter 2. The opinion dynamics are simulated over a one-year period, running in parallel with the vaccination uptake simulations for a single vaccination season, which are reported on an annual basis.

To simulate opinion dynamics, inter-community interaction is introduced using the mixing parameter μ, which represents the proportion of inter-community connections relative to the total number of connections within the community. The analysis begins with interaction involving a single external community, followed by scenarios involving multiple interacting communities. Each of the interacting communities is initialized with the same network size and topological structure as the under-vaccinated community. The inter-community interaction scheme can be seen in **Figure 3.2**.

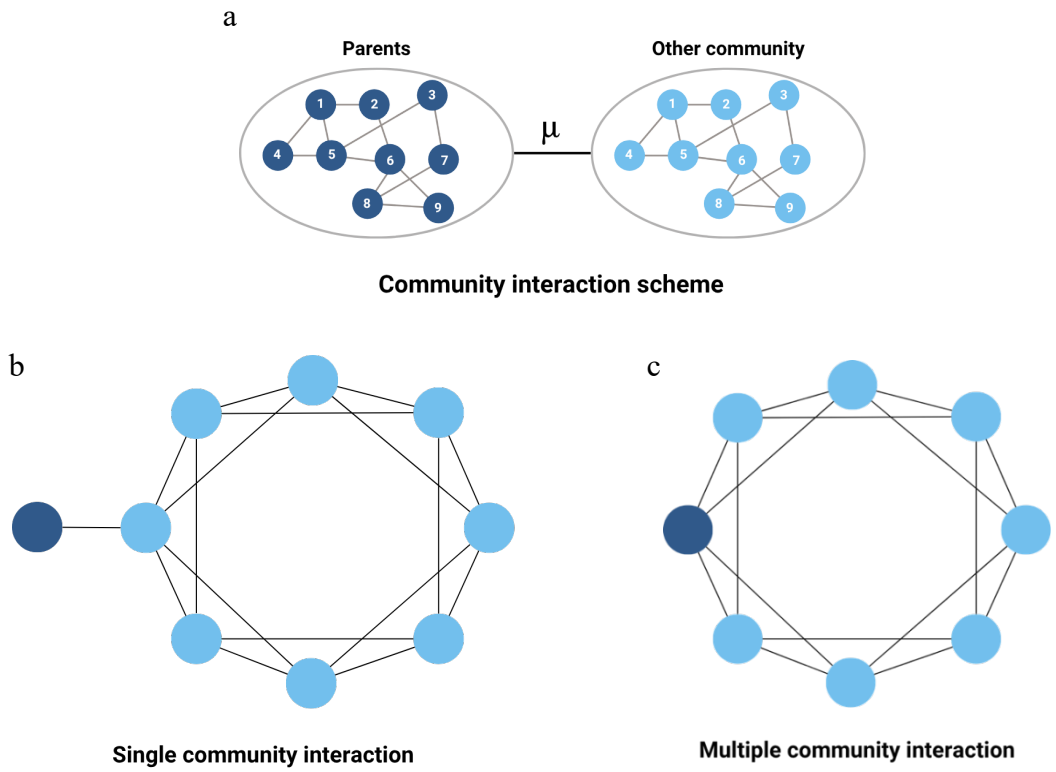


Figure 3.2. Modelled inter-community interaction of the under-vaccinated community with other communities. (**a**) Connections with other communities are generated based on the mixing parameter (μ), which defines the proportion of inter-community links relative to total connections in the under-vaccinated community. There are two scenarios: **(b)** Where the under-vaccinated community interacts with only one other community. **(c)** Where it interacts with multiple communities. All communities are constructed using a log-normal degree distribution fitted to empirical network data from 75 villages in India (Banerjee et al., 2013), with inter-community mixing (μ) incorporated into the fitted connection structure.

The next consideration concerns the frequency with which individuals update their opinions regarding vaccination. Evidence indicates that opinion change related to routine immunisation tends to occur gradually over extended periods, often in parallel with broader trends of polarization (Lee and Sibley, 2020). Rather than shifting on a daily or monthly basis, such updates typically unfold over the course of several years. Furthermore, parents do not revise their views at fixed or regular intervals but rather in response to salient external events, such

as the spread of information about adverse events, vaccine scares, or outbreaks of disease (Greyson and Bettinger, 2022; Torracinta et al., 2021). Based on this evidence of limited updating frequency when there is no external event, it is assumed that individuals update their opinions up to three times per year. Accordingly, the simulation incorporates three opinion update events over the one-year period.

In the opinion formation dynamics model, interactions with other communities are initially treated as *internal* processes, driven solely by interpersonal exchanges among households based on their respective stances toward vaccination. The first set of simulations focuses exclusively on these inter-household interactions.

Subsequently, the model incorporates *external* events, such as vaccine scares and large outbreaks, that can trigger shifts in opinion. Vaccine scares are simulated based on the occurrence of adverse events following immunisation (AEFI), with the probability derived from the estimated risk of febrile seizures after measles vaccination, which occurs at a rate of approximately 1 in 1,700 doses (Di Pietrantonj et al., 2021) A scare is assumed to be activated even after a single reported adverse event. In contrast, a large outbreak is defined as the occurrence of five or more symptomatic measles cases (World Health Organization, 2009). During these external events, households engage in simultaneous opinion exchange and discussion related to the event.

The opinion dynamics simulation will implement similar global parameter values from the vaccination decision model in community levels such as the social norm influence (α) and decision noise (k). For the opinion simulation, global parameters related with the households' and communities' interactions are assigned as listed in **Table 3**.

In this model, neighbouring communities are assumed to exhibit stronger support for vaccination than the under-vaccinated community, as reflected in their lower perceived vaccination relative cost (v_{RC}). The under-vaccinated community is simulated with v_{RC} values ranging from 0.5 to 1.0, indicating varying degrees of opposition to vaccination. In contrast, neighbouring communities are initialized with v_{RC} = 0.3, representing a more favourable view toward vaccination. To simulate how strong the households adhere to their current opinions, assimilation bias (b) is incorporated and assumed to operate uniformly across all communities, with a global bias parameter b = 1.

Table 3. Global parameter values for opinion dynamics simulations

Parameters	Description	Value
$v_{RC}\ other\ community$	Vaccination relative cost in other communities	0.3
$b_{i,j}$	Assimilation bias in under-vaccinated and other communities	1
μ	Inter-community connection proportion	0.3
w_{inter}	Weight of inter-community connection	0.5
w_{intra}	Weight of intra-community connection	1
w_{ii}	Self-weight (how strong a household trust their own opinion)	1

For the interaction, households are assumed to interact more frequently and more strongly with those in closer proximity. Proximity is operationalized based on community membership: households within the same community are considered "closer" than those in different communities. The mixing parameter (μ) defines the degree of inter-community connectivity, with a maximum allowable value of 0.5. Values of $\mu > 0.5$ would imply that the communities are no longer separate, so they are excluded from the model. To simulate social distance, the model differentiates the weights of intra- and inter-community connections. Each household is also assigned a constant self-weight of 1. It is assumed that households place greater influence on connections within their own community than on those with external contacts. Accordingly, for the global parameter setup, the intra-community weight w_{intra} is set to 1, while the inter-community weight w_{inter} is set to 0.5. To emphasize the effect of social interaction, no difference in self-weight (w_{ii}) is assigned across households; all are set to 1, both in under-vaccinated and neighbouring communities.

3.3 Results and Discussion

This sub chapter evaluates the behavioural, social, and epidemiological dynamics based on the modelling framework developed in Chapter 2. Results and discussions are organised to progress from individual psychology to community behaviour, then to outbreak dynamics,

behavioural vaccine effectiveness, opinion change, inter-community structure, and exogenous shocks. Throughout the results and discussions, perceived vaccination relative cost (v_{RC}) is used as the primary attitudinal axis, while willingness (Ψ), final vaccinated households (V_f), and cumulative infected households (I_f) are evaluated as the principal outcomes. Since this chapter does not implement formal statistical testing but rather focuses on qualitative assessment of vaccination decision simulation results, the term "significant" reflects qualitative differences among outcomes, rather than the result of a statistical test.

3.3.1 Vaccination willingness

In this section, sensitivity analysis result for all parameters involved in constructing household willingness to vaccinate are presented. The parameters analysed include the perception of vaccination relative cost (v_{RC}) in a household, vaccine coverage in the neighbourhood (θ), social norm degree (α) and decision noise (k) as defined in Eq.2.5 in Chapter 2. Building on previous work that highlights the central role of vaccination cost perception in shaping willingness to vaccinate (Bauch and Earn, 2004; Wang et al., 2016), this parameter is placed on the x-axis. The effects of other parameters are therefore examined in relation to how they influence willingness (Ψ) across different values of v_{RC}.

Willingness to vaccinate is influenced by the epidemiological context in which individuals make decisions. Intuitively, individuals are more likely to vaccinate when an outbreak occurs in their vicinity, compared to when there is no prominent infection nearby. To account for this contextual difference in decision-making, the sensitivity analysis of psychological parameters is stratified by whether households are exposed to an infected neighbour or not.

As expected, the willingness to vaccinate is higher when there is infected neighbour around the household. However, as can be seen on **Figure 3.3**, the individuals' willingness (Ψ) to vaccinate their children are sensitive to vaccination relative cost (v_{RC}), vaccine coverage in the neighbourhood (θ), social norm degree (α) and decision noise (k). As an important element for decision to vaccinate, there is a critical point of v_{RC}. In a situation of without infected neighbour, the willingness to vaccinate is suppressed to zero when the v_{RC} reaches 0.4, and from that point, other parameter are not sensitive anymore to influence willingness. On contrary, in the with infected neighbour setting, the critical point of v_{RC} is around 0.8, where the Ψ remains stable up to that level and the Ψ is decreased after that point for θ and α analysis.

However, households with lower k still maintain their willingness even when the vaccination relative cost is almost the same with being infected.

The vaccine coverage in the household's neighbourhood (θ) influences the willingness to vaccinate their children, either with or without infected neighbour. As has been mentioned before, in the absence of infected neighbour, when the vaccine relative cost (v_{RC}) exceeds 0.4, willingness in all vaccine coverage settings drop to zero and becomes insensitive to further changes in θ as can be seen in **Figure 3.3a**. Interestingly in **Figure 3.3e**, a notable pattern emerges in the presence of an infected neighbour: even under outbreak conditions, the willingness is suppressed based on proportion of vaccination coverage in the neighbourhood. A higher vaccine coverage in the neighbourhood will translate to higher willingness to vaccinate. However, it is important to note that the social norm degree (α) in the θ simulation is assigned in 0.7, a relatively higher value indicating a strong tendency for households to conform to prevailing social norms.

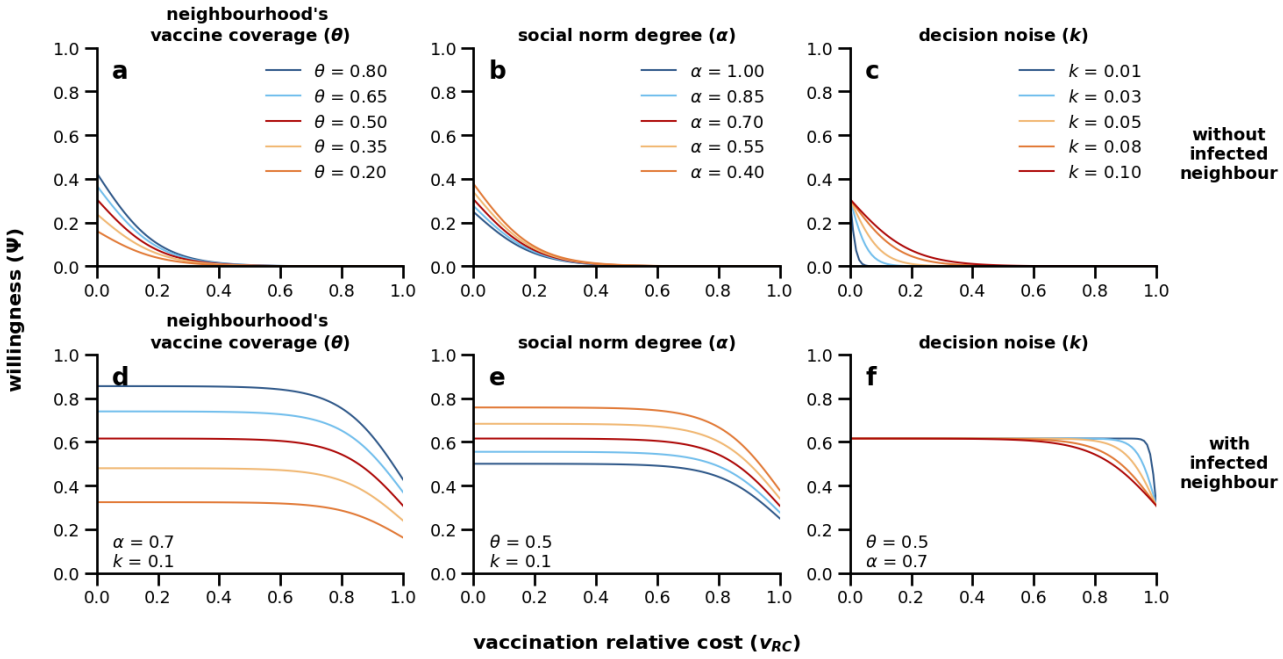


Figure 3.3. Individual's willingness to vaccinate. The willingness to vaccinate (Ψ) represents the probability that a household intends to vaccinate its children, determined by the household's perceived vaccination relative cost (v_{RC}), Willingness is shown as a function of neighbourhood vaccine coverage (θ) in **(a, d)**, social norm degree (α) in **(b, e)**, and decision noise (k) in **(c, f)**. The first row shows scenario where the household encounters an uninfected neighbour, and the second row shows encounters with an infected neighbour. Global parameter values (α = 0.7, k = 0.1, θ = 0.5) are used unless varied and are indicated by the red solid line in each subplot.

In this sensitivity analysis, a range of values for the social norm degree (α) is further explored although empirical evidence estimates the influence of subjective norms on vaccination

willingness to be approximately 0.7 (Chu et al., 2021). Alongside the proportion of vaccinated individuals in the neighbourhood, α also modulates willingness to vaccinate—though its effect is more pronounced in the setting where households encounter an infected neighbour (**Figure 3.3e**), and relatively minimal when no infections are present (**Figure 3.3b**). In under-vaccinated communities, households that exhibit strong conformity to social norms (higher α) may show reduced willingness to vaccinate during outbreaks, particularly when surrounded by low neighbourhood coverage. In contrast, households that are less influenced by social norms (lower α) demonstrate greater responsiveness to the presence of infection, exhibiting higher willingness to vaccinate when faced with an infected neighbour, even if surrounded by low neighbourhood coverage.

Decision noise (k) represents the degree of bounded rationality in how households represent their vaccination problem dilemma. A lower value of k indicates that a household is more capable of selecting the option with an optimal utility. This effect is clearly observed in the simulation. In the absence of infection (**Figure 3.3c**), households with the lowest k values are willing to vaccinate only when the v_{RC} is minimal. In contrast, when an infected neighbour is present (**Figure 3.3f**), these same households are still willing to vaccinate even when the cost of vaccination is almost the same with the cost of disease.

This section has examined the psychological constructs of willingness to vaccinate within the framework of the Theory of Planned Behaviour (TPB) (Ajzen, 1991). The sensitivity analysis demonstrates how the subjective norm of the social environment can suppress willingness, even during a prominent outbreak. Households are less likely to vaccinate when vaccination coverage in the surrounding neighbourhood is low.

The finding that households vaccinate less when neighbourhood coverage is low highlights the importance of considering vaccination as a complex contagion (Centola and Macy, 2007; Guilbeault et al., 2018), in which social influence plays a critical role in shaping costly decisions such as vaccination. When households evaluate vaccination solely on perceived cost, willingness increases substantially in the presence of an infected neighbour (**Figure 3.4a**).

In contrast, when social influence is incorporated into the decision model, the same situation results in lower willingness modulated by vaccination coverage in the neighbourhood (**Figure 3.4b**). The suppression of willingness to vaccinate through social influence helps explain why

under-vaccinated communities often remain hesitant even during disease outbreaks (Christianson et al., 2020; Zucker et al., 2020; Parker et al., 2006).

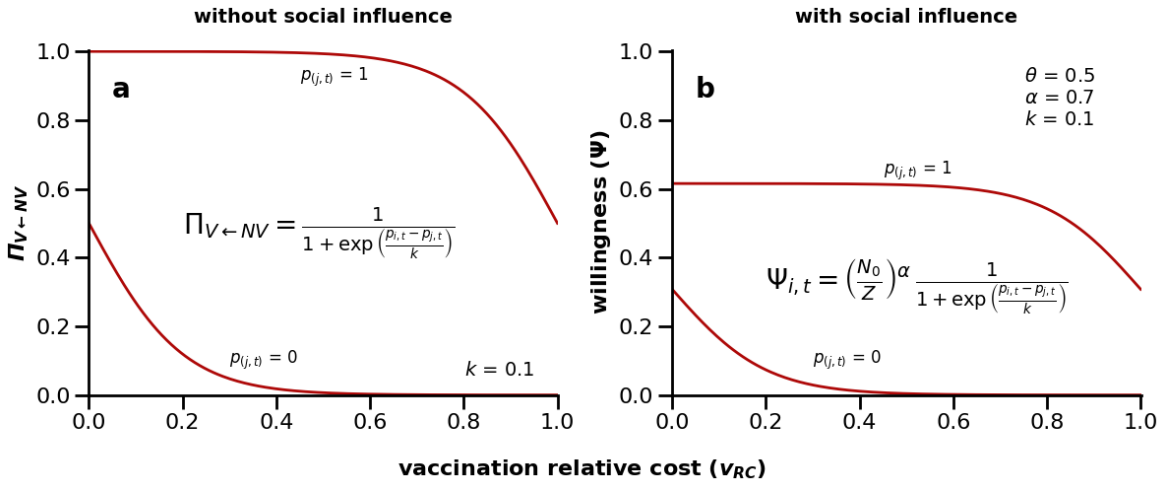


Figure 3.4. Probability of vaccination comparison of two decision models: **(a)** without social influence, based on Eq.2.2 from Chapter 2, and **(b)** with social influence, based on Eq.2.5 from Chapter 2. Here $p_{(j,t)}$ assigns a random neighbour's fate, whether infected ($p_{(j,t)}$=1) or not infected ($p_{(j,t)}$=0). $\frac{N_0}{Z}$ is equal to θ, assigns vaccination coverage in neighbourhood.

Even before vaccination behaviour is adopted, psychological analysis can reveal states of mind that act as obstacles to vaccination. In this context, the willingness analysis draws on the definition of vaccine hesitancy as a "state of indecisiveness," distinct from vaccination behaviour itself (Bussink-Voorend et al., 2022; Goldenberg, 2021; Larson, 2022). At this stage, individuals are already less inclined to vaccinate when fewer adopters are present in their surroundings.

3.3.2 Vaccination behaviour

Having examined household willingness to vaccinate from a psychological perspective, we now turn to the behavioural dimension of collective vaccination in under-vaccinated community. In this section, the willingness is simulated over one-year period, and the percentage of vaccinated household is calculated at the day 365. The average percentage across multiple simulations is presented in **Figure 3.5**, which displays the sensitivity of vaccination relative cost (v_{RC}), initial vaccination coverage (V_i), social norm strength (α), and decision noise (k) to influence final vaccinated household (V_f) under both outbreak and no-outbreak conditions.

In general, the perception of vaccination relative cost (v_{RC}) plays a critical role in shaping vaccination behaviour within under-vaccinated communities. As shown in **Figure 3.5a – c**, in the absence of an outbreak, when $v_{RC} \leq 0.4$, vaccine coverage can reach the 95% herd immunity threshold for measles. This suggests that the critical threshold of v_{RC} for $k = 0.1$ in a no-outbreak setting is approximately 0.4. In other words, if the perceived cost of vaccination is equal to or less than 40% of the perceived cost of infection, herd immunity can be achieved in a community. However, if we look at **Figure 3.5c**, the threshold is modulated by decision noise (k), as the lower k is translated to lower v_{RC} required to achieve herd immunity.

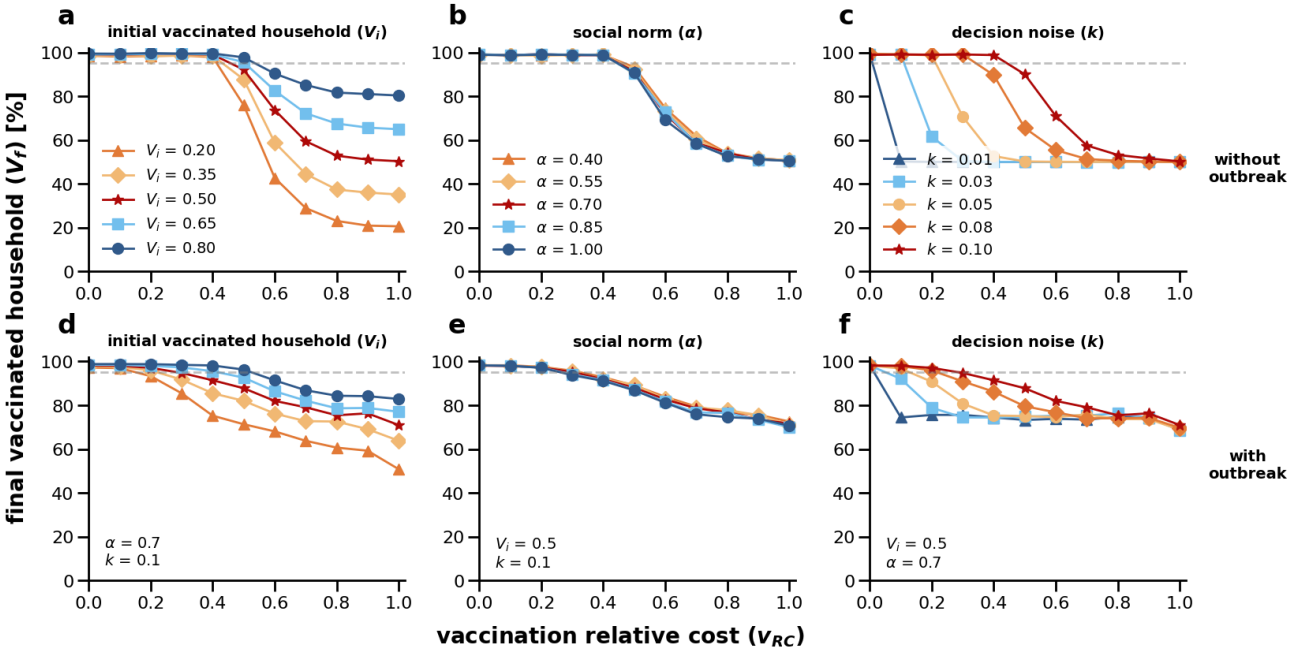


Figure 3.5. Collective vaccination behaviour in under-vaccinated communities with and without outbreak. Final vaccinated household (V_f) is shown as a function of the perceived vaccination relative cost (v_{RC}) and modulated by **(a, d)** initial vaccination coverage (V_i), **(b, e)** social norm (α) and **(c, f)** decision noise (k). The first row presents scenarios with an outbreak, and the second row presents scenarios without an outbreak. Global parameter values ($\alpha = 0.7$, $k = 0.1$ and $V_i = 0.5$) are used unless varied and are indicated by the red star symbol and solid line in each subplot.

Different dynamics emerge under outbreak conditions, as illustrated in **Figure 3.5d-f**. Even when $v_{RC} \leq 0.4$ and $k = 0.1$, the final vaccinated household (V_f) does not reach the herd immunity threshold. This is despite the expectation that willingness to vaccinate would increase in the presence of an outbreak. As elaborated in the next section on epidemiological dynamics, at the same v_{RC} level, fewer children are ultimately vaccinated because many become infected before receiving vaccination. The high transmissibility of measles results in a faster infection rate compared to the rate at which vaccination can be administered. It is important to note that in the outbreak setting, children who are infected during the simulation are no longer eligible

to receive the vaccine for the remainder of the outbreak period, which constrains the maximum achievable vaccination coverage.

The initial vaccinated (V_i) is sensitive toward the final vaccinated household (V_f) when the v_{RC} is larger than the critical point. In no outbreak setting as depicted in **Figure 3.5a**, the V_f is dispersed when the $v_{RC} > 0.4$. However, when the $v_{RC} > 0.8$, all the households in the community decide not to vaccinate their children. In comparison, when there is a measles outbreak, the critical point of v_{RC} is reduced to 0.1, as shown in **Figure 3.5d**. After that point, the V_f is dispersed based on V_i and the community will not reach herd immunity threshold especially when the initial vaccinated household is minimal.

In contrast to the psychological analysis of willingness, the collective behaviour simulations suggest that social norm strength (α) loses influence once decisions aggregate at the community level, showing little effect on the final proportion of vaccinated households (V_f). As can be seen on **Figure 3.5b** and **3.5e**, there is no significant difference on various α value as the lines exhibit minimal separation. In the individual's willingness (**Figure 3.3b** and **3.3e**), θ is held fixed at 0.5, while in the collective vaccination simulation, θ is no longer fixed but evolved as households vaccinate. The α may influences willingness, but the effect saturates as households start vaccinating and the V_f is increased.

As expected, when there is no outbreak (**Figure 3.5c**), lower values of k, indicating better representation of the vaccination problem, lead to a lower critical threshold for vaccination relative cost (v_{RC}) to reach herd immunity. However, an interesting pattern emerges in the outbreak setting (**Figure 3.5f**), where lower k unexpectedly leads to lower V_f. This result is counterintuitive, as one would anticipate that during an outbreak, households with better problem representation (lower k) would be more likely to vaccinate as a response. Yet, the simulations indicate that these "more rational" households do not achieve higher coverage under outbreak conditions.

This section demonstrates the presence of a critical threshold of v_{RC} required to maintain herd immunity and prevent measles outbreaks within a community. When decision noise (k) is set at 0.1, herd immunity requires $v_{RC} \leq 0.4$, with lower values of k necessitating even lower thresholds. For simplicity, the results in this section operationalize vaccine hesitancy as $v_{RC} > 0.4$. Consistent with Section 3.3.1 (Vaccination willingness), households are unwilling to

vaccinate their children once v_{RC} exceeds this threshold. Collective vaccination behaviour similarly fails to achieve herd immunity under no-outbreak conditions when $v_{RC} > 0.4$. This operational definition of the v_{RC} threshold aligns with conceptualizations of vaccine hesitancy as a *state of mind* rather than a behaviour (Bussink-Voorend et al., 2022; Goldenberg, 2021; Larson, 2022).

As discussed in Chapter 2, decision noise (k) represents bounded rationality (Simon, 1990), reflecting the fact that individuals cannot fully represent the complexity of a decision made under risk, such as vaccination. The parameter k is therefore incorporated into the decision model. Unlike other parameters, however, k is difficult to quantify empirically. The relative cost of vaccination (v_{RC}) can be approximated by asking caregivers to compare the perceived burden of vaccination with the risk of infection, while social norm strength (α) can be probed by assessing the likelihood of conforming to the decisions of immediate contacts. By contrast, k can only be inferred indirectly and must be assumed within specific contexts: higher values are more appropriate for decisions regarding novel pathogens, where individuals have limited understanding of the problem, whereas lower values apply to routine immunisations.

Theoretically, this presents a challenge for established vaccines such as measles. Individuals may assume they already possess a complete understanding of both the disease and the vaccine, resulting in lower values of k. Yet lower k corresponds to the need for an even lower perception of v_{RC} for households to adopt vaccination, thereby posing additional challenges for sustaining herd immunity against measles. Moreover, in the context of a highly infectious outbreak such as measles, individuals with lower k may delay vaccination to the extent that transmission outpaces their decision-making, undermining the effectiveness of reactive vaccination as a control strategy.

3.3.3 Epidemiological outcomes

Having previously examined the psychological and behavioural dynamics of vaccination, this section now focuses on the epidemiological dynamics of measles outbreaks in under-vaccinated communities. Two outcomes are tracked at the end of the one-year simulation (day 365): the percentage of households with infected child (I_f) and with breakthrough infections (B_f). Breakthrough infection is defined as infection occurring despite prior vaccination and includes asymptomatic cases. This section analyses how vaccination relative cost (v_{RC})

influences both I_f and B_f, and how these effects are modulated by initial vaccinated household (V_i), social norm (α) and decision noise (k).

Overall, **Figure 3.6** supports earlier findings from the behavioural dynamics analysis, showing that perceived vaccination relative cost (v_{RC}), initial vaccinated household (V_i), and decision noise (k) significantly influence the epidemiological outcomes of measles transmission. In **Figure 3.6a** and **3.6b**, a clear threshold is observed: when $v_{RC} \leq 0.1$, both the final epidemic size and the cumulative number of breakthrough infections remain low. Beyond this critical point, outcomes become more variable and are strongly modulated by the level of initial vaccination coverage in the community. As expected, lower V_i leads to higher infection rates. A second threshold appears at $v_{RC} = 0.4$, beyond which cumulative measles cases plateau. Beyond this point, changes in perceived vaccination cost exert little additional influence on transmission.

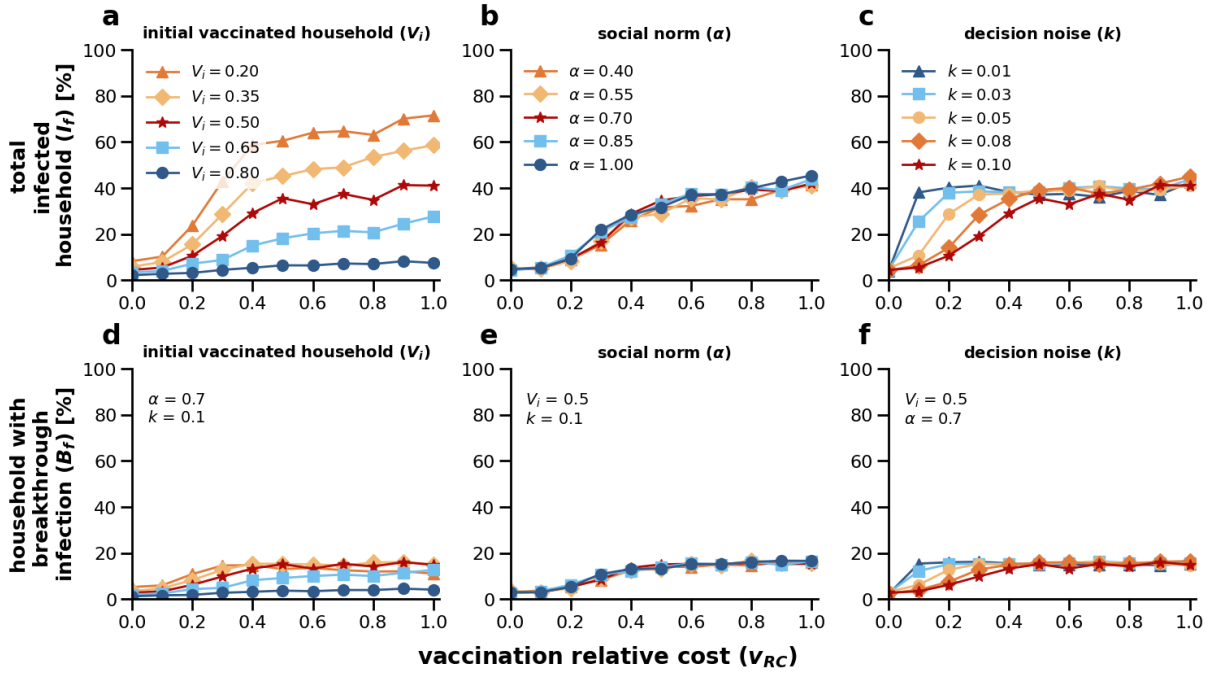


Figure 3.6. Epidemiological dynamics of measles outbreaks in under-vaccinated communities. The percentage of cumulative infections (I_f) is shown in the first row, and the percentage of cumulative breakthrough infections (B_f) in the second row. Outcomes are analysed as a function of the perceived vaccination relative cost (v_{RC}), modulated by: **(a, d)** initial vaccinated household (V_i), **(b, e)** social norm (α), and **(c, f)** decision noise (k). Global parameter values ($\alpha = 0.7$, $k = 0.1$ and $V_i = 0.5$) are used unless varied and are indicated by the red star symbol and solid line in each subplot.

The social norm degree (α) does not appear to significantly influence the epidemiological dynamics of measles transmission in under-vaccinated communities, consistent with its limited

role in collective vaccination behaviour. Since α has minimal effect on collective vaccination (**Figure 3.5b** and **3.5e**), and any boost/delay it causes is small compared with the measles spread, therefore its effect on individual willingness is diminished further in shaping the infection outcome.

However, **Figure 3.6a** and **3.6b** reveal a clear relationship between perceived vaccination cost (v_{RC}) and outbreak size. Both figures highlight two critical thresholds of v_{RC}: at 0.1 and 0.4. When $v_{RC} > 0.1$, infection levels increase substantially, indicating heightened transmission. Beyond $v_{RC} = 0.4$, the spread of infection begins to plateau, suggesting that additional increases in perceived cost have diminishing influence on overall epidemic size.

In the decision noise (k) analysis shown in **Figure 3.6c** and **3.6f**, the critical threshold at $v_{RC} = 0.4$ remains evident. Beyond this point, changes in v_{RC} no longer significantly affect measles transmission within the community. However, another pattern emerges at the lower end of the v_{RC} spectrum. Even when $v_{RC} = 0.1$, lower values of k produce substantially greater cumulative case counts compared to higher k values. This counterintuitive finding, that lower decision noise (i.e., more rational decision-making) increases infections when $v_{RC} \leq 0.4$, aligns with earlier results showing reduced vaccination uptake among more rational households during outbreaks.

This section identifies two critical thresholds of v_{RC} that shape outbreak dynamics in under-vaccinated communities: 0.1 and 0.4. When $v_{RC} \leq 0.1$, infections remain negligible because households vaccinate rapidly, outpacing measles transmission. Beyond this point, infections diverge according to initial vaccination coverage, reaching a plateau once $v_{RC} \geq 0.4$. At this second threshold, epidemic size varies substantially with the community's initial coverage.

These findings indicate that when the perceived relative cost of vaccination exceeds 0.4, the effectiveness of reactive vaccination is severely limited. Although willingness to vaccinate increases during outbreaks, a high perception of cost still results in substantial transmission, with outcomes determined largely by pre-outbreak coverage. In hesitant communities ($v_{RC} > 0.4$), epidemic size depends primarily on initial vaccination levels, underscoring the critical role of preventive vaccination over reactive strategies.

Households with lower decision noise experience larger epidemics when vaccination cost is minimal. This counterintuitive result arises because "more rational" households respond too

late in the context of a highly contagious disease like measles. By the time they decide to vaccinate, infection may already have occurred. In this setting, decision noise can act as a protective determinant, aligning with studies showing that noise may enhance collective adaptive behaviour (Bak-Coleman et al., 2021; Shirado and Christakis, 2017; Yates et al., 2009).

3.3.4 Behavioural vaccine effectiveness

The previous section showed that final breakthrough infections (B_f) are influenced by perceived vaccination relative cost (v_{RC}), initial vaccination coverage (V_i), and decision noise (k). Measles transmission can also outpace vaccination efforts, particularly when V_i is low and v_{RC} is high. This section examines whether these psychological and behavioural factors also affect vaccine effectiveness in the context of vaccine hesitancy. To capture this, *Behavioural Vaccine Effectiveness* (BVE) is introduced.

The term BVE is implemented to emphasize that while *Vaccine Effectiveness* (VE) has a standardized epidemiological definition referring to biological protection against infection and disease, BVE instead captures the realized effectiveness of vaccination once psychological and behavioural dynamics are considered**.** For that purpose, BVE is formally defined as:

$$BVE = 1 - \left(\frac{AR_{vacc}/V_i}{AR_{unvacc}/(1 - V_i)} \right) \tag{3.1}$$

AR_{vacc} refers to the attack rate among finally vaccinated households, while AR_{unvacc} is the attack rate among finally unvaccinated households. This formulation enables evaluation of vaccine effectiveness relative to vaccination behaviour. The BVE is also standardized to initial vaccination coverage (V_i), emphasizing the contribution of initial coverage in protecting the community against measles infection.

To capture the realised protection conferred by vaccination, the number of breakthrough infections (B_f) are assessed among all households that were ultimately vaccinated (V_f) at the end of each simulation. Since B_f and V_f are initially calculated as percentages, they are converted into absolute household counts by multiplying with the total number of household (N) before computing AR_{vacc}:

$$AR_{vacc} = \frac{B_f}{V_f} \tag{3.2}$$

To maintain clarity, the same notation (e.g., B_f, I_f, V_f) is applied when referring to either proportions or absolute numbers, depending on the context.

Since the total number of infected households (I_f) at the end of the simulation include both vaccinated and unvaccinated individuals, the attack rate among unvaccinated households (AR_{unvacc}) are isolated by subtracting the number of breakthrough infections (B_f) from the total infected (I_f), and dividing by the number of households that remain unvaccinated at the end of the simulation ($N - V_f$):

$$AR_{unvacc} = \frac{I_f - B_f}{N - V_f} \tag{3.3}$$

Given that the social norm degree (α) shows minimal sensitivity in influencing both total infections (I_f) and breakthrough infections (B_f), it is excluded from the subsequent BVE analysis. Instead, the analysis focuses only on three factors: the perceived vaccination relative cost (v_{RC}), the initial vaccination coverage (V_i) and decision noise (k). **Figure 3.7** presents the influence of these three factors on BVE.

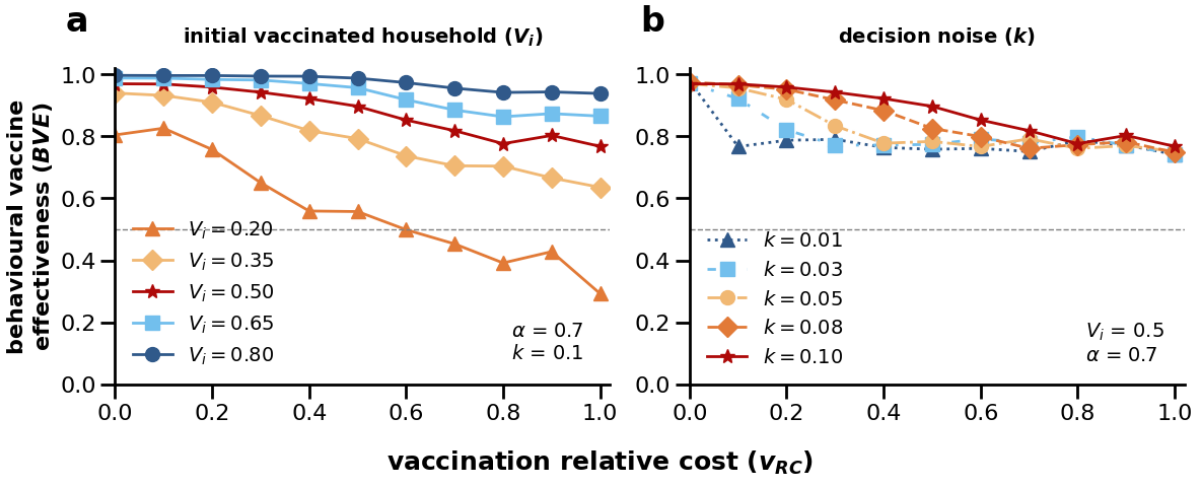


Figure 3.7. Behavioural vaccine effectiveness (BVE) in under-vaccinated communities against measles infection. BVE is shown as a function of the perceived vaccination relative cost (v_{RC}), modulated by **(a)** initial vaccinated households (V_i) and **(b)** decision noise (k). The horizontal dotted grey line indicates the threshold of $VE = 0.5$. Global parameter values (are $\alpha = 0.7$, $k = 0.1$ and $V_i = 0.5$) are used unless varied and are represented by the red star symbol and solid line in each subplot.

Figure 3.7a illustrates that the perception of vaccination relative cost (v_{RC}) significantly influences vaccine effectiveness (BVE) in the population. As v_{RC} increases, BVE declines — indicating that when more households perceive vaccination as costly, its overall effectiveness in preventing infection is reduced. This is particularly concerning in the context of highly transmissible diseases like measles, where vaccines are otherwise highly efficacious. Under conditions of low initial vaccination coverage (V_i = 0.2), the higher value of perceived vaccination relative cost can suppress BVE to below the critical threshold of 0.5, which is used to define an effective vaccine.

Figure 3.7b reveals that the suppression of BVE is more pronounced when decision noise (k) is minimal. Specifically, even at a relatively low v_{RC} value of 0.1, communities with the lowest k values already exhibit a notable reduction in BVE. However, beyond this point, BVE stabilizes at around 0.8, even as v_{RC} increases—assuming an initial vaccination coverage (V_i) of 50%. Overall, the influence of k on BVE diminishes once $v_{RC} \geq 0.8$, suggesting that the impact of decision rationality is constrained under conditions of high perceived vaccination relative cost.

It is important to emphasize that the reduction in BVE observed in the simulation does not reflect the biological effectiveness of the measles vaccine. Empirical evidence indicates that a single dose of the measles vaccine provides approximately 95% protection against infection (Di Pietrantonj et al., 2021). Instead, the reduction in BVE observed here reflects the influence of psychological and behavioural factors on vaccination dynamics at the community level. As illustrated in **Figure 3.7**, both the perceived relative cost of vaccination (v_{RC}) and the level of vaccine coverage prior to an outbreak (V_i) can significantly erode the effectiveness of an otherwise highly efficacious vaccine in an under-vaccinated community. This shows how psychological and behavioural aspects can undermine the impact of a vaccine, even when its biological performance is optimal.

3.3.5 Opinion formation

In this section, interaction is introduced between an under-vaccinated community ($v_{RC} \geq 0.5$) and neighbouring communities with lower v_{RC} and higher coverage sufficient to achieve herd immunity. This setting reflects persistent low-coverage groups embedded within generally well-vaccinated populations (Jenness et al., 2021; Khan et al., 2018; Klinkenberg et al., 2022). The simulations examine whether opinion exchange with neighbouring communities alters

vaccination dynamics, with v_{RC} allowed to change through an opinion formation process. External events such as vaccine scares or outbreaks are excluded here (addressed separately in Section 3.3.7), and opinion updates are assumed to occur three times within a one-year vaccination season to illustrate the impact of inter-community influence.

Assimilation bias (b) is responsible for opinion polarization between under-vaccinated community (orange line) and the neighbouring communities (blue line), as demonstrated in **Figure 3.8**. When there is no b in all communities, the households in under-vaccinated community will consolidate their opinion to follow the larger sentiment of vaccination in general population. Accordingly, the vaccination is increased in the under-vaccinated community. On contrary, in a scenario with bias, the opinion is polarized, and the under-vaccinated community maintains their low vaccination while general population can reach herd immunity.

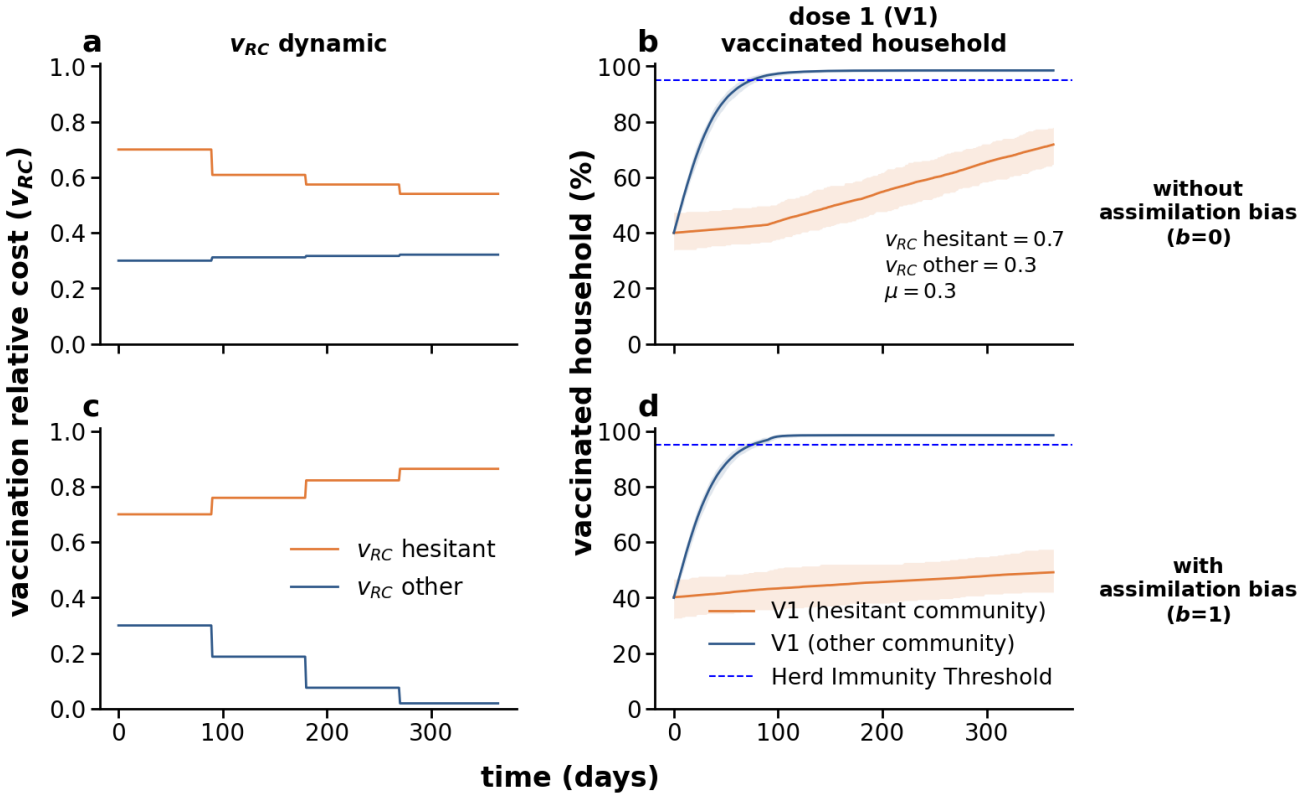


Figure 3.8. Perception of vaccination relative cost (v_{RC}) and vaccination dynamics in under-vaccinated (v_{RC} = 0.7) and neighbouring pro-vaccination communities (v_{RC} = 0.3). The under-vaccinated community interacts with four other communities, and opinion formation with and without assimilation bias is compared. Households vaccinate based on v_{RC}, with no external events simulated. Lines show means and shaded areas show 95% confidence intervals across runs.

Next, opinion updating is simulated with a sensitivity analysis of three parameters in the opinion formation model: assimilation bias (b_i), inter-community mixing (μ), and inter-community connection weight (w_{inter}). As part of the analysis, scenarios are compared in which the under-vaccinated community interacts with either a single neighbouring community or with multiple communities, thereby incorporating inter-community interaction, which is discussed further in **Section 3.3.6 Inter-community interaction**.

Overall, all opinion formation model parameters influence the update of perceived vaccination relative cost (v_{RC}), as shown in **Figure 3.9**. However, the degree of sensitivity is modulated by the number of interacting communities. As can be seen in the right column in **Figure 3.9**, multiple interacting communities environment enables a lower updated v_{RC} compared to when there is only one interacting community. Greater inter-community interaction leads to a perception that vaccination is less costly. Nonetheless, the ability of the opinion update process to shift the under-vaccinated community's perception in favour of vaccination is limited when the initial v_{RC} is extremely high. The greater the initial disparity between the under-vaccinated community's v_{RC} and the neighbouring community's v_{RC} of 0.3, the more likely the update will increase the high v_{RC} in the under-vaccinated community, thereby reinforcing opinion polarization about vaccination.

A closer examination of each opinion formation parameter reveals specific insights into their respective effects on opinion dynamics. **Figure 3.9a-b** highlight a marked difference in assimilation bias (b) between values of 1 and values greater than 1. As anticipated, higher bias leads to an increase in v_{RC} after interactions with pro-vaccine communities, reinforcing prior hesitant opinions. However, this effect appears to plateau for $b \geq 2$, suggesting diminishing marginal impact of stronger bias.

Among the analysed parameters as shown in **Figure 3.9**, inter-community mixing (μ) shows the greatest sensitivity to opinion updates, as illustrated in **Figure 3.9c-d**. As expected, increased mixing leads to reduced polarization: the more connected the under-vaccinated community is with households from other communities, the lower the resulting v_{RC} values following interaction.

Figure 3.9e-f illustrate the effect of inter-community connection weight (w_{inter}) on opinion polarization. When w_{inter} is lower, households in the under-vaccinated community assign less

importance to perspectives from outside their own group. As a result, polarization increases, reinforcing the divide between the under-vaccinated and their neighbouring communities.

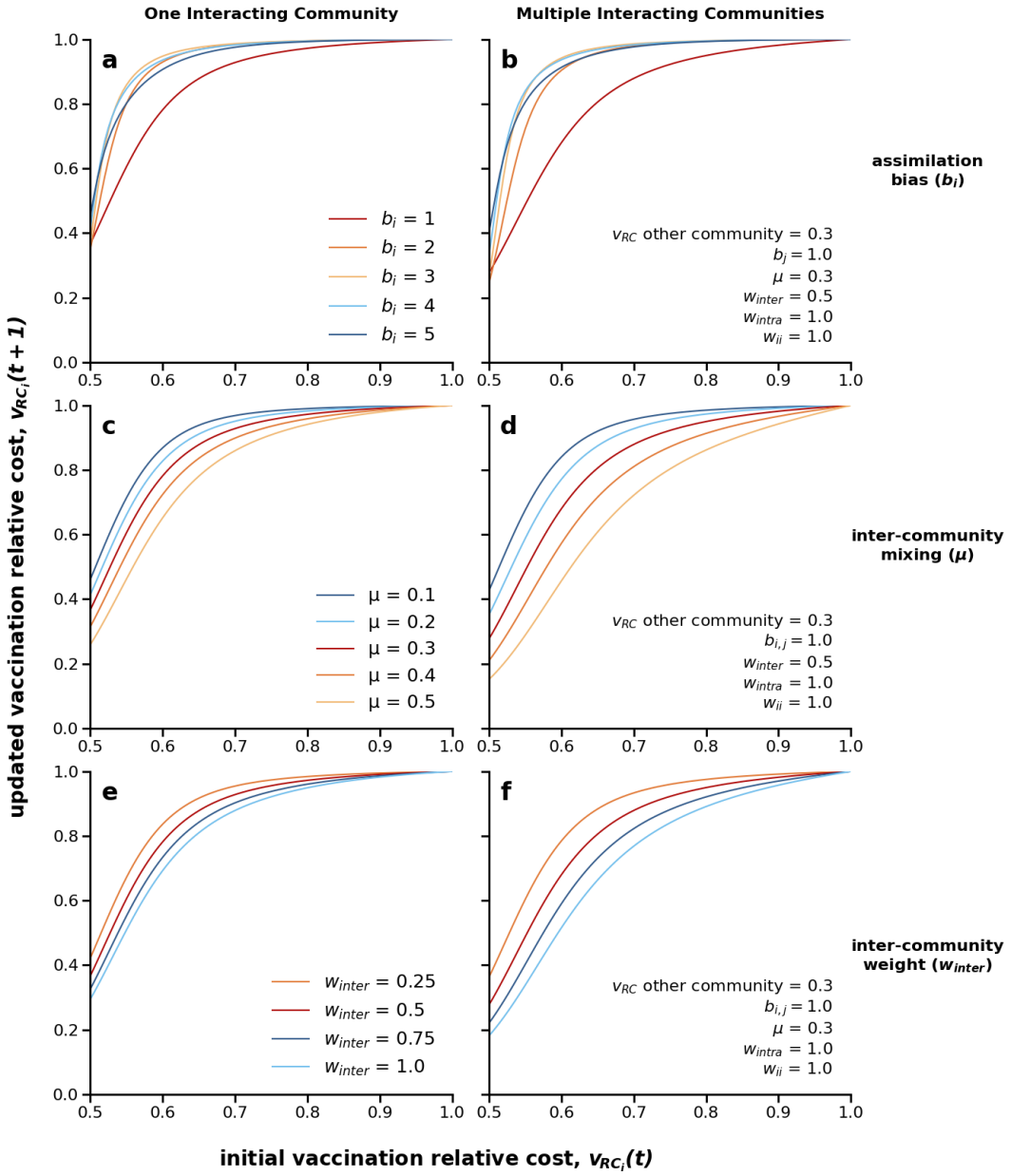


Figure 3.9. Update of perceived vaccination relative cost in an under-vaccinated community following interaction with other communities. The under-vaccinated community is simulated to initially oppose vaccination ($v_{RC} \geq 0.5$), while the neighbouring communities supports vaccination with $v_{RC} = 0.3$. In the multiple interacting communities, the under-vaccinated community is simulated to interact with 4 other communities. Opinion updates are simulated to occur three times over the course of one year, representing the maximum assumed frequency of opinion change without any external events. Global parameter values ($b_i = 1$, $\mu = 0.1$, $w_{intra} = 1$, and $w_{inter} = 0.5$) are used unless varied and are indicated by the solid red line in each subplot.

Next, sensitivity analysis of all three parameters related with opinion formation is conducted, to look at their influences toward final vaccinated household (V_f) in under-vaccinated

community. In contrast with the opinion update about vaccination as demonstrated in **Figure 3.9**, the opinion formation parameters are not sensitive to vaccination behaviour.

As can be seen in **Figure 3.10**, there is no significant difference of uptake between differing parameter values of assimilation bias (b), inter-community mixing (μ), and weight (w_{inter}). However, there is one exception on the b when there is only one interacted community (**Figure 3.10a**). In that scenario, when $b = 1$, the V_f is slightly different with other b setups.

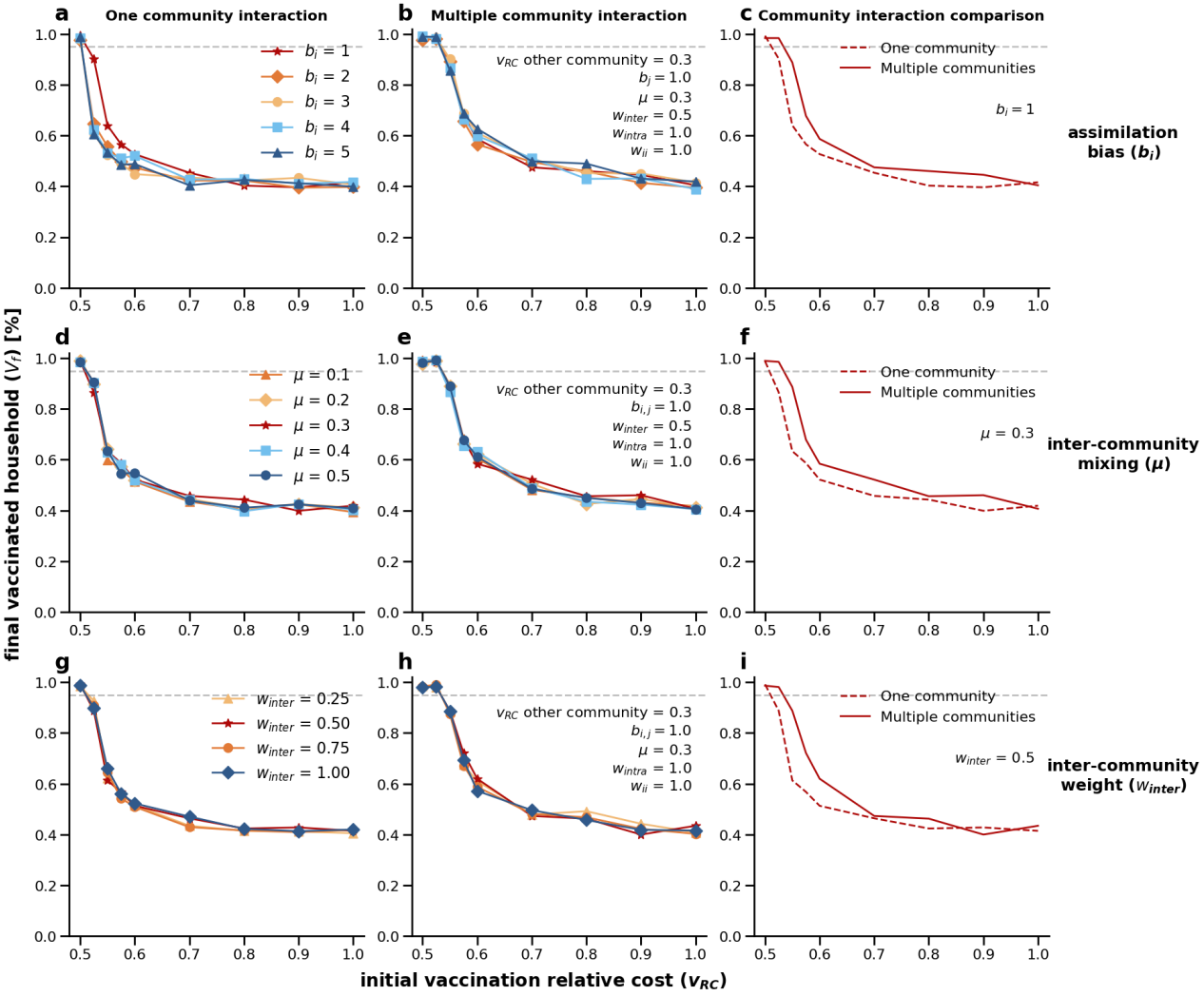


Figure 3.10. Final vaccinated household (V_f) in the under-vaccinated community following opinion updates about vaccination. Final vaccinated household (V_f) is shown after opinion updates occurring concurrently with the vaccination season at days 90, 180, and 270. Initial vaccinated household for dose 1 is set to 0.4 in both the under-vaccinated and the 4 neighbouring communities. The x-axis indicates the initial perceived vaccination relative cost (v_{RC}) in the under-vaccinated community prior to the updates. Global parameter values ($b_{ij} = 1, \mu = 0.3, w_{inter} = 0.5, w_{intra} = 1, w_{ii} = 1$) are used unless varied and are indicated by the solid red line in each subplot.

Although the opinion formation parameters are not sensitive to influence final vaccinated household percentage, **Figure 3.10** demonstrates a notable difference in vaccination coverage between scenarios involving interaction with only one neighbouring community and those involving multiple communities. Lower vaccination coverage is observed in the under-vaccinated community when interaction is limited to only one interacting community.

This section demonstrates the effect of assimilation bias in shaping opinions and driving polarization between under-vaccinated communities and the general population. When bias is present, under-vaccinated communities that predisposed to oppose vaccination maintain their low coverage, whereas communities supportive of vaccination rapidly achieve herd immunity. This polarizing outcome reflects the role of cognitive bias in sustaining vaccine hesitancy, as previously discussed by Goldenberg (2021).

This section also shows that social isolation contributes to low vaccination coverage in under-vaccinated communities. Coverage is lower when interaction is limited to a single neighbouring group compared with multiple connections. The following section explores in more detail how inter-community interaction shapes vaccination dynamics.

3.3.6 Inter-community interaction

The analysis in the preceding section showed that parameters in the opinion formation model, such as assimilation bias (b), inter-community mixing (μ), and inter-community weight (w_{inter}), exhibit limited sensitivity in influencing vaccination coverage within an under-vaccinated community. By contrast, the number of interacting communities had a more substantial effect on vaccination dynamics. Building on these findings, this section examines how the structure of inter-community interaction shapes vaccination outcomes.

To analyse this influence, three scenarios are compared: (1) an isolated under-vaccinated community, (2) interaction with a single neighbouring community, and (3) interaction with multiple communities. The network topology is further differentiated by the presence or absence of social segregation, which is modelled based on households' bias to assimilate differing opinions and the relative weighting of inter- versus intra-community ties. Social segregation is operationalised by assigning an assimilation bias of $b_{i,j} = 1$ across all households and discounting inter-community weights such that $w_{inter} = 0.5 w_{intra}$. This "with assimilation

bias" scenario is contrasted with a "without assimilation bias" scenario, in which the parameter values are assigned as $b_{i,j} = 0$ and $w_{inter} = w_{intra} = 1$.

Overall, more connected under-vaccinated communities have a higher vaccination uptake. As demonstrated in **Figure 3.11**, under-vaccinated communities which interact with only one other community (orange line) have a lower final vaccinated household (V_f), compared with when they interact with multiple communities (blue lines), even under similar inter-community mixing (μ) proportion.

However, this connectivity benefit is suppressed with the existence of assimilation bias. When the bias exists (**Figure 3.11a–c**), the difference between single and multiple community interaction is less pronounced than in the no bias scenario (**Figure 3.11d–f**).

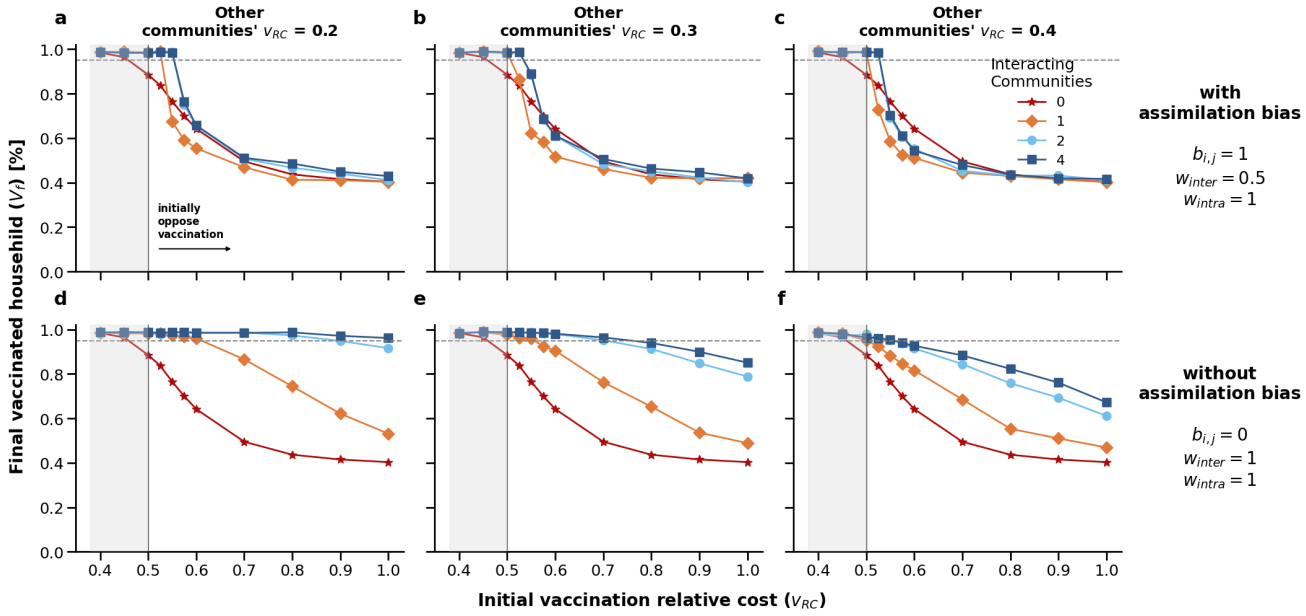


Figure 3.11. Final vaccinated household (V_f) in an under-vaccinated community influenced by inter-community opinion exchange. Final vaccinated household (V_f) is shown as a function of the initial perceived vaccination relative cost (v_{RC}) in the under-vaccinated community and the number of neighbouring communities it interacts with. Simulations are run under two conditions: with assimilation bias **(a–c)** and without assimilation bias **(d–f)**. Opinions are updated three times during the one-year vaccination season, with initial vaccination coverage set at 40% in all communities. Global parameter values are inter-community mixing (μ) = 0.3 and self-weight (w_{ii}) = 1.

Extending results from previous section, assimilation bias also modulates vaccination behaviour across various connectivity scenarios in under-vaccinated community. As shown in **Figure 3.11a–c**, there is a steep decline in final vaccinated household (V_f) when the initial

perceived vaccination relative cost (v_{RC}) exceeds the mid-range ($v_{RC} \approx 0.5$), and this effect is amplified when the neighbouring communities have a higher v_{RC} (e.g. when the other communities' v_{RC} is 0.4, compared with when the v_{RC} is 0.2). The neighbouring communities' opinion on vaccination also influences the vaccination coverage in the under-vaccinated community. In **Figure 3.11c**, final coverage is shown to fall below the no-interaction baseline (red line), indicating that neighbouring communities' opinions can have a backfiring effect within certain ranges of v_{RC} (around 0.525 to 0.8). In general, when the initial v_{RC} in the under-vaccinated community is higher ($v_{RC} \geq 0.8$), there is no significant new vaccination in that community, regardless of the level of community connectivity or the neighbouring communities' opinions on vaccination.

In contrast to the suppression of vaccination coverage observed under biased assimilation setting, **Figure 3.11d-f** show a relatively higher vaccination coverage in the under-vaccinated community without assimilation bias. There is no steep decline as seen when assimilation bias is present, and the decrease in coverage follows a linear pattern that correlates with increasing initial v_{RC}. In this unbiased setting, the influence of neighbouring communities' opinions on vaccination is still observable. As it is evident in comparison of **Figure 3.11d** and **3.11f**, the higher v_{RC} in the neighbouring communities also suppresses coverage in the under-vaccinated community.

The result in this section demonstrates that along with assimilation bias, community isolation is also responsible to hesitancy in under-vaccinated community. These findings extend previous work on the formation and implications of social segregation and polarization (Axelrod, 1997; Morales et al., 2019; Sunstein, 1999). Consistent with the concept of homophily, individuals tend to form connections with others who share similar views on vaccination, and these clusters reinforce shared attitudes (Alvarez-Zuzek et al., 2022). Such spatial clustering of vaccine hesitancy fosters segregation of under-vaccinated communities from the general population. This study further demonstrates that greater isolation of under-vaccinated communities, amplified by assimilation bias, reduces the likelihood that they will align their vaccination behaviour with the higher coverage levels of the general population.

3.3.7 External events

Previous section describes opinion formation and vaccination dynamics under the assumption that the perceived vaccination relative cost (v_{RC}) is shaped solely through opinion exchange

among households. In this section, external events that influence the v_{RC} dynamics are also simulated. Specifically, two opposing types of external events are considered: vaccine and disease scares. The vaccine scare happens due to adverse events following immunisation, while disease scare happens due to outbreaks of measles in the community. The former event will increase v_{RC}, while the latter will decrease v_{RC}.

This section simulates two scenarios: without and with an outbreak. In the no-outbreak scenario, the only possible external event is a vaccine scare, as vaccination occurs without measles transmission. In the outbreak scenario, both vaccine and outbreak scares are simulated concurrently, with vaccination and infection seeds introduced at the start of the simulation.

Initially, the effect of external events is examined by comparing simulations with and without their influence. The simulations model vaccination in an under-vaccinated community interacting with four neighbouring communities. The surrounding communities are assumed to support vaccination, with the perceived vaccination relative cost (v_{RC}) set to 0.3, while the under-vaccinated community is assigned v_{RC} = 0.7 when this parameter is not under analysis. Sensitivity analyses are conducted on inter-community mixing (μ), the effect of external events (h_v), and the initial v_{RC} in the under-vaccinated community. In these analyses, no outbreak is introduced, and the only external effect considered is a vaccine scare due to adverse events following immunisation. To ensure a balanced comparison with scenarios of without external events, households also update their opinions three times per year along with the occurrence of external events. Three scenarios of adverse event probability are compared: no vaccine risk, a risk of 1/1700 (based on the probability of febrile seizures following measles vaccination; Di Pietrantonj et al., 2021), and a hypothetical scenario of tenfold higher risk (1/170).

To capture the overall sustained shift in the perceived vaccination relative cost (v_{RC}) throughout the one-year vaccination season, the time-averaged difference of the area under the curve ($\overline{\Delta_{AUC}}$) between the baseline condition of without vaccine risk ($v_{RC}base$) and the comparison scenario with vaccine risk ($v_{RC}comparison$) is calculated using equation:

$$\overline{\Delta_{AUC}} = \frac{1}{365}\int_{0}^{365}\left(v_{RC}comparison(t) - v_{RC}base(t)\right)dt \qquad (3.4)$$

This metric provides an integrated measure of how much higher or lower v_{RC} remains in the presence of vaccine risk over the course of one year, compared to the no-risk baseline. In this

analysis, probabilities of adverse events (1/1700 and 1/170) are each compared with the no-adverse-event scenario. By quantifying the difference, the analysis highlights the extent to which vaccine scares alter the trajectory of v_{RC} dynamics in under-vaccinated communities. A positive $\overline{\Delta_{AUC}}$ indicates that the perceived vaccination cost remains higher under a vaccine scare scenario, while a negative value would indicate a relative reduction.

As expected, external events influence v_{RC} dynamics in under-vaccinated communities. As shown in **Figure 3.12**, more frequent adverse events lead to higher v_{RC} values, reinforcing perceptions of vaccination as costly. This pattern is consistent across all parameters analysed.

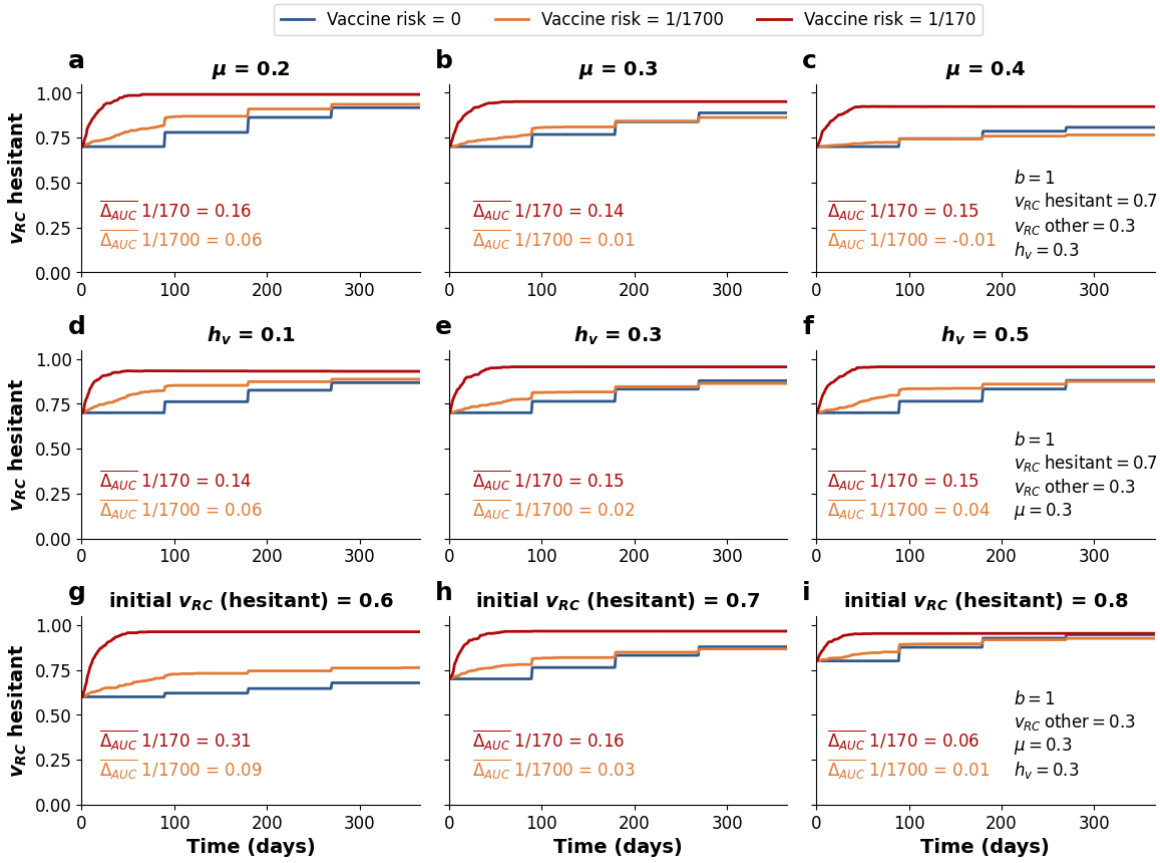


Figure 3.12. Perception of vaccination relative cost (v_{RC}) trend comparison under different vaccine risk scenarios. Trends in perceived vaccination relative cost (v_{RC}) are compared across vaccine risk settings. **(a–c)** Effects of inter-community mixing (μ). **(d–f)** Effects of vaccine scare (h_v). **(g–i)** Effects of the initial v_{RC} in the hesitant community. Time-averaged difference between the curves ($\overline{\Delta_{AUC}}$) are calculated based on difference with no vaccine risk. All simulations assume assimilation bias ($b = 1$) in under-vaccinated (hesitant) community and the interacting communities. The plotted trends are average from 100 simulations.

When adverse events are infrequent, only inter-community mixing (μ) shows sensitivity in altering v_{RC}. As illustrated in **Figure 3.12a-c**, with an adverse event probability of 1/1700, higher values of μ result in lower overall v_{RC} and reduce the gap between scenarios with and

without adverse events. This finding indicates that a more mixed under-vaccinated community remains resilient to infrequent adverse event.

Other parameters do not substantially affect v_{RC} dynamics. Simulations of vaccine scare strength (h_v) show no significant variation across values. Differences observed among h_v values are attributable to randomness, as indicated in **Figure 3.12d-f**, where no robust pattern emerges in mean $\overline{\Delta_{AUC}}$. Furthermore, initial v_{RC} strongly shapes the dynamics, even in the absence of vaccine scares. As demonstrated in **Figure 3.12g-i** higher initial v_{RC} produces faster increases in v_{RC} over time in all vaccine risk scenarios.

Building on the analysis of parameter sensitivity to external events, the next step is to examine the dynamics of v_{RC} alongside vaccination over time, expressed as the percentage of households in each community type. The effect of bias is examined by comparing simulations without assimilation bias (b = 0) and with assimilation bias ($b = 1$). The analysis focuses on the impact of a vaccine scare, modelled with an adverse event probability of 1 in 1,700 vaccinations. An additional comparison is made with a hypothetical scenario of substantially higher adverse event probability (1 in 17 vaccinations) to test whether frequent adverse events can suppress both under-vaccinated and neighbouring communities.

Figure 3.13 illustrates the effect of assimilation bias (b) on v_{RC} and vaccination dynamics. When assimilation bias is present in all communities, a polarization of v_{RC} emerges under infrequent vaccine adverse events (**Figure 3.13c**). Even a small probability of an adverse event increases v_{RC} in under-vaccinated community, while in other communities that have a lower v_{RC} (0.3), opinions still consolidate in support of vaccination, reflected by a reduction in v_{RC}. Consequently, vaccination coverage in under-vaccinated communities shows no substantial increase, whereas other communities achieve the herd immunity threshold. However, when the adverse event is simulated with 100-fold higher probability (**Figure 3.13e-f**), all communities oppose vaccination, and no communities can reach herd immunity threshold.

Following the simulation without an outbreak, focused solely on vaccination uptake, the analysis is extended to a scenario in which an outbreak is initiated by a single infection in an under-vaccinated community. In this setting, two simultaneous scares occur: a vaccine and a disease scare.

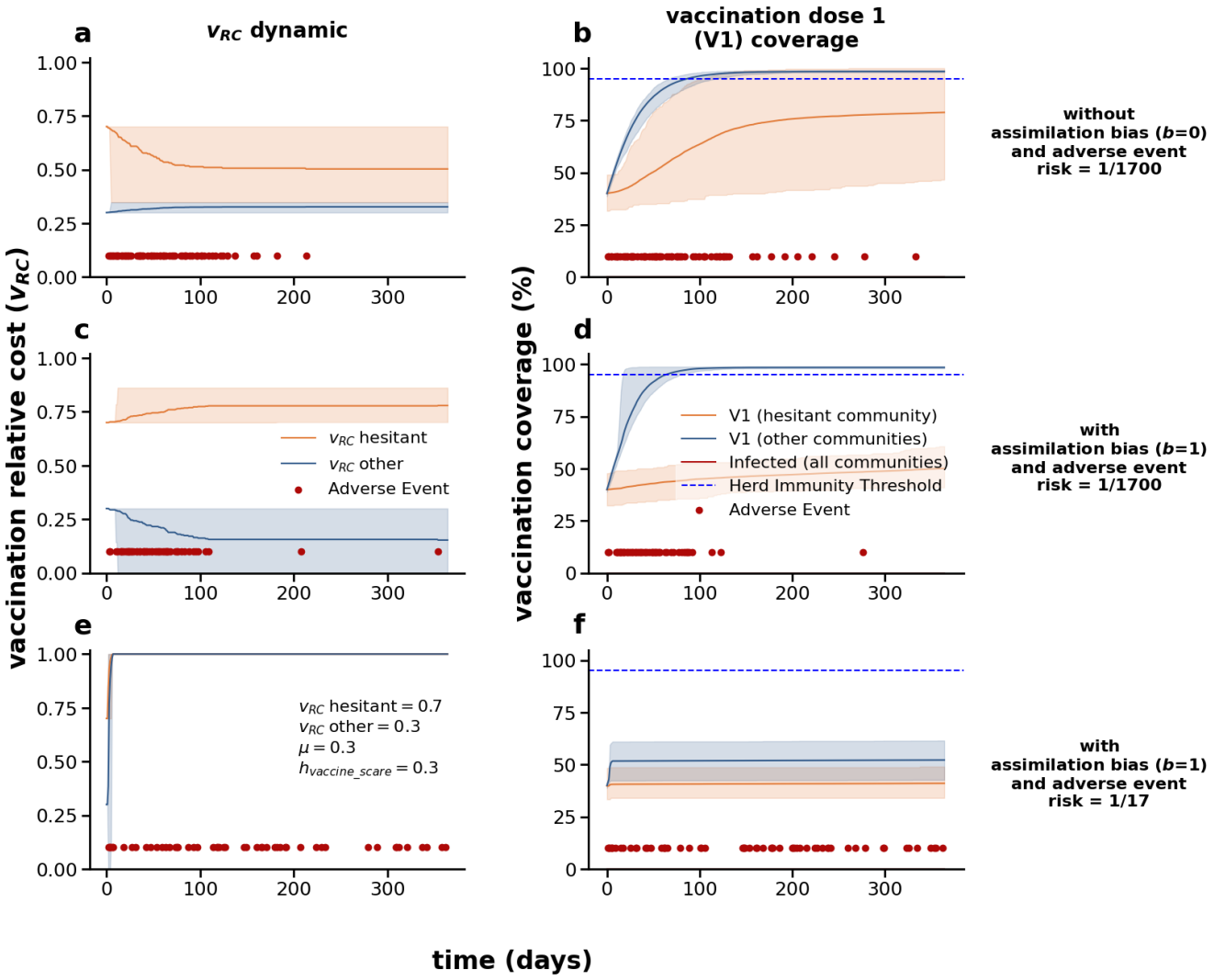


Figure 3.13. Perception of vaccination relative cost (v_{RC}) and vaccination coverage dynamics among households in under-vaccinated community and other communities when there is no measles outbreak. Either one under-vaccinated community (orange line) and other communities (blue line) are simulated simultaneously during one-year vaccination campaign. The lines show the mean v_{RC} and dose 1 vaccination trend from 100 simulations, while the colour-shade shows 95% confidence interval from all simulation runs. Each row represents various assumptions of assimilation bias (b) and adverse event risk.

Figure 3.14 demonstrates that assimilation bias (b) broadens the range of v_{RC} dynamics, as indicated by the wider orange shading in **Figure 3.14c** (b = 1) compared to **Figure 3.14a** (b = 0). Even with a prominent outbreak, v_{RC} can still increase in under-vaccinated communities when assimilation bias is present. This broader v_{RC} range translates into a relative suppression of vaccination coverage in under-vaccinated communities, as the mean coverage (orange line) is lower in **Figure 3.14d** compared to **Figure 3.14b**.

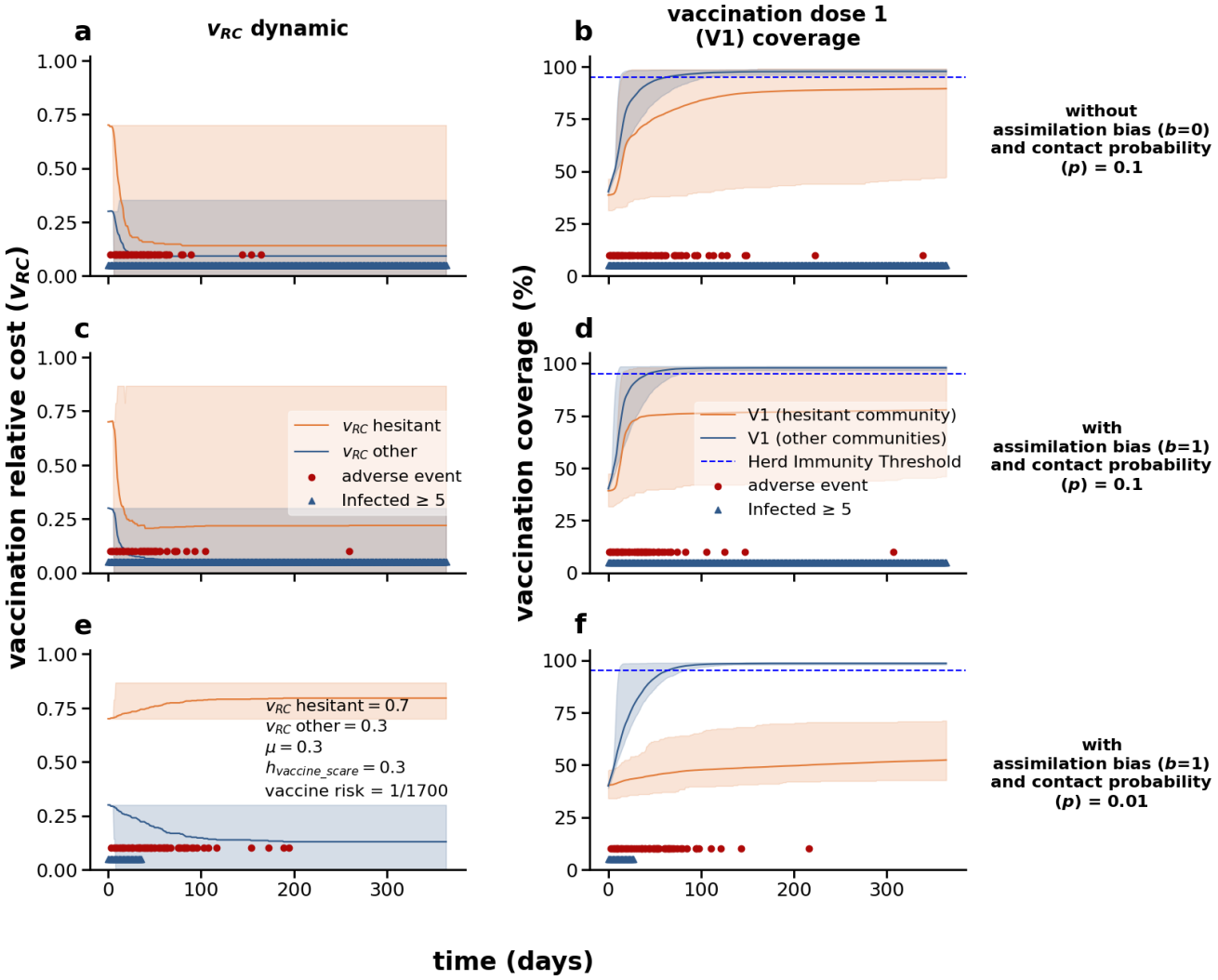


Figure 3.14. Perception of vaccination relative cost (v_{RC}) and vaccination coverage dynamics among households in under-vaccinated community and other communities when there is measles outbreak. Either one under-vaccinated community (orange line) and other communities (blue line) are simulated simultaneously during one-year vaccination campaign along with one seed of infection in the under-vaccinated communities. The lines show the mean v_{RC} and dose 1 vaccination trend from 100 simulations, while the colour-shade shows 95% confidence interval from all simulation runs.

Under a hypothetical scenario with a tenfold reduction in contact probability and the presence of assimilation bias (**Figure 3.14e-f**), v_{RC} becomes polarized between under-vaccinated and other communities. Each community reinforces its prior stance on vaccination, resulting in persistently low coverage in the under-vaccinated community, while other communities achieve herd immunity.

Assimilation bias (b) has been found to influence the dynamics of v_{RC} and the resulting vaccination coverage when external events occur. The next analysis examines b together with the external event parameter (h). It begins with simulations of vaccination in the absence of outbreaks, considering only a vaccine scare, with its effect measured as h_v. Initial vaccination

coverage in all communities is set at 40%, and the probability of an adverse event is fixed at 1 in 1,700 vaccinations.

In **Figure 3.15a**, the presence of assimilation bias (b) is shown to suppress vaccination coverage among households in under-vaccinated community, especially when opposition to vaccination is strong. When $v_{RC} \geq 0.8$, there is no vaccination among households in the under-vaccinated community if $b \geq 1$. However, a higher coverage can be reached under modest opposition ($v_{RC} < 0.6$) if $b = 1$. When $b > 1$, there is a steep decline of coverage even with modest opposition. By contrast, the vaccine scare effect (h_v) is not sensitive to influence final vaccine coverage among households in under-vaccinated community. As can be seen in **Figure 3.15b**, there is no difference of V_f under various values of h_v.

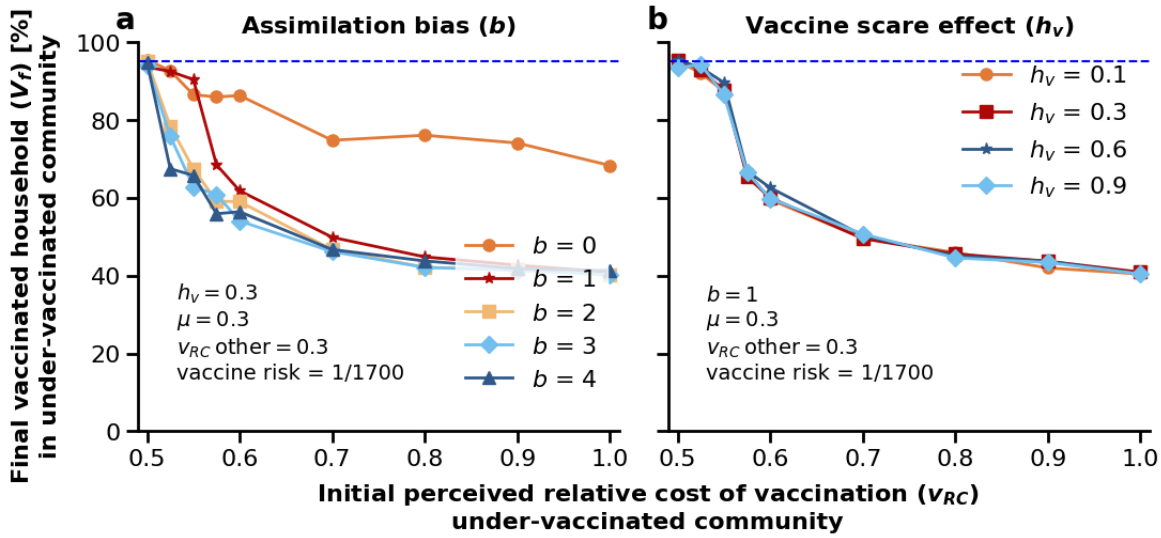


Figure 3.15. Final vaccinated household percentage following vaccine scare in under-vaccinated community without an outbreak. Final vaccinated household percentage is shown as a function of the initial perceived vaccination relative cost (v_{RC}) in the under-vaccinated community, simulated over a one-year vaccination schedule. The under-vaccinated community interacts with four neighbouring communities that support vaccination ($v_{RC} = 0.3$). The final vaccinated household percentage is the mean averaged from 50 simulations. The blue dashed line at 95% vaccinated coverage is the herd immunity threshold for measles. When the parameter is not being analysed, the global parameter values are $h_v = 0.3$, $b = 1$, $\mu = 0.3$, and v_{RC} other community = 0.3 and are depicted with starred line in each sub plot.

Next, simultaneous vaccination and outbreak events are simulated to analyse the effects of assimilation bias (b) and disease scare (h_d) on the final proportions of vaccinated and infected households in the under-vaccinated community. Both types of scare (vaccine- and disease-related) are incorporated within the same simulation. The outbreak is seeded by a single infection introduced into the under-vaccinated community. As in previous simulation, the initial vaccination coverage in all communities is set at 40%.

As shown in **Figure 3.16a**, assimilation bias (b) is sensitive to influence V_f but only on a slight effect when $b = 0$, and there is no significant difference on vaccination coverage when $b \geq 1$.

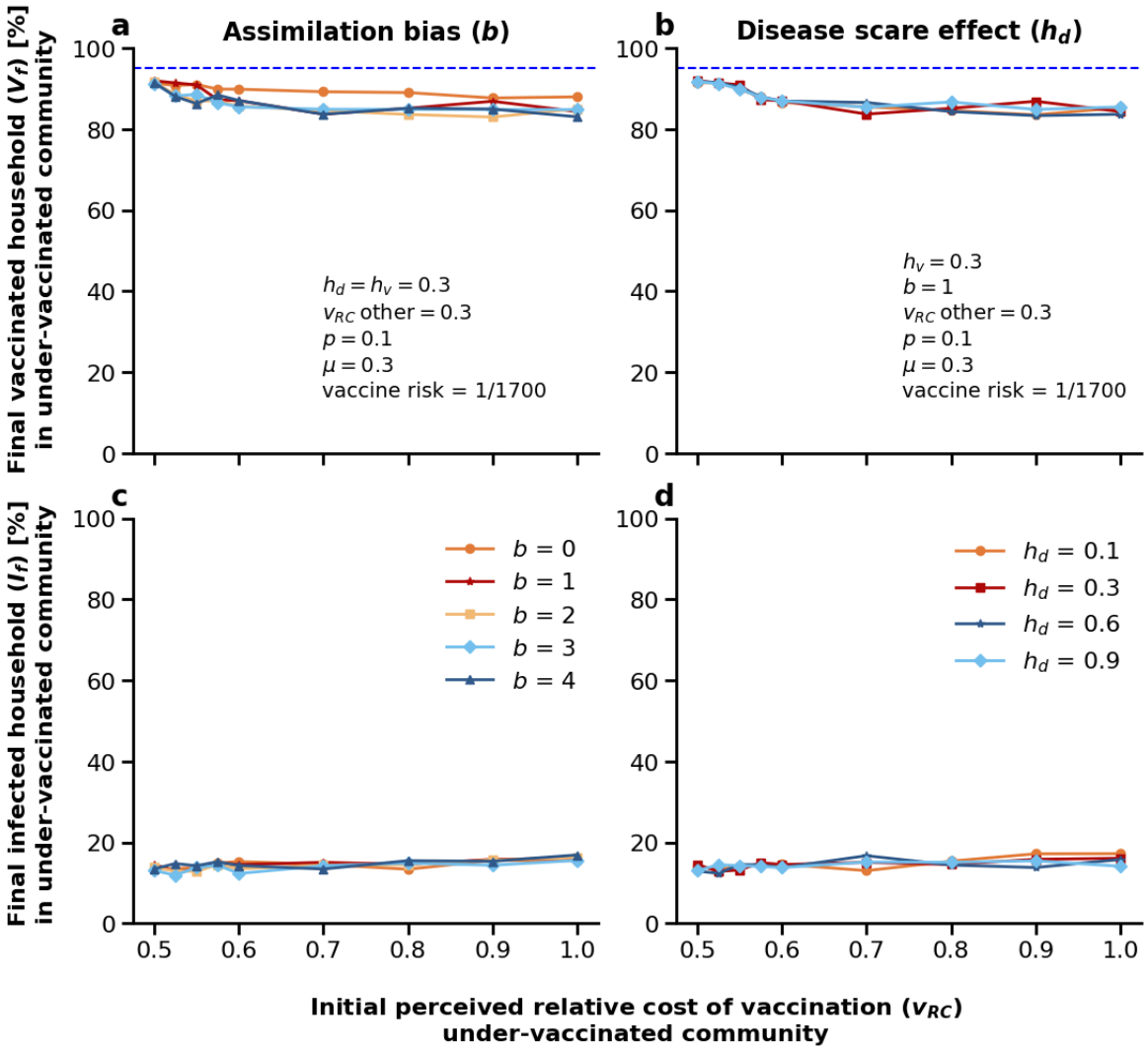


Figure 3.16. Final vaccinated and infected household percentages following vaccine and disease scares in an under-vaccinated community with an outbreak. Final outcomes are shown as a function of the initial perceived vaccination relative cost (v_{RC}) in the under-vaccinated community, simulated over a one-year vaccination schedule. The under-vaccinated community interacts with four neighbouring communities that support vaccination ($v_{RC} = 0.3$). From 100 simulations, average of **(a–b)** Final vaccinated household percentages and **(c–d)** Final infected household percentages are plotted based on assimilation bias (b) in the first column and disease scare effect (h_v) in the second column. When the parameter is not being analysed, the global parameter values are $h_v = 0.3$, $b = 1$, $\mu = 0.3$, and v_{RC} other community = 0.3 and are depicted with starred line in each sub plot.

Moreover, bias does not significantly influence infected households as can be seen in **Figure 3.16c**. **Figure 3.16b** and **3.16d** indicates that disease scares (h_d) do not significantly influence final vaccinated (V_f) and infected households (I_f) in under-vaccinated communities during a measles outbreak. Together with the results from **Figure 3.12d-f** and **Figure 3.15b**, this

demonstrates that external events are not sensitive determinants of V_f and I_f. In contrast to the dynamics observed in the absence of an outbreak, during a measles outbreak even v_{RC} is insensitive to I_f and has only minimal influence on V_f in under-vaccinated communities, suggesting that other parameters are more decisive in shaping the outcomes.

Even under opinion exchange settings, initial vaccination coverage (V_i) remains influential for V_f and I_f during measles outbreak as demonstrated in **Figure 3.17**. When $v_{RC} \leq 0.55$, V_f follows V_i, and beyond this point, V_f becomes more variable, although higher initial coverage still tends to yield higher final coverage. By contrast, the proportion of infected households is inversely related to initial vaccination coverage, with no observable effect of v_{RC}. These results extend the findings from Section 3.3.2 Vaccination behaviour and 3.3.3 Epidemiological outcomes, reinforcing that initial vaccination coverage is the most critical determinant of measles transmission and vaccination dynamics when there is outbreak in communities with $v_{RC} > 0.4$.

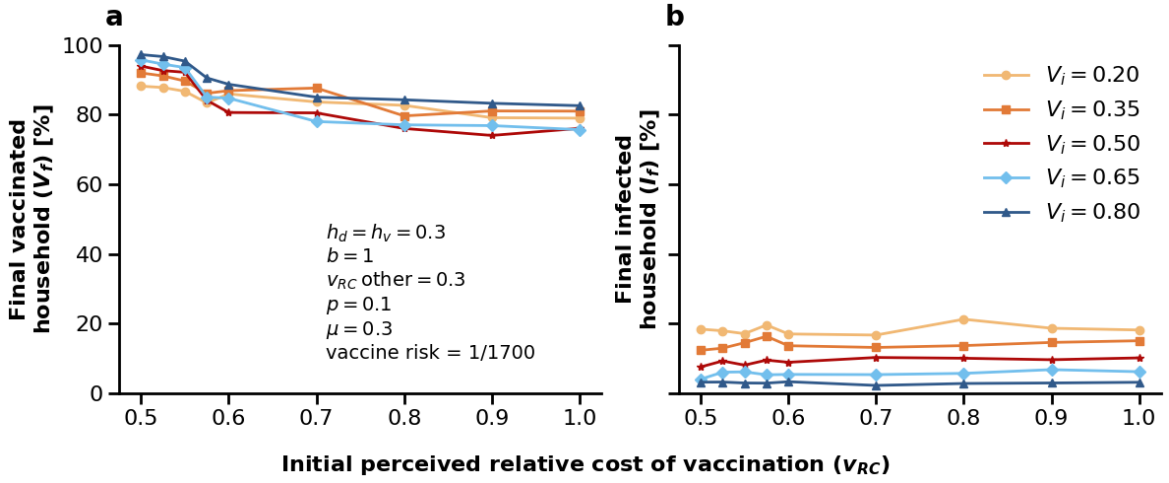


Figure 3.17. Final vaccinated and infected household percentages following vaccine and disease scares in an under-vaccinated community with an outbreak. Final outcomes are shown as a function of the initial perceived vaccination relative cost (v_{RC}) in the under-vaccinated community, simulated over a one-year vaccination schedule. The under-vaccinated community interacts with four neighbouring communities that support vaccination ($v_{RC} = 0.3$). From 100 simulations, average of **(a)** Final vaccinated household percentages and **(b)** Final infected household percentages are plotted based on initial vaccination coverage (V_i) in under-vaccinated community. The global parameter values are $h_d = h_v = 0.3$, $b = 1$, v_{RC} other community = 0.3, $p = 1$, $\mu = 0.3$, and vaccine risk = 1/1700.

This section demonstrates that the frequency of external events is a key determinant of v_{RC} dynamics. The more frequent adverse events occur, the more rapidly household opinions shift in opposition to vaccination. Under conditions of highly frequent adverse events, no other parameters show sensitivity in shaping v_{RC} dynamics. By contrast, when external events occur at a moderate frequency, households in under-vaccinated communities are more likely to align

their views with the general population, where vaccination coverage is higher, provided there is sufficient inter-community mixing.

Assimilation bias anchors households to their prior vaccination stance, even in the face of both vaccine and disease scares. As a result, under-vaccinated communities may increase their perceived vaccination relative cost during a measles outbreak, thereby suppressing vaccination behaviour despite elevated infection risk. Assimilation bias is especially influential in shaping final vaccination levels when no outbreak occurs, whereas external event effects show limited sensitivity in influencing either vaccinated or infected households in both outbreak and non-outbreak settings.

Interestingly, once a measles outbreak occurs in communities that already oppose vaccination, even the perceived vaccination cost (v_{RC}) is no longer a sensitive determinant of vaccination or infection outcomes, even under the influence of both vaccine and disease scares. These findings extend results from models without opinion updating and external events, which demonstrate that initial vaccination coverage plays a decisive role in shaping both final vaccination levels and epidemic size when communities are predisposed against vaccination. This finding underscores the importance of preventive rather than reactive immunisation in determining the vaccination and measles dynamics in under-vaccinated community.

3.4 Conclusions

The results in this chapter have illustrated mechanisms underlying several complex phenomena related to vaccine hesitancy, offering behavioural, social, and epidemiological insights into how vaccination decisions evolve in under-vaccinated communities. The results show that individuals' willingness to vaccinate is strongly shaped by their social environment. Households are less inclined to vaccinate their children when vaccination is uncommon among their neighbours, highlighting the critical role of social influence in reinforcing hesitancy. This dynamic reflects vaccination as a form of complex contagion, where costly behaviours require social reinforcement to spread.

The analyses also identify a critical threshold in the perceived vaccination relative cost (v_{RC}) that determines whether herd immunity can be achieved in one community. When v_{RC} remains below this threshold, vaccination uptake is sufficient to sustain herd immunity in the absence of an outbreak. Once v_{RC} exceeds the threshold, collective vaccination behaviour is suppressed,

and herd immunity becomes unattainable. Outbreak simulations further demonstrate that reactive vaccination is only effective when a community's perceived vaccination cost remains below this threshold. In communities where v_{RC} is high, percentage of infected households are inversely related to pre-outbreak vaccination levels. Linking back to the relationship between v_{RC} and the resulting coverage, persistently low vaccination coverage emerges as a consequence of high perception of vaccination cost within the community. As a result, when there is an outbreak in under-vaccinated community, the reactive vaccination effectiveness can be constrained by the underlying high v_{RC}. This underscores the limited utility of reactive vaccination in under-vaccinated community.

The opinion formation analysis demonstrates that assimilation bias entrenches opposition to vaccination in under-vaccinated communities, even when they interact with pro-vaccine communities. Biased assimilation strengthens prior attitudes and sustains low uptake, contributing to persistent coverage gaps among under-vaccinated community with general population.

Inter-community interaction simulations reveals that community isolation amplifies vaccine hesitancy and fosters polarization between under-vaccinated groups and the general population, along with assimilation bias. More isolated communities sustain lower coverage, whereas better-connected ones are more likely to converge toward higher vaccination levels.

The frequency of external events plays a critical role in shaping opinions and vaccination dynamics in under-vaccinated communities. More frequent vaccine scares reduce both pro-vaccination opinion and uptake, whereas more frequent disease scares increase them. Under conditions of moderate vaccine scare, greater inter-community mixing dampens the negative impact, suggesting that social connectivity can buffer communities against shocks to vaccine confidence.

In the absence of an outbreak, assimilation bias and the perceived relative cost of vaccination are important determinants of final coverage under vaccine scare scenarios. However, during a measles outbreak, both parameters exert only minor influence on final vaccination and negligible impact on infection outcomes. Notably, even under the influence of external events, initial coverage remains the critical factor, highlighting the importance of preventive over reactive immunisation in shaping both vaccination and disease dynamics in under-vaccinated communities.

3.5 Limitations

Several mechanisms underlying vaccine hesitancy have been elaborated in this chapter. While the results in this chapter provide useful insights into vaccination decision dynamics, its findings should be interpreted in light of several simplifying assumptions and constraints. Vaccination decisions were modelled at the household level, with parents assumed to be the decision makers and any infected child represented as one infected household. This approach omits intra-household heterogeneity, such as variation in children's ages or diverging parental preferences. Adults were assumed to be immune and children fully susceptible, excluding the effects of adult transmission and maternal immunity.

Both vaccination behaviour and measles transmission were simulated through the same household contact network, defined by a log-normal degree distribution fitted to 75 Indian villages and fixed at 150 households following the "Dunbar number." This assumption overlooks the possibility that infections and behaviours spread through different channels, such as physical versus virtual connections.

Vaccine availability was assumed to be immediate once a household decided to vaccinate, allowing the analysis to focus on demand-side dynamics but neglecting barriers to access that exist even in well-resourced settings. External events were also simulated in selected communities rather than the general population, making adverse events rarer in the simulations; therefore, inferencing these findings to wider populations should be done with caution.

Finally, the simulations in this chapter relied on an agent-based modelling approach, which faces inherent limitations in computational scalability. Simplifying agents to the household level, embedding them in inter-household social networks, and representing collective dynamics at the community scale enabled both tractability and reproducibility. Given that routine childhood vaccination, such as measles immunisation, is typically decided at the household level by parents, the modelling approach used here provides a reasonable and representative framework for examining childhood vaccination decision dynamics in community level.

Chapter 4 Estimating Perceived Relative Cost of Vaccination

4.1 Introduction

In Chapter 3, the vaccination decision dynamics demonstrates that perceived vaccination relative cost (v_{RC}) is critical in determining vaccination behaviour in a community. However, the v_{RC} is not directly observable in routine health information systems. Current immunisation programmes record and report vaccination uptake and incidence of vaccine-preventable diseases, but they do not systematically collect data on perceptions around vaccination. As a result, the practical utility of v_{RC} is constrained by data availability.

In this chapter, we aim to develop a method for estimating v_{RC} in a population using routinely reported vaccination uptake and incidence data through inverse problem estimation. To do so, we employ the agent-based vaccination decision model introduced in Chapter 2 and show how it is possible to infer the temporal dynamics of v_{RC} in a given population using administrative data routinely collected through immunisation programmes. Because v_{RC} is inferred indirectly, not all model parameters in the vaccination decision model can be identified separately from the observed data. The identifiability of the estimated parameters is discussed further in Section 4.4.

A psychological belief about vaccination should be distinguished from actual vaccination behaviour (Bussink-Voorend et al., 2022; Goldenberg, 2021; Larson, 2022), of which there is a record in the uptake data. People can still vaccinate due to external pressures, such as vaccine mandates, yet their hesitancy persists. Therefore, the model introduced in this chapter adds value in addressing vaccine hesitancy by enabling the monitoring of temporal trends in the cognitive state toward vaccination within a population.

As a use case, this chapter applies the method for estimating v_{RC} to provincial-level data containing measles vaccination uptake and incidence in Indonesia. Although the average vaccine coverage has been declining (Figueiredo et al., 2020; Wiegand et al., 2023) nationally, vaccination uptake varies substantially across provinces (as elaborated in the descriptive analysis later in this chapter). Some provinces have maintained consistently high or low uptake

over many years, even during disruptions due to Covid-19 pandemic or boosting in the catch-up periods of supplementary immunisation activities. The diversity in uptake across provinces makes Indonesia an appropriate use case for implementing the v_{RC} estimation method.

Indonesia is classified as a country with endemic measles transmission, and most of its province have no significant access constraints to vaccination services. Almost all provinces report measles case each year, despite the vaccine being provided free of charge. While vaccination access is generally adequate, some outermost and remote regions still experience accessibility challenges. Therefore, the lessons from this chapter are most applicable to settings where measles remains endemic and access barriers to vaccination are minimal.

4.2 Methods

To estimate the temporal dynamics of perceived vaccination relative cost (v_{RC}) across Indonesian provinces, this chapter implements a framework proposed by Monti et al. (2023). This framework supports the use of agent-based modelling (ABM) by initially transforming the ABM into a deterministic emulator to make it scalable to population-level data and to efficiently learn from observed data while inferring underlying hidden variable(s). The framework is thus well-suited for estimating the hidden variable v_{RC} from observed vaccination uptake and measles incidence, while implementing an agent-based vaccination decision model.

The framework follows the Generalized Expectation Maximization (GEM) algorithm (Dempster et al., 1977), as implemented in Monti et al. (2023). The GEM is an iterative process of Expectation (E-Step) and Maximization (M-Step) steps which are simulated through multiple iterations (epochs). The generalized term in the GEM reflects the process of learning through the series of data in the model. In the context of estimating v_{RC}, the workflow can be summarised as follows:

1. E-Step: Given the current v_{RC} values, simulate vaccination uptake and measles incidence.
2. M-Step: Compare simulated outcomes with observed data and compute the loss.
3. Repeat the alternating E- and M-steps through several iterations (epochs), updating v_{RC} at each iteration in an attempt to minimise the loss.

This Methods section explains the step-by-step process of the analysis. Initially, the administrative data are pre-processed to mitigate over-reporting of vaccination and under-reporting of cases. A preliminary calibration process of global and province specific parameters takes place before the GEM steps (the main "machine" of the analysis), as elaborated subsequently. Because GEM performs best when supplied with an optimal initial working estimate of v_{RC}, the method used to obtain this preliminary estimate is also outlined. Finally, the model framework is concluded by a reconciliation procedure of the estimated v_{RC} from the GEM. This reconciliation step transforms the raw and potentially noisy v_{RC} estimates into smoother and more behaviourally interpretable trajectories.

4.2.1 Dataset

This analysis uses administrative data of annual measles-containing-vaccine dose 1 (MCV-1) uptake and monthly measles incidence per 1 million population for each province in Indonesia during 2017-2023 vaccination seasons. Data were obtained from Indonesian Health Profile repository published by Indonesian Ministry of Health (Kementerian Kesehatan Republik Indonesia, 2024). The MCV-1 data are generated from measles-rubella vaccination dose 1 (MR-1) uptake, which is available on an annual timescale, while the measles incidence is probed from monthly reports of suspected cases. The vaccination data are collated from number of vaccine recipients and the target-children denominator, while the monthly reports of suspected cases are compared with total number of population denominators from official statistics. Both the vaccination and suspected cases datasets are available for all provinces and are published annually by the Indonesian Ministry of Health (Kementerian Kesehatan Republik Indonesia, 2024).

Measles incidence data in Indonesia was probed from monthly surveillance reports of suspected cases, defined as fever with maculopapular rash unless laboratory testing confirmed as another pathogen, for which a symptom onset date is recorded (Kementerian Kesehatan Republik Indonesia, 2020). In the Indonesian context, case finding is predominantly based on clinical symptoms suggesting measles, as laboratory confirmation covers only a small proportion of suspect, only 16-63% of total cases in 2018-2022 (Chacko, 2023). Consequently, in this study, the incidence was calculated based on total suspected cases each month from the Ministry of Health report, divided by annual population estimates from the Indonesian Central Bureau of Statistics.

Considering the potential for over- and under-reporting in the administrative data, a scaling procedure is applied to the vaccination uptake and measles incidence data (further description of the adjustment can be found in **Appendix A** Reported data adjustment). The MR-1 reported data is adjusted using the WUENIC (WHO-UNICEF estimates of national immunisation coverage) scaling approach (Burton et al., 2009), calculated by comparing WUENIC estimates and administrative data reported to WHO (World Health Organization and UNICEF, 2025). Conversely, provincial measles incidence is adjusted using national surveillance performance metrics from CDC (Chacko, 2023), considering that the reported incidence depends on surveillance capacity. It should be noted here that the WUENIC and surveillance capacity scales are available only at the national level, while the MR-1 and the measles incidence data are disaggregated by provinces. Therefore, for this analysis, it is assumed that the over-reporting of vaccination and under-reporting of incidence scales are homogenous across provinces.

To account for disruptions during the Covid-19 pandemic and the implementation of supplementary immunisation activities (SIA) within the study period, several adjustments are implemented. Vaccination service access and case detection were reduced in 2020-2021 due to lockdowns, therefore simple multipliers ($r_y < 1$) are applied to weight-down vaccination capacity and reported incidence in those years. SIAs, which increase vaccination uptake, are represented through temporary increases in month specific vaccination capacity based on the schedule of the SIAs. The SIA enhancement is implemented in 2017 for provinces in Java and Bali islands, in 2018 for provinces outside of Java-Bali, and in 2022 for nationwide campaign to catch vaccination gap coverage due to Covid-19 related service disruption.

4.2.2 Parameter calibration

The achieve optimal learning, the GEM model requires several parameters to be specified before estimating the perceived vaccination relative cost v_{RC}. Rather than relying on ad hoc hand-tuning, a sequential calibration procedure is implemented. This calibration comprises of two stages:

1. a global search for parameters governing the objective (loss) function and the learning dynamics.
2. a province-specific search for monthly vaccination capacity ($monthly_{cap}$); and year-specific estimation of incidence sensitivity ($risk_{scale}$) and hesitant fraction (π_h).

Global level parameter calibration

At the global level, five parameters are calibrated across all province-year pairs in the dataset:

- ω_{vac}: the relative weight of uptake in the objective (loss) function. At this stage, the incidence weight is fixed at $\omega_{inc} = 1$, and $\omega_{vac} > 1$ is used to prioritize uptake fitting over incidence.
- $\sigma_{vac}, \sigma_{inc} > 0$: scale parameters for the uptake and incidence squared-error terms (interpreted as Gaussian noise scale).
- lr: the learning rate used in the M-Step to update v_h and v_o.
- $risk_{scale}$: initially fitted at the global level and later refitted separately for each province-year.

At this stage, $monthly_{cap}$ is fixed at 1/12 for all provinces and will be recalibrated for each province in the next stage.

The model is run across all province-year pairs using combinations of all five global parameter sets, and the mean loss per epoch is recorded. To efficiently explore the five-dimensional parameter space, a three-stage continuous search is implemented using low-discrepancy sampling and progressive zooming (Klein et al., 2023). The low discrepancy sampling provides broad uptake of the five-dimensional parameter space with fewer evaluations than the standard random or grid searches. The progressive zooming then narrows the search around promising regions, allowing the algorithm to efficiently refine the best parameter combination candidates without exploring the full global space. This combination offers a computationally efficient yet robust strategy for tuning the global parameters set.

In Stage 1, n_1 = 48 candidates of parameter sets are generated using Halton-based Latin hypercube design within predefined bounds (linear scale for ω_{vac} and logarithmic scale for $\sigma_{vac}, \sigma_{inc}, lr,$ and $risk_{scale}$). A coarse ranking of candidate parameter sets is obtained by running each configuration for a reduced number of epochs.

In Stage 2, a refined local search is performed in the neighbourhood of the top candidate from Stage 1. The search interval is reduced to 50% of the original range around the selected candidate values, and n_2 = 24 new parameter sets are drawn.

In Stage 3, the search space is further narrowed to 20% of the original range around the best-performing candidate from Stage 2. A final set of n_3 = 12 parameter refinements is sampled and evaluated by re-running the model using the full number of epochs.

The three-stage search implements a constant halving schedule ($48 \rightarrow 24 \rightarrow 12$), anchored on n_3= 12 for evaluations that were computationally feasible under full set of 30 epochs. Stage 1 and 2 use reduced number of epochs to obtain a coarse ranking from the set of broad candidates, while stage 3 implements full epoch to concentrate on fewer candidates.

For each candidate combination, the loss $\mathcal{L}$ is computed for every province-year pair as defined in Eq.4.10. The mean loss across all province-year pairs at each epoch is then recorded, and the epoch with the minimum mean loss is selected and used as the base configuration for objective function and learning rate for M-Step.

Province level parameter calibration

It is assumed that each province has its own maximum capacity to deliver vaccination each month ($monthly_{cap}$). This monthly trend is assumed to be constant year on year. However, population sensitivity to reported measles incidence ($risk_{scale}$), and the proportion of hesitant individuals is allowed to vary each year (π_h). Here, calibration is performed in two steps, initially calibrating constant $monthly_{cap}$ and evolving $risk_{scale}$ for each province, then calibrating dynamic π_h across provinces. In both steps, the GEM algorithm is implemented with a lower number of epochs.

In calibrating the $monthly_{cap}$ and $risk_{scale}$, the hesitant population fraction is initially held fixed at π_h = 0.05 based on MMR vaccine hesitancy estimate (Gilkey et al., 2016), and the global parameter values resulting from the previous calibration stage are applied to all provinces. For each province, the $risk_{scale}$ search is limited to the range of monthly reported incidence experienced by the province, ensuring that the parameter search of $risk_{scale}$ is consistent with local scale of disease incidence.

The parameter search is conducted through a nested grid search of a linear grid of six candidates for $monthly_{cap} \in [0.05, 0.1]$ for each province p, and a log-space grid of each candidates for $risk_{scale}$ in every province-year p, y. Each parameter candidate is proposed as an initial guess of a GEM process, and fits for each year are scored according to the mean data loss at the best

epoch. For each $monthly_{cap}$ candidate, the optimal per year $risk_{scale}$ is identified and the minimal losses are recorded. Then, losses are averaged across years and the $monthly_{cap}$ with the smallest average loss being selected. Finally, the corresponding year-by-year $risk_{scale}$ associated with the winning cap is retained for the next process of calibrating the proportion of hesitant community (π_h) for each year.

The proportion of hesitant individuals in one province is allowed to vary, enabling the model to separate stable perception of vaccination relative cost (v_{RC}) from possible temporal changes in sub-population composition due to local events, campaigns or social changes that can affect the structure of local communities, but at the provincial level they only appear as gradual dynamics of v_{RC}. To allow the π_h to be varied dynamically over the year, the perceived vaccination relative cost (v_h and v_o) should be assigned as constant over the year during the π_h calibration. Yet the constraint $v_h > v_o$ is still enforced.

Calibration proceeds via two alternating steps that iterate across epochs: Step A to update constant v_h and v_o using the latest π_h, and Step B to update π_h using the latest constant v_h and v_o. These alternating steps are repeated for an assigned number of epochs.

In the initial Step A, for a given province p, provisional hesitant fraction π_h for each province is used to estimate a single pair of constant v_h and v_o, that minimise the average loss over the years in that province. For the initial step, π_h is assigned as constant over the year, along with the produced v_h and v_o.

Then for Step B, the fixed v_h and v_o from the initial step are then implemented to estimate π_h over the year for each province p. The optimal $\pi_{h,y}$ is searched over a grid of π_h values for each year, with smoothing penalties applied in logit space to ensure temporal coherence of π_h over the years. The resulting yearly π_h values are then implemented back into Step A.

These alternating steps are iterated after a maximum number of epochs has been achieved. By this point, both (v_h, v_o) and $\pi_{h,y}$ have stabilised and yield a consistent parameter value from the alternating steps.

4.2.3 Generalized Expectation-Maximization implementation

Expectation step (E - Step)

In the E-Step, the model simulates the expected vaccination uptake and the consequential incidence based on the assumed v_{RC}. To allow the agent-based model (ABM) to be compared to population-based data for both vaccination uptake and incidence, the ABM is transformed into a deterministic form.

The reported incidence is mapped into perceived risk of infection for each month in each province. In the ABM, the perceived risk of infection $p_{j,t}$ represents the risk signal household j receives when interacting with neighbouring household t. Perceived risk $p_{j,t}$ = 1 if t has a previous history of infection or is currently infected and $p_{j,t}$ = 0 otherwise. For the deterministic transformation, the binary risk indicator is transformed into an exponential saturating function ($p_{j,t} \rightarrow pr_t$), that maps monthly incidence I_t to the risk of measles infection perceived by the population each month t according to:

$$pr_t = 1 - \exp\left(- \frac{I_t}{risk_{scale}} \right) \tag{4.1}$$

A unique $risk_{scale}$ for each province-year reflects time varying incidence sensitivities for each province. A smaller $risk_{scale}$ indicates that the population is more reactive to incidence. It is assumed that populations are reactive to disease pressure, but their sensitivity to such a response saturates. A major outbreak will give rise to higher level of fear, but after reaching a certain level, the level of fear will not increase dramatically.

Here, vaccination is scheduled weekly, i.e. the population makes weekly vaccine uptake decisions. The perceived risk of infection pr_t is then compared with the perceived relative cost of vaccination v_{RC} to compute willingnes to vaccinate each week Ψ_w using the vaccination decision model:

$$\Psi_w = \theta^{\alpha} \frac{1}{1 + \exp\left(\frac{v_{RC} - pr_t}{k}\right)}, \qquad \theta = \frac{N_0}{Z} \tag{4.2}$$

Another deterministic transformation is adapted into the willingness equation. In the ABM setting, each household evaluates vaccination popularity in their neighbourhood. For the

deterministic update, vaccination popularity θ is assigned at the population level according to the same year's vaccination uptake data (V_y) for the v_{RC} estimation task and previous year's vaccination uptake data (V_{y-1}) for prediction task. For 2017, the first year of the analysis, θ takes that year's vaccine uptake.

Population heterogeneity also contributes to localised patterns of vaccine uptake. Clusters of hesitant communities can form pockets of under-vaccinated children despite high general population coverage (Anis et al., 2021; Masters et al., 2020). The model considers different vaccination popularity between hesitant (θ_h) and other communities (θ_o). The hesitant communities have a lower vaccination popularity ($\theta_h < \theta_o$) which is determined by $\delta_\theta \in (0, 1)$. The hesitant and other communities' vaccination popularity are assigned by:

$$\theta_h = \delta_\theta . V_{y-1}, \qquad \theta_o = V_{y-1} \tag{4.3}$$

In this study, vaccination popularity in the vaccine hesitant community is assigned as half of the general population (δ_θ = 0.5).

Since there is a different vaccination popularity in hesitant and other communities, vaccination uptake is calculated separately for those distinct community types. By considering the vaccination willingness each week, the successful vaccination each month in hesitant ($V_{h,t}$) and other ($V_{o,t}$) communities are calculated by:

$$V_{h,t} = 1 - \left(1 - \Psi_{h,w}\right)^{\frac{52}{12}},$$

$$V_{o,t} = 1 - \left(1 - \Psi_{o,w}\right)^{\frac{52}{12}}. \tag{4.4}$$

The successful monthly vaccination is a compounded probability of vaccination over several weekly independent iterations for 52 weeks divided by 12 months a year. At this point, the $monthly_{cap}$ is relaxed to 0.08, enabling complete uptake within a year.

Since the available dataset is in population uptake, the community type uptakes are converted to population uptake (V_t) that are determined by proportion of hesitant community (π_h) in the population.

$$V_t = \pi_h V_{h,t} + (1 - \pi_h) V_{o,t} \tag{4.5}$$

To account for the maximum number of vaccination doses that can be administered each month, a $monthly_{cap}$ is imposed on the simulated uptake in the population. Conversely, during Supplementary Immunisation Activities (SIA), this cap is increased and multiplied by a SIA multiplier for a specific province-year based on the SIA schedule. It is assumed in this study that there was an increased $1.5 \times monthly_{cap}$ during SIAs.

Susceptible fraction S_0 is initialized for each year y, by calculating the average of the three preceding years' annual vaccination uptake. If there are less than three years retrospective data available, the data is computed by averaging the available year data, while for 2017, the S_0 is equal to $1 - V_{12}^{obs}$ from the 2017 data. The $S_0 \geq 0.0013$ is calculated by dividing the Indonesian crude annual birth rate of 0.016 by 12 months. It means that even for 100% uptake in previous vaccination campaign, there is still possibility of measles cases in the population given the new birth cohort.

The vaccination at each month t determines the susceptible fraction at the end of that month ($S_t = 1 - V_t^{sim}$). Furthermore, the susceptible fraction at month t determines the course of infection at the next month $t + 1$, and the simulated incidence is:

$$I_t^{sim} = \lambda_y \, S_{t-1} \, r_y \tag{4.6}$$

To account for Covid-19 related disruption which limit vaccination and disease course, a multiplier $r_y < 1$ is implemented for 2020 and 2021 (r_{2020}: 0.4 ; r_{2021}: 0.6).

The λ_y is an estimated force of infection for each province-year. The λ_y is fitted by regressing the observed incidence in a month (I_t^{obs}) on the remaining susceptible from previous months (S_{t-1}) divided by Covid-19 multipliers (r_y):

$$\lambda_y = \frac{\sum_t^m S_{t-1} I_t^{obs}}{r_y \sum_t^m S_{t-1}^2} \tag{4.7}$$

Here is the recap of the deterministic process in the expectation step (E-Step). At the start of each year, the size of the susceptible population (S_0) is calculated for each province. Then the reported measles incidence I_t^{obs} is used to estimate perceived measles risk for that month (pr_t), which will further determine willingness to vaccinate each week $\Psi_{w,t}$ for both hesitant communities and general population. The willingness is then applied to produce simulated

vaccination uptake in the population V_t^{sim} at the end of each month. The remaining susceptible fraction $S_t = 1 - V_t^{sim}$ represents the population at risk for infection at the start of next month. Overall, within each year, the deterministic flow is:

$$I_t^{obs} \rightarrow pr_t \rightarrow \Psi_{w,t} \rightarrow V_t^{sim} \rightarrow S_t \rightarrow I_{t+1}^{sim}$$

Although measles is typically a seasonal disease in endemic settings (Moss and Griffin, 2012), either driven by school calendars (Fine and Clarkson, 1982), or climatic cycles (Ferrari et al., 2008), evidence from Indonesia does not support a consistent seasonal pattern. Autocorrelation analysis, Seasonal-Trend decomposition via Loess (STL), and Kruskal-Wallis tests all show no significant seasonal signal (**Appendix B** Seasonality analysis of measles).

Measles transmission in Indonesia during 2017-2023 therefore appears to be driven by sporadic outbreak events rather than a predictable seasonal cycle, and this analysis proceeds under the assumption of no seasonality of measles incidence. If the model is implemented in settings with explicit seasonal pattern, the data can be incorporated into the model either by removing the seasonal component from the observed incidence during dataset pre-processing, or by introducing an explicit seasonal forcing into the incidence calculation in this E-Step.

After the uptake and incidence have been simulated simultaneously, the next step is to measure discrepancies between reported and simulated data.

Objective (loss) function

In the objective function, the discrepancies between reported and simulated data are calculated, and the calculated loss will further be minimised in the Maximization Step (M-Step). Here, a Gaussian negative log-likelihood (NLL) is implemented into uptake and incidence loss calculation, since discrepancies between $I^{obs} - I^{sim}$ and $V^{obs} - V^{sim}$ are real-valued and continuous. The Gaussian NLL therefore provides a convenient and numerically stable loss function for penalising continuous data – model discrepancies.

The incidence dataset contains a monthly series of measles reported case, so the Gaussian NLL for incidence (I_{NLL}) implements mean of monthly series (m) over the course of one year:

$$I_{NLL} = \frac{1}{m} \sum_{t=1}^{m} \frac{\left(I_t^{obs} - I_t^{sim}\right)^2}{2\,\sigma_{inc}^2}, \qquad t = 1, \dots, m \tag{4.8}$$

In contrast, only annual uptake data of MCV-1 vaccination is available, so the NLL is only calculated at the year-end point only. The vaccine uptake NLL (V_{NLL}) is then calculated by:

$$V_{NLL} = \frac{\left(V_y^{obs} - V_{12}^{sim}\right)^2}{2\sigma_{vac}^2} \tag{4.9}$$

The σ_{inc} and σ_{vac} represent the residual distributions for incidence and uptake respectively. These σ's set expectation of mismatch between observed data and the model's best achievable fit and are calibrated from the data prior to running the GEM model.

Finally, the total loss balances the NLL from incidence and uptake by considering each weight of importance (ω_{inc}, ω_{vac}):

$$\mathcal{L} = \omega_{inc} \,.\, I_{NLL} + \omega_{vac} \,.\, V_{NLL} \tag{4.10}$$

Weight of incidence ω_{inc} and weight of vaccination ω_{vac} encode preference between incidence and vaccination NLL. The $\omega_{vac} > \omega_{inc}$ are set in this study, since the main objective is in estimating the v_{rc}. A higher ω_{vac} is prioritized for adjusting to v_{rc} to match the reported annual vaccine uptake, even if incidence fit degrades.

Maximization step update (M-Step)

The purpose of the Maximization Step (M-Step) is to minimize loss by performing gradient descent step of the perceived vaccination relative cost (v_{RC}) value. In the M-Step, the gradient of the loss is computed, and simultaneously moves v_{RC} in the direction that decreases the loss. Along with the vaccination popularity difference, it is assumed that there is a difference of v_{RC} in hesitant (denoted with v_h) and other communities (v_o).

The GEM algorithm implemented in this study applies gradient-based optimization, in which the parameter values are iteratively updated following the direction that most reduces the model's loss (discrepancies between observed and simulated data). To enhance the optimization task, the v_h and v_o are initially transformed into unconstrained space of mean (u_m) and difference (u_d) through logit transformation. First, v_h and v_o are linearly rescaled into (0, 1) before the logit transformation:

$$s_h = \frac{v_h - v_{min}}{v_{max} - v_{min}}, \qquad s_o = \frac{v_o - v_{min}}{v_{max} - v_{min}},$$

$$z_h = log\left(\frac{s_h}{1 - s_h}\right), \qquad z_o = log\left(\frac{s_o}{1 - s_o}\right). \tag{4.11}$$

Then the unconstrained parameter u_m (mean) and u_d (difference) are computed as:

$$u_m = \frac{z_h + z_o}{2},$$

$$u_d = softplus^{-1}(z_h - z_o). \tag{4.12}$$

where $$softplus^{-1}(y) = \log(e^y - 1)$$

The logit transformation maps the v_h and v_o values from bounded and stable range (0, 1), into an unbounded linear space $(-\infty, +\infty)$ which is more suitable for gradient-based optimization.

After the logit transformation into unconstrained space, the u_m and u_d are mapped back into v_h and v_o for base loss computation $\mathcal{L}(u_m, u_d)$:

$$d = softplus(u_d), \qquad z_h = u_m + \frac{d}{2}, \qquad z_o = u_m - \frac{d}{2},$$

$$v_h = v_{min} + (v_{max} - v_{min})\sigma(z_h), \tag{4.13}$$

$$v_o = v_{min} + (v_{max} - v_{min})\sigma(z_o).$$

where $$softplus(x) = \log(1 + e^x),\ \sigma(x) = \frac{1}{1 + e^{-x}}.$$

Instead of the raw value, the base loss computation implements the after-transformation value to the unconstrained space of v_h and v_o to address consistency with the u_m and u_d mapping, along with enforcement of the rule: $v_{max} > v_h > v_0 > v_{min}$.

In unconstrained space, u_m and u_d are perturbed by small amount of d_u, and then mapped back to new v_h and v_o. Using the new v_h and v_o, the loss is recomputed and approximate derivative of the gradient direction are:

$$\frac{\partial \mathcal{L}}{\partial u_m} \approx \frac{\mathcal{L}(u_m + d_u, u_d) - \mathcal{L}(u_m, u_d)}{d_u},$$

$$\frac{\partial \mathcal{L}}{\partial u_d} \approx \frac{\mathcal{L}(u_m, u_d + d_u) - \mathcal{L}(u_m, u_d)}{d_u}. \tag{4.14}$$

Then the gradient descent step in unconstrained space moves opposite to the gradient direction with learning rate lr to find new u_m and u_d:

$$u_{m_new} = u_m - lr.\frac{\partial \mathcal{L}}{\partial u_m},$$

$$u_{d_{new}} = u_d - lr.\frac{\partial \mathcal{L}}{\partial u_d}. \quad (4.15)$$

If the $\frac{\partial \mathcal{L}}{\partial u} > 0$, it means that there is a higher loss in the perturbed than the base u. Then the u_{new} must move into opposing direction by reducing the value to minimize the loss. Conversely, if increasing u reduces the loss, the updated u_{new} value should be increased.

After the gradient optimization process, then the u_{m_new} and u_{d_new} are converted back to updated v_h and v_o. A new loss is then evaluated again in this point and the updated v_h, v_o and loss are then recorded.

4.2.4 Perceived vaccination relative cost (v_{RC}) estimation and reconciliation

Perceived vaccination relative cost (v_{RC}) estimation

The GEM procedure requires proper initialization of v_{RC} in the hesitant (v_h) and other (v_o) communities across multiple years in each province. A data-driven initialization of v_h and v_o are conducted through two options: (i) grid search for first year for each province, and (ii) implement previous year's best $v_{gen}(y-1)$ for the subsequent years.

For the grid search, candidate values of $v \in [v_{min}, v_{max}]$ are being iterated, by initially assuming that $v_o = v_h = v$. For each candidate v, monthly uptake over a single year is simulated to produce simulated vaccine uptake over a year (V_y^{sim}). The best value of v is selected based on which one produces the smallest squared difference of the simulated and observed uptake:

$$v^* = \arg min_v \left(V_y^{sim} - V_y^{obs}\right)^2 \quad (4.16)$$

After the best v^* for this grid search has been found, the rule $v_h > v_o$ is implemented by converting v^* into an initial value before the GEM algorithm begins updating:

$$v_0^{(0)}(y) = v^*, \qquad v_h^{(0)}(y) = v^* + gap \tag{4.17}$$

where gap is a fixed constant to ensure $v_h > v_o$. Both values are clipped to an allowable domain $[v_{min}, v_{max}]$. Then the v_h and v_o are mixed into general perceived cost $v_{gen}(y)$ for a given year:

$$v_{gen}(y) = \pi_h(y)v_h(y) + \big(1 - \pi_h(y)\big)v_o(y) \tag{4.18}$$

The $v_{gen}(y)$ represents perceived vaccination relative cost in the general population for year y in one province, while it is recalled that π_h gives the proportion of hesitant households in each province-year.

For the subsequent year, the general perception of vaccination relative cost from previous year $v_{gen}(y-1)$ is used directly:

$$v_0^{(0)}(y) = v_{gen}(y-1), \qquad v_h^{(0)}(y) = v_0^{(0)}(y) + gap. \tag{4.19}$$

Both grid-search for the first year and the carry over best v_{RC} produce one initialized pair of $(v_0^{(0)}(y), v_h^{(0)}(y))$ for every year in one province.

The next step for v_{RC} estimation is the iterative GEM updating by iterating through several epochs. For each epoch, the GEM process goes year by year inside each province. The M-Step will update the $v_o(y)$ and $v_h(y)$ through minimizing loss using the objective function, and then the E-Step will simulate uptake and incidence using the updated $v_o(y)$ and $v_h(y)$. The EM fitting is conducted separately for each province, assuming that the behavioural dynamics are independent within each province.

Reconciliation of v_{RC} trend estimation

The GEM process produces raw $v_o(y)$ and $v_h(y)$ which can show dramatic fluctuations over the years. This happens because the GEM process optimizes the hidden variable v_{rc} for each year to fit both the vaccine uptake and incidence data. The fluctuated v_{rc} can be statistically correct but behaviourally irrelevant, because shifts in perceived cost of measles vaccination happen gradually, not dramatically over the years (Torracinta et al., 2021). Therefore, to derive a behaviourally coherent and interpretable result of the v_{rc} trend, a post-estimation reconcilitian procedure is conducted to the raw $v_o(y)$ and $v_h(y)$ data.

First, the median of each year difference of the perceived vaccination relative cost between hesitant and other communities $\delta(y) = v_h(y) - v_o(y)$ is computed to find each province constant difference (δ_{const}). The δ_{const} is subject to minimal gap δ_{min} between two community types to ensure that $v_h > v_0$. The raw yearly difference $\delta(y)$ is clipped to the interval [0, δ_{max}] to avoid extreme difference (δ_{max} = 0.6). This procedure of finding δ_{const} follows the assumption that the relative difference in the perceived vaccination cost between hesitant and other communities is stable over the period of analysis.

Next, the yearly general level of vaccination cost perception $v_{gen}(y)$ in each province is smoothed using quadratic penalty on year-to-year difference:

$$v_{gen}^{sm} = \arg\min_{x_1,\dots,x_T} \sum_{y=1}^{T} \Big(x_y - v_{gen}(2)\Big)^2 + \lambda_{post} \sum_{y=2}^{T} \big(x_y - x_{y-1}\big)^2 \tag{4.20}$$

This smoothing procedure penalises drastic change of general perception of vaccination cost in the population over the years. This reflects the assumption that the general perception of vaccination relative cost is changed gradually over the years.

Finally, the constant difference (δ_{const}) and the smoothed general perception of vaccination cost (v_{gen}^{sm}) are reconciled into the $v_o(y)$ and $v_h(y)$:

$$v_h^{rec}(y) = v_{gen}^{sm}(y) + \big(1 - \pi_h(y)\big)\delta_{const},$$

$$v_o^{rec}(y) = v_{gen}^{sm}(y) - \pi_h(y)\delta_{const}. \tag{4.21}$$

along with final bounding step to ensure $v_h^{rec}(y), v_o^{rec}(y) \in [v_{min}, v_{max}]$. The final reconciliation process also includes calculating the reconciled v_{RC} for general population each year in one province:

$$v_{gen}^{rec}(y) = \pi_h(y)v_h^{rec}(y) + \big(1 - \pi_h(y)\big)v_o^{rec}(y) \tag{4.22}$$

4.2.5 In-sample model fit and uncertainty quantification

In-sample model fit is evaluated by measuring agreement between simulated and reported data of MCV-1 uptake and measles mean monthly incidence, and by quantifying uncertainty through the posterior predictive distribution. Agreement is assessed using mean absolute error

(MAE) and coefficient of determination (R^2), and uncertainty is expressed as 95% Bayesian credible intervals derived via Markov Chain Monte Carlo (MCMC) sampling.

MAE is measured differently for MCV-1 uptake and measles incidence, reflecting the distinct statistical properties for each outcome and to ensure comparability across provinces. For MCV-1 uptake, the absolute MAE is used directly given that uptake is bounded on [0,1]. For measles incidence, however, the MAE is normalised by the provincial mean incidence to account for wide variation in baseline incidence across provinces. Without normalisation, provinces with inherently higher incidence would produce larger absolute errors simply due to scale, making cross-provincial comparison unfair. The resulting normalised MAE is therefore scale-invariant and represents the error as a fraction of the typical incidence level in each province.

The reporting noise parameters of the reported data were specified as modelling assumption in the absence of province-level validation data. Although the MCV-1 uptake and measles incidence reported data have been normalised with WUENIC and surveillance performance scales, both scales only apply at the national level, and there is still possibility of reporting noise at the provincial level. For reported data of MCV-1 uptake, the reporting noise was set to 10%. For measles incidence, the reporting noise was set to 10% of each province's highest reported monthly incidence, with a minimum threshold of 1 per million incidence per month to ensure numerical stability in provinces with very low or near-zero incidence.

To quantify parameter uncertainty, a Bayesian inference framework was adopted in which six model parameters were jointly estimated for each province-year from the reported MCV-1 uptake and mean monthly measles incidence. The jointly estimated six parameters are the perceived vaccination relative cost of hesitant and non-hesitant communities (v_h, v_o), the proportion of the hesitant communities (π_h), the monthly cap of vaccination delivery ($monthly_{cap}$), the perceived $risk_{scale}$, and the yearly force of infection (λ_y).

Prior distributions of parameter values were specified to be minimally restrictive, allowing the data to drive parameter estimation while keeping values within plausible bounds. Uniform priors were specified for the bounded behavioural parameters with v_h and v_o constrained to [0.01, 0.99], π_h to [0.01, 0.50], and $monthly_{cap}$ to [0.03, 0.20]. Log-uniform priors were assigned to the positive epidemiological scale parameters, with $risk_{scale}$ bounded to [0.05, 500] and λ_y to [0.01, 500]. Additionally, the perceived vaccination relative cost in hesitant communities was constrained to be higher than of the other communities ($v_h > v_o$).

The joint posterior distribution over all six parameters was estimated simultaneously using Markov Chain Monte Carlo (MCMC), performed using *emcee* sampler (Foreman-Mackey et al., 2013). *emcee* is a Python implementation of affine-invariant ensemble sampler for MCMC, in which multiple chains called "walkers" explore the parameter space simultaneously by proposing new parameter combinations based on the current positions of other walkers. Affine invariance means the sampler performs equally well regardless of the scale or correlation structure of the parameters, making it well-suited to models with parameters of varying magnitude without requiring manual tuning of step sizes. The performance of the MCMC is evaluated by autocorrelation time and acceptance fraction. There is no universally accepted threshold for autocorrelation time, but shorter values are preferable (Foreman-Mackey et al., 2013), and the acceptance fraction should be in the range of 0.2 to 0.5 (Gelman et al., 1996).

4.2.6 Out-of-sample validation

This section describes an out-of-sample validation methods, distinct from the in-sample model evaluation in Section 4.2.5, to assess the model's ability to predict measles vaccination uptake and incidence using parameters calibrated on years other than the year being predicted. In Section 4.2.5, the model was evaluated through agreement and uncertainty between simulated and reported data, where the simulated data were generated from parameters calibrated on the reported data of a given year and then evaluated against the same data. The circularity arises from the refitting of the force of infection (λ_y) which is obtained by regression on the observed monthly incidence (I_t^{obs}) of the same year (Eq.4.7), while the same I_t^{obs} also enters the perceived risk of infection (pr_t) that drives willingness to vaccinate (Eq.4.1). The behavioural parameters, namely perceived vaccination relative cost (v_{RC}), vaccine hesitant communities proportion in the population (π_h) and the incidence sensitivity ($risk_{scale}$), were also fitted to the reported data and then evaluated against data from the same year. Although the model is designed for estimation rather than prediction, an out-of-sample validation provides a stronger test of whether the model captures vaccination behaviour and disease dynamics beyond the data used to calibrate it.

The out-of-sample validation followed a rolling-origin design with an expanding fitting window (Tashman, 2000), in which the reported data series for 2017-2023 were divided into two folds, each consisting of a fitting and a test period. In the first fold, the model was fitted to the 2017–2021 data and used to predict 2022. In the second fold, the fitting period was

expanded to 2017-2022 and the model was used to predict 2023. Data from the test year were not used for fitting, except in the reference settings described below. Each fold was evaluated across the 34 provinces. The national data were excluded from the analysis because they are an aggregate of the provincial data. The two folds therefore produced 68 held-out province-years for the out-of-sample prediction test.

Within each fitting period, the province-specific monthly vaccination capacity ($monthly_{cap}$), and province-year-specific force of infection (λ_y), incidence sensitivity ($risk_{scale}$), perceived vaccination relative cost in hesitant and other communities (v_h, v_o), and hesitant fraction (π_h) were estimated using data from the fitted years period only. The monthly vaccination capacity is assumed to be constant over the years and therefore applied unchanged to the test year. The capacity boost from the 2022 SIA was supplied to the 2022 test year based on the scheduled SIA months in each province, since SIA schedules are planned and known before implementation. The rules for carrying forward the parameters values from the fitting period to the test period are described in **Table 4**:

Table 4. Carry-forward rule of the behavioural parameters and the force of infection.

Parameters	**Carry-forward rule**
Force of infection (λ_y)	Mean of the fitted years period
Incidence sensitivity ($risk_{scale}$)	Geometric mean of the fitted years estimates
Perceived vaccination relative cost (v_h, v_o)	Estimated and reconciled from the final fit year
Hesitant fraction (π_h)	Estimated from the final fit year

Measles incidence in the dataset is driven mainly by irregular outbreaks rather than by a seasonal cycle (Appendix B Seasonality analysis of measles), therefore the carried-forward value for force of infection (λ_y) is the mean of the fitted period. In contrast, the carried-forward incidence sensitivity ($risk_{scale}$) was the geometric mean of the fitted years value, considering this parameter is fitted on a log-spaced grid (Section 4.2.2). The carried-forward values for perceived vaccination relative cost (v_h, v_o) and hesitant fraction (π_h) were from the final year of the fitting period, since both parameters are already smoothed over time (Section 4.2.2 for π_h and Section 4.2.4 for v_h, v_o).

Prediction was repeated under five information settings (S1 – S5), which differ in how much the model may learn from the test years. Each setting is defined by three factors; whether the behavioural parameters ($risk_{scale}, v_h, v_o, \pi_h$), the force of infection (λ_y) and the incidence which influence perceive risk of measles infection (p_{rt}) in Eq.4.1, adopt carry-forward value from fitted years or re-estimated from the test year data, as can be seen in **Table 5**. Specifically for S5, the incidence data for measles risk perception is simulated by the model.

Table 5. Information settings of the prediction model.

Setting	Behavioural parameters ($risk_{scale}, v_h, v_o, \pi_h$)	Force of infection (λ_y)	Incidence entering measles perceived risk (Eq.4.1)
S1	Re-estimated on the test year	Re-estimated on the test year	Reported data
S2	Re-estimated on the test year	Carried forward	Reported data
S3	Carried forward	Re-estimated on the test year	Reported data
S4	Carried forward	Carried forward	Reported data
S5	Carried forward	Carried forward	Model-generated

The five information settings were ordered by how much information they use from the test year, from the most informed to a full forecast. S1 is the most informed setting, because the behavioural parameters and λ_y were re-estimated on the test years and the reported incidence enters the perceived risk of infection (pr_t) in Eq.4.1. S2 differs from S1 only in that the λ_y was carried forward from the fitting period. In S3 and S4, the behavioural parameters are carried forward from the fitting period, while λ_y is either re-estimated on the test year (S3) or carried forward (S4). Comparing S1 with S2, and S3 with S4, therefore isolates the effect of refitting λ_y on the test year, which is the source of the circularity described at the first paragraph in this section. Finally, S5 is the full forecast setting, in which the model simulates vaccination uptake and measles incidence without using any data from the test year. The only difference between S4 and S5 is the incidence entering the perceived risk of infection, so comparing these two settings isolates the contribution of reported incidence to predicted uptake. Because S1–S4 all use reported incidence from the test year, they serve as reference settings, and S5 is the only setting that constitutes a true out-of-sample prediction.

The model's prediction of vaccination uptake and measles incidence in the test years were compared against simple baseline models. For vaccination uptake, the baselines were last year's uptake, the provincial mean uptake over the fitting period, a linear trend in uptake over

the fitting period, and a lagged uptake–incidence model. For measles incidence, the baselines were the incidence in the same month of the final fitting year and the provincial mean incidence for each calendar month over the fitting period.

The predictions of all models were compared with the reported annual MCV-1 uptake and the reported mean monthly measles incidence using the mean absolute error (MAE), as in the in-sample evaluation (Section 4.2.5). The uptake error was calculated on its original scale [0, 1], whereas the incidence error was calculated on a logarithmic scale, because incidence varies by several orders of magnitude across provinces and years. The predictive performance of each model was then summarised using a skill score, which measures the accuracy of a predictor relative to a reference forecast (Murphy, 1988; Tashman, 2000). For an accuracy measure whose perfect value is zero, such as the MAE used in this analysis, the skill score is:

$$skill\ score = 1 - \frac{MAE\ (predictor)}{MAE\ (reference)} \tag{4.23}$$

The skill score is zero when the predictor is as accurate as the reference, positive when the predictor is more accurate than the reference, and negative when it is less accurate. It reaches a maximum of one for a perfect prediction.

The uncertainty of the skill score was estimated using a paired bootstrap over provinces. In each of 10,000 bootstrap resamples, 34 provinces were drawn with replacement, and both held-out years of each selected province were retained together. The skill score was recomputed for each resample, and the 95% percentile intervals was implemented as the confidence interval. Provinces, rather than province-years, were resampled to account for the dependence between the two held-out years (2022 and 2023) within the same province. The pairing between the predictor and the reference was preserved in every resample, so that both were always evaluated on the same set of province-years.

4.3 Results

4.3.1 Measles vaccination and incidence trends in Indonesia

There are persistence and polarizing trends of measles-containing-vaccine dose 1 (MCV-1) uptake across provinces in Indonesia. **Figure 4.1a** shows that provinces with low uptake in 2023 had sustained low uptake since 2017, whereas provinces with high uptake in 2023

maintained their high uptake over the same period. The pattern of high and low uptake even persisted during supplementary immunisation activities (SIAs) which are conducted in 2017 for provinces in Java and Bali islands (home to more than half of children in the country), in 2018 for provinces outside of Java-Bali and in 2022 for a nationwide campaign following Covid-19 pandemic. During the Covid-19 pandemic (2020-2021) there was a restriction of vaccination service, and the provinces with persistently low uptake have the lowest drop of MCV-1 vaccination during that period. Moreover, the discrepancies between the low and high uptake provinces gradually widen over time, with the low uptake provinces having a progressively lower uptake.

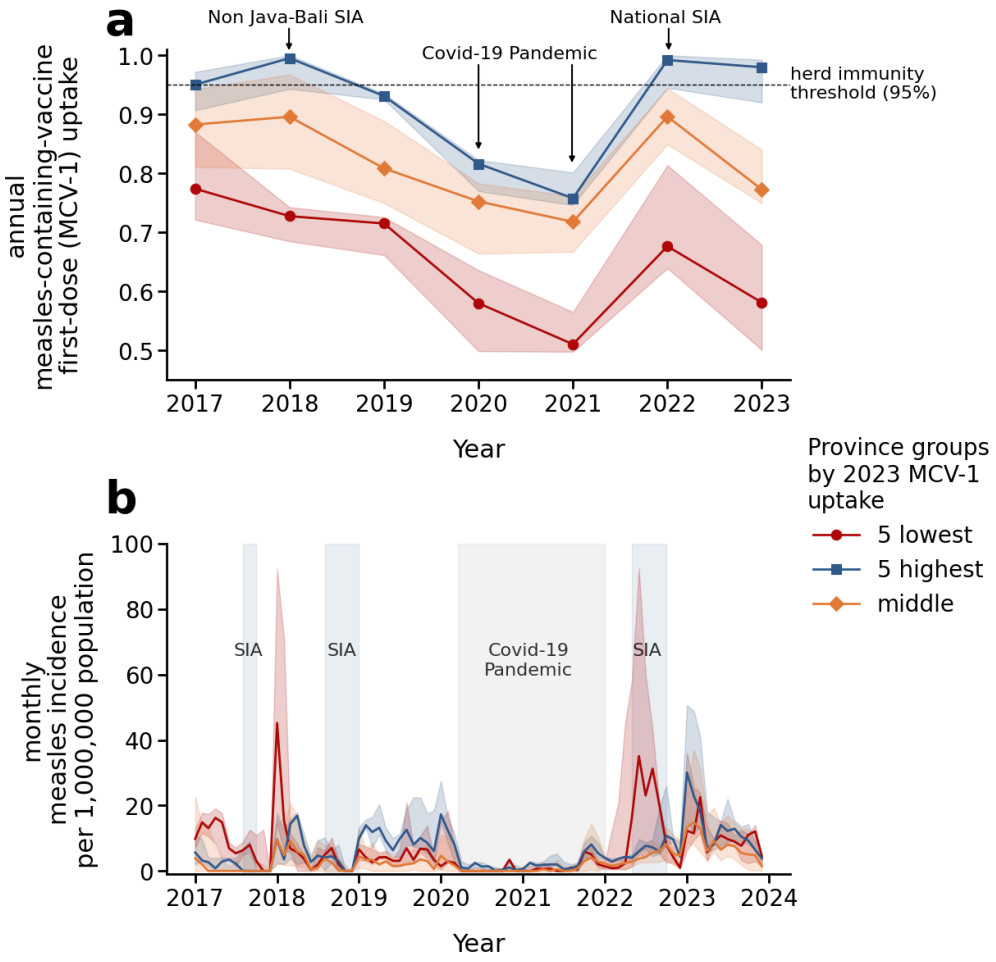


Figure 4.1. Indonesian reported measles vaccination uptake and incidence. **(a)** The national MCV1 uptake divided by 5 provinces with lowest, middle and 5 highest uptake in 2023 data, after adjustment with WUENIC scale. Note the trend dynamics are increased during supplementary immunisation activities (SIA) and decreased during Covid-19 pandemics. **(b)** The national monthly incidence of measles, after adjustment with the national surveillance capacity for each year. The lines represent the median and the shaded areas represent the interquartile range. The surveillance capacity data are not available in 2017, then no incidence adjustment for that year.

As expected, provinces with the lowest vaccination uptake over the years have the greatest risk of large measles outbreaks. **Figure 4.1b** highlights two prominent national flares, in 2018 and 2022, which happened in provinces with the lowest MCV-1 uptake. Following decline of vaccination uptake due to Covid-19, Indonesia experienced a nationwide measles outbreak in 2023. However, the lowest uptake provinces were less affected, because they had already experienced large outbreaks earlier in 2022. Moreover, the 2023 nationwide outbreak had a lower incidence than the localized outbreaks in the least vaccinated provinces in 2022.

4.3.2 In-sample model fit

In-sample model fit is assessed using mean absolute error (MAE), coefficient of determination (R^2), and 95% Bayesian credible intervals from the posterior predictive distribution. **Figure 4.2** presents the MAE and R^2 diagnostics, while **Figure 4.3** and **Figure 4.4** show the credible intervals for MCV-1 uptake and mean monthly measles incidence from Markov Chain Monte Carlo (MCMC) simulation.

The model achieves a small mean absolute error (MAE) for both MCV-1 uptake and measles incidence across provinces (**Figure 4.2a-b**). The maximum MAE for MCV-1 uptake is 0.065, observed in Papua province, while the maximum normalised MAE for incidence is 0.283, observed in Maluku province. Furthermore, the error is negatively associated with both reported MCV-1 uptake (Pearson r = -0.58, $p < 0.001$) and reported measles incidence (r = -0.41, $p < 0.05$), indicating that provinces with lower vaccination coverage or lower baseline incidence tend to exhibit larger errors.

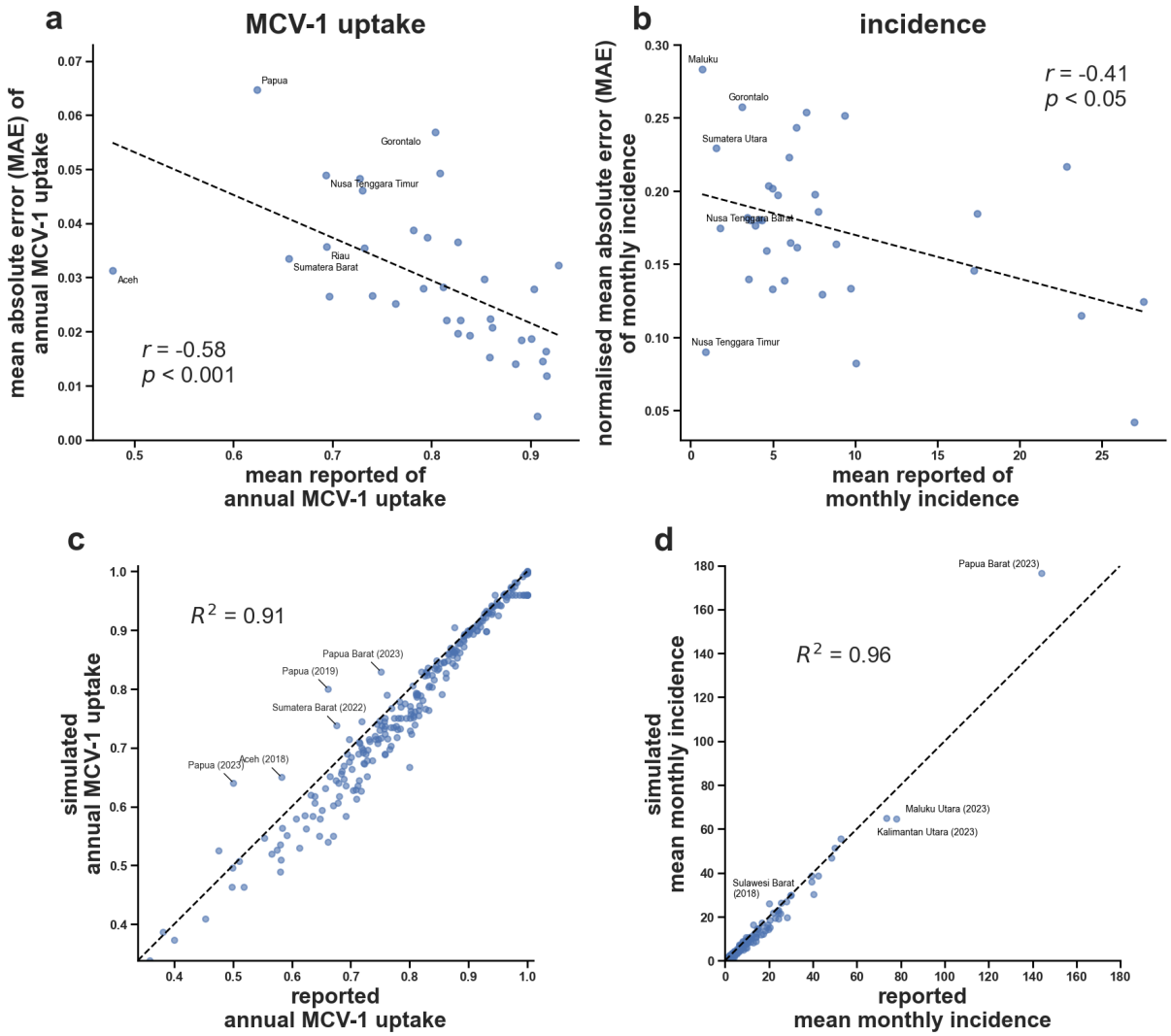


Figure 4.2. Evaluation of model accuracy for MCV-1 uptake and measles incidence across Indonesian provinces. (**a**) Correlation between provincial mean reported annual MCV-1 uptake and mean absolute error (MAE) of annual MCV-1 uptake. (**b**) Correlation between provincial mean reported monthly measles incidence and normalised MAE of monthly incidence. In panels a and b, each point represents a province, and the Pearson correlation coefficient is shown. (**c-d**) Agreement between simulated and reported annual MCV-1 uptake and mean monthly incidence. In panels c and d, the dashed lines denote the 1:1 line and the coefficient of determination (R^2) is shown. In panel b and d, incidence is expressed per 1 million population.

There is strong agreement between simulated and reported data for MCV-1 uptake and mean monthly measles incidence, as reflected in the high coefficient of determination (R^2 = 0.91 for uptake and R^2 = 0.96 for incidence) shown in **Figure 4.2c-d**. However, simulated MCV-1 uptake is predominantly lower than the reported values, as most data points lie below the 1:1 diagonal line. In contrast, the measles incidence data points are clustered closely around the 1:1 diagonal line, with the exception of Papua Barat (2023), where the model simulates a higher incidence rate than reported. For further reference, the basic and effective reproductive number for each province-year is provided in **Appendix D** Basic and effective reproductive number

The performance of the *emcee* MCMC sampler for analysing model uncertainty was evaluated using acceptance fraction and integrated autocorrelation time (IAT) following Foreman-Mackey et al. (2013). Across all evaluated province-year combinations, acceptance fraction ranged from 0.23 to 0.34 (mean = 0.27), falling within the recommended range of 0.2 to 0.5 (Gelman et al., 1996). The maximum IAT ranged from 27.7 to 36.0 steps (mean = 31.3) from a total run length of 300 steps, which corresponded to a steps-to-IAT ratio of 8.3 to 10.8, consistent with the recommendation of running the sampler for approximately 10 x IAT steps (Foreman-Mackey et al., 2013). The full diagnostic results of the MCMC are reported in Supplementary Document 1. Together, these diagnostics indicate that the sampler achieved adequate convergence and mixing across all province-year combinations, providing reliable uncertainty quantification.

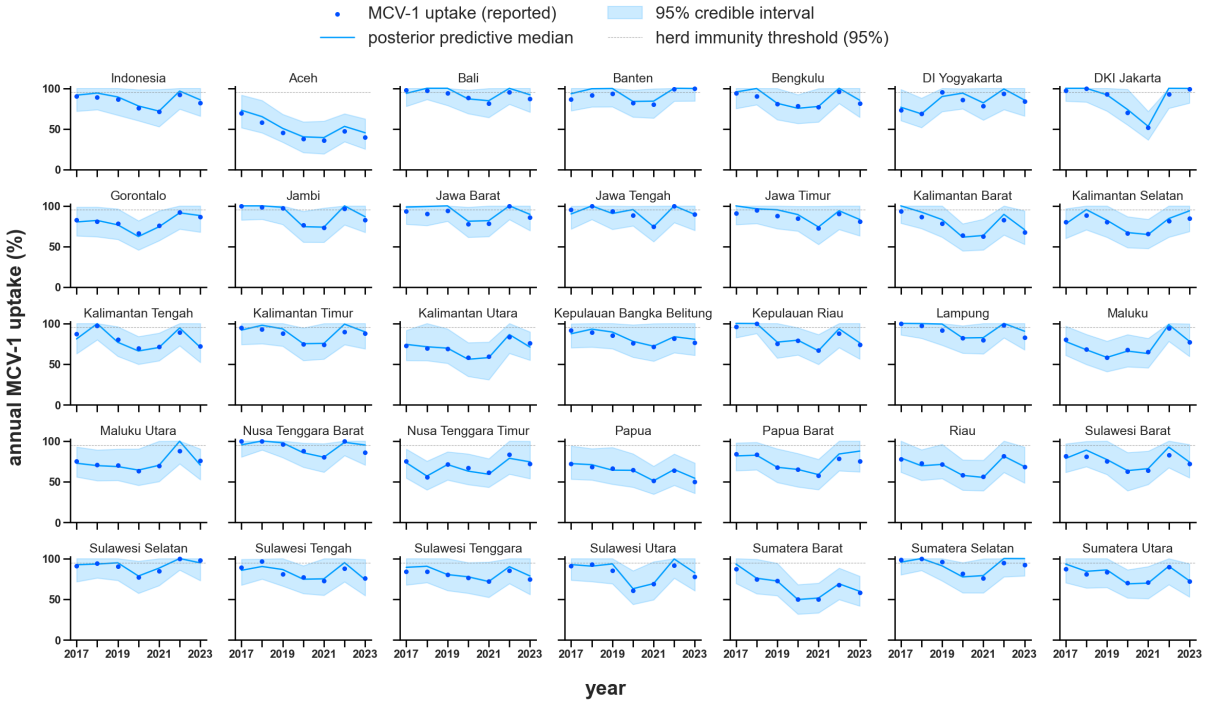


Figure 4.3. Posterior predictive distribution of provincial measles-containing vaccine dose 1 (MCV-1) uptake in Indonesia, 2017–2023. The reported annual MCV-1 uptake (blue dots) is shown along with the median prediction from the posterior predictive distribution (blue line). The shaded blue bands represent the 95% Bayesian credible interval, derived from 1,000 posterior predictive samples drawn via Markov Chain Monte Carlo (MCMC) sampling of the six-parameter joint posterior (v_h, v_o, π_h, $monthly_{cap}$, $risk_{scale}$, λ_y). Given the observed data and model, the true value lies within this interval with 95% probability. The dashed horizontal line shows the required 95% herd immunity threshold for measles.

The chosen method of MCMC simulation with affine-invariant ensemble sampler (Foreman-Mackey et al., 2013) produces an appropriate fit to the observed temporal patterns of MCV-1 vaccination uptake over the 2017-2023 study period (**Figure 4.3**). In most provinces, the

posterior predictive median tracks the reported uptake closely, and the 95% credible intervals generally envelop the reported data points. The model also captures key national patterns in uptake trends, including the decline during the Covid-19 pandemic in 2020-2021 and the subsequent increase during supplementary immunisation activities (SIA) in 2022.

In contrast, the model shows greater uncertainty in fitting the reported measles incidence compared to MCV-1 uptake, although it captures the general magnitude and trend of incidence across provinces (**Figure 4.4**). In general, the posterior predictive median of incidence tends to be lower than the reported data points, with the exception of Aceh, Nusa Tenggara Timur, Papua Barat and Sulawesi Barat, where the posterior median intersects with the reported data points. The reported incidence is generally within the 95% credible interval band, with the exception to Jambi (2022), Kalimantan Tengah (2019) and Kepulauan Bangka Belitung (2017), as detailed in the full list of reported MCV-1 uptake and measles incidence data with their 95% credible intervals in Supplementary Document 2.

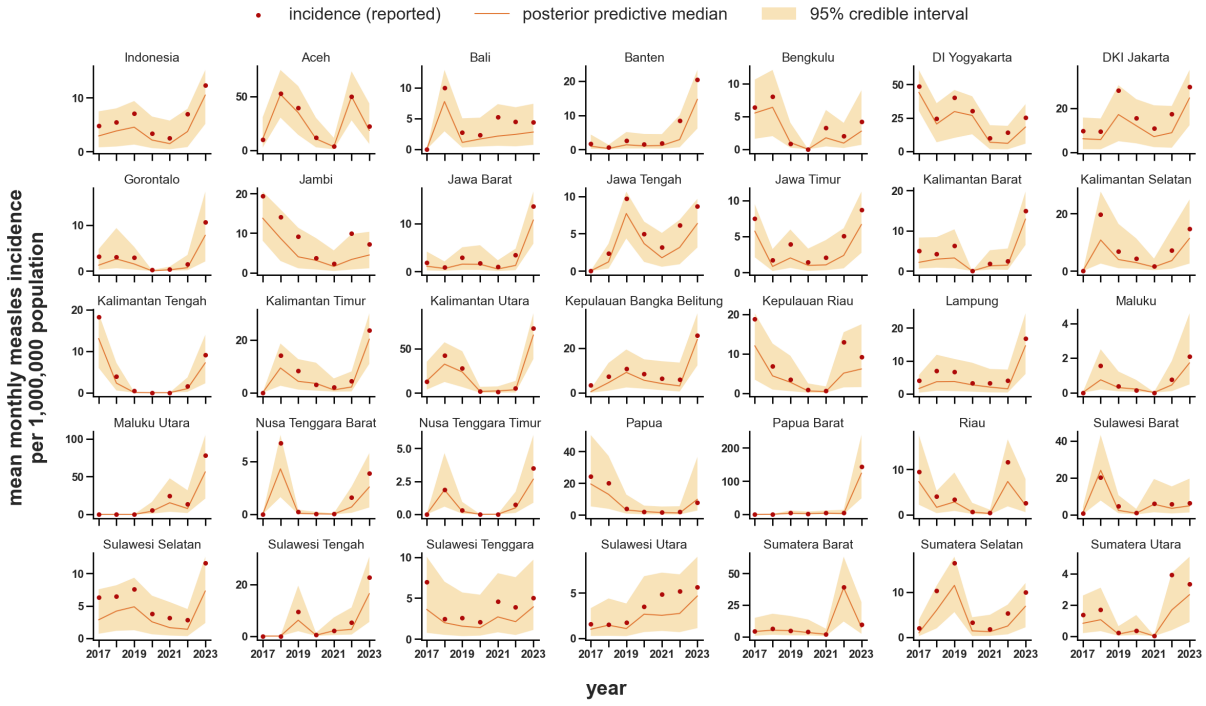


Figure 4.4. Posterior predictive distribution of provincial measles incidence in Indonesia, 2017–2023. The reported mean monthly measles incidence (per 1 million population) is shown in red dots along with the median prediction from the posterior predictive distribution (orange line). The shaded orange bands represent the 95% Bayesian credible interval, derived from 1,000 posterior predictive samples drawn via MCMC sampling of the six-parameter joint posterior (v_h, v_o, π_h, $monthly_{cap}$, $risk_{scale}$, λ_y). Given the observed data and model, the true incidence lies within this interval with 95% probability.

Overall, the model achieves a close fit to the reported data on vaccination uptake and measles incidence, accurately reproducing the temporal dynamics of both vaccination behaviour and

disease transmission across provinces in Indonesia. The posterior predictive median captures the trajectories of reported MCV-1 uptake and measles incidence, and the 95% credible intervals envelop the reported data points for both outcomes. Together, the strong agreement between simulated and observed patterns and the well-calibrated uncertainty bands demonstrate the reliability of the model for estimating the perceived vaccination relative cost (v_{RC}), an unreported behavioural parameter that governs vaccination decision-making and its effect on disease transmission. The estimated v_{RC} values are presented in the following subsection.

4.3.3 Estimated perceived vaccination relative cost (v_{RC})

The estimated perceived vaccination relative cost (v_{RC}) shown in **Figure 4.5** represents the reconciled general population perception of vaccination. These v_{RC} values are reconciled by smoothing the v_{RC} estimates, which fluctuate over the years to fit the vaccination uptake and measles incidence data. The v_{RC} reconciliation is aimed at obtaining a behaviourally interpretable trend. Further elaboration on the v_{RC} estimation process: (i) the fitted and reconciled general population v_{RC} trends; (ii) reconciled v_{RC} trajectories for the hesitant and other communities; and (iii) reconciled v_{RC} over time alongside vaccination uptake and measles incidence is provided in **Appendix E** Estimated v_{RC} list.

Across Indonesia, there is a general pattern of increasing perceived vaccination relative cost (v_{RC}) over the study period, beginning in many provinces in 2018 and progressing through 2023. The national-level v_{RC} trend (top-left panel) also exhibits a similar trajectory to the provincial-level pattern, suggesting that there is a nationwide increasing trend of negative sentiment toward measles vaccination.

While the majority of provinces show increasing v_{RC} patterns, some provinces exhibit distinct behaviours. Sulawesi Selatan and Sulawesi Tenggara show decreasing v_{RC} trends, suggesting improved attitude toward vaccination. Meanwhile, DI Yogyakarta, Gorontalo and Maluku display relatively stable v_{RC} trajectories, implying more consistent perception toward measles vaccination across years despite fluctuations in vaccine uptake or incidence. These differences highlight heterogeneity of vaccination perception among provinces in Indonesia.

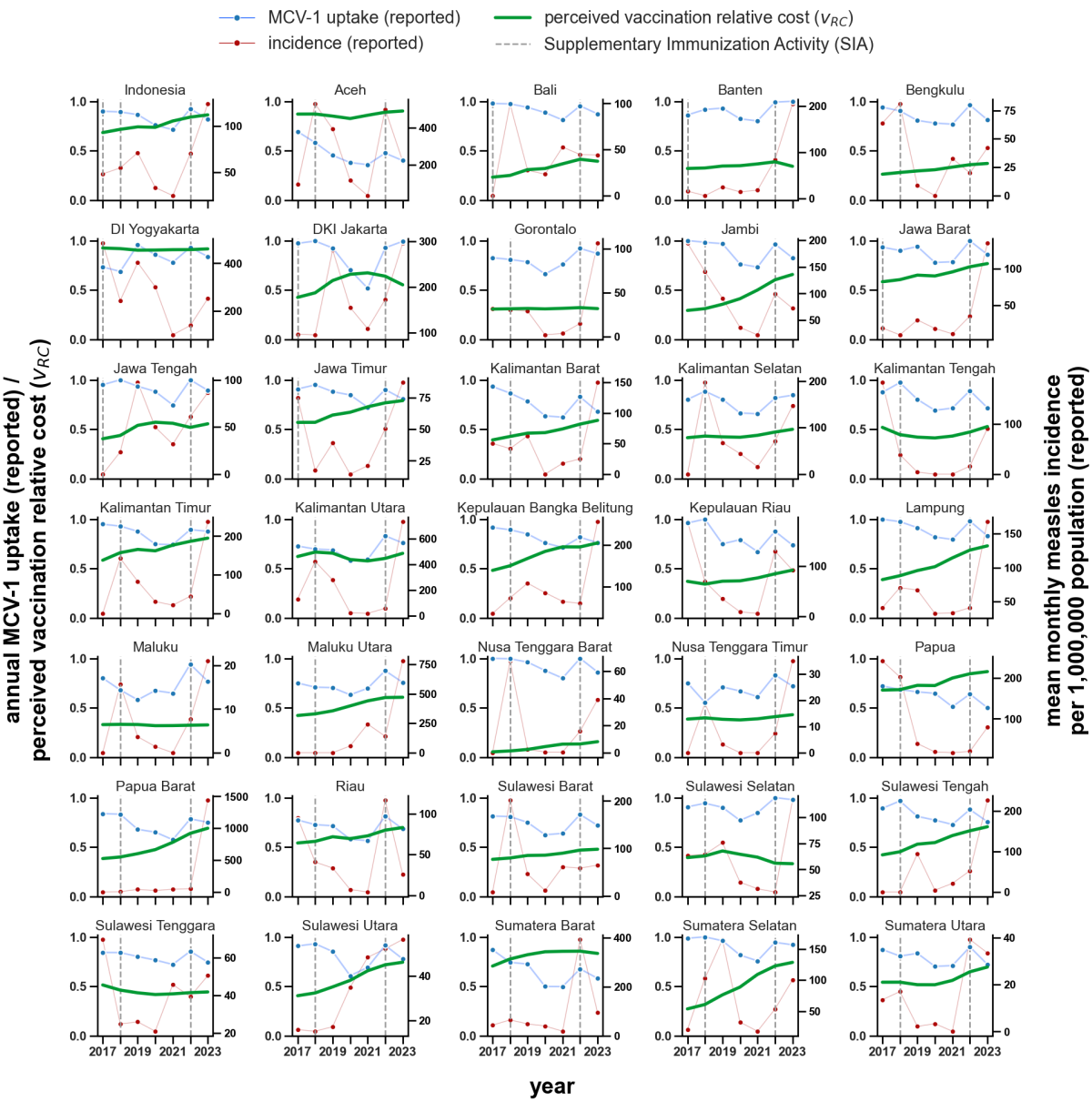


Figure 4.5. Trend of perceived vaccination relative cost (v_{RC}) in Indonesian provinces along with the reported MCV-1 uptake and mean monthly measles incidence, 2017 – 2023. National level analysis is shown in Indonesia panel (top-left), showing increasing trend of v_{RC} (green line) over the years. In general, the annual MCV-1 uptake (blue points) is increased during supplementary immunisation activity (SIA) (grey dashed line), and there is an increasing measles incidence (red points) in 2023.

The model is designed to separate v_{RC}, as a psychological variable, from external shocks such as Covid-19 disruptions and supplementary immunisation activities (SIA) boosting. Although the MCV-1 uptake is lower in 2020-2021 due to Covid-19-related service disruption, the v_{RC} trend does not exhibit sharp increases during these years, indicating that the temporary reduction of uptake was not driven by change of perception toward vaccination. Conversely, vaccination uptake increases during SIA do not correspond to sudden decrease in v_{RC},

confirming that the improved uptake stems from supply-side interventions rather that improvement in demand of vaccination.

During the nationwide measles outbreak in 2023, only 3 provinces (Bali, Banten and DKI Jakarta) exhibited a decline in v_{RC}. In most other provinces, the v_{RC} either remained constant or increased during the same period. This general upward trend in perceived vaccination cost aligns with the reduction in MCV-1 uptake observed after the 2022 SIA campaign. In contrast, the three provinces showing a decrease of v_{RC} in 2023 demonstrated more favourable uptake patterns. Banten and DKI Jakarta achieved higher uptake in 2023 compared with the SIA levels in 2022, while Bali experienced a slight decline in uptake but reported a similar incidence rate with the 2022 data.

The spatial evolution of v_{RC} across Indonesia is shown in **Figure 4.6**, revealing a clear pattern of geographic heterogeneity. Some provinces exhibit a consistently high v_{RC}, the most prominent example being Aceh, the westernmost province on the map with persistent dark red colour. While other provinces maintain a persistently low v_{RC} like Nusa Tenggara Barat, a province in the south of central Indonesian region with consistent dark green color. These behavioural patterns remain stable over time, persisting both before and after the Covid-19 pandemic in 2020-2021.

In addition to the spatial variation, gradual temporal shifts are also evident. **Figure 4.6** again demonstrates that there is an increasing trend of the v_{RC} across Indonesia, with many provinces becoming progressively darker on the maps over time. By 2023, almost all provinces in Sumatra (the western island) exhibit a high v_{RC}, with several approaching levels at which the perceived relative cost of vaccination is almost equivalent to the perceived cost of measles infection.

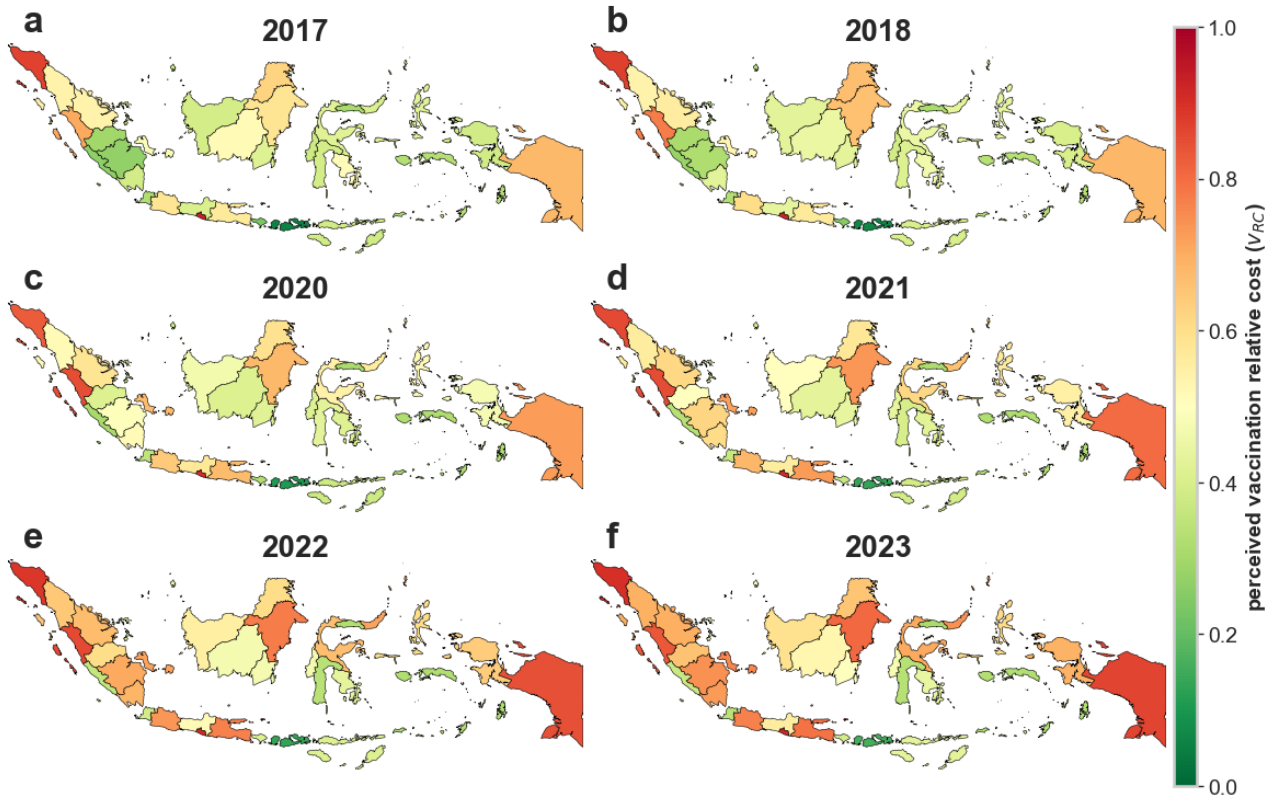


Figure 4.6. Spatial distribution and temporal evolution of provincial perceived vaccination relative cost (v_{RC}) in Indonesia, 2017 to 2023. The figure shows reconciled v_{RC} estimate in general population for each province.

The annual v_{RC} was significantly correlated with both MCV-1 uptake and measles incidence (**Figure 4.7**). Specifically, there was a moderate negative association between MCV-1 uptake and v_{RC} (r = -0.39, p < 0.05), indicating that lower vaccination coverage is associated with higher perceived vaccination relative cost. In contrast, a moderate positive association was observed between measles incidence and v_{RC} (r = 0.33, p < 0.05), suggesting that higher incidence is associated with higher perceived relative vaccination cost. The relationships are expected, as the high perceived relative vaccination cost is correlated with both low vaccination uptake and high incidence respectively.

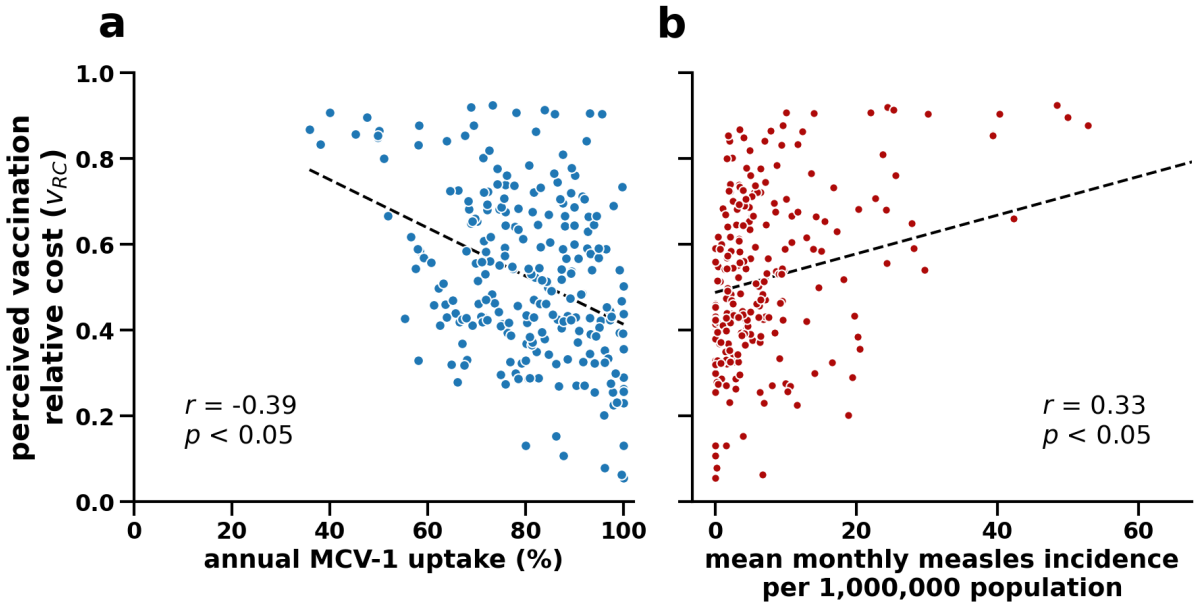


Figure 4.7. Correlation of annual measles-containing-vaccine dose 1 (MCV-1) and mean monthly measles incidence with perceived vaccination relative cost (v_{RC}) in Indonesian provinces, 2017 – 2023. The association of both MCV-1 (blue dots) and measles incidence (red dots) with the v_{RC} were measured with Pearson correlation.

The analysis is further extended to assess accessibility barriers, operationalised using poverty rate and distance to primary care facilities. The poverty rate is the percentage of the population living below the poverty line, measured by the ability to purchase daily nutritional requirements of 2,100 calories per person and to acquire non-food basic needs, including housing, clothing, education, and healthcare. The poverty rate for each province is measured and published annually by the Indonesian Central Bureau of Statistics.

Distance to primary care is measured by travel time based on a modelling study by Bosch et al. (2025), categorised as the percentage of the provincial population with more than 1 hour travel time to the nearest primary care facility. Primary care is the health service delivery unit that administers routine immunisation for children in Indonesia. The distance measurement accounts for terrain, land cover, road infrastructure, and seasonal conditions including both dry and monsoon seasons. The accessibility data were collected in 2025, while the MCV-1 and v_{RC} data span 2017-2023. To enable better comparison with the cross-sectional accessibility data, the longitudinal MCV-1 uptake and v_{RC} data were averaged across years for each province, assuming that provincial accessibility patterns remained relatively constant and that the 2025 accessibility data are representative of the 2017-2023 period.

Both poverty rate and distance to primary care facility are associated with annual MCV-1 uptake but not with the perceived vaccination relative cost (v_{RC}). There is a statistically significant but weak negative association between annual MCV-1 uptake and poverty rate (r = -0.25, p <0.05), whereas the association between v_{RC} and poverty rate is not statistically significant (r =-0.02, p = 0.78) (**Figure 4.8a-b**). Similarly, there is a statistically significant moderate negative association between MCV-1 uptake and distance to primary care facility (r = -0.43, p < 0.001), whereas the association between v_{RC} and distance is not statistically significant (r = 0.06, p = 0.64) (**Figure 4.8c-d**).

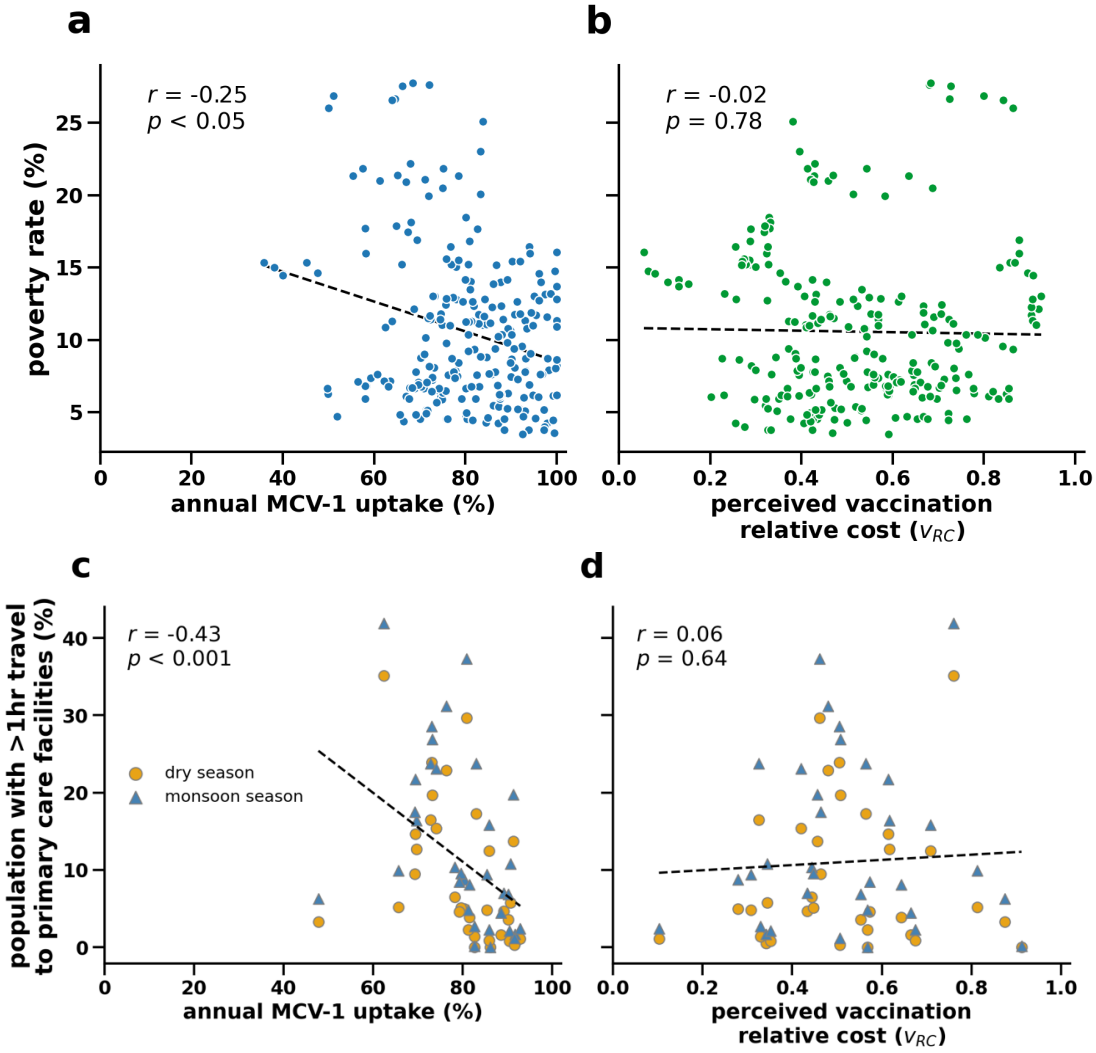


Figure 4.8. Association of annual measles-containing-vaccine dose 1 (MCV-1) uptake and perceived vaccination relative cost (v_{RC}) with poverty rate and distance to primary care facilities in Indonesian provinces, 2017-2023. Panels (**a-b**) show correlation with poverty rate, and panels (**c-d**) show correlation with distance to primary care facilities. The poverty rate represents the percentage of the population living below the poverty line. Distance is measured as the percentage of the population requiring more than one hour of travel time to reach a primary care facility (Bosch et al., 2025), either during dry (orange circle) or monsoon season (blue triangles). The annual MCV-1 and v_{RC} data are averaged for panel c-d to match with the available 2025 travel time data. All correlations were measured using Pearson correlation coefficient.

4.3.4 Out-of-sample validation

Section 4.3.2 showed that the model closely reproduces vaccination uptake and measles incidence in the same years for which it was calibrated. However, this in-sample procedure raises an issue of circularity, even though the model achieves its objective of estimating the perceived vaccination relative cost (v_{RC}) in a given year, as shown in Section 4.3.3. This section therefore reports whether the model can predict vaccination uptake and measles incidence using parameters calibrated on other years.

Figure 4.9a–b shows the mean absolute error (MAE) of predictions under the five information settings, which differ in whether parameters are re-estimated on the test year or carried forward from the fitting period. In S1, where the behavioural parameters and the force of infection (λ) were re-estimated on the test year and the reported incidence entered the perceived risk of infection, the MAE was 0.109 for MCV-1 uptake and 2.6 cases per million population for mean monthly measles incidence. Refitting λ on the test year reduced the incidence error three- to four-fold, as shown by the comparisons between S1 and S2 (MAE 2.6 vs 9.6) and between S3 and S4 (MAE 3.0 vs 9.9) (**Figure 4.9b**). In contrast, refitting λ had no effect on the uptake error (S1 and S2: 0.109; S3 and S4: 0.126) (**Figure 4.9a**). In the full forecast setting (S5), where no data from the test year were used, the model produced the lowest uptake error of all settings (MAE 0.089). The incidence error in S5 (MAE 9.5), however, remained similar to the other settings in which λ was carried forward.

The full forecast setting (S5) predicted MCV-1 uptake more accurately than S1 (MAE 0.089 vs 0.109), even though S1 used parameters estimated on the test year (**Figure 4.9a**). S5 is the only setting that implements model-generated incidence, which predicts lower incidence in 52 out of 68 (76.5%) held-out province-year compared to reported data, as can be seen in Supplementary Document 3. Those lower incidence is reflected in predicted lower uptake of S5 compared to settings using reported incidence (S1-S4). As for comparison, S5 predicts a lower uptake compared to S4 in 51 out of 68 (75%) held-out province-year. The two held-out years, 2022 and 2023, were marked by measles outbreaks in Indonesia following the Covid-19 pandemic, yet MCV-1 uptake did not rise in response. This is consistent with the increasing trend of v_{RC} estimated over the study period (**Figure 4.5**) which rose in most provinces and declined in only three during the 2023 outbreak (Section 4.3.3). Because v_{RC} was increasing, the carried-forward value from the fitting period was lower than the v_{RC} of the test year.

Consequently, combining the higher reported incidence with the lower carried-forward v_{RC} raised the simulated perceived risk of infection without the increase in perceived vaccination cost, which further inflated the predicted MCV-1 uptake.

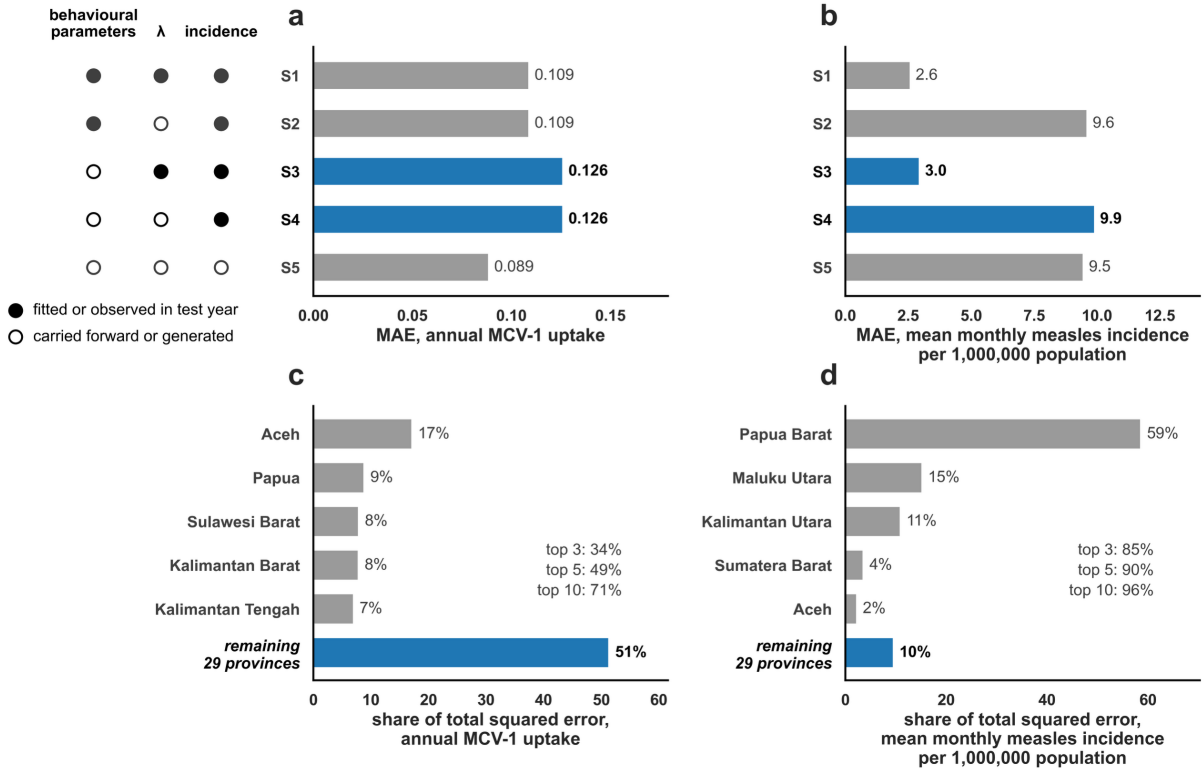


Figure 4.9. Mean absolute error (MAE) of the models prediction along with the share of error across provinces. Panel (a-b) show MCV-1 uptake and measles incidence MAE across various information settings, which distribute whether the parameters and observations are carried-forward from fitted years or implemented from test year. Panel (c-d) show contribution of error from provinces, which are concentrated on few provinces for incidence, and more distributed for MCV-1 uptake. The data show pooled performance from two held-out years fold in 2022 and 2023. The behavioural parameters are $risk_{scale}, v_h, v_o, \pi_h$.

In the full forecast setting (S5), the incidence prediction error was concentrated in a few provinces. To show how the error is distributed across provinces, each province's share of the total squared error was calculated (**Figure 4.9c–d**). For incidence, Papua Barat alone contributed more than half of the total squared error (59%), mainly due to its large outbreak in 2023, and five provinces together accounted for 90% (**Figure 4.9d**). In comparison, the uptake error was more evenly distributed across provinces, although five provinces still accounted for almost half of the total squared error (49%) (**Figure 4.9c**).

With 2022 and 2023 as the held-out years and the previous years as the fitting period, the predicted uptake is correlated with the reported uptake across 68 held-out province-years (r = 0.62, $p < 0.001$) (**Figure 4.10a**). The model tended to over-predict vaccination uptake, with the

five highest predicted error provinces (as can be seen in **Figure 4.9c**) are in 2023 held-out year, one year after the SIA campaign, when the uptake was fell back toward its pre-SIA level. In contrast, the model tended to under-predict incidence, although predicted and reported incidence were correlated on logarithmic scale (r = 0.55, p < 0.001) (**Figure 4.10b**). Of the five largest discrepancies province-year in incidence (as can be seen in **Figure 4.9d**), two were in Aceh and Sumatera Barat in 2022, when measles outbreaks occurred in the five provinces with the lowest vaccination coverage, including these two provinces (**Figure 4.1b**). The other three were in Papua Barat, Maluku Utara and Kalimantan Utara in 2023.

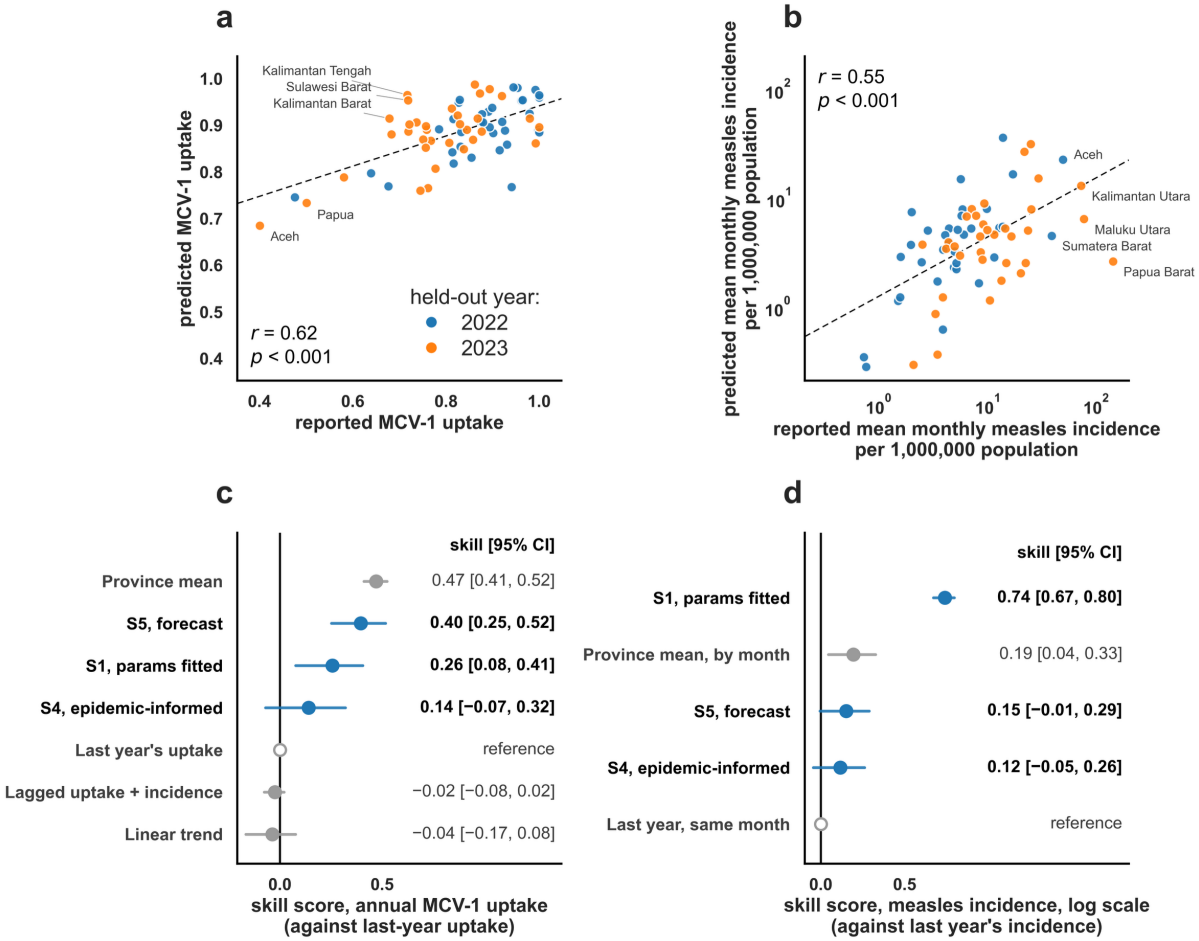


Figure 4.10. Predicted-reported data association and skill score of various information settings against baseline models. Panel (a-b) show association between predicted and reported data of MCV-1 uptake and measles incidence across two held-out years. Panel (c-d) show skill score of the model against last year data as the benchmark model to predict MCV-1 uptake and measles incidence. The skill score shown is pooled across two held-out years (2022 and 2023).

The skill scores, pooled across the 2022 and 2023 folds, are shown in **Figure 4.10c–d**, with last year's data as the reference. For MCV-1 uptake, the provincial mean achieved the highest skill score (0.47 [95% CI 0.41–0.52]), reflecting the persistence of uptake within provinces

over time. Among the information settings, the full forecast setting (S5) achieved the highest skill (0.40 [95% CI 0.25–0.52]), followed by S1 (0.26 [95% CI 0.08–0.41]) for predicting uptake. Both outperformed last year's uptake, the lagged uptake–incidence model and the linear trend model, neither of which performed better than last year's uptake. For measles incidence, S1 achieved the highest skill score (0.74 [95% CI 0.67–0.80]), outperforming all other models, including the provincial monthly mean (0.19 [95% CI 0.04–0.33]). However, this advantage arises from refitting λ on the incidence of the test year and is therefore subject to the circularity issue described in Section 4.2.6. Without any information from the test year, S5 performed only slightly better than last year's incidence (0.15 [95% CI −0.01 to 0.29]), and its confidence interval included zero.

4.4 Discussions

There is an increasing trend of perceived vaccination relative cost (v_{RC}) across Indonesian provinces between 2017 and 2023, with several provinces approaching values close to 1. Within the framework of Health Belief Model (HBM) (Becker et al., 1974; Rosenstock, 1974a, 1974b), v_{RC} can be interpreted as a proxy for perception toward vaccination. Individuals weigh the perceived risk of vaccination against its perceived benefits, and v_{RC} represents the psychological cost of accepting to take the vaccine compared with the expected cost of becoming infected. A value of v_{RC} = 1 therefore indicates that vaccination is perceived to be as costly as infection, and this judgment of v_{RC} is then compared with a social norm to produce willingness based on the Theory of Planned Behaviour model (Ajzen, 1991). Therefore, the rising v_{RC} which is estimated to have occurred across provinces can be directly translated into a declining willingness to vaccinate.

A marked upwards trend for v_{RC} is observed beginning in 2018, coinciding with the measles-rubella (MR) supplementary immunisation campaigns implemented outside the Java-Bali region. The campaigns was severely disrupted following declarations by Islamic clerics that the MR vaccine was forbidden due to the porcine-derived components used for its production (Rochmyaningsih, 2018). Although the campaign later resumed after intensive dialogue with Islamic clerical organisations, implementation remained challenging, particularly in more conservative provinces. This was most evident in Sumatra, where two-thirds of Indonesia's unvaccinated children resided during the MR campaign period (Pronyk et al., 2019). These events are reflected in the estimated v_{RC} trajectories, with many provinces beginning to show

rising v_{RC} from 2018 onwards. By 2023, excessive v_{RC} levels were especially prominent across provinces in Sumatra.

The estimated v_{RC} in this study is associated with both MCV-1 uptake and measles incidence. As expected, higher v_{RC} corresponds to lower MCV-1 uptake and subsequently higher measles incidence. More notably, the estimated v_{RC} is distinct from the behavioural measure of MCV-1 uptake itself. While annual MCV-1 uptake is significantly correlated with provincial poverty rate and distance to primary care facilities, v_{RC} is not significantly associated with either indicator. This suggests that the model is able to estimate a psychological determinant of vaccination decision-making, the v_{RC}, that is not associated with structural economic and accessibility constraints.

The Generalized Expectation Maximization (GEM) inspired model in this chapter achieves a close fit to the reported data, with a maximum annual vaccination uptake error of approximately 6% and a measles incidence error of around 5 cases per million population. The strong agreement between simulated and reported values ($R^2 \approx 0.91$ for uptake and $R^2 \approx 0.96$ for incidence) supports the robustness of the estimated v_{RC} trajectories. Achieving this fit requires data preprocessing using WHO/UNICEF estimates of national immunisation coverage (WUENIC) and surveillance performance, followed by multi-stage calibration from national to province-year parameters, and simplified assumptions of vaccination-disease dynamics. It is important to note as well that the province-year specific parameters (sensitivity to disease risk and the proportion of hesitant communities) are directly inferred from the dataset using GEM, as these parameter values are not always directly observable.

Despite the strong agreement between simulated and reported data, several important patterns should be noted. The model tends to simulate slightly lower vaccination uptake than what is reported administratively, highlighting the critical role of accurate population denominators, particularly in settings with uncertain counts of eligible children. Additionally, a notable discrepancy emerges in the 2023 measles outbreak in Papua Barat (a province with limited access to health service), where the incidence is simulated to be substantially larger than reported, suggesting potential under-detection of cases.

The uncertainty of the model estimates is quantified using the affine-invariant ensemble sampler implemented in *emcee* (Foreman-Mackey et al., 2013). The sampler diagnostics indicate adequate convergence and mixing across all province-year combinations, with

acceptance fractions and integrated autocorrelation times falling within recommended ranges. The resulting 95% Bayesian credible intervals for MCV-1 uptake generally envelop the reported data points across provinces, indicating that the model achieves reasonable precision in capturing vaccination uptake dynamics. The credible intervals for measles incidence are comparatively wider than those for MCV-1 uptake, and the posterior predictive median for incidence tend to be lower than the reported values in most provinces. Nevertheless, the reported incidence generally falls within the 95% credible interval, with only three province-year combinations lying outside this range, suggesting that the model captures the plausible range of measles incidence despite limited precision at the point estimate level.

It should be noted that the reporting noise parameters in the MCMC sampler were specified as modelling assumptions in the absence of province-level validation data. Although the reported MCV-1 uptake and measles incidence have been normalised using national-level WUENIC and surveillance performance-scales, these adjustments do not account for provincial-level reporting variability, and the assumed noise levels may not fully reflect the true measurement uncertainty in each province.

The out-of-sample validation shows that the model has predictive ability beyond reproducing the data it was calibrated on. The circularity mainly affects the prediction of measles incidence rather than MCV-1 uptake: refitting the force of infection (λ) on the test year reduces the incidence error three- to four-fold but has no effect on the uptake error. When no information from the test year is used, the model predicts MCV-1 uptake better than last year's uptake, a linear trend, or a combination of last year's uptake and incidence. This reflects an advantage of the model's structure, which separates the gradual change in perceived vaccination relative cost (v_{RC}) from temporary supply-side disruptions, such as the Covid-19 service restrictions and SIA campaigns. However, the model does not outperform the provincial mean. This is expected, because provincial MCV-1 uptake in Indonesia is persistent over time, consistent with the spatially stable and gradually changing v_{RC} estimated in this chapter. The advantage of the model over the provincial mean therefore lies not in the predictive accuracy but in how the model can distinguish between supply and demand constraints. A provincial mean of uptake combines vaccination perception and accessibility constraints into a single value, whereas the model separates the two. As shown in **Figure 4.8**, MCV-1 uptake is associated with poverty rate and distance to primary care facilities, whereas v_{RC} is not. Furthermore, the behavioural parameters estimated from earlier years, including v_{RC}, retain their predictive value in later

years. This suggests that the model captures a persistent behavioural characteristic of each province rather than an artefact of year-by-year fitting.

The out-of-sample validation also reveals the limits of the incidence component of the model. Supplying the reported incidence of the test year to the perceived risk of measles infection reduces the accuracy of the predicted MCV-1 uptake. When the reported incidence is higher than the model-generated incidence, the model predicts an increase in vaccination that is not observed in the reported MCV-1 uptake. This highlights the role of v_{RC} in the model. In most provinces, v_{RC} remained constant or increased during the 2022 and 2023 outbreaks, which suppressed vaccination uptake despite the higher risk of infection. When v_{RC} is carried forward from earlier years, its value is lower than in the test year, so its suppressing effect on uptake is underestimated. Combined with the higher reported incidence during the outbreaks, this inflates the predicted uptake. Furthermore, the deterministic model with an averaged force of infection for each province cannot capture measles outbreaks in endemic settings, which are driven by pockets of unvaccinated individuals and case importation. Therefore, the model is better suited to monitoring vaccination perception, operationalised as v_{RC}, than to forecasting outbreaks. These prediction ability findings should be interpreted with caution, as the validation covers only two held-out years, both of which were atypical due to post-pandemic recovery, a nationwide vaccination campaign and a nationwide outbreak.

As this chapter implements inverse problem to estimate perceived vaccination relative cost (v_{RC}) from routinely available vaccination uptake and measles incidence data, the model is subject to parameter identifiability limitations. The parameters governing the loss function and the learning dynamics ($\omega_{vac}, \omega_{inc}, \sigma_{vac}, \sigma_{inc}, lr$) are calibrated by loss minimisation across the whole dataset. They are therefore tuning parameters, rather than quantities identifiable from the observations, although $\omega_{vac} > 1$ and $\omega_{inc} = 1$ are assigned deliberately to give greater weight to fitting vaccination uptake than incidence. The province-level calibration allows the measles incidence sensitivity ($risk_{scale}$), and the proportion of hesitant individuals (π_h) to vary each year to fit the reported data of uptake and incidence. These parameters may therefore absorb discrepancies between the model and the data to focus on the v_{RC} estimation and should not be interpreted as direct measurements. Nevertheless, the force of infection (λ_y) is informed by the monthly incidence, but it also absorbs provincial differences in case detection not captured by the national surveillance adjustment, so it should be read as an effective force of infection.

While the provincial v_{RC} trend is the most identifiable hidden parameter, since the annual vaccination uptake responds to it directly, its value is subject to several entanglements. First, v_h, v_o and π_h affect the data only through their combined effect on population uptake (Eq. 4.5), so different combinations can produce the same observed uptake. Their separate values are determined by the modelling assumptions (the $v_h > v_o$ constraint, the fixed δ_θ, the constant $\delta_{constant}$ and the smoothing of π_h), rather than by the data. Second, v_{RC} trades off against $risk_{scale}$ (Eq.4.1 and 4.2) to determine vaccination willingness. While in low-incidence years, the perceived risk is close to zero regardless of the $risk_{scale}$, making $risk_{scale}$ effectively unidentifiable. Finally, the absolute level of v_{RC} is conditional on the fixed values of k, α and δ_θ which are assumed in this study. The estimated v_{RC} is therefore most robust to be inferred as a relative quantity, in its trends within provinces and its differences between provinces, rather than as an absolute measurement.

Therefore, the hidden variable v_{RC} inferred in this chapter should not be interpreted as a direct measurement of households' perception toward vaccination. Rather, it represents a model implied behavioural variable that reconciles observed vaccination uptake and disease incidence under the assumed vaccination decision and disease transmission models. Although the model achieves strong agreement with reported data and the MCMC sampler provides uncertainty quantification around the model parameters, the estimates of v_{RC} remain conditional on model structure, data quality, the multi-stage calibration pipeline, and the assumed reporting noise levels. Therefore, the inferred trajectories of v_{RC} are best interpreted comparatively across provinces over time, rather than as absolute estimates of the psychological construct.

4.5 Conclusions

This chapter introduces a model capable of estimating the perceived vaccination relative cost (v_{RC}) trajectories using routine reports of measles vaccination uptake and incidence. The model generates a quantitative measurement of vaccination perception in a population, where the direct measurements of the psychological variable are not always available. While accuracy of the model depends on the quality of the available dataset, multistage calibration, and simplified assumptions about vaccination-disease dynamics, the results demonstrate that hidden variables related to vaccination perception can be inferred even in imperfect data settings. Finally, the model provides a foundation for integrating vaccination perception inference into

immunisation programme monitoring and for designing more responsive strategies to address vaccine hesitancy.

Chapter 5 Strategies to Address Vaccine Hesitancy

5.1 Introduction

This chapter aims to examine the effectiveness of interventions designed to address vaccine hesitancy through simulation. In this chapter, evidence from controlled experimental and observational studies that relate to vaccination behaviour are translated into the modelling framework developed in Chapter 2, which captures individual decision-making within social networks. While these studies are typically conducted in controlled settings, embedding their behavioural mechanisms within this network-based model allows their group-level implications to be explored under more complex and heterogenous social conditions.

Vaccine hesitancy is a complex issue, and vaccination behaviour in under-vaccinated communities should be understood as a complex adaptive system, in which behaviours are interdependent among households (Plsek, 2001). Studies evaluating interventions to address vaccine hesitancy are commonly designed to minimise contextual confounding in order to isolate intervention effectiveness. However, these contextual factors are intrinsic to real-world settings and can substantially shape vaccination behaviour, including through social connections and cognitive biases that influence individual judgement. These contextual factors shape whether interventions can be successfully implemented and help explain variation in vaccination uptake across communities (Adamu et al., 2024). The effectiveness of behavioural health interventions, such as vaccination, depends not only on the intervention mechanism itself, but also on how malleable the intervention is in practice and how accommodating the community's social connections are (May et al., 2016).

Although several interventions have been reported to increase vaccine uptake, the overall quality of evidence remains low, and there is limited agreement regarding their effectiveness in addressing vaccine hesitancy (Dubé et al., 2015; Sadaf et al., 2013). This lack of strong agreement reflects the difficulty of translating effects observed in controlled or individual-level evaluations into complex vaccination behaviour. In light of this limited agreement, this chapter

simulates interventions by embedding evidence on their efficacy in modifying psychological determinants of vaccination within the complex dynamics of vaccination behaviour.

Within this chapter, interventions are organised into three groups, ordered by increasing level of stringency: (i) communication and information interventions, (ii) influencer-based or network interventions, and (iii) mandates or requirements.

These three intervention groups function under different mechanisms in the vaccination decision-making process. Communication interventions operate by shaping individual perceptions toward vaccination and the associated disease risk, thereby reducing the perceived vaccination relative cost (v_{RC}) and ultimately increasing the willingness to vaccinate. This intervention group includes debunking or corrective communication, which reactively addresses misinformation related to vaccination, and prebunking or inoculation strategy, which proactively builds resistance to misinformation. Influencer interventions target social process by introducing vaccine-promoter agents into social networks, thereby inducing coordination to vaccinate through interpersonal influence. Finally, mandates- or requirements-based interventions, represent the most stringent intervention group and act by altering the payoff structure of the decision making.

Although both communication and mandate strategies influence vaccination behaviour through the perceived vaccination relative cost (v_{RC}), they operate through distinct mechanisms. Communication interventions work by reducing the v_{RC} by changing individual subjective evaluation of vaccination, reflecting a cognitive shift toward vaccination. In contrast, vaccine mandates do not primarily seek to change vaccination perception, but they re-map the vaccination from a perceived cost into explicit payoff, where non-compliance carries tangible consequences (like access restrictions, penalties or withdrawal of promised benefits). In the mandate settings, vaccination is relatively advantageous even in the absence of changes in vaccination perceptions.

After modelling vaccination behaviour at the population level in Chapter 4, this chapter returns to simulating vaccination behaviour at the community level. Interventions are implemented at this level to examine both their effectiveness and underlying mechanisms to increase vaccine uptake. In addition, when simulating mandate strategies, we distinguish between an individual's willingness and the collective vaccination behaviour, two distinct concepts which should be given equal importance in addressing vaccine hesitancy.

By simulating interventions that target cognition, social coordination and incentive structures through a network-based vaccination decision model, this chapter clarifies why interventions that are effective in a controlled setting may fail to scale. It also explores under which psychological and social network conditions different intervention approaches are likely to succeed.

5.2 Methods

5.2.1 Network, vaccination and disease models

Simulations are performed in a synthetic social network representing connective agents who can make decisions about vaccination. Each agent represents a household who interacts with other agents based on a degree (connection) distribution. This connectivity between agents influences how they access information around them about disease and vaccination status. In this chapter, 150 households are generated to represent a community, following Dunbar's number of stable group membership (Dunbar, 1992; Hill and Dunbar, 2003) and the underlying connectivity network is calibrated to an empirical network of villages in India (Banerjee et al., 2013). Each household represents a caregiver who decides whether to vaccinate their children with measles vaccination dose 1. It is assumed that during that period, the child within each household is susceptible against measles infection, and the disease is transmitted through the social network among households.

Interventions are implemented within one vaccination season and we assume that individuals can make decisions about their vaccination status on a daily basis, with households members being vaccinated the day after a decision to vaccinate them is made. The default simulation scenario assumes that vaccination uptake is zero at the initial time point, and that vaccination willingness (Ψ) is influenced by the vaccination popularity in the community (V_p), along with vaccination popularity in the neighbourhood (θ).

$$\Psi = \left(V_p + \theta\right)^{\alpha} * \frac{1}{1 + \exp\left(\frac{v_{RC} - p_{(j,t)}}{k}\right)} \tag{5.1}$$

In the general formulation of willingness, V_p stands for the vaccination uptake from the previous season – as mentioned above in this chapter, each vaccination season is re-initiated with no vaccination in the community ($V_p = 0$) as well as in the neighbourhood ($\theta = 0$). The

initial zero vaccination coverage reflects households with less than one year old children who need to vaccinate their children against measles at each vaccination season.

This chapter is focused on vaccination decisions in the absence of an outbreak, due to the significant importance of proactive compared to reactive vaccination following an outbreak, as elaborated in Chapter 3. However, we also investigate scenarios with measles transmission in the community to compare influencers seeding effect in vaccination and disease transmission.

5.2.2 Parameters

In this chapter, the terms vaccine hesitancy and under-vaccination are used to describe related phenomena operating at different levels of decision-making. Hesitancy refers to household-level attitudes and decision states, including delayed vaccination, low willingness to vaccinate, or higher perceived vaccination relative cost. To avoid stigmatized labelling at the group level, under-vaccination is used to describe community-level hesitancy and is operationalised through vaccine popularity within the community. Therefore, in the analysis, communities are grouped into three levels: high, moderate and low under-vaccination, based on vaccine popularity (V_p) in the community: 0.4, 0.8 and 0.95.

The network-based vaccination decision and disease model implements general parameter values as described in Chapter 2 Modelling Vaccine Hesitancy. For clarity, the behavioural based parameters for the vaccination decision model are listed in **Table 6**, while a detailed parameter list for the transmission model can be found in Chapter 2 (Section 4.2 - Measles model description). Each intervention will have their own specific parameter to influence vaccination decision as elaborated in their respective sub-section.

Table 6. Global parameter values in interventions to address vaccine hesitancy simulation.

Parameters	Description	Value
V_p	Vaccination popularity in the community	[0.4, 0.8, 0.95]
α	Degree of social norm influence	0.7
k	Decision noise	0.1
b	Assimilation bias	1

5.2.3 Interventions model

Communication Strategies

Communication strategies are modelled to alter household's perception of vaccination relative cost (v_{RC}) and are divided into prebunking and debunking strategies. Prebunking is simulated as being conducted prior to exposure to misinformation, therefore its utility depends on the occurrence of misinformation against vaccination. Debunking strategies specifically refer to communication about disease risk; this particular Health Belief Model determinant (Rosenstock, 1974a, 1974b), has been shown to reduce v_{RC} (Brewer et al., 2007; Horne et al., 2015). For clarity, the term *risk communication* is used to describe debunking strategies, which are simulated both with and without the presence of misinformation.

Both communication strategies groups are also influenced by assimilation bias (b), which is also applied in the simulation. Households that support vaccination will have a greater receptivity to messages that support vaccination and vice versa for hesitant households (they will have a greater receptivity to message that oppose vaccination). Assimilation bias can influence efficacy of risk communication and misinformation to alter household's receptivity to communication strategies, while prebunking is indirectly affected by prior exposure to misinformation.

To account for any bias, information gate parameter (g) is implemented in each community of households to scale the impact of risk communication and misinformation. The biased assimilation (b) during communication strategies is implemented through the gate receptivity g, that depends on the communication recipient's prior stance toward vaccination, which is proxied by prior perceived vaccination relative cost (v_{RC}^{prior}). We distinguish gate receptivity based on whether it applies to risk communication (g_{risk}) or misinformation (g_{mis}) as follows:

$$g_{risk} = \frac{\left(1 - v_{RC}^{prior}\right)^b}{\left(1 - v_{RC}^{prior}\right)^b + \left(v_{RC}^{prior}\right)^b}$$
$$g_{mis} = \frac{\left(v_{RC}^{prior}\right)^b}{\left(1 - v_{RC}^{prior}\right)^b + \left(v_{RC}^{prior}\right)^b} \quad (5.2)$$

The relationship of how gate receptivity (g) is influenced by assimilation bias (b), based on the prior perceived vaccination relative cost (v_{RC}^{prior}) is depicted in **Figure 5.1**:

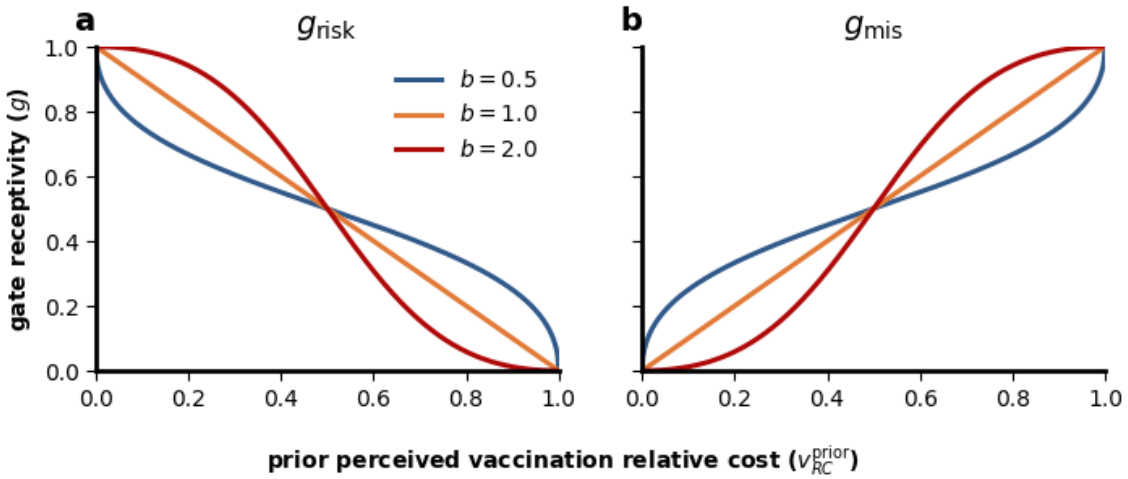


Figure 5.1. Communication strategies gate receptivity (g) based on prior perceived vaccination cost (v_{RC}^{prior}) of households. The figures show effect of assimilation bias (b) to (a) gate receptivity toward risk communication (g_{risk}), and (b) gate receptivity toward misinformation against vaccination (g_{mis}). Households that support vaccination ($v_{RC} < 0.5$) have a higher receptivity to risk communication. On contrary, the hesitant households ($v_{RC} > 0.5$) have a higher receptivity to misinformation against vaccination.

To account for the effect of misinformation, evidence from a trial assessing exposure to a vaccine-critical website is implemented (Betsch et al., 2010). The vaccine-critical website provides narratives framing vaccination as risky, and exposure to these narratives increases perceived vaccination risk, measured by change of vaccine perception grading (B = 0.857) on a 1-7 scale (with 7 indicating full agreement with the statement that "vaccinating causes considerable risks"). The evidence is implemented in calculating increased of perceived vaccination relative cost in the community due to misinformation (Δv_{RC}^{M}):

$$\Delta v_{RC}^{M} = \frac{B}{7-1} = \frac{0.857}{6} \approx 0.143$$

Then the v_{RC} after exposure to misinformation is:

$$v_{RC}^{post-M} = v_{RC}^{prior} + \Delta v_{RC}^{M}\, g_{mis} \tag{5.3}$$

Other researches have also reported the effect of misinformation on vaccination decision, but these have not been implemented in this study because either their results are measured as percentage reductions of respondents who intent to vaccinate (Loomba et al., 2021), or because the reported decrease of vaccine attitude is moderated by anger evaluated through multiple frames of misinformation message (Featherstone and Zhang, 2020). For a focus on the perceived vaccination relative cost analysis, instead of the collective behaviour effect and the

diversity of misinformation messaging frames, we do not incorporate evidence from those other studies.

Prebunking strategies can be implemented to mitigate the effect of misinformation. There are two types of prebunking: issue-based and technique-based. For the issue-based, people are supplied with information about potential misinformation and the respective refutations, while for the technique-based, people are pre-exposed to methods of misinformation so that they can better recognise unreliable information. Issue-based prebunking strategies have resulted in a Cohen's d = 0.43 difference on attitude toward vaccination (making it more favourable) compared with people without the intervention (Banas and Rains, 2010). Conversely, when people who were trained with technique-based misinformation a Cohen's d = 0.37 difference in vaccination perception was observed when compared with the control group (Roozenbeek et al., 2022).

Although both prebunking types have slightly similar efficacy to prevent misinformation, the issue-based type too specific to be able to address the vast, dynamic, and expanding misinformation content. People need to be updated regularly for any misinformation content that might arise in the community. Conversely, the technique-based training can cater to various contents given the same misinformation techniques are broadly applied to different products.

In this chapter, the technique-based prebunking evidence is implemented into the model, and the community is assumed to be exposed with known misinformation technique. If the community has been inoculated against misinformation, then the updated perceived vaccination relative cost v_{RC}^{post-P} is:

$$v_{RC}^{post-P} = v_{RC}^{prior} + \left(1 - d_{prebunking}\right)\Delta v_{RC}^{M} g_{mis} \tag{5.4}$$

The risk communication works in altering risk of infection (r_i) perception. Recall that the v_{RC} as constructed by Health Belief Model (HBM) as elaborated in Chapter 2 is:

$$v_{RC} = \frac{c_v}{b_v} = \frac{c_v}{v_c . r_i} \tag{2.3}$$

where the v_{RC} is the balance between the perceived cost of vaccination (c_v) and the perceived benefit of protection from disease (b_v) from vaccination, and v_c captures individual's confidence in the vaccine effectiveness and trust in the vaccination program.

Here risk communication strategy has a significant but small effect on perception of disease risk (d = 0.161, p = 0.047) (Parsons et al., 2018). The Cohen's d effect size can change initial r_i to produce perceived infection risk after communication r_{i_comm}:

$$r_{i_{comm}} = r_i \left(1 + d_{debunking}\right) \tag{5.6}$$

Considering that r_i is assigned as 1, and c_v, v_c are constant during the intervention, then the v_{RC} after risk communication becomes:

$$without\ misinformation:\ v_{RC}^{post-D} = \frac{v_{RC}^{prior}}{1 + d_{debunking} g_{risk}}$$

$$with\ misinformation:\ v_{RC}^{post-D} = \frac{v_{RC}^{post-M}}{1 + d_{debunking} g_{risk}} \tag{5.7}$$

If both risk communication and prebunking are conducted together after a misinformation outbreak in a community, then the updated perceived vaccination relative cost is:

$$v_{RC}^{post-PD} = \frac{v_{RC}^{prior} + \left(1 - d_{prebunking}\right)\Delta v_{RC}^{M} g_{mis}}{1 + d_{debunking} g_{risk}} \tag{5.8}$$

The communication strategy is assumed to have a homogenous effect across all households in the community. The gate receptivity (g) and assimilation bias (b) are also assumed to be fixed and are computed at time 0. This homogeneity and single activation setup at initial time step are conducted to avoid a feedback loop between the outcome of interest (v_{RC}) and its potential modulators, namely the communication strategy and the gate receptivity.

Influencer Strategy

Influencer strategy refers to potential role of well-connected agents in the social network in promoting vaccination within the community. We assume this can act passively as these "influencers" do not deliberately mean to alter vaccination perception in a cognitive sense but simply state themselves as vaccine supporters which can induce social coordination within the community to vaccinate. In the influencer's strategy, vaccine promoters are the heads of households in the community. In each vaccination season, the first individuals to receive vaccination are those in influencer households.

Intuition will lead us to believe that if the most popular agents within a community are the first to be vaccinated, vaccination uptake would speed up due to their popularity (*World Health Organization*, 2020). However, vaccination is a costly behaviour, therefore it cannot be modelled as a simple contagion which can be distributed easily by the most popular agent. Vaccination is a complex contagion instead, in which agents need to coordinate with the others to see whether the behaviour is legitimate. Due to the social reinforcement requirement, there can be countervailing influence which can hamper vaccine adoption. Therefore, in the influencers strategy, the most popular individuals are tested and compared with other types of network centrality: the lowest degree centrality, diffusion centrality, and k-core centrality.

Diffusion centrality was used to identify households with high potential to initiate information spreading through a few steps of social contact (Banerjee et al., 2014). In practice, diffusion central households can be identified through repeated nominations of individuals who are known to disseminate information quickly. For an undirected network with adjacency matrix A, diffusion centrality of household i is defined as:

$$DC_i = \sum_{t=1}^{T} 1^T (qA)^t e_i \tag{5.9}$$

where q is each connection transmission probability and T is the maximum number of steps through which information can spread. In this study, q was set to 1 to focus the behavioural transmission in vaccination willingness, while T was set as 3, corresponding to short and realistic chain of interpersonal communication among highly knitted community.

The diffusion centrality of node i (DC_i) is calculated by initiating seeding that originates from node i only, represented by vector e_i. The vector e_i assigns a value of 1 to node i and 0 to all other nodes, thereby capturing a unit shoch originating exclusively from node i. The resulting diffusion centrality measures the total amount of influence that can be generated by node i through the network over T diffusion steps.

The k-core centrality indicates how strongly a household is embedded in a tightly connected group, where each household maintains multiple connections with others in the same group (Seidman, 1983). The k-core seeding is implemented by first computing the coreness index of each household using the standard k-core decomposition of the social network. This type of centrality has been found to be the most efficient spreader of disease and rumour in social

network with SIR (susceptible-infectious-recovered) and SIS (susceptible-infectious-susceptible) models (Kitsak et al., 2010).

Mandates/Incentives

In the mandatory vaccination setting, the psychological state v_{RC} is transformed from perceived cost to net benefit, which is assigned as $v_{RC} < 0$. The vaccination campaign is simulated in an under-vaccinated community through different v_{RC} to compare the effect of transforming v_{RC} from cost to benefit, to evaluate the intervention effect towards vaccine uptake behaviour.

The households' willingness to vaccinate is also evaluated when a vaccine mandate is implemented, to develop a comparison between vaccination behaviour and willingness. To provide a better distinction between the behaviour and willingness, the vaccination popularity (V_p) is assigned as minimal (V_p = 0.01) during each simulated vaccination season. This allows us to focus on local social influence in the neighbourhood and how it relates to v_{RC}, since the interaction between these two determinants will subsequently influence a particular household's willingness to vaccine despite the overall vaccination behaviour in the community.

5.3 Results

To simulate interventions in a community with different levels of under-vaccination, a perceived vaccination relative cost (v_{RC}) is assigned to be consistent with the existing vaccine popularity (V_p) of each community. As described in the Methods section, V_p serves as a proxy for community level hesitancy, with V_p = 0.4, 0.8 and 0.95 representing high, moderate, and no hesitancy in the community, respectively. Although V_p is used as a proxy, the *hesitancy* term is avoided and instead we use the term *under-vaccination*, which can be measured using existing vaccine uptake data from the community.

For each V_p scenario, vaccination dynamics are simulated over a single vaccination season under baseline conditions, starting from zero vaccination coverage. By baseline we mean a scenario with no implemented interventions, and no change in perceived cost of vaccination (v_{RC}). The v_{RC} is homogenous across all households in the community. Households' vaccination willingness (Ψ) evolves as a function of vaccination popularity in the neighbourhood (θ) and the community-wide vaccination popularity (V_p). The value of v_{RC} is

calibrated such that the final vaccination uptake after one season matches the corresponding community popularity ($V_f = V_p$).

Figure 5.2 shows the relationship between v_{RC} and final vaccination uptake (V_f), illustrating a surprising commonality in the v_{RC} that produces the desired uptake for each assumed V_p. Following this v_{RC} calibration, all subsequent simulations are conducted using the corresponding V_p/v_{RC} pair. This setup allows interventions to be evaluated under comparable baseline uptake conditions across high, moderate and low under-vaccination communities.

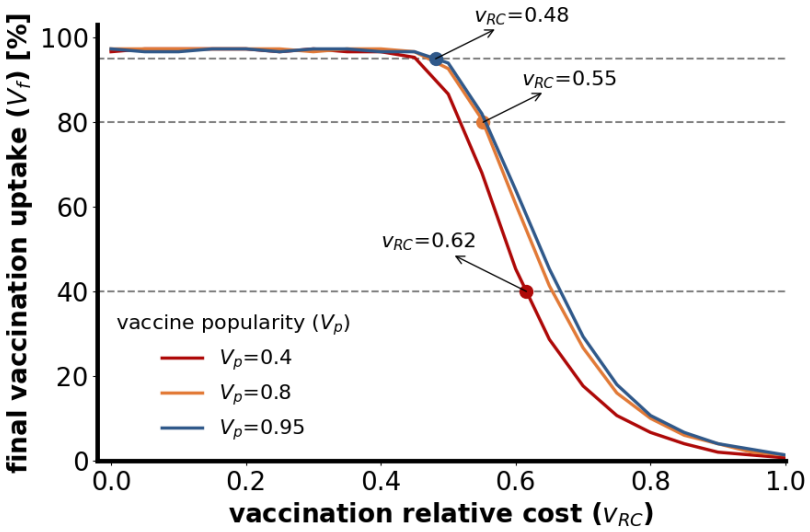


Figure 5.2. Vaccination uptake stability as a function of perceived vaccination relative cost (v_{RC}). Lines show the median final vaccination uptake after one vaccination season. Dashed horizontal line shows v_{RC} for each vaccine popularity (V_p) = [0.4, 0.8, 0.95]. Vaccination is simulated in a synthetic community of 150 households, with connectivity distribution follows empirical network of households in one village (Banerjee et al., 2013). The vaccination season is simulated for 365 days, and households can make vaccination decisions daily. Results are based on 100 simulation runs. Global parameter values are social norm (α) = 0.7 and decision noise (k) = 0.1.

5.3.1 Communication Strategies

Communication strategies are evaluated under two conditions: risk communication in the absence of misinformation against vaccination, and both risk communication and prebunking communication strategies implemented under misinformation conditions. Effectiveness of prebunking can only be assessed when there is an outbreak of misinformation, therefore before we describe the communication strategies, the effect of misinformation is evaluated. Risk communication is simulated both as a pre-emptive intervention in the absence of misinformation and as a corrective intervention following misinformation exposure.

Figure 5.3 shows the effect of risk communication in the absence of misinformation across communities with different prior vaccination popularity (V_p) and levels of assimilation bias (b). Under the same b level, the increase in vaccination uptake is largest in highly under-vaccinated communities ($V_p = 0.4$), smaller in moderately under-vaccinated communities ($V_p = 0.8$), and minimal in low under-vaccinated communities ($V_p = 0.95$). In high and moderate under-vaccination communities, higher assimilation bias (b) is associated with reduced increase in uptake following risk communication, although in moderate under-vaccination communities there is no difference of uptake between $b = 1$ and $b = 2$. By contrast, in low under-vaccination community, there is no difference of increasing uptake across various levels of assimilation bias (b).

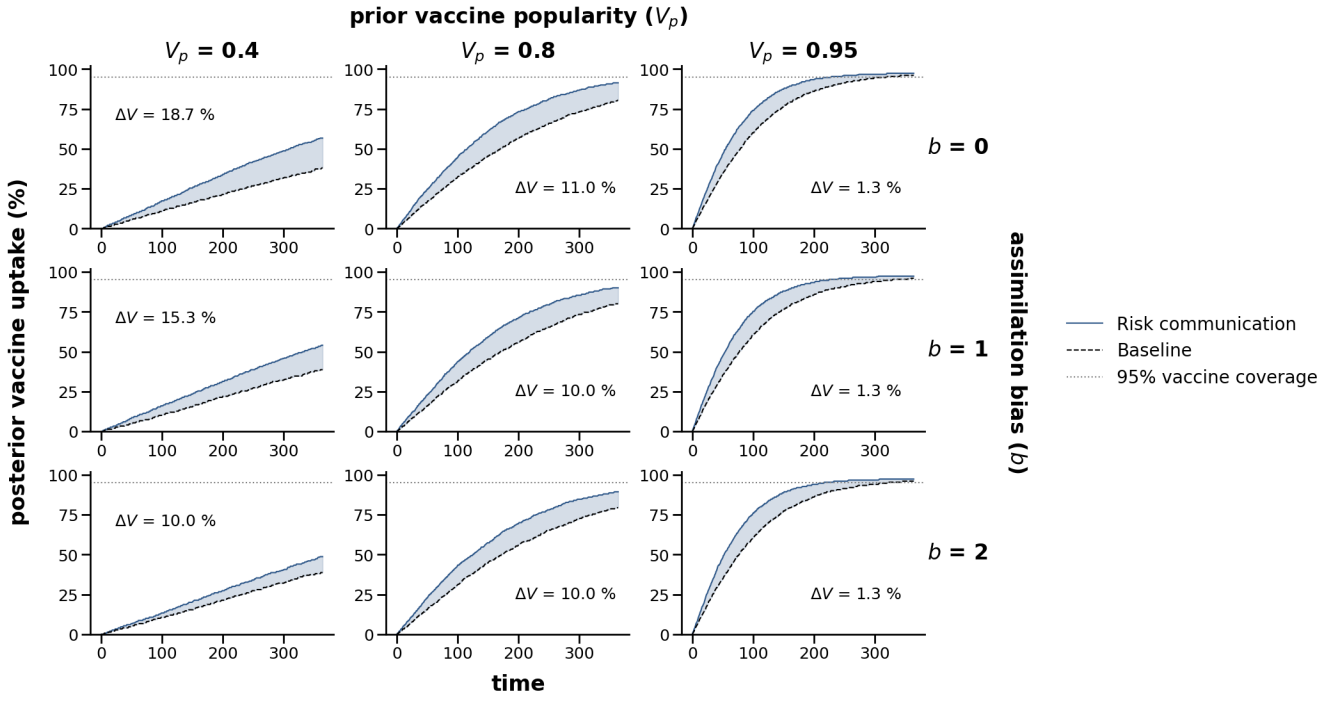


Figure 5.3. Effect of risk communication to increase vaccination uptake in one community, based on prior vaccination popularity (V_p) and assimilation bias (b). Lines show median of vaccination uptake for one community consisting of 150 households. The final vaccination coverage difference (ΔV) is measured at the end of the vaccination season (time = 365) for both the run with and the run without risk communication. The median is calculated from 100 simulations. Global parameter values are social norm (α) = 0.7 and decision noise (k) = 0.1.

Before assessing communication strategies following misinformation, the effect of misinformation alone is evaluated. **Figure 5.4** shows that misinformation decreases vaccination uptake across all community types. The magnitude of this reduction depends on both prior vaccine popularity and assimilation bias. In high and moderate under-vaccinated communities ($V_p = [0.4, 0.8]$), increasing assimilation bias leads to a larger reduction in

uptake, while in low under-vaccination communities ($V_p = 0.95$), higher assimilation bias is associated with a smaller decline in uptake. Within the same level of bias, the communities with moderate under-vaccination suffer the highest loss of uptake due to misinformation.

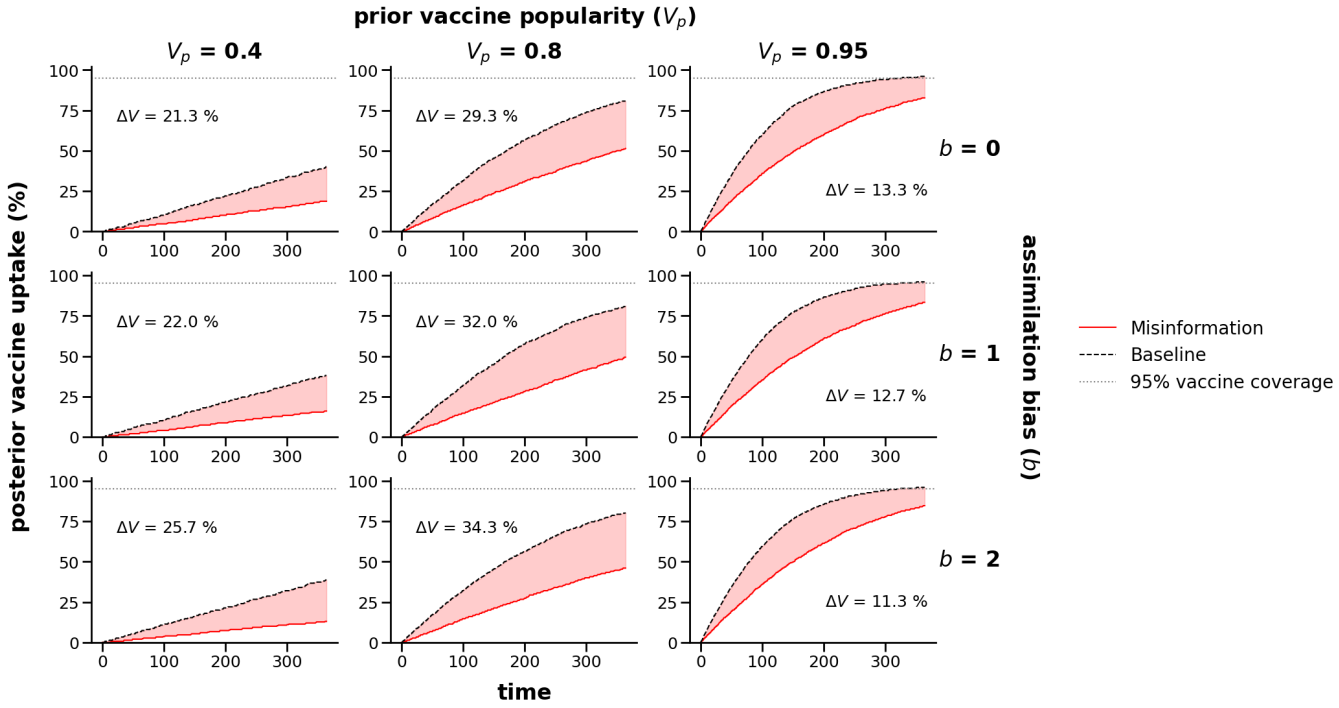


Figure 5.4. Effect of misinformation against vaccination to decrease uptake in one community, based on prior vaccination popularity (V_p) and assimilation (b). Lines show median of vaccination uptake for one community consisting of 150 households. The final vaccination coverage difference (ΔV) is measured at the end of vaccination season (time = 365). The median is calculated from 100 simulations. Global parameter values are social norm (α) = 0.7 and decision noise (k) = 0.1.

Figure 5.5 presents the effect of communication strategies implemented after misinformation exposure. When applied independently, risk communication produces larger increases in vaccination uptake in moderate and low under-vaccination communities compared to prebunking. In highly under-vaccinated communities, risk communication and prebunking produce almost similar increases in uptake when implemented separately, signalling a reduced effectiveness of risk communication in these communities' group.

When prebunking is applied prior to misinformation and followed by risk communication, the combined strategy yields the largest increase in vaccination uptake across all community types. In the least under-vaccinated communities, combined interventions can recover uptake to the pre-misinformation level. However, the recovery of uptake remains constrained by prior vaccine popularity. In high and moderate under-vaccinated communities, even the combined communication strategy does not restore uptake to pre-misinformation level.

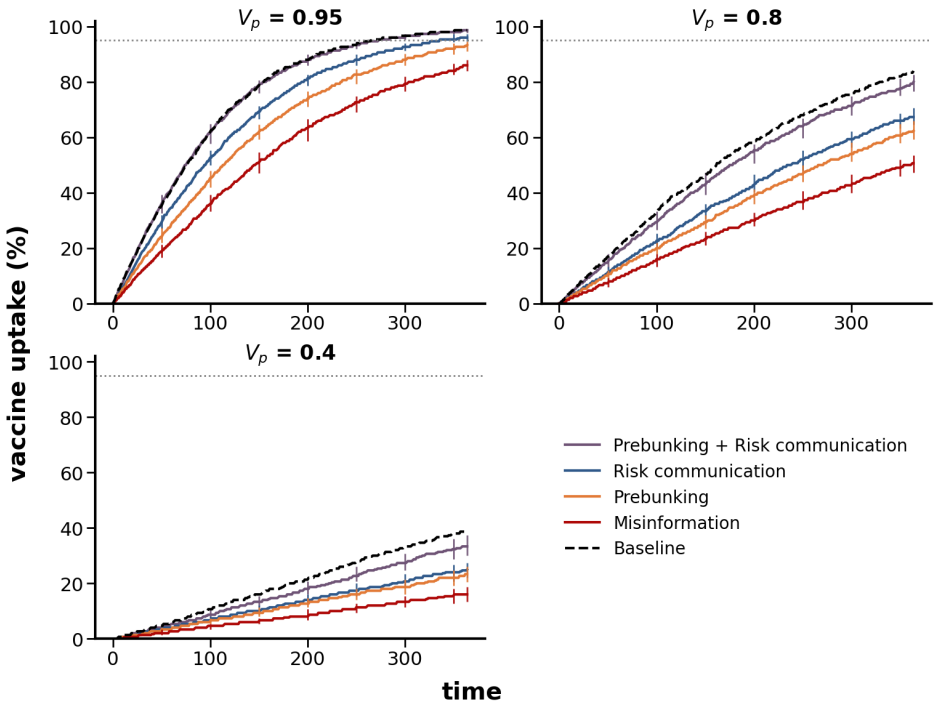


Figure 5.5. Efficacy of communication strategies to increase uptake under influence of misinformation against vaccination. Lines show median vaccination uptake across 1000 simulation runs, with the interquartile range (IQR) shown at 50-day intervals. Simulations are conducted in a synthetic community of 150 households with assimilation bias (b) = 1, social norm (α) = 0.7 and decision noise (k) = 0.1.

5.3.2 Influencer-Based Strategies

In this intervention, vaccination is initiated in a select subset households within the community chosen based on network centrality measures. These selected households are referred to as *influencers* and provide social signals of vaccine adoption to other households in the community, thereby leveraging vaccination uptake through social influence. To isolate the effect of social influence, the perceived vaccination relative cost (v_{RC}) is assumed to be homogenous across households within a community. **Figure 5.6** compares the effects of different influencer selection strategies on vaccination uptake and measles transmission.

Figure 5.6a-c show vaccination uptake trajectories of each influencer strategy under varying prior vaccine popularity (V_p). In the high (V_p = 0.4) and moderate (V_p = 0.8) under-vaccinated community scenarios, initiating vaccination in the households with most connectivity and high diffusion reach produces the largest increase in vaccination uptake. A summary of the differences between all influencer strategies is presented in **Figure 5.6d**, which shows the median and interquartile range of final vaccination uptake after one vaccination season in highly under-vaccinated communities (V_p = 0.4).

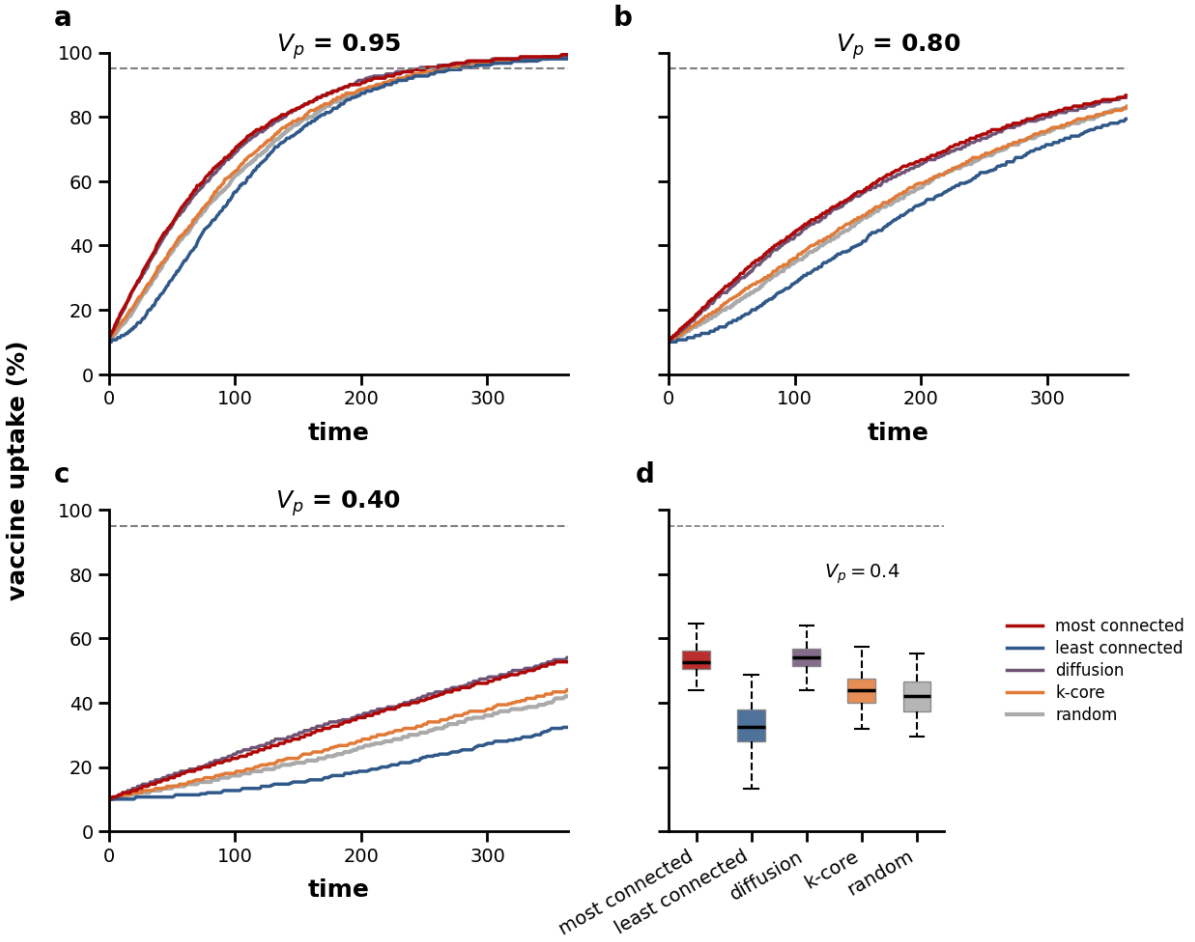


Figure 5.6. Comparisons of influencers strategies effectiveness to vaccination uptake. The vaccinations are simulated through different level of vaccine popularity (V_p) in the community **(panel a-c)**. **(d)** The median and IQR of final vaccination uptake in highly under-vaccinated communities ($V_p = 0.4$). Each influencer strategy is implemented by initiating vaccination with 15 households in a synthetic under-vaccinated community of 150 households. It is assumed that vaccination is available each day for one year vaccination season and no opinion updating. Each line represents the influencers strategy effect to vaccination uptake which is measured by median from 1000 simulations. The general parameters values are social norm (α) = 0.7 and decision noise (k) = 0.1.

5.3.3 Mandatory Vaccination Strategy

Mandatory vaccination is evaluated by distinguishing between vaccination behaviour, measured by collective uptake in the community, and vaccination willingness (Ψ), measured at the household level. Mandatory vaccination is modelled by assigning a negative perceived vaccination relative cost ($v_{RC} < 0$), representing a shift of v_{RC} from perceived cost to perceived net payoff from vaccination.

Figure 5.7 summarises the effect of mandatory vaccination on collective vaccine uptake dynamics and household willingness. Under mandatory vaccination, vaccine uptake rapidly

approaches full coverage, as shown in **Figure 5.7**a-**b** (red line and red bar), with all households in the community vaccinated extremely quickly.

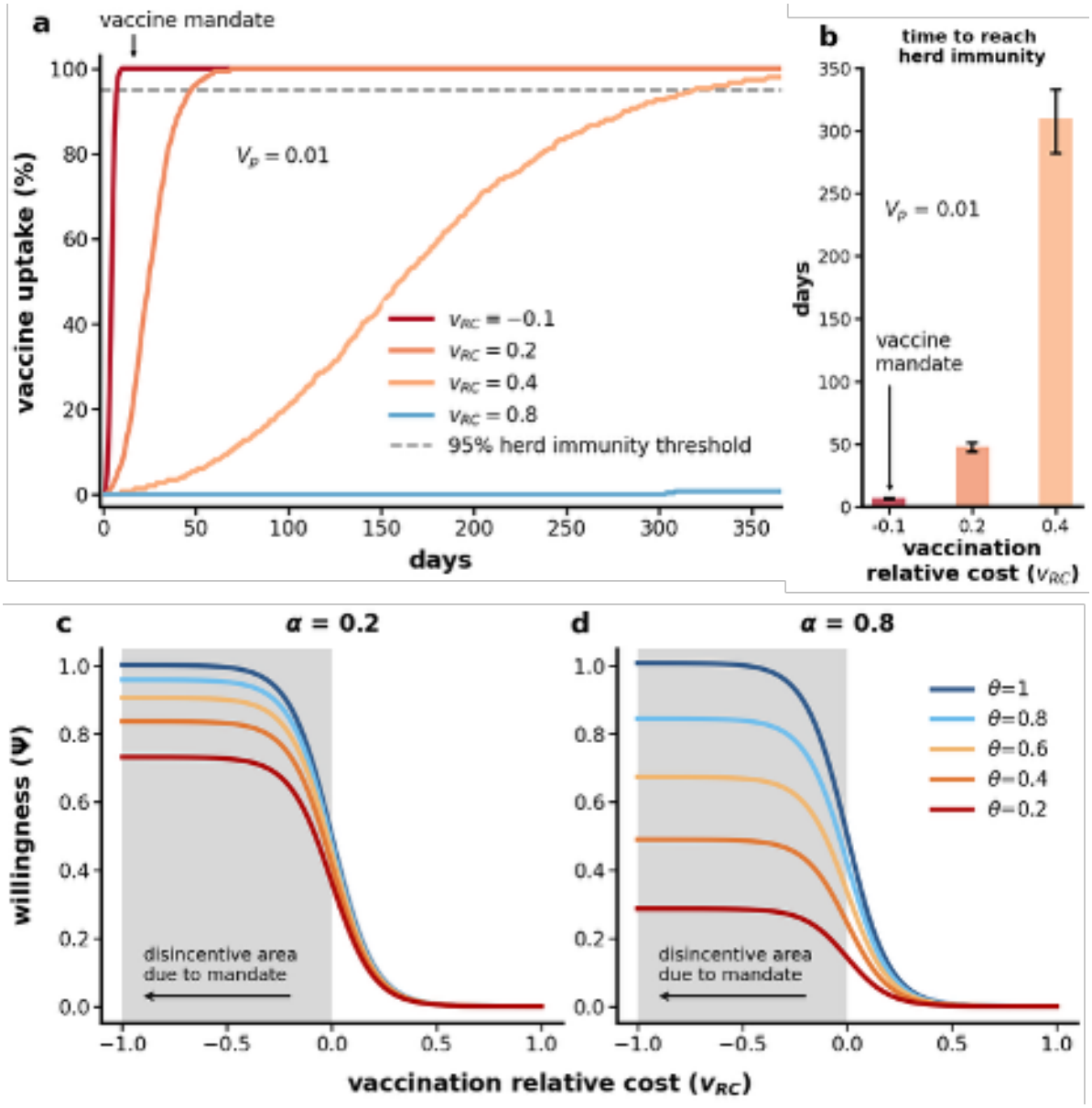


Figure 5.7. Efficacy of mandatory vaccination in a community. **(a)** Vaccination trajectories under different scenarios of perceived vaccination relative cost (v_{RC}). When mandatory vaccination is implemented, the v_{RC} is assigned as < 0, modelled as perceived payoff instead of cost. **(b)** Time in days to reach 95% herd immunity under different v_{RC} settings. Panels **(c-d)** show vaccination willingness (Ψ) of households based on vaccination popularity in their neighbourhoods, according to whether they are less (α = 0.2) or more (α = 0.8) likely to conform with social norms. The general parameter value is decision noise (k)= 0.1.

By contrast, although mandatory vaccination can increase household willingness to vaccinate, the willingness is not homogenous across households. **Figure 5.7c-d** shows that willingness is reduced when vaccine popularity in the neighbourhood is low. This reduction in willingness is more pronounced among households with higher conformity to social norms (α = 0.8).

5.4 Discussion

This chapter examined the effectiveness of interventions to address vaccine hesitancy by embedding behavioural mechanisms identified in experimental and observational studies within a network-based vaccination decision model. By simulating interventions in a community of households that target perceptions, social influence, and incentive structures, the results clarify both the limits of commonly proposed strategies and the conditions under which they are likely to succeed.

Across all intervention groups, two general insights emerge. Firstly, interventions that modify individual perceptions or incentives do not necessarily translate into sustained collective vaccination uptake once psychological and social determinants are considered. These constraints are evident in the limited effectiveness of communication strategies in highly under-vaccinated communities, and in the lower vaccination willingness observed in under-vaccinated neighbourhoods, even under mandatory vaccination. Secondly, in a highly under-vaccinated community, higher vaccination uptake can be achieved by inducing socially driven activation through households with high connectivity or those most likely to diffuse information to others.

5.4.1 Communication interventions: perception change under social influences and assimilation bias

Communication strategies were modelled as interventions that reduce the perceived vaccination relative cost (v_{RC}) by altering subjective evaluations of vaccination and disease risk. Here, we simulate that the changes of v_{RC} are induced by modulating the perception of disease risk (Brewer et al., 2007; Horne et al., 2015), as messages focused on vaccination benefits have been known to backfire (Nyhan et al., 2014). Although both perception of disease risk and vaccination confidence are elements of the Health Belief Model used to construct the perceived vaccination relative cost, communicating disease risk is the only effective intervention for reducing the perceived vaccination relative cost. Based on this understanding, we implement evidence on the efficacy of communicating disease risk (Parsons et al., 2018) to simulate risk communication. Our results show that risk-focused communication can increase vaccination uptake. Surprisingly, conducting risk communication in the absence of misinformation can generate a larger increase of uptake in most under-vaccinated communities,

compared to other community types. However, this increase is constrained by assimilation bias, where the larger bias reduces the increase of uptake in most under-vaccinated community. Yet this finding underscores the importance of communicating risk from vaccine-preventable diseases even for the most under-vaccinated communities.

Prebunking strategies, which aim to build resistance to misinformation (Roozenbeek et al., 2022a, 2022b; van der Linden, 2022), are simulated to perform better when combined with subsequent risk communication, and to be less effective than risk communication alone. Combination of prebunking and risk communication can achieve an optimal recovery of uptake following misinformation, although in most under-vaccinated community, the combined communication strategy cannot recover the pre-misinformation uptake. This suggests that inoculation against vaccine misinformation is not a substitute for communicating disease risks; in fact, they complement each other.

This chapter also finds that social influence is a key determinant of the effectiveness of communication strategies, in line with results in Chapter 3 showing that households are less inclined to vaccinate their children when vaccination is perceived as less popular. The interventions were also simulated by considering assimilation bias (Lord et al., 1979), which captures the tendency for individuals to accept or reject information in line with their prior stance. This bias diminishes risk communication effectiveness and magnifies misinformation effect. Together, these findings provide a theoretical-based illustration of how social influence and assimilation bias can jointly constrain the effectiveness of communication strategies against misinformation, addressing the need for integrative modelling to explain the complex interplay between cognitive and social dynamics under misinformation, as highlighted by Ecker et al. (2022).

These findings provide a mechanistic explanation of why communication strategies that perform well in controlled settings can fail to scale: social influence interacts with assimilation bias to constrain how much communication interventions can shift behaviour, even when the communication content is accurate and well-designed.

5.4.2 Influencers strategies: evaluating most popular promoter myth

Influencer-based interventions were designed by initiating vaccination through households selected based on their network centrality. A common assumption in public health practice is that targeting the most popular or well-connected individuals will accelerate behavioural adoption (*COVID-19 Vaccine Safety Communication*, 2020). The simulations in this chapter evaluate this assumption.

Vaccination is a costly decision, as no vaccine is entirely free from side effects. Because of this inherent cost, a sufficient fraction of neighbours who have already adopted vaccination is required to convince households to vaccinate their children, consistent with social influence determinants of behaviour in the Theory of Planned Behaviour (Ajzen, 1991) and the Increasing Vaccination Model (Brewer, 2021; Brewer et al., 2017). Results from Chapter 3 (Section 3.3.1 - Vaccination willingness) further elaborate the importance of social influence in increasing vaccination intention in under-vaccinated communities. Therefore, vaccination behaviour should be considered as a complex contagion (Guilbeault et al., 2018), as its adoption requires social reinforcement across the community.

In this study, simulations show that in highly under-vaccinated communities, targeting the most connected households generates larger increases in vaccination uptake than initiating vaccination among the least connected households. This result appears to contradict the general understanding of complex contagion, which suggests that collective behavioural change spreads more effectively when initiated from the network periphery (Centola, 2021), where households have fewer neighbours. The apparent contradiction arises largely from the network topology: in a social network with a log-normal degree distribution, the heavy right tail indicates the presence of highly connected households (**Figure 3.1**). These highly connected households can reach many neighbours quickly, and each adoption updates the locally perceived popularity of vaccination for a large number of secondary households simultaneously. In contrast, the least connected households update perceived vaccination popularity for very few secondary households. As a result, the social signal remains trapped in small pockets of the neighbourhood and behaviour diffuses slowly.

Another finding also supports the importance of exposure for increasing vaccination. This chapter further demonstrates that vaccinations are transmitted vastly when seeded by

households with high diffusion centrality. Households with high diffusion centrality are positioned such that information originating from them is expected to reach a larger portion of the network over multiple steps, even if they do not have the highest number of connections around them. This type of household can be identified by asking community members who will be most suited to spread information or "gossip" (Banerjee et al., 2019).

This chapter also finds that households with high k-core centrality are not the most effective spreaders, as k-core seeding produces vaccination uptake levels similar to those achieved by random seeding. This result contradicts the findings of Kitsak et al. (2010), who showed that k-core centrality is a more effective spreading measure than degree (most-connected) centrality in social network. This discrepancy arises from differences in the underlying transmission process. Kitsak et al. (2010) model the diffusion through susceptible-infected-recovered and susceptible-infected-susceptible dynamics, in which the transmission can occur through contact with a single infected neighbour and does not account for social influence and judgment of perceived vaccination relative cost that precede the vaccination decision.

As shown in the simulations above, initiating vaccination from the most connected and most diffusive households generates the highest vaccination uptake. Beyond this behavioural benefit, targeting these households also supports disease containment. Households with high connectivity can serve as superspreaders of infectious disease transmission (Lloyd-Smith et al., 2005) and vaccinating them effectively optimises both vaccination behaviour and disease prevention in the community. Overall, these findings support the utility of current influencer-based intervention practices that initiate vaccination from the most connected individuals to increase vaccination uptake.

5.4.3 Mandatory vaccination: decoupling willingness from behaviour

Mandatory vaccination represents the most stringent intervention class, and it is modelled to operate by altering the payoff structure of the vaccination decision. In the simulations shown here, mandates rapidly induce coverage values above the herd immunity threshold by shifting vaccination from a perceived cost to a perceived net payoff.

Interventions that shape behaviour like mandatory vaccination, may directly influence behaviour without improving willingness (Ajzen, 1991; Brewer et al., 2017). Therefore, the

distinctions between behaviour and willingness are preserved in this chapter, which found that the behavioural compliance to vaccination is not necessarily accompanied by a uniform increase in willingness to vaccinate. The simulations reveal that willingness remain suppressed in neighbourhoods where vaccination is less popular, especially among households with higher conformity to social norms.

This decoupling of willingness from behaviour has important implications. Although mandates can achieve immediate coverage targets, they do not necessarily generate supportive social influence and may leave hesitancy problem unresolved. Furthermore, introducing mandatory vaccination can induce resentment among individuals with prior negative attitude toward vaccination (Betsch, 2016), and avoidance of future voluntary vaccination (Sprengholz et al., 2022).

The negative attitude is probed as a higher perceived vaccination relative cost in this thesis and manifested in a lower uptake within a community. Therefore, implementing mandatory vaccination in under-vaccinated community may generate higher dissent and lower future uptake. In this sense, mandates may increase coverage in the short term while allowing hesitancy to persist at the households' level, potentially leading to renewed decline in uptake once the coercive intervention is relaxed.

5.4.4 Implications for scaling interventions

Taken together, the simulations in this chapter clarify why interventions that demonstrate efficacy in controlled or individual-level studies may struggle when scaled to under-vaccinated communities. In experimental settings, interventions are typically evaluated under conditions that minimise social environments and assimilation bias. As a result, intervention mechanisms that successfully alter perceptions or incentives in controlled settings often fail to translate into sustained collective vaccination uptake when embedded within social network with the embedded complexities. Interventions fail to scale because behaviour is embedded in socially heterogeneous systems where the same intervention produces uneven reinforcement and response.

Taken together, the simulations in this chapter clarify why interventions that demonstrate efficacy in controlled or individual-level studies may struggle when scaled to under-vaccinated communities. In experimental settings, interventions are typically evaluated under conditions

that minimise social influence and assimilation bias, both of which are inherent to real-world settings and can shape vaccination outcomes following implementation (Adamu et al., 2024). As a result, when implemented, there is a lack of strong agreement regarding effectiveness of interventions in addressing vaccine hesitancy (Dubé et al., 2015; Sadaf et al., 2013). The same intervention can produce different outcomes when implemented across communities with varying social and cognitive contexts.

Alongside the challenges of implementing interventions to address hesitancy in highly under-vaccinated communities, the results in this chapter provide guidance for intervention design. Inducing vaccination behaviour in highly under-vaccinated communities is most effectively initiated at the most connected households or through households that are most likely to diffuse information about vaccination adoption. Despite the inherently low popularity of vaccination and the presence of assimilation bias in such communities, the utility of communicating infection risk to increase vaccination uptake should not be neglected. Misinformation has a substantial effect in reducing vaccination uptake. Therefore, prebunking is important for inoculating communities against misinformation. However, prebunking should be accompanied by risk communication to achieve optimal effectiveness. By contrast, mandates are effective in rapidly increasing uptake by altering payoff structures, but they do so without resolving underlying hesitancy and may suppress willingness in under-vaccinated neighbourhoods with high conformity to social norms.

5.5 Conclusions

This chapter examined the effectiveness of interventions to address vaccine hesitancy by embedding empirically grounded behavioural mechanisms within a network-based vaccination decision model. By simulating communication strategies, influencer-based interventions, and mandates under varying levels of community under-vaccination, the chapter clarifies not only which interventions increase vaccination uptake, but why their effects differ across social and psychological contexts.

Across all intervention classes, a central finding is that increasing vaccination uptake is not solely a matter of altering individual perceptions or incentives. Instead, intervention efficacy is strongly conditioned by social influence and motivated reasoning. Communication strategies that successfully reduce perceived vaccination relative cost (v_{RC}) at the individual level can produce limited or uneven gains when assimilation bias and social countervailing feedback are

present. Even when communication is accurate and evidence-based, its impact is constrained in highly under-vaccinated communities by selective receptivity and weak social reinforcement. These results provide a mechanistic explanation for why communication interventions that perform well in controlled or individual-level studies may fail to scale in under-vaccinated communities.

Influencer-based strategies simulation results in this chapter confirm the importance of seeding vaccination through the most connected and the most diffusive households, consistent with the common assumptions of initiating vaccination campaign through the most popular individuals (*COVID-19 Vaccine Safety Communication*, 2020). The most connected and diffusive households provide a greater exposure to vaccination behaviour, which was simulated to produce higher vaccination uptake in highly under-vaccinated communities compared to other influencer strategies (least connected, k-core, and random seedings). These results demonstrate that in highly under-vaccinated communities, wider community exposure is more important than strong reinforcement within local neighbourhoods.

Mandatory vaccination emerges as the most effective intervention for rapidly achieving high coverage in the community, but its effects do not extend to the households' willingness. The simulations reveal a distinction between behaviour and willingness under mandates, particularly in under-vaccinated neighbourhoods with strong conformity to social norms. While mandates can deliver short-term coverage gains, they leave underlying hesitancy unresolved and may risk suppressing future voluntary uptake once coercive incentives are relaxed.

Several limitations should be acknowledged. Firstly, the model assumes homogeneity in perceived vaccination relative cost (v_{RC}), assimilation bias, and communication effects within each community. While this design choice isolates the community-level mechanisms, real-world settings exhibit substantial within-community heterogeneity that may amplify or attenuate intervention effects. Secondly, communication strategies are implemented as single, time-zero shocks with fixed effect sizes derived from experimental studies. In practice, communication is iterative, adaptive, and embedded within evolving information environments, which may alter both magnitude and persistence of effects. Lastly, the synthetic social networks used in the simulations are static, and although parameterised using empirical degree distributions, they cannot fully capture the dynamics of relationship formation or institutional channels of influence.

Despite these limitations, the chapter provides a coherent and theoretically grounded framework for evaluating interventions under realistic social constraints. By integrating cognition, social coordination, and incentive structures within a network-based vaccination decision model, the analysis serve its aim to explain under which conditions interventions succeed or fail. The findings underscore the necessity of designing vaccination policies that are sensitive to social influence and motivated reasoning.

More broadly, this work demonstrates the high utility of mechanistic modelling for informing vaccination policy. By formalising the processes through how vaccination decisions emerge and interact within networks of decision-making agents, the framework allows intervention strategies to be simulated prior to implementation and enabling identification of community-based contexts in which they are likely to scale or backfire. As vaccine hesitancy becomes increasingly prominent, with clusters of under-vaccinated communities becoming apparent, the framework presented in this chapter provides a principled basis for designing interventions that are effective in addressing vaccine hesitancy.

Chapter 6 General Discussions and Conclusions

In trying to investigate the ever-persistent vaccine hesitancy problem, this thesis tackles four objectives: (i) formulate a vaccination decision model integrating multidisciplinary understanding of the vaccine hesitancy phenomenon; (ii) elucidate complex mechanisms of vaccine hesitancy; (iii) infer temporal dynamics of vaccination perception from routine administrative data; (iv) simulate implementations of interventions to address vaccine hesitancy.

The development of an integrated framework to study vaccine hesitancy is achieved by initially constructing a unified model of vaccination decision making, which is elaborated in Chapter 2. The subsequent Chapter 3 demonstrates the integrated model and approaches the disentanglement of complex phenomena related with vaccine hesitancy. Chapters 4 and 5 show model implementations, where in Chapter 4, the model is used to estimate perceived vaccination relative cost (v_{RC}) using routinely collected immunisation and disease incidence data. Finally, in Chapter 5, the model is implemented to simulate and evaluate effectiveness of interventions to address vaccine hesitancy, which are grouped into three intervention classes: communication, influencers and mandate.

6.1 Summary of findings

Chapter 2 presented an exploration of the theoretical and methodological foundations used to model vaccine hesitancy in this thesis. Grounded in health behaviour theories, opinion formation, epidemiological dynamics and network science, our approach combines these perspectives to construct an integrated modelling framework that captures both individual and collective vaccination behaviour. The vaccination decision model developed in this study implements two key drivers of vaccination derived from the Theory of Planned Behaviour and the Increasing Vaccination Model: self-perception and social influence. These behavioural dynamics are coupled with an individual-based transmission model that is fitted to empirical vaccination uptake and disease incidence data. Finally, synthetic social networks are deployed to simulate co-evolving behaviour and disease spread through communities and populations.

The results in Chapter 3 have illustrated mechanisms underlying several complex phenomena related to vaccine hesitancy, offering behavioural, social, and epidemiological insights into how vaccination decisions evolve in under-vaccinated communities. The results show that individuals' willingness to vaccinate is strongly shaped by their social environment. The analyses also identify a critical threshold in the perceived vaccination relative cost that determines whether herd immunity is achievable. Outbreak simulations further demonstrate the limited utility of reactive vaccination in under-vaccinated communities where the perceived vaccination relative cost exceeds the critical threshold, as the proportion of households infected following an outbreak is inversely correlated with the level of vaccination coverage prior to the outbreak. The compounded high perceived vaccination relative cost and low social influence to vaccinate are responsible for hesitancy persistence despite a prominent outbreak.

The opinion formation analysis in Chapter 3 demonstrates that assimilation bias entrenches opposition to vaccination in under-vaccinated communities, even when they interact with pro-vaccine communities. Inter-community interaction simulations further reveal that community isolation along with assimilation bias amplifies vaccine hesitancy and fosters polarization between under-vaccinated groups and the general population with relatively higher vaccination uptake. Notably, even under the influence of external events, initial coverage remains the critical factor, highlighting the importance of preventive over reactive immunisation in shaping both vaccination and disease dynamics in under-vaccinated communities.

There is an increasing trend of perceived vaccination relative cost across Indonesian provinces between 2017 and 2023, with several provinces approaching values close to 1. The Generalized Expectation Maximization (GEM) inspired model in Chapter 4 achieves a close in-sample fit to the reported data, and the reported values of vaccination uptake and incidence generally fall within the 95% Bayesian credible intervals derived from MCMC sampling. The out-of-sample validation shows that the close in-sample fit of measles incidence, but not of vaccination uptake, reflects circularity of refitting force of infection on the incidence of the same year. Without any information from the predicted year, the model predicted vaccination uptake better than last year's uptake and a linear trend, and comparably to the provincial mean, but had limited ability to predict measles incidence. This indicates the limited utility of the model as an outbreak predictive tool.

The perceived vaccination relative cost estimated from earlier years retained their predictive value in later years, indicating that the behavioural parameter captures a persistent

characteristic of each province rather than an artefact of year-by-year fitting. However, the hidden variable of perceived vaccination cost inferred in Chapter 4 should not be interpreted as a direct measurement of households' perception toward vaccination, but rather as a supporting tool to monitor vaccine perception trajectories in the population over time. Overall, this study demonstrates the utility of the proposed model for estimating perceived vaccination relative cost, a hidden variable that cannot be directly observed from routinely reported data alone.

Chapter 5 examined the effectiveness of interventions to address vaccine hesitancy by embedding behavioural mechanisms identified in experimental and observational studies within a network-based vaccination decision model. Communication strategies can produce limited or uneven gains when assimilation bias and social countervailing feedback are present, yet risk communication confers higher benefit of increasing uptake when implemented in the lower vaccinated communities. Implementation of prebunking strategies against misinformation cannot replace risk communication in correcting the biases resulting from misinformation spread in under-vaccinated communities. In highly under-vaccinated communities, targeting the most connected and highly diffusive households generates larger increases in vaccination uptake, supporting current practices that prioritise well-connected individuals and those most likely to diffuse information ("gossip") within the community. Mandatory vaccination emerges as the most effective intervention for rapidly achieving high uptake in the community, but its effects are not mirrored in households' willingness to vaccinate. While households do decide to vaccinate, their willingness remains suppressed by low popularity of vaccination within their vicinity.

6.2 Context

This thesis is developed under an assumption of heterogeneous vaccination uptake. Clusters of under-vaccinated communities can emerge despite high uptake levels in the general population (Brownwright et al., 2017; Klinkenberg et al., 2022; Masters et al., 2020). The clustering is caused by the mutual phenomena of homophily and social influence (Alvarez-Zuzek et al., 2022), where individuals are more likely to relate with others with the same attributes, and those relationships between people with same characteristics enforce their perceptions and behaviour.

The first unifying claim of the thesis is also related with the clustering phenomenon: **social influences transform individual's perception of vaccination into collective dynamics that may constrain behaviour**. The social norm determinant to behaviour can not only promote preference for conducting a behaviour but also induce behavioural restriction, especially in under-vaccinated communities. Households can be less willing to vaccinate, even under outbreak and mandatory vaccination, if there are less vaccinated households around them, as can be seen in Chapter 3 (**Figure 3.3**) and Chapter 5 (**Figure 5.7**).

The thesis claim on the importance of social influence shifts the paradigm of vaccination behaviour transmission in social networks from simple to complex contagion. Complex contagion applies to costly decisions, where adoption of a new behaviour occurs only after a sufficient proportion of people around an individual have already adopted that behaviour (Centola and Macy, 2007; Guilbeault et al., 2018). As no vaccination is entirely free from adverse events, vaccination constitutes a "costly" decision and therefore requires complex contagion mechanisms to trigger behavioural adoption.

However, simulations of vaccination campaign in highly under-vaccinated communities in this thesis contradict the general understanding of complex contagion, which suggests that collective behavioural change spreads more effectively when initiated from the network periphery with sparse connectivity (Centola, 2021). This would imply fewer connections promote stronger social reinforcement when a neighbour adopts vaccination. By contrast, this thesis shows that initiating vaccination with the least connected households generates smaller increases in general population uptake than random seeding. Conversely, vaccination campaigns are most effective when initiated through the most connected and highly diffusive households (Chapter 5 – **Figure 5.6**). These results underscore that, in highly under-vaccinated communities, social influence is more optimal to be delivered through wider exposure of vaccination behaviour across the community rather than through strong reinforcement within small local neighbourhoods.

Modelling vaccination through a social network enables further disentanglement of social influence effects. This study found that community isolation, moderated by assimilation bias, increases vaccine hesitancy and fosters polarisation between under-vaccinated communities and the surrounding general population - **Figure 3.10** (Chapter 3). Beyond homophily and social contagion, which can generate clusters of hesitant communities (Alvarez-Zuzek et al., 2022), households in highly knitted and isolated communities are likely to converge in opinion

under assimilation bias, reinforcing their prior stance toward vaccination. Therefore, in communities where households already perceive vaccination as costly, the high perceived cost is likely to persist over time.

Altogether, the social influence and community isolation with assimilation bias act as constraints towards vaccination in under-vaccinated communities, given their resistance to external shocks such as disease outbreaks and vaccine mandates. This underscores the importance of the social environment in shaping households' vaccination decisions in protection against disease.

The second unifying claim of the thesis is that **there is a critical threshold of vaccine perception in determining stability of vaccine uptake in one community**. The vaccine perception is operationalised in this thesis as perceived vaccination relative cost, and once the perceived vaccination relative cost exceeds this threshold, collective vaccination decreases and herd immunity becomes unreachable.

This critical threshold remains significant during a measles outbreak. Reactive vaccination is only effective when perceived vaccination relative cost in one community is below the critical threshold. When perceived vaccination relative cost is above the threshold, the cumulative infected percentage is inversely associated with the initial vaccination coverage in the community, as can be seen in Chapter 3 - **Figure 3.6**, including when an external shock of disease scare is considered (**Figure 3.17**).

This study also found that extreme values of perceived vaccination cost can suppress the effectiveness of the highly efficacious measles vaccine. To explain this phenomenon, behavioural vaccine effectiveness (BVE) is operationalised in this thesis, distinct from the optimal biological effectiveness of the measles vaccine. This study found a lower BVE after a measles outbreak in under-vaccinated communities, and BVE was suppressed to below 0.5 in highly under-vaccinated communities with higher perceived vaccination relative cost (**Figure 3.7**). This underscores how behavioural and psychological factors can undermine a biologically highly efficacious vaccine.

Because vaccination uptake is an outcome of inherent perceived vaccination relative cost, it can be inferred that communities that are under-vaccinated against measles have an underlying high perceived vaccination cost. Given that under-vaccinated communities are also most likely

to experience outbreaks (Dimala et al., 2021; Leong and Wilder-Smith, 2019; Phadke et al., 2016), this finding underscores the constraints of relying on reactive vaccination following measles outbreaks in under-vaccinated communities. However, this result should be interpreted cautiously, due to the assumption of full susceptibility among unvaccinated children, which was used to isolate the role of pre-outbreak vaccination coverage and the underlying perceived vaccination cost in shaping epidemic magnitude. Nevertheless, the result highlights the importance of interventions to address hesitancy and increase pre-emptive vaccination, rather than relying on reactive vaccination following outbreaks.

The out-of-sample validation in Chapter 4 provides empirical evidence consistent with this claim. The measles outbreaks in Indonesia in 2022 and 2023 were not followed by an increase in vaccination uptake, as the estimated perceived vaccination relative cost remained constant or increased in most provinces during those years. When the model was supplied with the reported outbreak incidence while carrying forward the lower perceived vaccination relative cost of earlier years, it predicted an increase in uptake that did not occur. This suggests that, in populations with a high perceived vaccination relative cost, outbreaks alone are insufficient to raise vaccination uptake, consistent with the persistence of hesitancy despite outbreaks simulated in Chapter 3.

Implementing communication strategies to alleviate the perceived vaccination cost is simulated to be effective in increasing uptake, yet the only successful communication strategy to reduce perceived vaccination relative cost is through disease risk communication (Brewer et al., 2007; Horne et al., 2015). Although communication strategies effectiveness is constrained by social influence and assimilation bias, risk communication can increase vaccination uptake - larger effects are expected in communities with lower vaccination rather than in communities with higher uptake. Implementing prebunking strategies to mitigate the harms of misinformation is not a substitute for risk communication. As shown in **Figure 5.5**, both prebunking and debunking are optimised when both are implemented as preventive and as a response against misinformation.

The third unifying claim of the thesis is **the disentanglement of the psychological construct of vaccination from the behavioural outcomes**. This distinction is most prominent in the simulation of mandatory vaccination, where the perceived relative cost of vaccination is shifted to net benefit. In the mandate setting, a failure to comply means loss of access to baseline service, therefore the compliance means a benefit of access. This study found that households'

willingness to vaccinate under mandatory vaccination is inherently depleted when there are less vaccinated households around them, despite explicitly high uptake (**Figure 5.7.**). Previous studies have reported indirect effects of vaccine mandates in igniting anger (Betsch, 2016) and avoidance to any future voluntary vaccination (Sprengholz et al., 2022). This study adds value by elaborating another challenge in implementing mandatory vaccination: the psychological level constraint due to suppressed support of vaccination in the neighbourhood. This distinction between behavioural and psychological states has been considered as well in defining vaccine hesitancy, where the hesitancy should be measured as the "state of mind" rather than the behaviour (Bussink-Voorend et al., 2022; Goldenberg, 2021; Larson, 2022).

To disentangle the psychological state from observed behaviour, this thesis proposes a method to estimate trends in the hidden variable of perceived vaccination relative cost from routinely reported vaccination uptake and measles incidence data in global immunisation programmes, as presented in Chapter 4. This work provides a foundation to monitor trajectories of population perception toward vaccination, complementing routine reports of uptake and incidence.

The out-of-sample validation further supports this disentanglement. The model predicted vaccination uptake better than last year's uptake and a linear trend because it separates the gradual change in perceived vaccination relative cost from temporary supply-side disruptions, such as service restrictions during the Covid-19 pandemic and supplementary immunisation activities. Although a provincial mean of uptake predicted as accurately as the model, it combines vaccination perception and accessibility constraints into a single value, whereas the estimated perceived vaccination relative cost is not associated with poverty rate or distance to primary care facilities. The value of the model therefore lies in identifying whether low uptake stems from vaccination perception or from access, rather than in improving the prediction of uptake itself.

6.3 Strengths, limitations and further works

In this thesis, the vaccine hesitancy phenomenon is studied through an integrated modelling framework grounded in health behaviour theories, opinion formation, network science and epidemiology. The unified vaccination decision model is implemented to study mechanisms underlying complex phenomenon of vaccine hesitancy in under-vaccinated communities, to infer comparative temporal dynamics of vaccination perception across multiple populations

using routinely available data, and to simulate interventions to address vaccine hesitancy to evaluate their effectiveness prior to implementation.

The vaccination decision model in this thesis is inspired by the Theory of Planned Behaviour (TPB) (Ajzen, 1991) and the Increasing Vaccination Model (IVM) (Brewer, 2021; Brewer et al., 2017). In both models, there is a distinction between willingness and behaviour, which helps to disentangle the psychological antecedents from the behavioural outcome. This differentiation enables a richer comparative analysis between behaviour and the underlying cognitive aspects of vaccination, as seen in supressed willingness during emergent outbreaks and under mandatory vaccination, despite an increasing vaccination behaviour. This enables examination of the underlying determinants of vaccine hesitancy, disentangled from observed vaccination behaviour.

Although vaccination determinants are represented in the vaccination decision model, perceived behavioural control (PBC) in TPB or direct behaviour change (DBC) in IVM are not yet fully included. PBC and DBC operate on top of household willingness by providing facilitating factors that expedite behavioural outcome. Interventions that provide such facilitating factors include strategies to ease access to vaccination, as well as approaches that directly shape behaviour through mandates, sanctions or requirements. Although external adjustment of PBC and DBC is simulated in mandatory vaccination settings in this thesis, other avenues to adjust them are not yet included.

The partial exclusion of PBC and DBC is also due to our focus on the demand side of the vaccination pipeline. Supply side problems related accessibility are treated as negligible, although accessibility barriers may still exist for some communities despite widespread vaccine availability in the general population (Qi et al., 2022). This study found that the estimated perceived vaccination relative cost was not associated with poverty rate or distance to primary care facilities, whereas vaccination uptake was, providing initial evidence that the estimate reflects perception rather than accessibility. However, further scrutiny through observational research is needed to disentangle accessibility from broader cost perceptions regarding vaccination. Overall, further methodological development is needed to incorporate more comprehensive PBC and DBC into vaccination modelling frameworks.

This thesis focuses on the simulation of vaccination decision making in small communities. This scaling decision enables a focus on pockets of communities with significantly lower

vaccination uptake, clustered within a wider population with relatively higher uptake (Brownwright et al., 2017; Klinkenberg et al., 2022; Masters et al., 2020). The decision is aligned with the implementation of an agent-based model (ABM) in a synthetic network of households. ABM is an appropriate choice given that vaccination uptake is not homogeneous across the population. However, ABM is bounded by available computational capacity. Therefore, the focus on under-vaccinated communities reflects a judgement to address the thesis aim while optimising computational capability and maintaining reproducibility for other researchers or public health programmes with limited access to high-performance computing.

However, this thesis cannot avoid the need for scalability enhancement, given that one of its aims is to estimate vaccination perception in populations. To address this aim, the ABM- and network-based vaccination decision model is transformed into a deterministic form to enable population-level scalability. The deterministic transformation is further implemented within an estimation model inspired by the Generalized Expectation Maximization (GEM) algorithm (Dempster et al., 1977; Monti et al., 2023). The estimation model can efficiently infer perceived vaccination relative cost trajectories that fit the reported vaccination uptake and measles incidence data. Its uncertainty was quantified using Markov Chain Monte Carlo (MCMC) sampling, and its predictive ability was evaluated out of sample. Nevertheless, the estimates remain conditional on the model structure, data quality and multi-stage calibration, and its result should not be treated as absolute measures of perception. Therefore, the inferred perceived vaccination relative cost is best interpreted as a signal of perception trends.

The out-of-sample validation of the estimation model covers only two held-out years, both of which were atypical due to post-pandemic recovery, a nationwide vaccination campaign and a nationwide outbreak. The validation also showed that the deterministic model, with an averaged force of infection in each province, cannot forecast measles outbreaks, which in endemic settings are driven by pockets of unvaccinated individuals and case importation. Moreover, carrying forward perceived vaccination relative cost from earlier years cannot anticipate changes in perception within the predicted year. Further work could extend the validation as additional years of data become available, incorporate stochastic transmission and case importation, and compare the model against a variant with province-invariant perceived vaccination relative cost.

Strategies to address vaccine hesitancy are simplified into three groups of interventions based on the working mechanism in augmenting vaccination behaviour: cognitive, social and

incentive-based. This simplification does not replace comprehensive and specific analysis of each possible intervention that can help reduce vaccine hesitancy, but rather it provides a principled basis to implement the specific interventions according to where they operate within the decision-making mechanism and the specific setting of under-vaccinated communities as subject of behavioural change. Further evidence on intervention efficacy can be incorporated into the vaccination decision model used, to evaluate any intervention of interest prior to scaling up in real world application.

Although this study considered heterogeneity in potentially infectious contacts for individuals within a prescribed social network, homogeneity assumptions still dominate the psychological constructs assigned to each household agent. Perceived vaccination relative cost, assimilation bias, social norm degree, decision noise index and intervention efficacy are assumed to be homogenous across households in each community. This approach is taken to isolate the effect of each psychological construct in producing a vaccination behaviour, as the inter-household variation could obscure the effect analysis. However, incorporating empirically informed heterogeneity in these vaccination determinants would strengthen the model's realism and external validity.

Another simplification concerns the assumption of identical connectivity structures for behavioural and disease transmission. Implementing identical connectivity enables direct comparison and clarifies the distinction between complex and simple contagion. However, this simplification abstracts from the reality that behaviour and disease have different modes of transmission; measles can spread through inter-household, school and workplace close in-person interactions, whereas vaccination behaviour can also spread through print media and online communications. Building on the renewed understanding of the distinction between complex transmission of vaccination and simple transmission of disease, further work incorporating more realistic behavioural and disease transmission pathways is needed to strengthen understanding of vaccine hesitancy.

6.4 Conclusions

This thesis addresses vaccine hesitancy and strategies to address it. The aim of this thesis is achieved through a unified modelling approach that integrates multidisciplinary perspectives from health behaviour, evolutionary game theory, statistical physics of human cooperation, social network topology and measles epidemiology. The thesis initially elaborates the

construction of the integrated model, then described the theoretical evaluation of vaccine hesitancy phenomena in under-vaccinated communities. The integrated model is subsequently implemented to estimate a psychological construct of vaccine perception from routine administrative data of vaccination uptake and measles incidence at the population level. Finally, the integrated model is also implemented to simulate intervention scale-up from controlled settings of experimental and observational research to real-world conditions characterised by social influence and cognitive bias.

From the pipeline of work in this thesis and the resulting findings, three thesis claims emerge: (i) social influence transforms household perception of vaccination into collective dynamics that may constrain behaviour, (ii) there is a critical threshold of vaccine perception determining the stability of vaccine uptake within a community, and (iii) psychological states should be disentangled from the vaccination behavioural outcome.

In addressing vaccine hesitancy, specific focus should be placed to ensure sufficient local reinforcement of vaccine adoption in the neighbourhoods. The most effective avenue to initiate vaccine campaigns in under-vaccinated communities is through the most popular and the most diffusive ones (those most likely to know "gossip" and distribute it within the community) households. Furthermore, communicating disease risk provides the greatest benefit for increasing uptake in the most under-vaccinated communities, as the intervention can reduce perceived vaccination cost despite current local reinforcement and bias against vaccination, to gradually reach herd immunity coverage. Finally, since this thesis considers both the behavioural and psychological constructs as being equally important in sustaining collective vaccination, monitoring willingness and vaccine perception should not be obscured by observed vaccination uptake alone.

To clarify and dissect the complex mechanisms of vaccine hesitancy, this thesis necessarily adopts a set of simplifications that abstract from the full behavioural complexity observed in real settings. Further work that relaxes these assumptions will be important to represent vaccine hesitancy with greater realism. Nevertheless, within these limits, this thesis offers an incremental contribution to the body of knowledge by providing a structured modelling framework to interpret how psychological state, social influence, and behavioural complexity can jointly shape vaccination outcomes.

Appendix

Appendix A Reported data adjustment

To account for under-reporting due to suboptimal surveillance, case counts were adjusted using two performance indicators: the non-measles–non-rubella (NMNR) discard rate and the proportion of suspected cases investigated within 48 hours. **Table A.1** shows Indonesia's surveillance performance for 2018-2022, based on data from CDC report (Chacko, 2023). For 2023, only NMNR data were available from WHO (*World Health Organization*, 2024).

Table A.1. Measles surveillance performance in Indonesia, 2018-2022

Characteristic	Year						Target
	2018	2019	2020	2021	2022	2023	
Non-measles non-rubella (NMNR) discard rate (per 100,000 population)	1.2	1.0	0.8	0.8	3.3	4.84	≥ 2
Suspected case investigated within 48 hours (%)	65	62	60	71	74	-	≥ 80

The reported data of measles-contained-vaccine dose 1 (MCV-1) vaccination uptake were adjusted with WHO/UNICEF estimates of national immunisation coverage (WUENIC) data (World Health Organization and UNICEF, 2025).

Figure A.1 presents both the monthly measles incidence and MCV-1 uptake, comparing the reported and adjusted data.

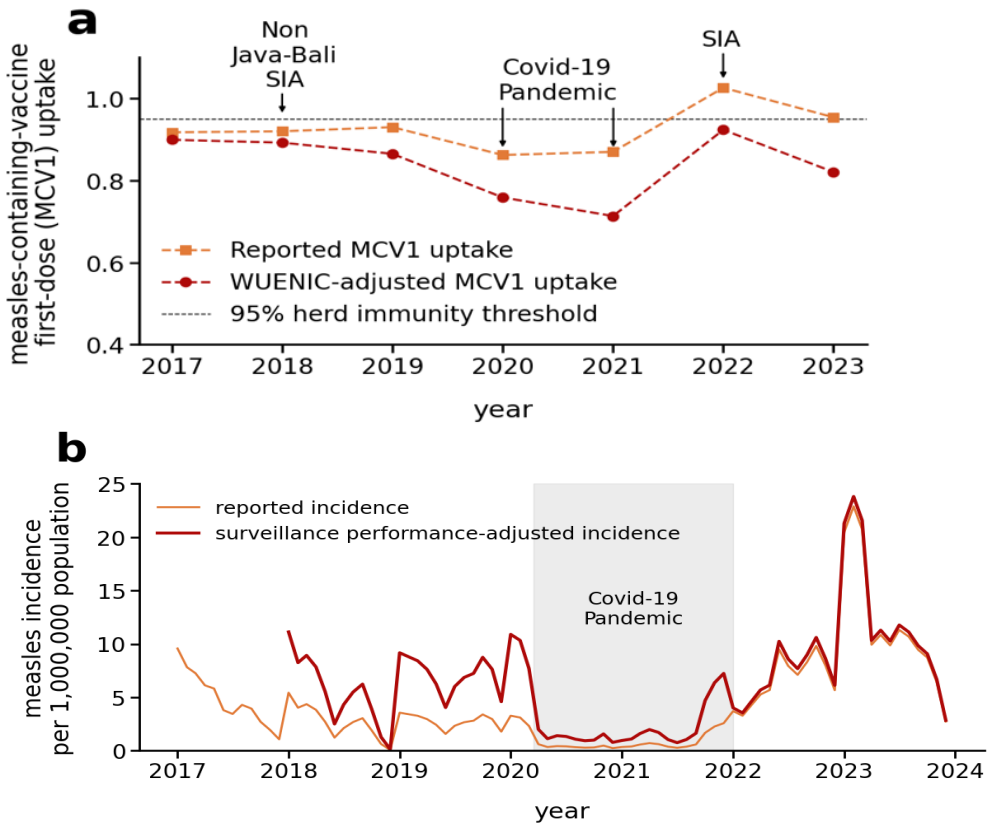


Figure A.1. The reported and adjusted MCV-1 uptake and measles incidence data of Indonesia. (a) Annual MCV-1 uptake in comparison with the WUENIC-adjusted data. **(b)** Monthly incidence per 1 million population in comparison with annual surveillance capacity data.

Figure A.1 shows that the gap between the reported and the WUENIC-scaled estimates widens over time. The non-Java-Bali SIA in 2018 did not help to reach the 95% herd immunity threshold. While the reported annual uptake exceeding 100% during the post Covid-19 pandemic SIA in 2022, the WUENIC-scaled uptake still fell short of the herd immunity threshold. In contrast, the reported incidence values increasingly converge with the surveillance adjusted incidence over the study period, indicating that the national surveillance performance in Indonesia improved during these years.

Following relaxation of contact intensity after lockdown and expected reduction of vaccination due to pandemic, Indonesia experienced a measles outbreak in 2023, with incidence peaking in January. Similar early year peaks were also observed in 2017 and 2018, suggesting a possible seasonal pattern in which measles incidence tends to rise at the start of the year. However, this visual pattern alone is insufficient to confirm seasonality, and further analysis is required to determine whether measles in Indonesia follows a consistent seasonal cycle.

Figure A.2 shows the association between measles-containing-vaccine dose (MCV-1) uptake with the subsequent annual measles incidence based on the lag years. The correlation was significant for 2 to 4 years lag, with the highest correlation happens in 3 years lag with negative correlation of MCV-1 uptake with annual measles incidence (r = -0.34).

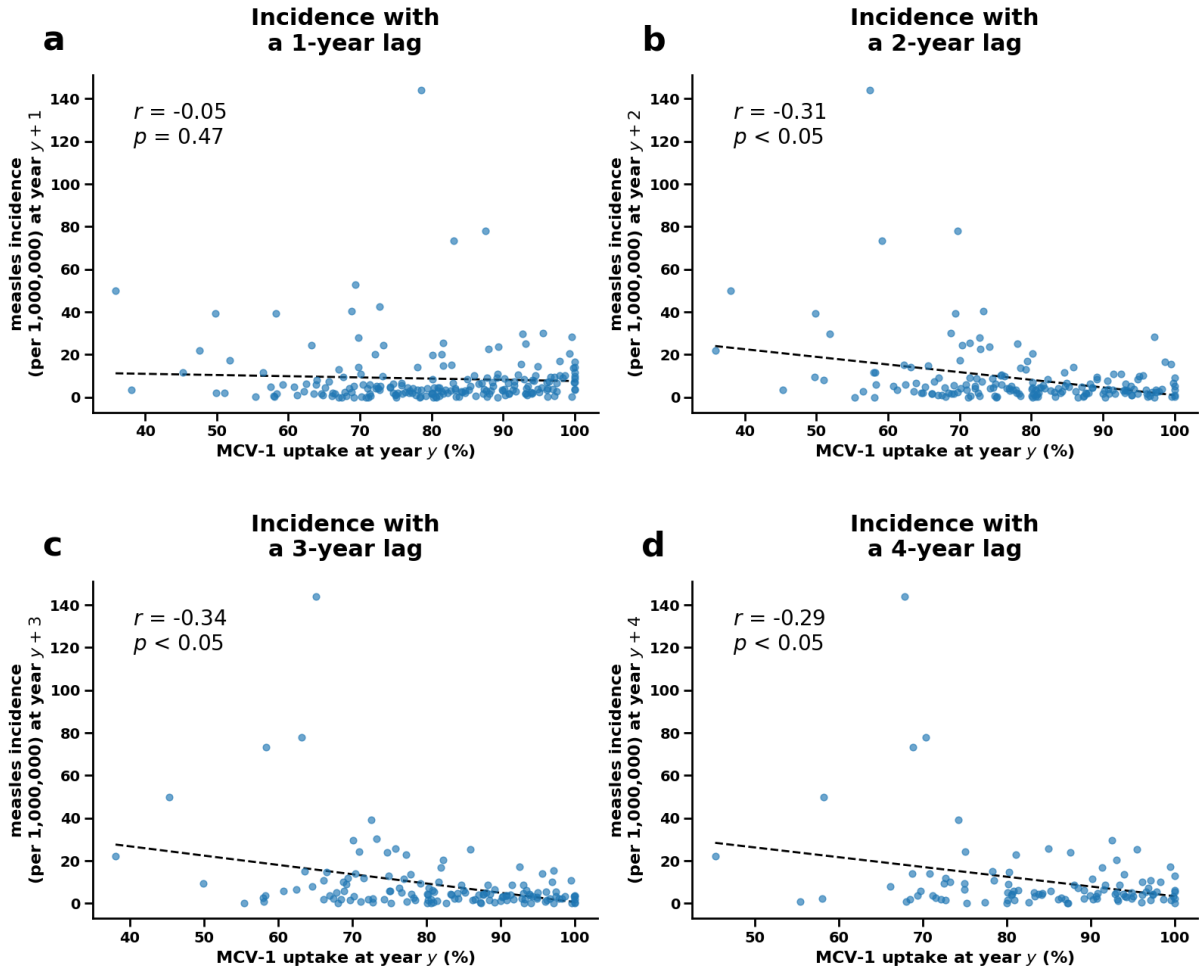


Figure A.2. Association of annual measles-containing-vaccine dose 1 (MCV-1) uptake with yearly measles incidence. The association is measured by Pearson's r based on the incidence year lag.

Appendix B Seasonality analysis of measles

Figure B.1 demonstrates that across the months, January is consistently the peak month of measles incidence in Indonesia. The median provincial incidence in January is around 8 per 1 million population. Incidence declines in the subsequent months, plateaus from April to July, rises modestly in August, then stabilizes before falling to a December low. Visual inspection of the monthly trend suggests that there is a seasonality of measles in Indonesia.

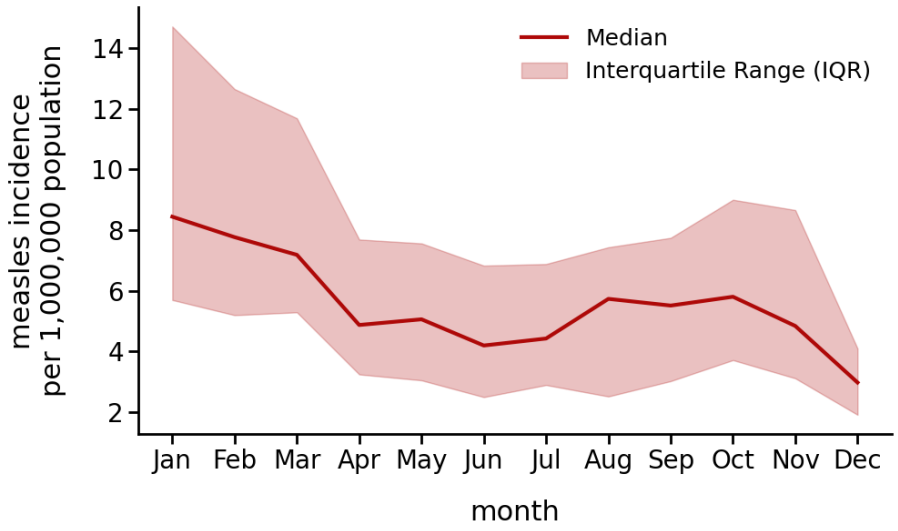


Figure B.1. Monthly seasonality trend of measles incidence across provinces in Indonesia. Trends in measles incidence are shown for 2017–2023. The median and interquartile range (IQR) are calculated from adjusted incidence across provinces, where adjustment accounts for national surveillance performance based on the non-measles–non-rubella discard rate and the percentage of timely case investigations.

However, to formally assess seasonality in measles incidence, a further analysis is conducted. The visual inspection of incidence trend is extended with (i) Autocorrelation Function (ACF), to quantify similarity in incidence across monthly lag, and (ii) Seasonal-Trend decomposition using Loess (STL) (Cleveland et al., 1990), to separates the incidence with the seasonality-adjusted trend.

To assess seasonality in measles incidence, the ACF yearly lags (at 12, 24, 36 and 48 months) are examined using the province-level time series. **Figure B.2a** shows no significant autocorrelation at these annual lags, indicating no seasonality. By contrast, the ACF exhibits strong positive autocorrelation at short lags (1-5 months), suggesting a measles outbreak persistence in a province. A high incidence month in one province is followed by other high months. Moreover, there is a negative autocorrelation around 16-36 lag months, suggestive of a multi-year epidemic cycle. During that period, the negative autocorrelation of incidence

indicates a temporary depletion of susceptible, although the correlation is not significant as the time points do not cross the significance bounds.

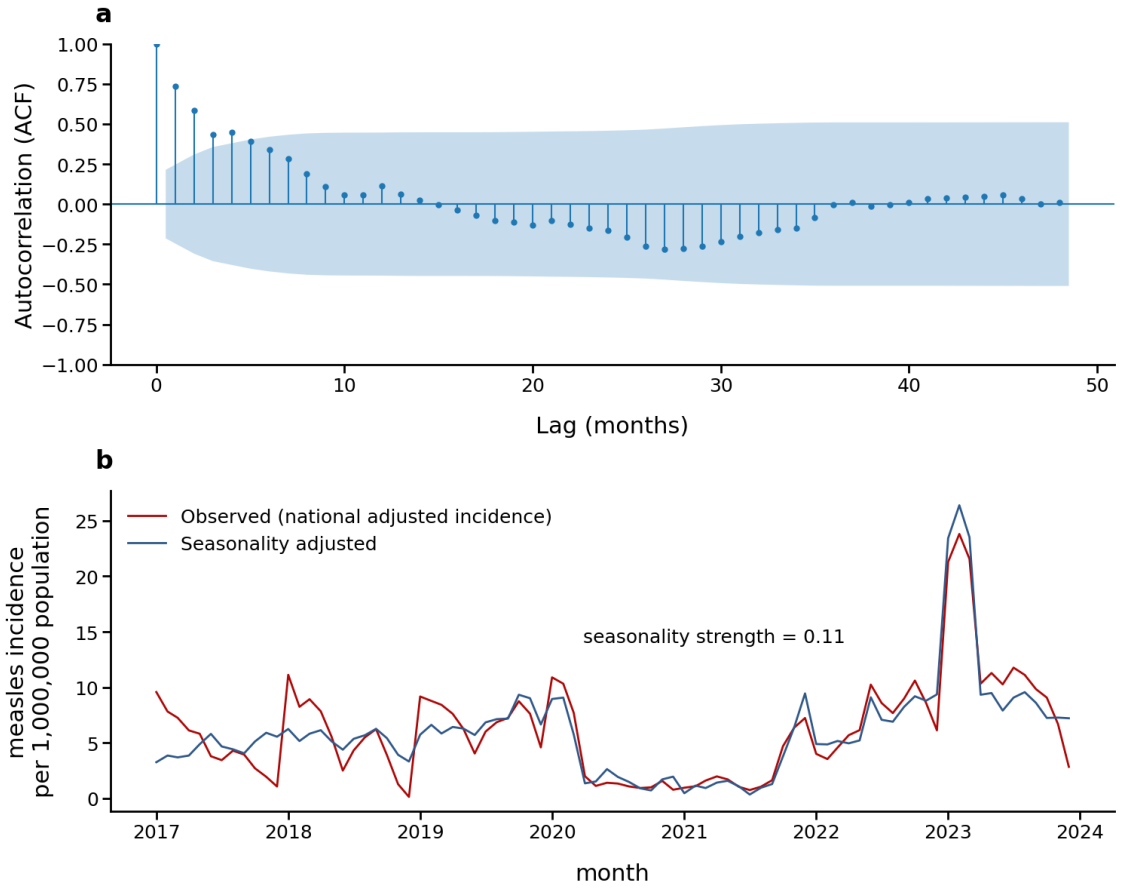


Figure B.2. Seasonality analysis of measles incidence in Indonesia. (a) Autocorrelation function (ACF), with the blue shading indicates the significance bounds. Bars extending beyond the bounds represent significant autocorrelation at the corresponding lag. **(b)** Seasonal–trend decomposition using Loess (STL), performed with a 12-month seasonal period and robust fitting to downweigh outliers.

Using STL decomposition (**Figure B.2b**), it is demonstrated that there is no seasonal pattern in measles incidence in Indonesia. A seasonality is indicated when the seasonality adjusted line (blue) is substantially flatter than the observed data series (red). The seasonality adjusted series is obtained by removing seasonal component (period = 12), computed from same month values across years. Estimates near the series boundaries (2017 – 2018) are less reliable due to edge effect. STL has no past data to estimate stable seasonal component in the early part of the series. From 2019 onward, the seasonality adjusted series closely tracks the observed incidence, indicating that the incidence is dominated by irregular outbreaks rather than seasonality pattern. This is consistent with the low seasonality strength, with only ~0.11 of the variance explained by seasonality.

Multiple seasonality tests likewise confirms that there is no seasonality of measles incidence in Indonesia. A Kruskal-Wallis test comparing median monthly incidence across provinces shows no month is systematically higher than the others (p-value = 0.4). An annual harmonic regression estimates a seasonal amplitude of ≈1.6 cases per 1 million, minor relative to observed peaks (>20 per 1 million in 2023 and ~10 in 2018 and 2020).

Table B.1. Seasonality test results of measles incidence in Indonesia

Test	Statistic	p-value
Kruskal-Wallis (across months)	H = 11.518	0.401
Harmonic regression (12-month)	Amplitude = 1.6 per 1 million	-
Ljung-Box Q (12)	52.22	<0.001

By contrast, the Ljung-Box test at 12-month lag was significant ($Q(12) = 52.22$, $p < 0.001$), indicating temporal autocorrelation persists at yearly interval. However, as has been shown by ACF plot in **Figure B.2a**, it is demonstrated that there is no sharp spike of autocorrelation at 12 lag months. Instead, the ACF plot shows a gradual decay of correlations after an outbreak (up to ~14 months lag), and negative correlation at longer lags (16 to 36 months). This pattern is consistent with prolonged outbreak decay and subsequent depletion of susceptible rather than a repeating annual cycle. Therefore, the significant Ljung-Box result reflects persistence of measles outbreak, not true seasonality.

Taken together, these analysis support the assumption that there is no seasonality of measles incidence in Indonesia during 2017-2023 period. The peak of cases is mainly driven by irregular outbreaks due to random events, rather than regular pattern of seasonality. Accordingly, the measles transmission is modelled with assumption of no seasonality.

Other methods such as spectral analysis, cosinor models, seasonal ARIMA (SARIMA), and Edwards' test were also considered to assess seasonality of measles incidence in Indonesia. However, they are less suitable for the available data and analysis aims. Spectral analysis requires long and stationary series, while the measles outbreak-driven data can produce irregular epidemics and multiple noisy peaks. Cosinor model is similar to harmonic regression, but to accommodate irregular peaks of measles incidence, it requires multiple overlapping waves, rather a single smooth yearly cycles. SARIMA is primarily a forecasting tools and less interpretable in assessing seasonality strength. Edward's test is mainly designed for circular

event data (e.g. counts of onset dates) rather than aggregated monthly incidence counts such as those in the available dataset.

Appendix C Parameter estimation

Global parameters for the objective (loss) function and the M-Step learning rate were calibrated using all province-year data. Optimization ran for up to 30 epochs. The selected global parameter values combination is reported in **Table C.1** (where $\mathcal{L}^*$ denotes the minimum mean loss across provinces at the selected epoch).

Table C.1. Global parameter values for the loss function and M-Step learning rate.

lr	$risk_{scale}$	σ_{cov}	σ_{inc}	ω_{cov}	$\mathcal{L}^*$
0.009	1.754	1.11	122.19	1.11	0.02

In the next stage, province-specific parameters were calibrated using the **Table C.1** values. For each province, a constant $monthly_{cap}$ and year-specific $risk_{scale}$ are estimated. Finally, by implementing the estimated $monthly_{cap}$ and $risk_{scale}$ values, the yearly proportion of hesitant communities π_h are calibrated for each province. The result of the province-year parameter calibration can be seen in Supplementary Document 4.

Appendix D Basic and effective reproductive number

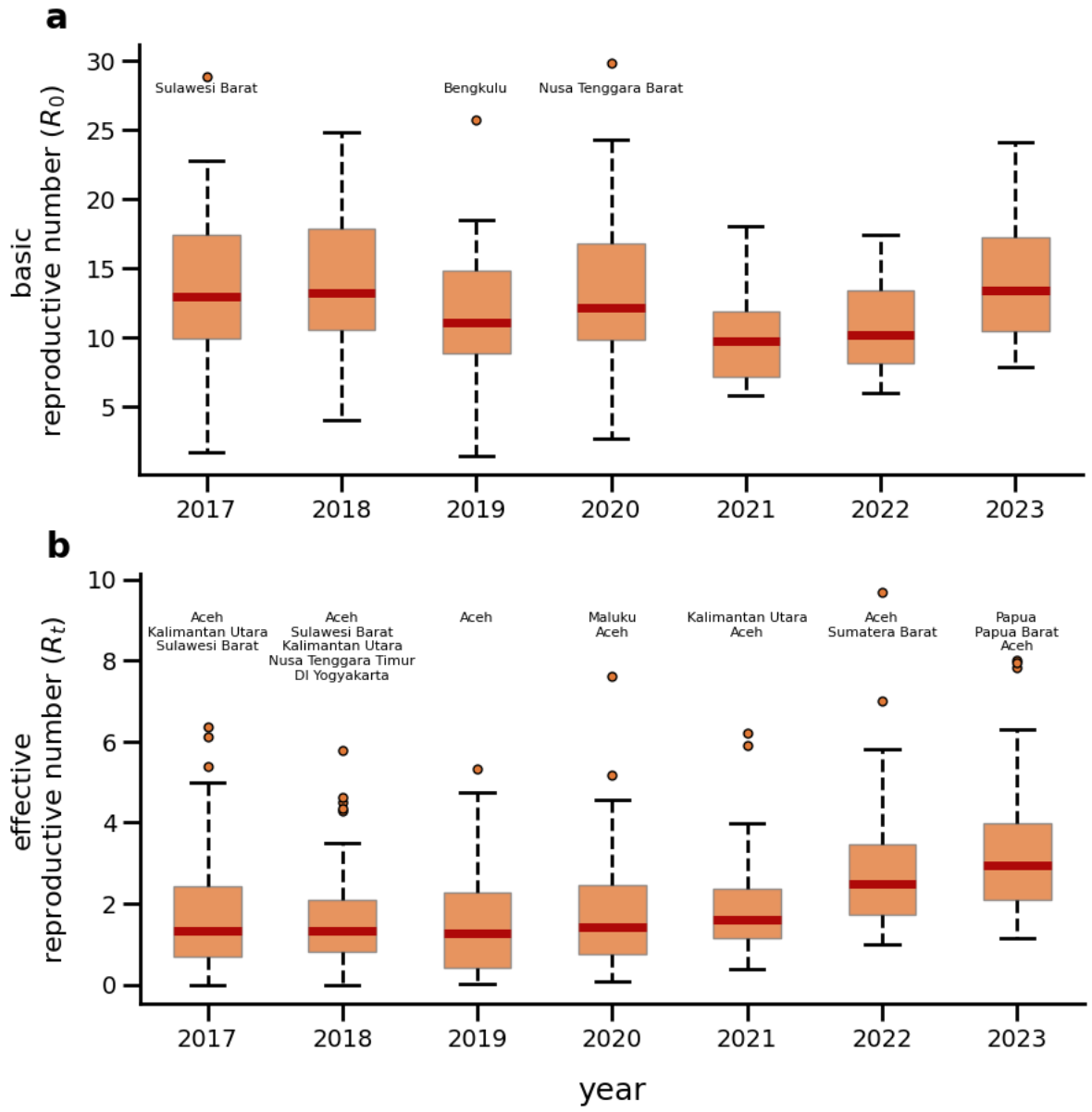


Figure D.1. Measles reproductive number for each vaccination season in Indonesia, 2017-2023. (a) The basic reproductive number (R_0) and **(b)** the effective reproductive number (R_t) are calculated with mean monthly incidence and the fitted force of infection (λ_y) for each vaccination season year. The duration of infectiousness is 6-10 days. The R_t for each year is calculated by considering average of vaccination uptake over the last 3 years, and the outliers provinces are sorted based on the R_t value.

To calculate the reproductive number, initially the transmission rate (β) is computed from yearly fitted force of infection (λ_y) from GEM (Generalized-Expectation Model) in Chapter 4:

$$\beta = \frac{\lambda_y}{I_{fraction}}; \qquad I_{fraction} = \frac{\bar{I}_y^{obs}}{10^6}$$

The $\bar{I}_y^{obs}$ is the mean monthly measles incidence per 1 million population for each year. Then the basic reproductive number (R_0) is calculated by considering duration of measles infectiousness (D) in 6-10 days (Hübschen et al., 2022).

$$R_0 = \beta \times D$$

The effective reproductive number (R_t) is calculated by looking at average of measles-containing-vaccine dose 1 (MCV-1) uptake ($\bar{V}$), which are calculated over the previous three years record.

$$R_t = R_o\,(1 - \bar{V})$$

The reproductive number dataset of measles infection in Indonesia during 2017-2018 vaccination seasons is provided in Supplementary Document 5.

Appendix E Estimated v_{RC} list

The raw v_{RC} estimates fluctuate to closely fit the reported data. For behavioural interpretability, these fluctuating trajectories are reconciled. **Figure E.1** compares the raw and reconciled general v_{RC} within each province. **Figure E.2** extends this by showing the reconciled general v_{RC} alongside the hesitant and other communities' trajectories. The reconciled perceived vaccination cost (v_{RC}) is also shown alongside the annual measles containing vaccine dose 1 (MCV1) uptake (**Figure E.3**) and incidence (**Figure E.4**). The full list of the v_{RC} for hesitant, other and in general population before and after the reconciliation is provided in Supplementary Document 6, along with the λ_y, $\mathcal{L}$ and δ_{const} for each province-year.

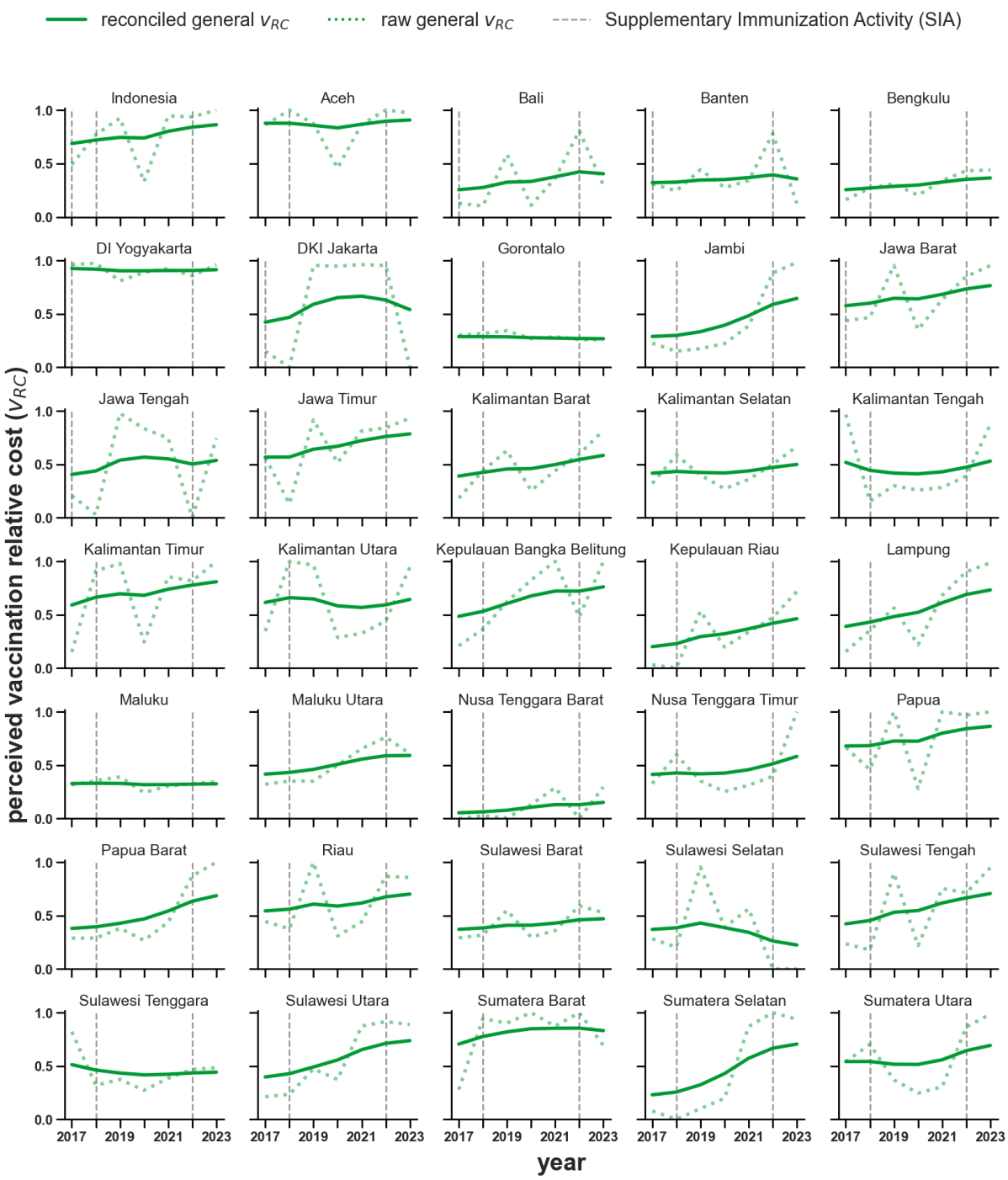


Figure E.1. Reconciled and raw perceived vaccination relative cost (v_{RC}) by provinces in Indonesia. Panels show the general population v_{RC}, which are a mixture of hesitant and other communities, and represents a general perception of v_{RC} in each province. Solid lines are reconciled trajectories, and dotted lines are raw estimates of v_{RC}. Vertical dashed lines indicate supplementary immunisation activity (SIA) periods.

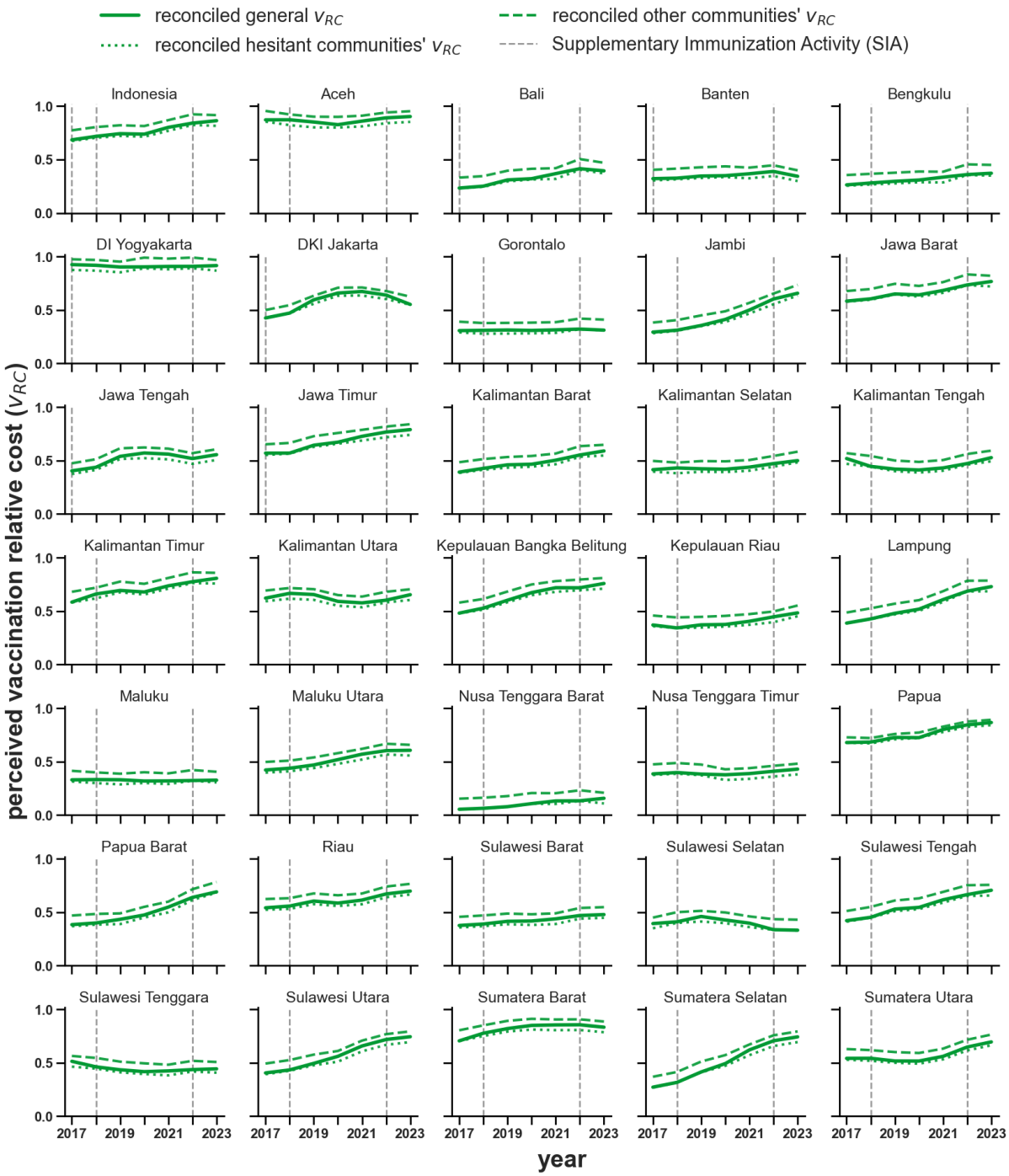


Figure E.2. Reconciled perceived vaccination relative cost (v_{RC}) by provinces, showing general population, hesitant, and other communities trajectories. The general series (straight line) is the mixture of hesitant (dotted) and other (dashed) communities, with the hesitant communities' proportion is initially set π_h = 0.05 before π_h calibration. Although in later calibration, the π_h is allowed to vary each year, the other communities proportion dominates the general population, so the other trajectory closely tracks the general trajectory. Vertical dashed lines indicate SIA periods.

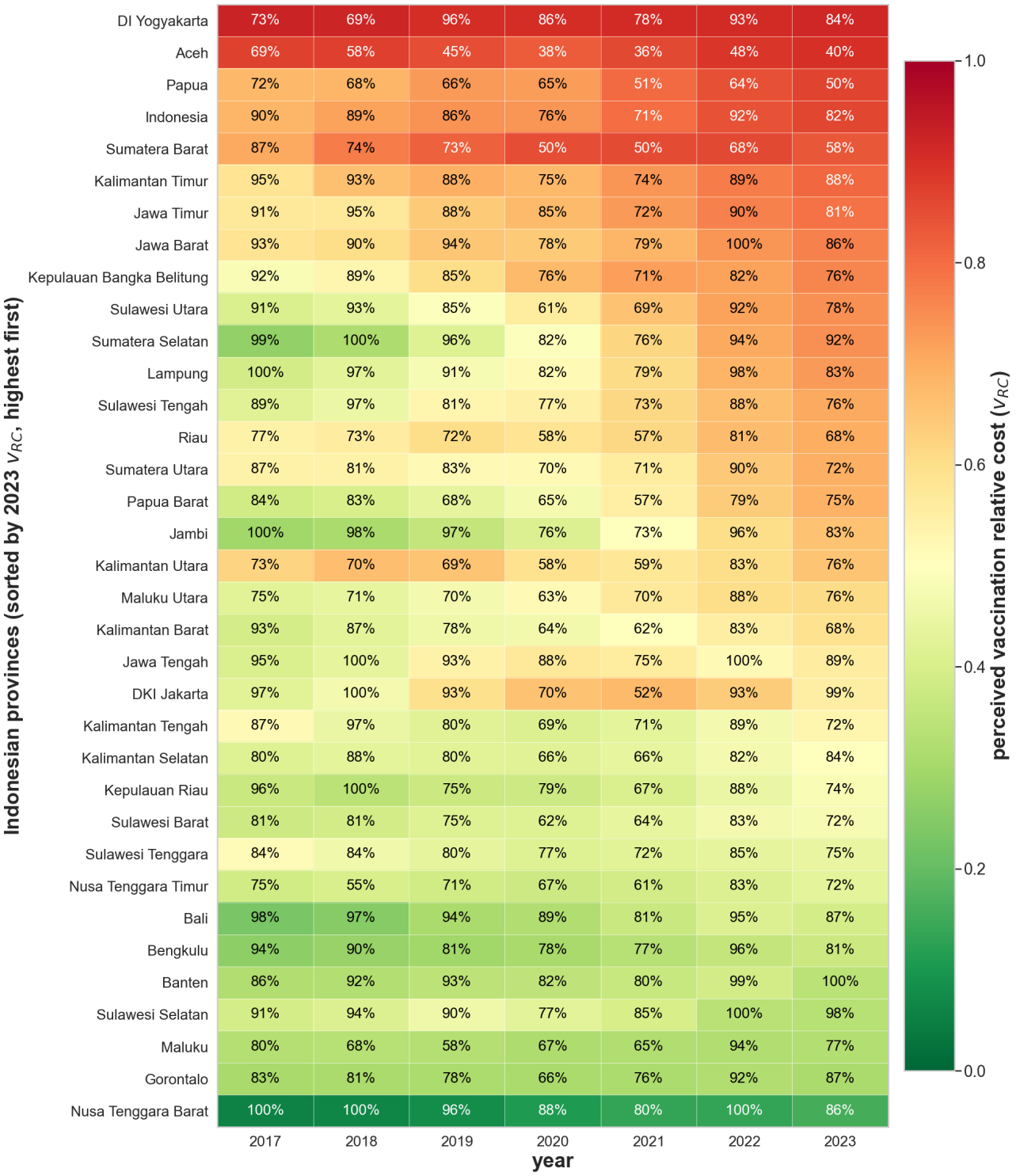


Figure E.3. Perceived vaccination relative cost (v_{RC}) across provinces in Indonesia, in comparison with reported measles-containing-vaccine dose 1 (MCV-1), 2017-2023. The v_{RC} value is reflected in the color scheme, while the annual MCV-1 uptake is on the label within each box. The provinces are sorted based on v_{RC} value in 2023.

.

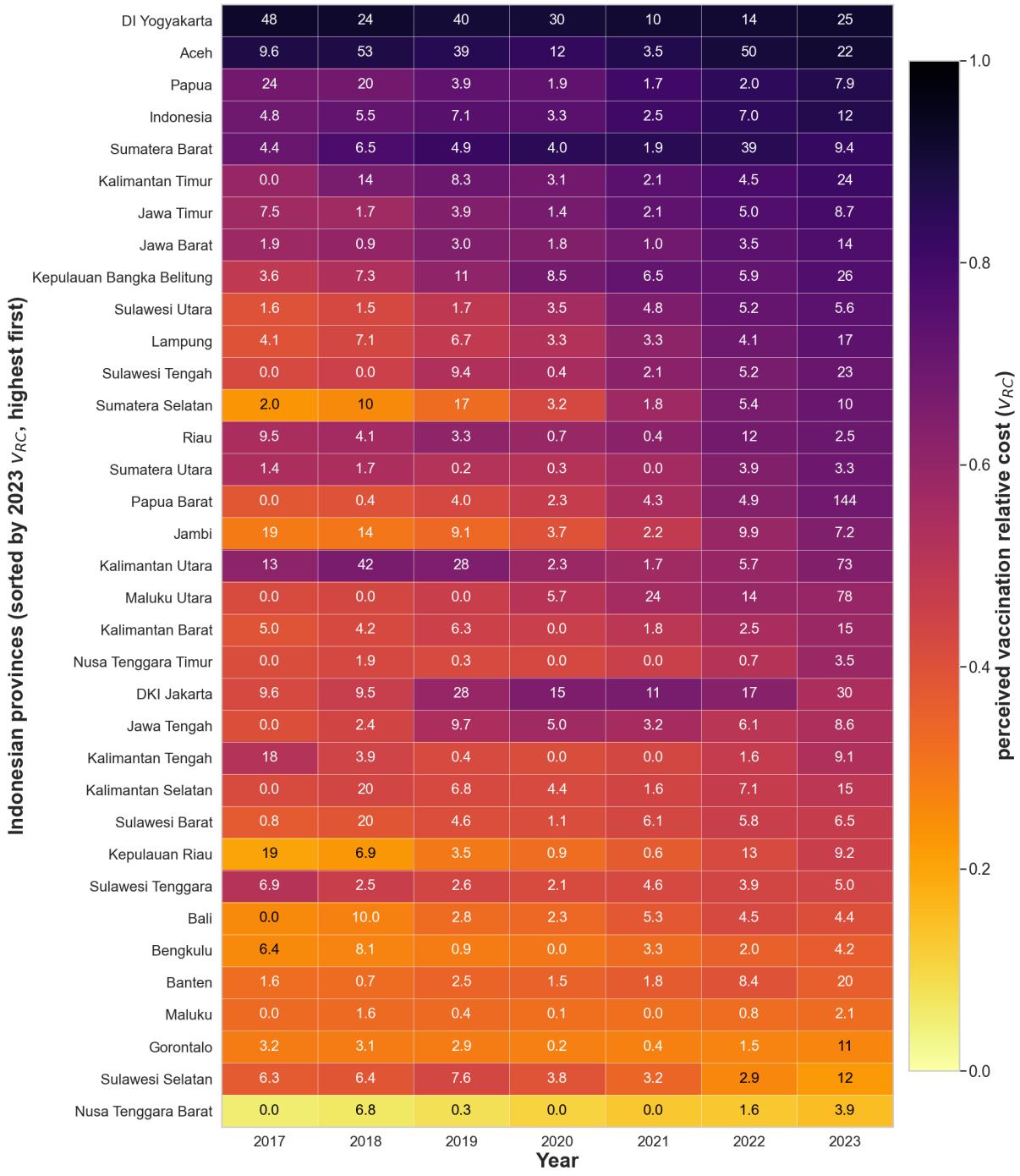


Figure E.4. Perceived vaccination relative cost (v_{RC}) across provinces in Indonesia, in comparison with reported mean monthly measles incidence per 1 million population, 2017-2023. The v_{RC} value is reflected in the color scheme, while the measles incidence is on the label within each box. The provinces are sorted based on v_{RC} value in 2023.

Bibliography

Acemoglu, D., Ozdaglar, A., 2011. Opinion Dynamics and Learning in Social Networks. Dyn. Games Appl. 1, 3–49. https://doi.org/10.1007/s13235-010-0004-1

Adamu, A.A., Ndwandwe, D., Jalo, R.I., Wiysonge, C.S., 2024. Positioning implementation science in national immunization programmes to improve coverage equity and advance progress toward Immunization Agenda 2030: An urgent global health imperative. Hum. Vaccines Immunother. 20, 2331872. https://doi.org/10.1080/21645515.2024.2331872

Ajzen, I., 1991. The theory of planned behavior. Organ. Behav. Hum. Decis. Process., Theories of Cognitive Self-Regulation 50, 179–211. https://doi.org/10.1016/0749-5978(91)90020-T

Albert, R., Jeong, H., Barabási, A.-L., 1999. Diameter of the World-Wide Web. Nature 401, 130–131. https://doi.org/10.1038/43601

Alvarez-Zuzek, L.G., Zipfel, C.M., Bansal, S., 2022. Spatial clustering in vaccination hesitancy: The role of social influence and social selection. PLoS Comput. Biol. 18, e1010437. https://doi.org/10.1371/journal.pcbi.1010437

Anderson, R.M., May, R.M., 1982. Directly Transmitted Infections Diseases: Control by Vaccination. Science 215, 1053–1060. https://doi.org/10.1126/science.7063839

Anis, E., Haas, E.J., Indenbaum, V., Singer, S.R., Warshavsky, B., Rishpon, S., Green, M.S., Mendelson, E., Grotto, I., Kaliner, E., Sadetzki, S., 2021. A prolonged, nationwide measles outbreak despite very high vaccination coverage in Israel, 2018-19. J. Infect. 83, 678–685. https://doi.org/10.1016/j.jinf.2021.09.025

Aral, S., Nicolaides, C., 2017. Exercise contagion in a global social network. Nat. Commun. 8, 14753. https://doi.org/10.1038/ncomms14753

Axelrod, R., 1997. The Dissemination of Culture: A Model with Local Convergence and Global Polarization. J. Confl. Resolut. 41, 203–226. https://doi.org/10.1177/0022002797041002001

Backhaus, I., Hoven, H., Kawachi, I., 2023. Far-right political ideology and COVID-19 vaccine hesitancy: Multilevel analysis of 21 European countries. Soc. Sci. Med. 335, 116227. https://doi.org/10.1016/j.socscimed.2023.116227

Bail, C.A., Argyle, L.P., Brown, T.W., Bumpus, J.P., Chen, H., Hunzaker, M.B.F., Lee, J., Mann, M., Merhout, F., Volfovsky, A., 2018. Exposure to opposing views on social media can increase political polarization. Proc. Natl. Acad. Sci. U. S. A. 115, 9216–9221. https://doi.org/10.1073/pnas.1804840115

Bak-Coleman, J.B., Alfano, M., Barfuss, W., Bergstrom, C.T., Centeno, M.A., Couzin, I.D., Donges, J.F., Galesic, M., Gersick, A.S., Jacquet, J., Kao, A.B., Moran, R.E., Romanczuk, P., Rubenstein, D.I., Tombak, K.J., Van Bavel, J.J., Weber, E.U., 2021. Stewardship of global collective behavior. Proc. Natl. Acad. Sci. 118, e2025764118. https://doi.org/10.1073/pnas.2025764118

Banas, J.A., Rains, S.A., 2010. A Meta-Analysis of Research on Inoculation Theory. Commun. Monogr. 77, 281–311. https://doi.org/10.1080/03637751003758193

Bandura, A., 2001. Self-efficacy and Health, in: Smelser, N.J., Baltes, P.B. (Eds.), International Encyclopedia of the Social & Behavioral Sciences. Pergamon, Oxford, pp. 13815–13820. https://doi.org/10.1016/B0-08-043076-7/03806-7

Banerjee, A., Chandrasekar, A.G., Duflo, E., Jackson, M.O., 2014. Gossip: Identifying Central Individuals in a Social Network. Natl. Bur. Econ. Res., NBER Working Paper Series.

Banerjee, A., Chandrasekhar, A.G., Duflo, E., Jackson, M.O., 2019. Using Gossips to Spread Information: Theory and Evidence from Two Randomized Controlled Trials. Rev. Econ. Stud. 86, 2453–2490. https://doi.org/10.1093/restud/rdz008

Banerjee, A., Chandrasekhar, A.G., Duflo, E., Jackson, M.O., 2013. The Diffusion of Microfinance. Science 341, 1236498. https://doi.org/10.1126/science.1236498

Barabási, A.-L., Albert, R., 1999. Emergence of Scaling in Random Networks. Science 286, 509–512. https://doi.org/10.1126/science.286.5439.509

Bauch, C.T., Earn, D.J.D., 2004. Vaccination and the theory of games. Proc. Natl. Acad. Sci. 101, 13391–13394. https://doi.org/10.1073/pnas.0403823101

Becker, M.H., Drachman, R.H., Kirscht, J.P., 1974. A New Approach to Explaining Sick-RoIe Behavior in Low-Income Populations. Am. J. Public Health 64, 205–216.

Bedson, J., Skrip, L.A., Pedi, D., Abramowitz, S., Carter, S., Jalloh, M.F., Funk, S., Gobat, N., Giles-Vernick, T., Chowell, G., de Almeida, J.R., Elessawi, R., Scarpino, S.V., Hammond, R.A., Briand, S., Epstein, J.M., Hébert-Dufresne, L., Althouse, B.M., 2021. A review and agenda for integrated disease models including social and behavioural factors. Nat. Hum. Behav. 5, 834–846. https://doi.org/10.1038/s41562-021-01136-2

Ben-Menachem, E., 2011. Vaccination and the Onset of Dravet Syndrome: Vaccination and the Onset of Dravet Syndrome. Epilepsy Curr. 11, 120–122. https://doi.org/10.5698/1535-7511-11.4.120

Betsch, C., 2016. Detrimental effects of introducing partial compulsory vaccination: experimental evidence. Eur. J. Public Health 26, 378–381. https://doi.org/10.1093/eurpub/ckv154

Betsch, C., Renkewitz, F., Betsch, T., Ulshöfer, C., 2010. The Influence of Vaccine-critical Websites on Perceiving Vaccination Risks. J. Health Psychol. 15, 446–455. https://doi.org/10.1177/1359105309353647

Bosch, L., Heyns, A., Debebe, Z., 2025. Health Care Access Come Rain or Shine: A Multifactorial Accessibility Study of Public Primary Health Care in Indonesia.

Brewer, N.T., 2021. What Works to Increase Vaccination Uptake. Acad. Pediatr., Raising Child and Adolescent Immunization Rates 21, S9–S16. https://doi.org/10.1016/j.acap.2021.01.017

Brewer, N.T., Chapman, G.B., Gibbons, F.X., Gerrard, M., McCaul, K.D., Weinstein, N.D., 2007. Meta-analysis of the relationship between risk perception and health behavior: The example of vaccination. Health Psychol. 26, 136–145. https://doi.org/10.1037/0278-6133.26.2.136

Brewer, N.T., Chapman, G.B., Rothman, A.J., Leask, J., Kempe, A., 2017. Increasing Vaccination: Putting Psychological Science into Action. Psychol. Sci. Public Interest 18, 149–207. https://doi.org/10.1177/1529100618760521

Broido, A.D., Clauset, A., 2019. Scale-free networks are rare. Nat. Commun. 10, 1017. https://doi.org/10.1038/s41467-019-08746-5

Brownwright, T.K., Dodson, Z.M., van Panhuis, W.G., 2017. Spatial clustering of measles vaccination coverage among children in sub-Saharan Africa. BMC Public Health 17, 957. https://doi.org/10.1186/s12889-017-4961-9

Bruine De Bruin, W., Parker, A.M., Galesic, M., Vardavas, R., 2019. Reports of social circles' and own vaccination behavior: A national longitudinal survey. Health Psychol. 38, 975–983. https://doi.org/10.1037/hea0000771

Burton, A., Monasch, R., Lautenbach, B., Gacic-Dobo, M., Neill, M., Karimov, R., Wolfson, L., Jones, G., Birmingham, M., 2009. WHO and UNICEF estimates of national infant immunization coverage: methods and processes. Bull. World Health Organ. 87, 535–541. https://doi.org/10.2471/BLT.08.053819

Bussink-Voorend, D., Hautvast, J.L.A., Vandeberg, L., Visser, O., Hulscher, M.E.J.L., 2022. A systematic literature review to clarify the concept of vaccine hesitancy. Nat. Hum. Behav. 6, 1634–1648. https://doi.org/10.1038/s41562-022-01431-6

Centers for Disease Control and Prevention, 2025. Measles Symptoms and Complications [WWW Document]. Measles Rubeola. URL https://www.cdc.gov/measles/signs-symptoms/index.html (accessed 3.19.25).

Centers for Disease Control and Prevention, 2024. Assessing Measles Outbreak Risk in the United States [WWW Document]. Natl. Cent. Immun. Respir. Dis. URL https://www.cdc.gov/ncird/whats-new/measles-outbreak-risk-in-us.html (accessed 1.28.25).

Centola, D., 2021. Chapter 17: Complex contagions, in: Research Handbook on Analytical Sociology.

Centola, D., 2010. The Spread of Behavior in an Online Social Network Experiment. Science 329, 1194–1197. https://doi.org/10.1126/science.1185231

Centola, D., Macy, M., 2007. Complex Contagions and the Weakness of Long Ties. Am. J. Sociol. 113, 702–734. https://doi.org/10.1086/521848

Chacko, S., 2023. Progress Toward Measles and Rubella Elimination — Indonesia, 2013–2022. MMWR Morb. Mortal. Wkly. Rep. 72. https://doi.org/10.15585/mmwr.mm7242a2

Chandrasekhar, A.G., Larreguy, H., Xandri, J.P., 2020. Testing Models of Social Learning on Networks: Evidence From Two Experiments. Econometrica 88, 1–32. https://doi.org/10.3982/ECTA14407

Christianson, B., Sharif-Mohamed, F., Heath, J., Roddy, M., Bahta, L., Omar, H., Rockwood, T., Kenyon, C., 2020. Parental attitudes and decisions regarding MMR vaccination during an outbreak of measles among an undervaccinated Somali community in Minnesota. Vaccine 38, 6979–6984. https://doi.org/10.1016/j.vaccine.2020.09.022

Chu, A., Gupta, V., Unni, E.J., 2021. Utilizing the Theory of Planned Behavior to determine the intentions to receive the influenza vaccine during COVID-19: A cross-sectional survey of US adults. Prev. Med. Rep. 23, 101417. https://doi.org/10.1016/j.pmedr.2021.101417

Cleveland, R.B., Cleveland, W.S., McRae, J.E., Terpenning, I., 1990. STL: A Seasonal-Trend Decomposition Procedure Based on LOESS. J. Off. Stat. 6, 3–73.

Clifford, P., Sudbury, A., 1973. A Model for Spatial Conflict. Biometrika 60, 581–588. https://doi.org/10.2307/2335008

Cole-Lewis, H., Perotte, A., Galica, K., Dreyer, L., Griffith, C., Schwarz, M., Yun, C., Patrick, H., Coa, K., Augustson, E., 2016. Social Network Behavior and Engagement Within a Smoking Cessation Facebook Page. J. Med. Internet Res. 18, e205. https://doi.org/10.2196/jmir.5574

COVID-19 Vaccines: Safety Surveillance Manual, 1st ed. ed, 2020. . World Health Organization, Geneva.

Cowan, L.D., Griffin, M.R., Howson, C.P., Katz, M., Johnston, R.B., Shaywitz, B.A., Fineberg, H.V., 1993. Acute encephalopathy and chronic neurological damage after pertusis vaccine. Vaccine 11, 1371–1379. https://doi.org/10.1016/0264-410X(93)90163-R

Dandekar, P., Goel, A., Lee, D.T., 2013. Biased assimilation, homophily, and the dynamics of polarization. Proc. Natl. Acad. Sci. 110, 5791–5796. https://doi.org/10.1073/pnas.1217220110

de Figueiredo, A., Larson, H.J., Reicher, S.D., 2021. The potential impact of vaccine passports on inclination to accept COVID-19 vaccinations in the United Kingdom: Evidence from a large cross-sectional survey and modeling study. EClinicalMedicine 40, 101109. https://doi.org/10.1016/j.eclinm.2021.101109

de Oliveira, S.A., Jin, L., Siqueira, M.M., Cohen, B.J., 2000. Atypical measles in a patient twice vaccinated against measles: transmission from an unvaccinated household contact. Vaccine 19, 1093–1096. https://doi.org/10.1016/s0264-410x(00)00338-8

Definition of a measles outbreak, 2009. , in: Response to Measles Outbreaks in Measles Mortality Reduction Settings: Immunization, Vaccines and Biologicals. World Health Organization, Geneva, p. 6.

DeGroot, M.H., 1974. Reaching a Consensus. J. Am. Stat. Assoc. 69, 118–121. https://doi.org/10.2307/2285509

Dempster, A.P., Laird, N.M., Rubin, D.B., 1977. Maximum Likelihood from Incomplete Data Via the *EM* Algorithm. J. R. Stat. Soc. Ser. B Stat. Methodol. 39, 1–22. https://doi.org/10.1111/j.2517-6161.1977.tb01600.x

DeStefano, F., Thompson, W.W., 2004. MMR vaccine and autism: an update of the scientific evidence. Expert Rev. Vaccines 3, 19–22. https://doi.org/10.1586/14760584.3.1.19

Di Pietrantonj, C., Rivetti, A., Marchione, P., Debalini, M.G., Demicheli, V., 2021. Vaccines for measles, mumps, rubella, and varicella in children. Cochrane Database Syst. Rev. 11, CD004407. https://doi.org/10.1002/14651858.CD004407.pub5

Dimala, C.A., Kadia, B.M., Nji, M.A.M., Bechem, N.N., 2021. Factors associated with measles resurgence in the United States in the post-elimination era. Sci. Rep. 11, 51. https://doi.org/10.1038/s41598-020-80214-3

Dong, E., Nixon, K., Gardner, L.M., 2024. A population level study on the determinants of COVID-19 vaccination rates at the U.S. county level. Sci. Rep. 14, 4277. https://doi.org/10.1038/s41598-024-54441-x

Dubé, E., Gagnon, D., MacDonald, N.E., 2015. Strategies intended to address vaccine hesitancy: Review of published reviews. Vaccine, WHO Recommendations Regarding Vaccine Hesitancy 33, 4191–4203. https://doi.org/10.1016/j.vaccine.2015.04.041

Dunbar, R.I.M., 1993. Coevolution of neocortical size, group size and language in humans. Behav. Brain Sci. 16, 681–694. https://doi.org/10.1017/S0140525X00032325

Dunbar, R.I.M., 1992. Neocortex size as a constraint on group size in primates. J. Hum. Evol. 22, 469–493. https://doi.org/10.1016/0047-2484(92)90081-J

Dunbar, R.I.M., Arnaboldi, V., Conti, M., Passarella, A., 2015. The structure of online social networks mirrors those in the offline world. Soc. Netw. 43, 39–47. https://doi.org/10.1016/j.socnet.2015.04.005

Eagan, R.L., Larson, H.J., de Figueiredo, A., 2023. Recent trends in vaccine coverage and confidence: A cause for concern. Hum. Vaccines Immunother. 19, 2237374. https://doi.org/10.1080/21645515.2023.2237374

Ecker, U.K.H., Lewandowsky, S., Cook, J., Schmid, P., Fazio, L.K., Brashier, N., Kendeou, P., Vraga, E.K., Amazeen, M.A., 2022. The psychological drivers of misinformation belief and its resistance to correction. Nat. Rev. Psychol. 1, 13–29. https://doi.org/10.1038/s44159-021-00006-y

Facciani, M., Lazić, A., Viggiano, G., McKay, T., 2023. Political network composition predicts vaccination attitudes. Soc. Sci. Med. 1982 328, 116004. https://doi.org/10.1016/j.socscimed.2023.116004

Featherstone, J.D., Zhang, J., 2020. Feeling angry: the effects of vaccine misinformation and refutational messages on negative emotions and vaccination attitude. J. Health Commun. 25, 692–702. https://doi.org/10.1080/10810730.2020.1838671

Ferrari, M.J., Grais, R.F., Bharti, N., Conlan, A.J.K., Bjørnstad, O.N., Wolfson, L.J., Guerin, P.J., Djibo, A., Grenfell, B.T., 2008. The dynamics of measles in sub-Saharan Africa. Nature 451, 679–684. https://doi.org/10.1038/nature06509

Figueiredo, A. de, Simas, C., Karafillakis, E., Paterson, P., Larson, H.J., 2020. Mapping global trends in vaccine confidence and investigating barriers to vaccine uptake: a large-scale retrospective temporal modelling study. The Lancet 396, 898–908. https://doi.org/10.1016/S0140-6736(20)31558-0

Fine, P.E.M., Clarkson, J.A., 1982. Measles in England and Wales—I: An Analysis of Factors Underlying Seasonal Patterns. Int. J. Epidemiol. 11, 5–14. https://doi.org/10.1093/ije/11.1.5

Foreman-Mackey, D., Hogg, D.W., Lang, D., Goodman, J., 2013. emcee: The MCMC Hammer. Publ. Astron. Soc. Pac. 125, 306. https://doi.org/10.1086/670067

Fridman, A., Gershon, R., Gneezy, A., 2021. COVID-19 and vaccine hesitancy: A longitudinal study. PLOS ONE 16, e0250123. https://doi.org/10.1371/journal.pone.0250123

Fryer, R.G., Jr, Harms, P., Jackson, M.O., 2019. Updating Beliefs when Evidence is Open to Interpretation: Implications for Bias and Polarization. J. Eur. Econ. Assoc. 17, 1470–1501. https://doi.org/10.1093/jeea/jvy025

Funk, S., Knapp, J.K., Lebo, E., Reef, S.E., Dabbagh, A.J., Kretsinger, K., Jit, M., Edmunds, W.J., Strebel, P.M., 2019. Combining serological and contact data to derive target immunity levels for achieving and maintaining measles elimination. BMC Med. 17, 180. https://doi.org/10.1186/s12916-019-1413-7

Gelman, A., Roberts, G., Gilks, W., 1996. Efficient Metropolis Jumping Rules, in: Bayesian Statistics. pp. 599–607.

Gilkey, M.B., McRee, A.-L., Magnus, B.E., Reiter, P.L., Dempsey, A.F., Brewer, N.T., 2016. Vaccination Confidence and Parental Refusal/Delay of Early Childhood Vaccines. PLOS ONE 11, e0159087. https://doi.org/10.1371/journal.pone.0159087

Gilmour, S., Kanda, M., Kusumi, E., Tanimoto, T., Kami, M., Shibuya, K., 2013. HPV vaccination programme in Japan. The Lancet 382, 768. https://doi.org/10.1016/S0140-6736(13)61831-0

Goldenberg, M., 2021. Vaccine Hesitancy: Public Trust, Expertise, and the War on Science. University of Pittsburgh Press, Pittsburgh, United States.

Goldenberg, M.J., 2016. Public Misunderstanding of Science? Reframing the Problem of Vaccine Hesitancy. Perspect. Sci. 24, 552–581. https://doi.org/10.1162/POSC_a_00223

Gostin, L.O., Hodge, J.G., Bloom, B.R., El-Mohandes, A., Fielding, J., Hotez, P., Kurth, A., Larson, H.J., Orenstein, W.A., Rabin, K., Ratzan, S.C., Salmon, D., 2020. The public health crisis of underimmunisation: a global plan of action. Lancet Infect. Dis. https://doi.org/10.1016/S1473-3099(19)30558-4

Greyson, D., Bettinger, J.A., 2022. How do mothers' vaccine attitudes change over time? SSM - Qual. Res. Health 2, 100060. https://doi.org/10.1016/j.ssmqr.2022.100060

Griffin, D.E., Lin, W.-H.W., Nelson, A.N., 2018. Understanding the causes and consequences of measles virus persistence. F1000Research 7, 237. https://doi.org/10.12688/f1000research.12094.1

Gualano, M., Olivero, E., Voglino, G., Corezzi, M., Rossello, P., Vicentini, C., Bert, F., Siliquini, R., 2019. Knowledge, attitudes and beliefs towards compulsory vaccination: a systematic review. Hum. Vaccines Immunother. 15, 918–931. https://doi.org/10.1080/21645515.2018.1564437

Guerra, F.M., Bolotin, S., Lim, G., Heffernan, J., Deeks, S.L., Li, Y., Crowcroft, N.S., 2017. The basic reproduction number (R0) of measles: a systematic review. Lancet Infect. Dis. 17, e420–e428. https://doi.org/10.1016/S1473-3099(17)30307-9

Guilbeault, D., Becker, J., Centola, D., 2018. Complex Contagions: A Decade in Review, in: Lehmann, S., Ahn, Y.-Y. (Eds.), Complex Spreading Phenomena in Social Systems: Influence and Contagion in Real-World Social Networks. Springer International Publishing, Cham, pp. 3–25. https://doi.org/10.1007/978-3-319-77332-2_1

Harris, K.M., Halpern, C.T., Whitsel, E.A., Hussey, J.M., Killeya-Jones, L.A., Tabor, J., Dean, S.C., 2019. Cohort Profile: The National Longitudinal Study of Adolescent to Adult Health (Add Health). Int. J. Epidemiol. 48, 1415–1415k. https://doi.org/10.1093/ije/dyz115

Herrera-Diestra, J.L., Meyers, L.A., 2019. Local risk perception enhances epidemic control. PLOS ONE 14, e0225576. https://doi.org/10.1371/journal.pone.0225576

Hill, R.A., Dunbar, R.I.M., 2003. Social network size in humans. Hum. Nat. 14, 53–72. https://doi.org/10.1007/s12110-003-1016-y

Holley, R.A., Liggett, T.M., 1975. Ergodic Theorems for Weakly Interacting Infinite Systems and the Voter Model. Ann. Probab. 3, 643–663.

Horne, Z., Powell, D., Hummel, J.E., Holyoak, K.J., 2015. Countering antivaccination attitudes. Proc. Natl. Acad. Sci. 112, 10321–10324. https://doi.org/10.1073/pnas.1504019112

Hotez, P., 2019. America and Europe's new normal: the return of vaccine-preventable diseases. Pediatr. Res. https://doi.org/10.1038/s41390-019-0354-3

Hübschen, J.M., Gouandjika-Vasilache, I., Dina, J., 2022. Measles. The Lancet 399, 678–690. https://doi.org/10.1016/S0140-6736(21)02004-3

Ikeda, S., Ueda, Y., Yagi, A., Matsuzaki, S., Kobayashi, E., Kimura, T., Miyagi, E., Sekine, M., Enomoto, T., Kudoh, K., 2019. HPV vaccination in Japan: what is happening in Japan? Expert Rev. Vaccines 18, 323–325. https://doi.org/10.1080/14760584.2019.1584040

Jenness, S.M., Aavitsland, P., White, R.A., Winje, B.A., 2021. Measles vaccine coverage among children born to Somali immigrants in Norway. BMC Public Health 21, 668. https://doi.org/10.1186/s12889-021-10694-z

Jusup, M., Holme, P., Kanazawa, K., Takayasu, M., Romić, I., Wang, Z., Geček, S., Lipić, T., Podobnik, B., Wang, L., Luo, W., Klanjšček, T., Fan, J., Boccaletti, S., Perc, M., 2022. Social physics. Phys. Rep., Social physics 948, 1–148. https://doi.org/10.1016/j.physrep.2021.10.005

Karsai, M., Iñiguez, G., Kaski, K., Kertész, J., 2014. Complex contagion process in spreading of online innovation. J. R. Soc. Interface 11, 20140694. https://doi.org/10.1098/rsif.2014.0694

Kementerian Kesehatan Republik Indonesia, 2024. Profil Kesehatan Indonesia.

Kementerian Kesehatan Republik Indonesia, 2020. Pedoman Surveilans Campak Rubella.

Kennedy, J., 2019. Populist politics and vaccine hesitancy in Western Europe: an analysis of national-level data. Eur. J. Public Health 29, 512–516. https://doi.org/10.1093/eurpub/ckz004

Khan, J., Shil, A., Prakash, R., 2018. Exploring the spatial heterogeneity in different doses of vaccination coverage in India. PloS One 13, e0207209. https://doi.org/10.1371/journal.pone.0207209

Kiang, M.V., Bubar, K.M., Maldonado, Y., Hotez, P.J., Lo, N.C., 2025. Modeling Reemergence of Vaccine-Eliminated Infectious Diseases Under Declining Vaccination in the US. JAMA 333, 2176–2187. https://doi.org/10.1001/jama.2025.6495

Kitsak, M., Gallos, L.K., Havlin, S., Liljeros, F., Muchnik, L., Stanley, H.E., Makse, H.A., 2010. Identification of influential spreaders in complex networks. Nat. Phys. 6, 888–893. https://doi.org/10.1038/nphys1746

Klein, A., Seeger, M., Archambeau, C., 2023. 19.4 Multifidelity Hyperparameter Optimization, in: Dive into Deep Learning. Cambridge University Press.

Klinkenberg, D., van Hoek, A.J., Veldhuijzen, I., Hahné, S., Wallinga, J., 2022. Social clustering of unvaccinated children in schools in the Netherlands. Epidemiol. Infect. 150, e200. https://doi.org/10.1017/S0950268822001455

Klymak, M., Vlandas, T., 2022. Partisanship and Covid-19 vaccination in the UK. Sci. Rep. 12, 19785. https://doi.org/10.1038/s41598-022-23035-w

Kobayashi, T., Nishiura, H., 2022. Transmission Network of Measles During the Yamagata Outbreak in Japan, 2017. J. Epidemiol. 32, 96–104. https://doi.org/10.2188/jea.JE20200455

Kreps, S.E., Kriner, D.L., 2023. Resistance to COVID-19 vaccination and the social contract: evidence from Italy. Npj Vaccines 8, 60. https://doi.org/10.1038/s41541-023-00660-8

Krug, E.G., Dahlberg, L.L., Mercy, J.A., Zwi, A.B., Lozano, R. (Eds.), 2002. The world report on violence and health. World Health Organization, Genève.

Kunda, Z., 1990. The case for motivated reasoning. Psychol. Bull. 108, 480–498. https://doi.org/10.1037/0033-2909.108.3.480

Laksono, B.M., De Vries, R.D., Duprex, W.P., De Swart, R.L., 2020. Measles pathogenesis, immune suppression and animal models. Curr. Opin. Virol. 41, 31–37. https://doi.org/10.1016/j.coviro.2020.03.002

Lane, S., MacDonald, N.E., Marti, M., Dumolard, L., 2018. Vaccine hesitancy around the globe: Analysis of three years of WHO/UNICEF Joint Reporting Form data-2015–2017. Vaccine 36, 3861–3867. https://doi.org/10.1016/j.vaccine.2018.03.063

Larson, H.J., 2022. Defining and measuring vaccine hesitancy. Nat. Hum. Behav. 6, 1609–1610. https://doi.org/10.1038/s41562-022-01484-7

Lee, C.H.J., Sibley, C.G., 2020. Attitudes toward vaccinations are becoming more polarized in New Zealand: Findings from a longitudinal survey. eClinicalMedicine 23. https://doi.org/10.1016/j.eclinm.2020.100387

Leong, W.-Y., Wilder-Smith, A.B., 2019. Measles Resurgence in Europe: Migrants and Travellers are not the Main Drivers. J. Epidemiol. Glob. Health 9, 294–299. https://doi.org/10.2991/jegh.k.191007.001

Leskovec, J., Krevl, A., 2014. SNAP Datasets: Stanford Large Network Dataset Collection.

Lievano, F.A., Helfand, R.F., Harpaz, R., Walls, L., Katz, R.S., Williams, I., Villamarzo, Y.S., Rota, P.A., Bellini, W.J., 2004. Lack of Evidence of Measles Virus Shedding in People with Inapparent Measles Virus Infections. J. Infect. Dis. 189, S165–S170. https://doi.org/10.1086/377715

Lloyd-Smith, J.O., Schreiber, S.J., Kopp, P.E., Getz, W.M., 2005. Superspreading and the effect of individual variation on disease emergence. Nature 438, 355–359. https://doi.org/10.1038/nature04153

Loomba, S., de Figueiredo, A., Piatek, S.J., de Graaf, K., Larson, H.J., 2021. Measuring the impact of COVID-19 vaccine misinformation on vaccination intent in the UK and USA. Nat. Hum. Behav. 5, 337–348. https://doi.org/10.1038/s41562-021-01056-1

Lord, C.G., Ross, L., Lepper, M.R., 1979. Biased assimilation and attitude polarization: The effects of prior theories on subsequently considered evidence. J. Pers. Soc. Psychol. 37, 2098–2109. https://doi.org/10.1037/0022-3514.37.11.2098

MacDonald, N.E., 2015. Vaccine hesitancy: Definition, scope and determinants. Vaccine 33, 4161–4164. https://doi.org/10.1016/j.vaccine.2015.04.036

Marinović, A.A.B., Swaan, C., Wichmann, O., van Steenbergen, J., Kretzschmar, M., 2012. Effectiveness and Timing of Vaccination during School Measles Outbreak. Emerg. Infect. Dis. 18, 1405–1413. https://doi.org/10.3201/eid1809.111578

Martin, E.K., Shearer, M.P., Trotochaud, M., Nuzzo, J.B., 2021. Outbreak response operations during the US measles epidemic, 2017–19. BMC Public Health 21, 620. https://doi.org/10.1186/s12889-021-10652-9

Masters, N.B., Eisenberg, M.C., Delamater, P.L., Kay, M., Boulton, M.L., Zelner, J., 2020. Fine-scale spatial clustering of measles nonvaccination that increases outbreak

potential is obscured by aggregated reporting data. Proc. Natl. Acad. Sci. U. S. A. 117, 28506–28514. https://doi.org/10.1073/pnas.2011529117

May, C.R., Johnson, M., Finch, T., 2016. Implementation, context and complexity. Implement. Sci. 11, 141. https://doi.org/10.1186/s13012-016-0506-3

Measles: Vaccine Preventable Surveillance Standards, 2018.

Mina, M.J., Kula, T., Leng, Y., Li, M., de Vries, R.D., Knip, M., Siljander, H., Rewers, M., Choy, D.F., Wilson, M.S., Larman, H.B., Nelson, A.N., Griffin, D.E., de Swart, R.L., Elledge, S.J., 2019. Measles virus infection diminishes preexisting antibodies that offer protection from other pathogens. Science 366, 599–606. https://doi.org/10.1126/science.aay6485

Mina, M.J., Metcalf, C.J.E., de Swart, R.L., Osterhaus, A.D.M.E., Grenfell, B.T., 2015. Long-term measles-induced immunomodulation increases overall childhood infectious disease mortality. Science 348, 694–699. https://doi.org/10.1126/science.aaa3662

Monti, C., Pangallo, M., De Francisci Morales, G., Bonchi, F., 2023. On learning agent-based models from data. Sci. Rep. 13, 9268. https://doi.org/10.1038/s41598-023-35536-3

Morales, A.J., Dong, X., Bar-Yam, Y., 'Sandy' Pentland, A., 2019. Segregation and polarization in urban areas. R. Soc. Open Sci. 6, 190573. https://doi.org/10.1098/rsos.190573

Moss, W.J., Griffin, D.E., 2012. Measles. The Lancet 379, 153–164. https://doi.org/10.1016/S0140-6736(10)62352-5

Müller, J., Tellier, A., Kurschilgen, M., 2022. Echo chambers and opinion dynamics explain the occurrence of vaccination hesitancy. R. Soc. Open Sci. 9, 220367. https://doi.org/10.1098/rsos.220367

Murphy, A.H., 1988. Skill Scores Based on the Mean Square Error and Their Relationships to the Correlation Coefficient. Mon. Weather Rev. 116, 2417–2424. https://doi.org/10.1175/1520-0493(1988)116%3C2417:SSBOTM%3E2.0.CO;2

Newman, M.E.J., 2006. Modularity and community structure in networks. Proc. Natl. Acad. Sci. 103, 8577–8582. https://doi.org/10.1073/pnas.0601602103

Nyhan, B., Reifler, J., Richey, S., Freed, G.L., 2014. Effective Messages in Vaccine Promotion: A Randomized Trial. Pediatrics 133, e835–e842. https://doi.org/10.1542/peds.2013-2365

Omer, S.B., Enger, K.S., Moulton, L.H., Halsey, N.A., Stokley, S., Salmon, D.A., 2008. Geographic clustering of nonmedical exemptions to school immunization requirements and associations with geographic clustering of pertussis. Am. J. Epidemiol. 168, 1389–1396. https://doi.org/10.1093/aje/kwn263

Ozawa, S., Clark, S., Portnoy, A., Grewal, S., Stack, M.L., Sinha, A., Mirelman, A., Franklin, H., Friberg, I.K., Tam, Y., Walker, N., Clark, A., Ferrari, M., Suraratdecha, C., Sweet, S., Goldie, S.J., Garske, T., Li, M., Hansen, P.M., Johnson, H.L., Walker, D., 2017. Estimated economic impact of vaccinations in 73 low- and middle-income countries, 2001-2020. Bull. World Health Organ. 95, 629–638. https://doi.org/10.2471/BLT.16.178475

Pandey, P., Kang, Y., Cooper, N., O'Donnell, M.B., Falk, E.B., 2021. Social networks and neural receptivity to persuasive health messages. Health Psychol. Off. J. Div. Health Psychol. Am. Psychol. Assoc. 40, 285–294. https://doi.org/10.1037/hea0001059

Parker, A.A., Staggs, W., Dayan, G.H., Ortega-Sánchez, I.R., Rota, P.A., Lowe, L., Boardman, P., Teclaw, R., Graves, C., LeBaron, C.W., 2006. Implications of a 2005 Measles Outbreak in Indiana for Sustained Elimination of Measles in the United States. N. Engl. J. Med. 355, 447–455. https://doi.org/10.1056/NEJMoa060775

Parsons, J.E., Newby, K.V., French, D.P., 2018. Do interventions containing risk messages increase risk appraisal and the subsequent vaccination intentions and uptake? – A systematic review and meta-analysis. Br. J. Health Psychol. 23, 1084–1106. https://doi.org/10.1111/bjhp.12340

Pastor-Satorras, R., Castellano, C., Van Mieghem, P., Vespignani, A., 2015. Epidemic processes in complex networks. Rev. Mod. Phys. 87, 925–979. https://doi.org/10.1103/RevModPhys.87.925

Perc, M., Jordan, J.J., Rand, D.G., Wang, Z., Boccaletti, S., Szolnoki, A., 2017. Statistical physics of human cooperation. Phys. Rep., Statistical physics of human cooperation 687, 14. https://doi.org/10.1016/j.physrep.2017.05.004

Petrova, V.N., Sawatsky, B., Han, A.X., Laksono, B.M., Walz, L., Parker, E., Pieper, K., Anderson, C.A., de Vries, R.D., Lanzavecchia, A., Kellam, P., von Messling, V., de Swart, R.L., Russell, C.A., 2019. Incomplete genetic reconstitution of B cell pools contributes to prolonged immunosuppression after measles. Sci. Immunol. 4, eaay6125. https://doi.org/10.1126/sciimmunol.aay6125

Phadke, V.K., Bednarczyk, R.A., Salmon, D.A., Omer, S.B., 2016. Association Between Vaccine Refusal and Vaccine-Preventable Diseases in the United States: A Review of Measles and Pertussis. JAMA 315, 1149–1158. https://doi.org/10.1001/jama.2016.1353

Pingali, S.C., Delamater, P.L., Buttenheim, A.M., Salmon, D.A., Klein, N.P., Omer, S.B., 2019. Associations of Statewide Legislative and Administrative Interventions With Vaccination Status Among Kindergartners in California. JAMA 322, 49–56. https://doi.org/10.1001/jama.2019.7924

Plsek, P., 2001. Redesigning Health Care with Insights from the Science of Complex Adaptive Systems, in: Crossing the Quality Chasm: A New Health System for The 21st Century. National Academy of Sciences, pp. 309–322. https://doi.org/10.1037/e317382004-001

Pronyk, P., Sugihantono, A., Sitohang, V., Moran, T., Kadandale, S., Muller, S., Whetham, C., Kezaala, R., 2019. Vaccine hesitancy in Indonesia. Lancet Planet. Health 3, e114–e115. https://doi.org/10.1016/S2542-5196(18)30287-0

Qi, F., Barragan, D., Rodriguez, M.G., Lu, J., 2022. Evaluating spatial accessibility to COVID-19 vaccine resources in diversely populated counties in the United States. Front. Public Health 10. https://doi.org/10.3389/fpubh.2022.895538

Ramsay, S., 2001. UK starts campaign to reassure parents about MMR-vaccine safety. The Lancet 357, 290. https://doi.org/10.1016/S0140-6736(05)71737-2

Ratzan, S.C., 2011. Vaccine Literacy: A New Shot for Advancing Health. J. Health Commun. 16, 227–229. https://doi.org/10.1080/10810730.2011.561726

Robinson, P., Wiley, K., Degeling, C., 2021. Public health practitioner perspectives on dealing with measles outbreaks if high anti-vaccination sentiment is present. BMC Public Health 21, 578. https://doi.org/10.1186/s12889-021-10604-3

Rochmyaningsih, D., 2018. Indonesian fatwa causes immunization rates to drop. Science 362, 628–629. https://doi.org/10.1126/science.362.6415.628

Roozenbeek, J., Traberg, C.S., van der Linden, S., 2022a. Technique-based inoculation against real-world misinformation. R. Soc. Open Sci. 9, 211719. https://doi.org/10.1098/rsos.211719

Roozenbeek, J., van der Linden, S., Goldberg, B., Rathje, S., Lewandowsky, S., 2022b. Psychological inoculation improves resilience against misinformation on social media. Sci. Adv. 8, eabo6254. https://doi.org/10.1126/sciadv.abo6254

Rosenstock, I.M., 1974a. The Health Belief Model and Preventive Health Behavior. Health Educ. Monogr. 2, 354–386. https://doi.org/10.1177/109019817400200405

Rosenstock, I.M., 1974b. Historical Origins of the Health Belief Model. Health Educ. Monogr. 2, 328–335.

Rota, P.A., Moss, W.J., Takeda, M., de Swart, R.L., Thompson, K.M., Goodson, J.L., 2016. Measles. Nat. Rev. Dis. Primer 2, 1–16. https://doi.org/10.1038/nrdp.2016.49

Sadaf, A., Richards, J.L., Glanz, J., Salmon, D.A., Omer, S.B., 2013. A systematic review of interventions for reducing parental vaccine refusal and vaccine hesitancy. Vaccine 31, 4293–4304. https://doi.org/10.1016/j.vaccine.2013.07.013

Sbarra, A.N., Mosser, J.F., Jit, M., Ferrari, M., Ramshaw, R.E., O'Connor, P., Krause, L.K., Rogowski, E.L.B., Portnoy, A., 2023. Estimating national-level measles case–fatality ratios in low-income and middle-income countries: an updated systematic review and modelling study. Lancet Glob. Health 11, e516–e524. https://doi.org/10.1016/S2214-109X(23)00043-8

Schenk, J., Abrams, S., Theeten, H., Damme, P.V., Beutels, P., Hens, N., 2021. Immunogenicity and persistence of trivalent measles, mumps, and rubella vaccines: a systematic review and meta-analysis. Lancet Infect. Dis. 21, 286–295. https://doi.org/10.1016/S1473-3099(20)30442-4

Seidman, S.B., 1983. Network structure and minimum degree. Soc. Netw. 5, 269–287. https://doi.org/10.1016/0378-8733(83)90028-X

Serafino, M., Cimini, G., Maritan, A., Rinaldo, A., Suweis, S., Banavar, J.R., Caldarelli, G., 2021. True scale-free networks hidden by finite size effects. Proc. Natl. Acad. Sci. 118, e2013825118. https://doi.org/10.1073/pnas.2013825118

Shankar, M., Hartner, A.-M., Arnold, C.R.K., Gayawan, E., Kang, H., Kim, J.-H., Gilani, G.N., Cori, A., Fu, H., Jit, M., Muloiwa, R., Portnoy, A., Trotter, C., Gaythorpe, K.A.M., 2024. How mathematical modelling can inform outbreak response vaccination. BMC Infect. Dis. 24, 1371. https://doi.org/10.1186/s12879-024-10243-0

Shattock, A.J., Johnson, H.C., Sim, S.Y., Carter, A., Lambach, P., Hutubessy, R.C.W., Thompson, K.M., Badizadegan, K., Lambert, B., Ferrari, M.J., Jit, M., Fu, H., Silal, S.P., Hounsell, R.A., White, R.G., Mosser, J.F., Gaythorpe, K.A.M., Trotter, C.L., Lindstrand, A., O'Brien, K.L., Bar-Zeev, N., 2024. Contribution of vaccination to improved survival and health: modelling 50 years of the Expanded Programme on Immunization. The Lancet 403, 2307–2316. https://doi.org/10.1016/S0140-6736(24)00850-X

Shirado, H., Christakis, N.A., 2017. Locally noisy autonomous agents improve global human coordination in network experiments. Nature 545, 370–374. https://doi.org/10.1038/nature22332

Simon, H.A., 1997. Models of Bounded Rationality, Volume 3: Empirically Grounded Economic Reason. The MIT Press. https://doi.org/10.7551/mitpress/4711.001.0001

Simon, H.A., 1990. Bounded Rationality, in: Eatwell, J., Milgate, M., Newman, P. (Eds.), Utility and Probability. Palgrave Macmillan UK, London, pp. 15–18. https://doi.org/10.1007/978-1-349-20568-4_5

Smith, L.E., Hodson, A., Rubin, G.J., 2021. Parental attitudes towards mandatory vaccination; a systematic review. Vaccine 39, 4046–4053. https://doi.org/10.1016/j.vaccine.2021.06.018

Sonoda, S., Nakayama, T., 2001. Detection of measles virus genome in lymphocytes from asymptomatic healthy children. J. Med. Virol. 65, 381–387. https://doi.org/10.1002/jmv.2045

Sprague, D.A., House, T., 2017. Evidence for complex contagion models of social contagion from observational data. PloS One 12, e0180802. https://doi.org/10.1371/journal.pone.0180802

Sprengholz, P., Felgendreff, L., Böhm, R., Betsch, C., 2022. Vaccination policy reactance: Predictors, consequences, and countermeasures. J. Health Psychol. 27, 1394–1407.

Stefkovics, Á., Albert, F., Ligeti, A.S., Dávid, B., Rudas, S., Koltai, J., 2024. Vaccination homophily in ego contact networks during the COVID-19 pandemic. Sci. Rep. 14, 15515. https://doi.org/10.1038/s41598-024-65986-2

Strategic Plan for measles and rubella elimination and sustenance in the WHO South-East Asia Region: 2024-2028, 2024. . World Health Organization.

Strebel, P.M., Papania, M.J., Gastañaduy, P.A., Goodson, J.L., 2018. Measles Vaccines, in: Plotkin's Vaccines. Elsevier, pp. 579-618.e21. https://doi.org/10.1016/B978-0-323-35761-6.00037-7

Sunstein, C.R., 1999. The Law of Group Polarization (No. 91), John M. Olin Program in Law and Economics Working Paper. The University of Chicago.

Szolnoki, A., Wang, Z., Perc, M., 2012. Wisdom of groups promotes cooperation in evolutionary social dilemmas. Sci. Rep. 2, 576. https://doi.org/10.1038/srep00576

Tashman, L.J., 2000. Out-of-sample tests of forecasting accuracy: an analysis and review. Int. J. Forecast., The M3- Competition 16, 437–450. https://doi.org/10.1016/S0169-2070(00)00065-0

Toole, J.L., Cha, M., González, M.C., 2012. Modeling the adoption of innovations in the presence of geographic and media influences. PloS One 7, e29528. https://doi.org/10.1371/journal.pone.0029528

Torracinta, L., Tanner, R., Vanderslott, S., 2021. MMR Vaccine Attitude and Uptake Research in the United Kingdom: A Critical Review. Vaccines 9, 402. https://doi.org/10.3390/vaccines9040402

Traulsen, A., Hauert, C., 2009. Stochastic evolutionary game dynamics, in: Reviews of Nonlinear Dynamics and Complexity. John Wiley & Sons, Ltd., pp. 25–61.

van der Linden, S., 2022. Misinformation: susceptibility, spread, and interventions to immunize the public. Nat. Med. 28, 460–467. https://doi.org/10.1038/s41591-022-01713-6

Virtanen, P., Gommers, R., Oliphant, T.E., Haberland, M., Reddy, T., Cournapeau, D., Burovski, E., Peterson, P., Weckesser, W., Bright, J., van der Walt, S.J., Brett, M., Wilson, J., Millman, K.J., Mayorov, N., Nelson, A.R.J., Jones, E., Kern, R., Larson, E., Carey, C.J., Polat, İ., Feng, Y., Moore, E.W., VanderPlas, J., Laxalde, D., Perktold, J., Cimrman, R., Henriksen, I., Quintero, E.A., Harris, C.R., Archibald, A.M., Ribeiro, A.H., Pedregosa, F., van Mulbregt, P., 2020. SciPy 1.0: fundamental algorithms for scientific computing in Python. Nat. Methods 17, 261–272. https://doi.org/10.1038/s41592-019-0686-2

Wakefield, A.J., 1999. MMR vaccination and autism. The Lancet 354, 949–950. https://doi.org/10.1016/S0140-6736(05)75696-8

Wang, Z., Bauch, C.T., Bhattacharyya, S., d'Onofrio, A., Manfredi, P., Perc, M., Perra, N., Salathé, M., Zhao, D., 2016. Statistical physics of vaccination. Phys. Rep., Statistical physics of vaccination 664, 1–113. https://doi.org/10.1016/j.physrep.2016.10.006

Weston, D., Hauck, K., Amlôt, R., 2018. Infection prevention behaviour and infectious disease modelling: a review of the literature and recommendations for the future. BMC Public Health 18, 336. https://doi.org/10.1186/s12889-018-5223-1

Wiegand, M., Eagan, R.L., Karimov, R., Lin, L., Larson, H.J., Figueiredo, A.D., 2023. Global Declines in Vaccine Confidence from 2015 to 2022: A Large-Scale Retrospective Analysis. https://doi.org/10.2139/ssrn.4438003

World Health Organization, 2026. Vaccines and immunization [WWW Document]. Vaccines Immun. URL https://www.who.int/health-topics/vaccines-and-immunization (accessed 1.2.26).

World Health Organization, 2019. Ten threats to global health in 2019 [WWW Document]. URL https://www.who.int/news-room/spotlight/ten-threats-to-global-health-in-2019 (accessed 1.2.26).

World Health Organization, UNICEF, 2025. WHO/UNICEF Estimates of National Immunization Coverage.

Wu, Z.-X., Zhang, H.-F., 2013. Peer pressure is a double-edged sword in vaccination dynamics. EPL Europhys. Lett. 104, 10002. https://doi.org/10.1209/0295-5075/104/10002

Yaqub, O., Castle-Clarke, S., Sevdalis, N., Chataway, J., 2014. Attitudes to vaccination: A critical review. Soc. Sci. Med. 112, 1–11. https://doi.org/10.1016/j.socscimed.2014.04.018

Yates, C.A., Erban, R., Escudero, C., Couzin, I.D., Buhl, C., Kevrekidis, I.G., Maini, P.K., Sumpter, D.J.T., 2009. Inherent noise can facilitate coherence in collective swarm motion. Proc. Natl. Acad. Sci. 106, 5464–5469. https://doi.org/10.1073/pnas.0811195106

Zhou, W.-X., Sornette, D., Hill, R.A., Dunbar, R.I.M., 2005. Discrete hierarchical organization of social group sizes. Proc. R. Soc. B Biol. Sci. 272, 439–444. https://doi.org/10.1098/rspb.2004.2970

Zucker, J.R., Rosen, J.B., Iwamoto, M., Arciuolo, R.J., Langdon-Embry, M., Vora, N.M., Rakeman, J.L., Isaac, B.M., Jean, A., Asfaw, M., Hawkins, S.C., Merrill, T.G., Kennelly, M.O., Morgenthau, B.M., Daskalakis, D.C., Barbot, O., 2020. Consequences

of Undervaccination — Measles Outbreak, New York City, 2018–2019. N. Engl. J. Med. 382, 1009–1017. https://doi.org/10.1056/NEJMoa1912514